iScience

CellPress

Article

Electrochemical Oxidative Clean Halogenation Using HX/NaX with Hydrogen Evolution

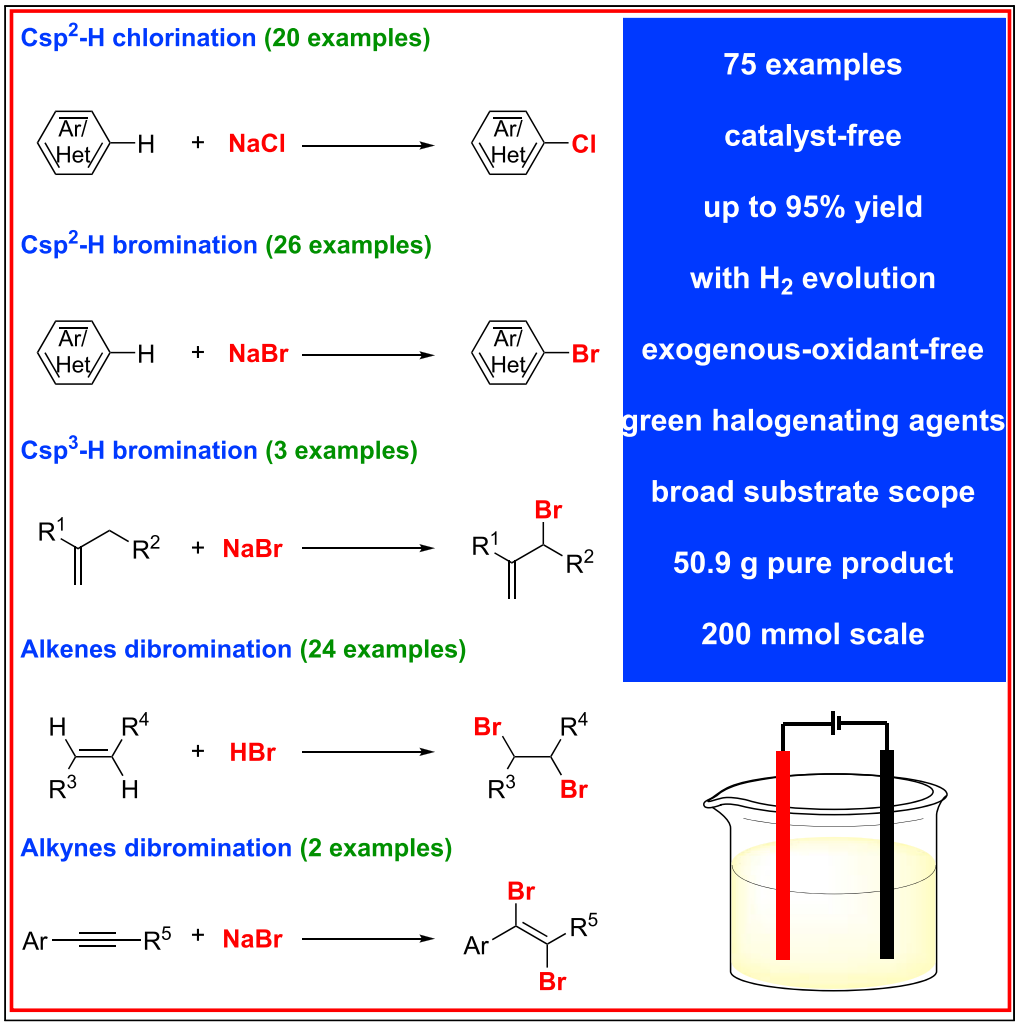

Yong Yuan, Anjin Yao, Yongfu Zheng, ..., Jing Zhao, Huilai Wen, Aiwen Lei

aiwenlei@whu.edu.cn

HIGHLIGHTS

Metal catalyst free and exogenous oxidant free

Commercially available, nontoxic, and green halogenating agents

Broad substrate scope

200-mmol-scale synthesis

Yuan et al., iScience *12*, 293–303
February 22, 2019
https://doi.org/10.1016/j.isci.2019.01.017

iScience

CellPress

Article

Electrochemical Oxidative Clean Halogenation Using HX/NaX with Hydrogen Evolution

Yong Yuan,[1,2,3] Anjin Yao,[1,3] Yongfu Zheng,[1,3] Meng Gao,[1] Zhilin Zhou,[1] Jin Qiao,[1] Jiajia Hu,[1] Baoqin Ye,[1] Jing Zhao,[1] Huilai Wen,[1] and Aiwen Lei[1,2,4,*]

SUMMARY

Organic halides (R-X) are prevalent structural motifs in pharmaceutical molecules and key building blocks for the synthesis of fine chemicals. Although a number of routes are available in the literature for the synthesis of organic halides, these methods often require stoichiometric additives or oxidants, metal catalysts, leaving or directing groups, or toxic halogenating agents. In addition, the necessity of employing different, often tailor-made, catalytic systems for each type of substrate also limits the applicability of these methods. Herein, we report a clean halogenation by electrochemical oxidation with NaX/HX. A series of organic halides were prepared under metal catalyst- and exogenous-oxidant-free reaction conditions. It is worth noting that this reaction has a broad substrate scope; various heteroarenes, arenes, alkenes, alkynes, and even aliphatic hydrocarbons could be applied. Most importantly, the reaction could also be performed on a 200-mmol scale with the same efficiency (86%, 50.9 g pure product).

INTRODUCTION

Organic halides (R-X) are compounds of high practical utility, which are not only important structural motifs in many pharmaceutical molecules and natural products (Hernandez et al., 2010; Jeschke, 2010; Butler and Sandy, 2009) but also key building blocks for the synthesis of fine chemicals via transition-metal-catalyzed oxidative/reductive cross-coupling reactions (Yue et al., 2018; Fairlamb, 2007; Nicolaou et al., 2005; Meijere and Diederich, 2004; Liu et al., 2017a). Consequently, practical and efficient methods to access this class of compounds are highly valuable. Extensive efforts have been made, and great achievement has been reached (Ye et al., 2018; Mo et al., 2010; Petrone et al., 2016; Rafiee et al., 2018; Liu et al., 2017b; Fu et al., 2017a; Wang et al., 2012; Wallentin et al., 2012; Liu and Groves, 2010; Murphy et al., 2007; Smith et al., 2002), such as the electrophilic aromatic substitutions (Barluenga et al., 2007; Prakash et al., 2004; David, 1976) and the directed C-H halogenations (Teskey et al., 2015; Schröder et al., 2015; Schröder et al., 2012; Bedford et al., 2011; Kakiuchi et al., 2009; Mei et al., 2008; Whitfield and Sanford, 2007; Wan, 2006). Although these methods have been widely used for the synthesis of organic halides (R-X), they still have one or more of the following limitations: (1) the use of hazardous and toxic X_2 (X = Br, Cl) as halogenating agents; (2) the need of stoichiometric amount of additives/exogenous oxidants; (3) the need of a metal salt as the catalyst; (4) the need of custom-built substrate bearing leaving or directing groups; (5) the necessity of employing different, often tailor-made, catalytic systems for each types of substrate; and (6) the harsh reaction conditions. Therefore, exploring an efficient and versatile method for the synthesis of various organic halides (R-X) with non-toxic and green halogenating agents under environmentally benign metal-catalyst-free and exogenous-oxidant-free reaction conditions would be highly desirable.

Electrochemical anodic oxidation presents the prospect of the efficient and environmentally benign synthesis of complex molecules and has attracted considerable interest (Tang et al., 2018a; Yoshida et al., 2018; Jiang et al., 2018; Yan et al., 2017; Pletcher et al., 2018; Francke and Little, 2014; Jutand, 2008; Sperry and Wright, 2006; Qiu et al., 2018; Xiong et al., 2017; Gieshoff et al., 2017; Fu et al., 2017b; Yang et al., 2017; Horn et al., 2016; Badalyan and Stahl, 2016; Kärkäs, 2018; Liu et al., 2018; Lyalin and Petrosyan, 2013; Raju et al., 2006; Kulangiappar et al., 2016; Tan et al., 2017). As part of our continuing studies in the area of electrochemical oxidative C-C and C-heteroatom bonds formation (Yuan et al., 2019; Tang et al., 2018b; Gao et al., 2018; Yuan et al., 2018a, 2018b, 2018c), we herein report a clean halogenation by exogenous-oxidant-free electrochemical oxidation. A series of significant organic halides (R-X) were prepared under

[1]National Research Center for Carbohydrate Synthesis, Jiangxi Normal University, Nanchang, Jiangxi 330022, P. R. China

[2]College of Chemistry and Molecular Sciences, the Institute for Advanced Studies (IAS), Wuhan University, Wuhan, Hubei 430072, P. R. China

[3]These authors contributed equally

[4]Lead Contact

*Correspondence: aiwenlei@whu.edu.cn

https://doi.org/10.1016/j.isci.2019.01.017

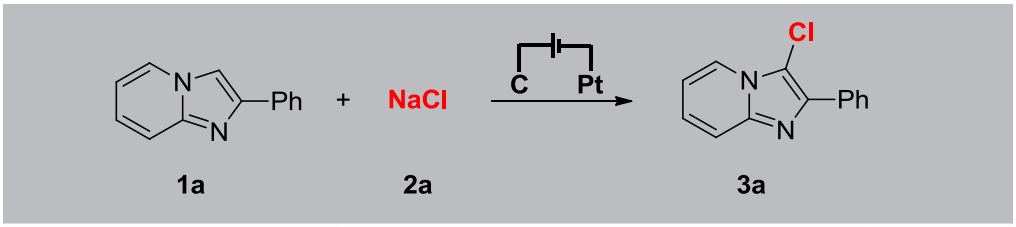

Entry	Variation from the Standard Conditions	Yield (%)[a]
1	None	81
2	HCl (aq.) instead of NaCl	49
3	LiCl instead of NaCl	34
4	KCl instead of NaCl	75
5	$MgCl_2$ instead of NaCl	44
6	$CaCl_2$ instead of NaCl	51
7	6 mA, 7 h	75
8	18 mA, 2.3 h	70
9	Carbon cloth cathode	61
10	Platinum plate anode	53
11	Without H_2O	69
12	MeCN instead of DMF	48
13	No electric current	ND

Table 1. Optimization of Electrochemical Oxidative C-H Chlorination

Reaction conditions: carbon rod anode, platinum plate cathode, constant current = 12 mA, **1a** (0.3 mmol), **2a** (2.0 equiv.), DMF (10.5 mL), H_2O (0.5 mL), 80°C, N_2, 3.5 h (5.2 F/mol).

ND, not detected.

[a]Isolated yields.

metal-catalyst-free and exogenous-oxidant-free reaction conditions with commercially available, nontoxic, and atom-efficient NaX/HX (aq.). It is worth noting that this electrochemical oxidative synthetic protocol has a broad substrate scope. Various heteroarenes, arenes, alkenes, alkynes, and even aliphatic hydrocarbons were suitable for this transformation.

RESULTS AND DISCUSSION

Imidazopyridines (Dyminska, 2015; Enguehard-Gueiffier and Gueiffier, 2007), especially C-3-substituted imidazopyridines, are often used as commercially available drugs including alpidem (Okubo et al., 2004), zolpidem (Langer et al., 1990), necopidem (Depoortere and George, 1991), and saripidem (Sanger, 1995). The introduction of a halogen moiety into the C-3 position of imidazopyridines has been considered to be important because the generated C-3 halogenated imidazopyridines are key intermediates for the synthesis of these drugs. Our investigation included 2-phenylimidazo[1,2-a]pyridine (**1a**) and sodium chloride (**2a**) as the starting materials for the synthesis of these class of significant C-3 halogenated imidazopyridines. As shown in Table 1, by employing a two-electrode system with carbon rod as the anode and platinum plate as the cathode, the desired C-H chlorination product **3a** was produced in 81% yield with a 12 mA constant current in an undivided cell (entry 1). A range of other chlorides were investigated, but all displayed lower effectiveness than sodium chloride (entries 2–6). Both decreasing the operating current to 6 mA and increasing the operating current to 18 mA led to slightly decreased reaction yields (entries 7–8). Then different electrode materials were surveyed, employing either carbon cloth as cathode or platinum plate as anode led to decreased reaction efficiency (entries 9–10). The effect of solvent was explored as

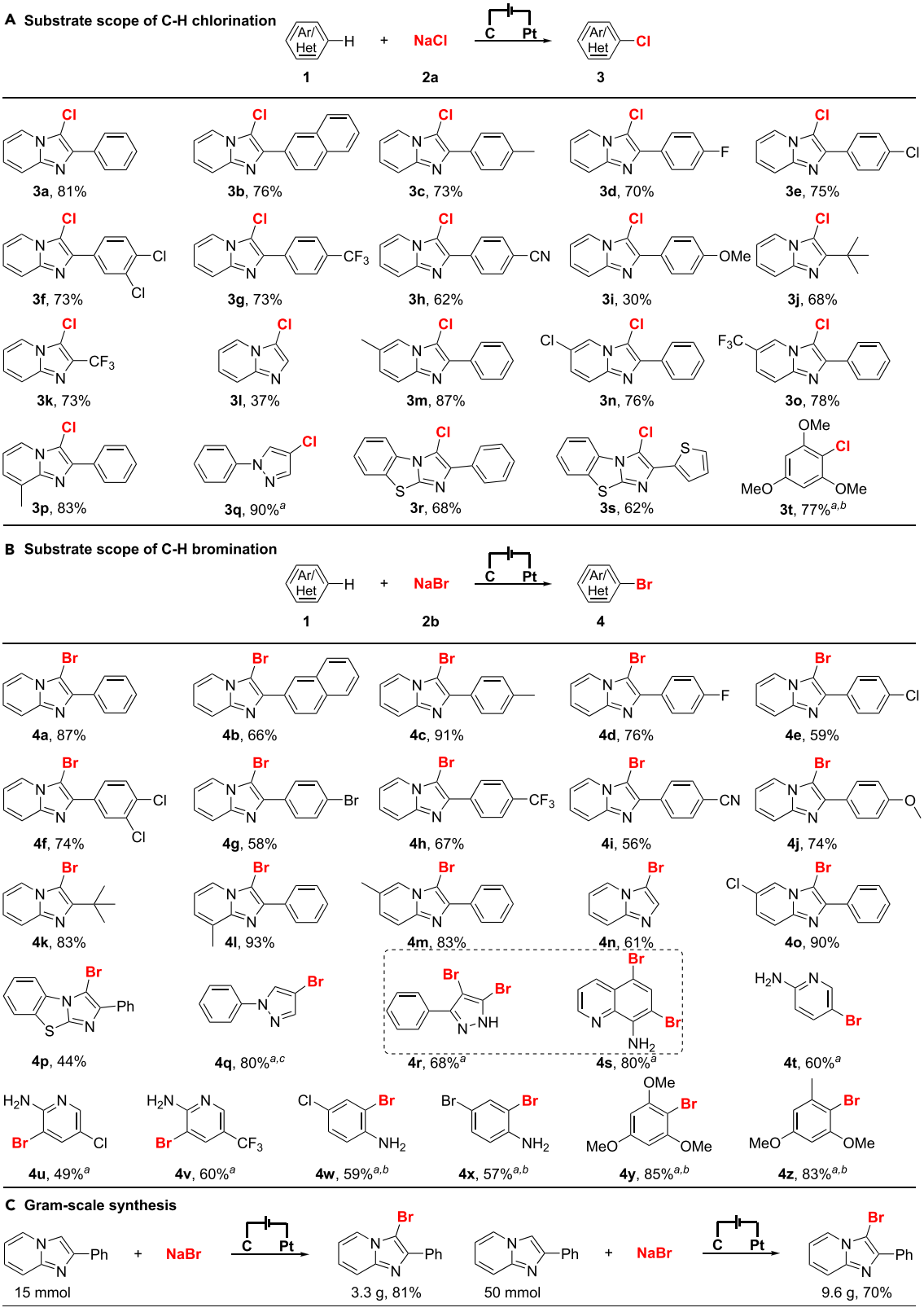
A Substrate scope of C-H chlorination
Ar/Het—H + NaCl → Ar/Het—Cl
1
2a
3
3a, 81%
3b, 76%
3c, 73%
3d, 70%
3e, 75%
3f, 73%
3g, 73%
3h, 62%
3i, 30%
3j, 68%
3k, 73%
3l, 37%
3m, 87%
3n, 76%
3o, 78%
3p, 83%
3q, 90%a
3r, 68%
3s, 62%
3t, 77%a,b
B Substrate scope of C-H bromination
Ar/Het—H + NaBr → Ar/Het—Br
1
2b
4
4a, 87%
4b, 66%
4c, 91%
4d, 76%
4e, 59%
4f, 74%
4g, 58%
4h, 67%
4i, 56%
4j, 74%
4k, 83%
4l, 93%
4m, 83%
4n, 61%
4o, 90%
4p, 44%
4q, 80%a,c
4r, 68%a
4s, 80%a
4t, 60%a
4u, 49%a
4v, 60%a
4w, 59%a,b
4x, 57%a,b
4y, 85%a,b
4z, 83%a,b
C Gram-scale synthesis
15 mmol
3.3 g, 81%
50 mmol
9.6 g, 70%

Figure 1. Substrate Scope for Electrochemical Oxidative C-H Halogenation

(A) Substrate scope of C-H chlorination.

(B) Substrate scope of C-H bromination.

(C) Gram-scale synthesis.

Reaction conditions: carbon rod anode, platinum plate cathode, constant current = 12 mA, **1** (0.3 mmol), **2a** (2.0 equiv.) or **2b** (4.0 equiv.), DMF (10.5 mL), H_2O (0.5 mL), 80°C, N_2, 3.5 h (5.2 F/mol), isolated yields.

[a]CH_3CN (10.5 mL), H_2O (0.5 mL), 75°C.

[b]**1** (2.0 equiv.), **2** (0.3 mmol).

[c]7.0 h.

well. When N,N-dimethylformamide was used as the sole solvent, 69% yield of **3a** could still be obtained (entry 11). However, when the reaction was performed using acetonitrile instead of N,N-dimethylformamide, an obvious loss of the yield was observed (entry 12). As was expected, no reaction could be observed in the absence of electric current (entry 13).

With the optimized reaction conditions in hand, the scope and generality of this clean halogenation was explored (Figure 1). With respect to the C-H chlorination (Figure 1A), diverse heteroarenes/arenes served as effective reaction partners with **2a** to form C-Cl bond. The phenyl- and naphthyl-substituted imidazo[1,2-a]pyridines showed good reactivity and gave the corresponding products in 81% and 76% yields (Figure 1A, **3a-b**), respectively. 2-Arylimidazo[1,2-a]pyridines bearing halogen substituents on the phenyl ring delivered the C-H chlorination products in good to high yields (Figure 1A, **3d-f**). Delightfully, strong electron-withdrawing groups such as trifluoromethyl and cyano at the *para* position of the phenyl ring of 2-phenylimidazo[1,2-a]pyridines nearly did not affect the reaction efficiency (Figure 1A, **3g-h**). By contrast, 2-phenylimidazo[1,2-a]pyridines bearing electron-rich group showed decreased reaction efficiency (Figures 1A, **3i**). It is worth noting that the substrates bearing *tert*-butyl, trifluoromethyl, and -H groups at the C-2 position of imidazo[1,2-a]pyridines also reacted smoothly and delivered the desired products in moderate to good yields (Figure 1A, **3j-l**). Moreover, imidazo[1,2-a]pyridines bearing various substituents such as methyl, chlorine, and trifluoromethyl groups at different positions of the pyridine ring all furnished the C-H chlorination products in high yields (Figure 1A, **3m-p**). Besides various imidazo[1,2-a]pyridines, 1-phenylpyrazole, benzo[*d*]-imidazo[2,1-*b*]thiazole derivatives, and very-electron-rich 1,3,5-trimethoxybenzene were also suitable substrates for this transformation, affording the desired products in 62%–90% yields (Figure 1A, **3q-t**).

We subsequently turned our attention to the C-H bromination (Figure 1B). To our delight, imidazo[1,2-a]pyridines bearing various substituents such as alkyl, alkoxy, halogen, cyano, and trifluoromethyl groups at different positions of the phenyl ring or pyridine ring all underwent clean transformations to generate the C-H bromination products in good to excellent yields (Figure 1B, **4a-o**). Notably, besides various imidazo[1,2-a]pyridines, other kinds of heteroarenes and arenes were also suitable for this transformation. For example, 2-aminopyridine, benzo[*d*]-imidazo[2,1-*b*]thiazole derivative, 1-phenylpyrazole, 3-phenylpyrazole, 8-aminoquinoline, and 2-aminopyridine derivatives all delivered the corresponding C-H bromination products in moderate to high yields (Figure 1B, **4p-v**). It is worth noting that for 3-phenylpyrazole and 8-aminoquinoline, the double C-H bromination products were the major products (Figure 1B, **4r-s**). In the case of electron-rich arenes, *p*-chloroaniline and *p*-bromoaniline afforded the corresponding C-H bromination products in good yields (Figure 1B, **4w-x**). The very-electron-rich arenes, such as 1,3,5-trimethoxybenzene and 3,5-dimethoxytoluene, gave the C-Br bond formation products in 85% and 83% yields (Figure 1B, **4y-z**), respectively. To examine the scalability of the exogenous-oxidant-free electrochemical oxidative C-H halogenation, reactions on the 15- and 50-mmol scale were performed (Figure 1C). The corresponding C-H halogenation products were afforded in 81% and 70% isolated yield, respectively (see Supplemental Information for details).

To shed light on the reaction mechanism for this electrochemical oxidative C-H halogenation, a series of control experiments were conducted. First, voltammograms of the substrates were recorded (see Figure S160 of the Supplemental Information for details). The oxidation peak of **1a** was observed in N,N-dimethylformamide (DMF)/H_2O at 1.59 V, whereas the oxidation peak of NaCl and NaBr were observed at 1.55 V and 1.40 V, respectively, which indicated that NaCl or NaBr was likely to be first oxidized under the electrolytic conditions. Moreover, under the standard optimized conditions, no homo-coupling product of **1a** was observed in either C-H chlorination or bromination (Figures 2A and 2B). These results further indicated that NaCl and NaBr are readily oxidized than **1a** in this electrochemical oxidative C-H halogenation. The reaction of **1a** with molecular Cl_2 and Br_2 in the absence of electricity was also investigated

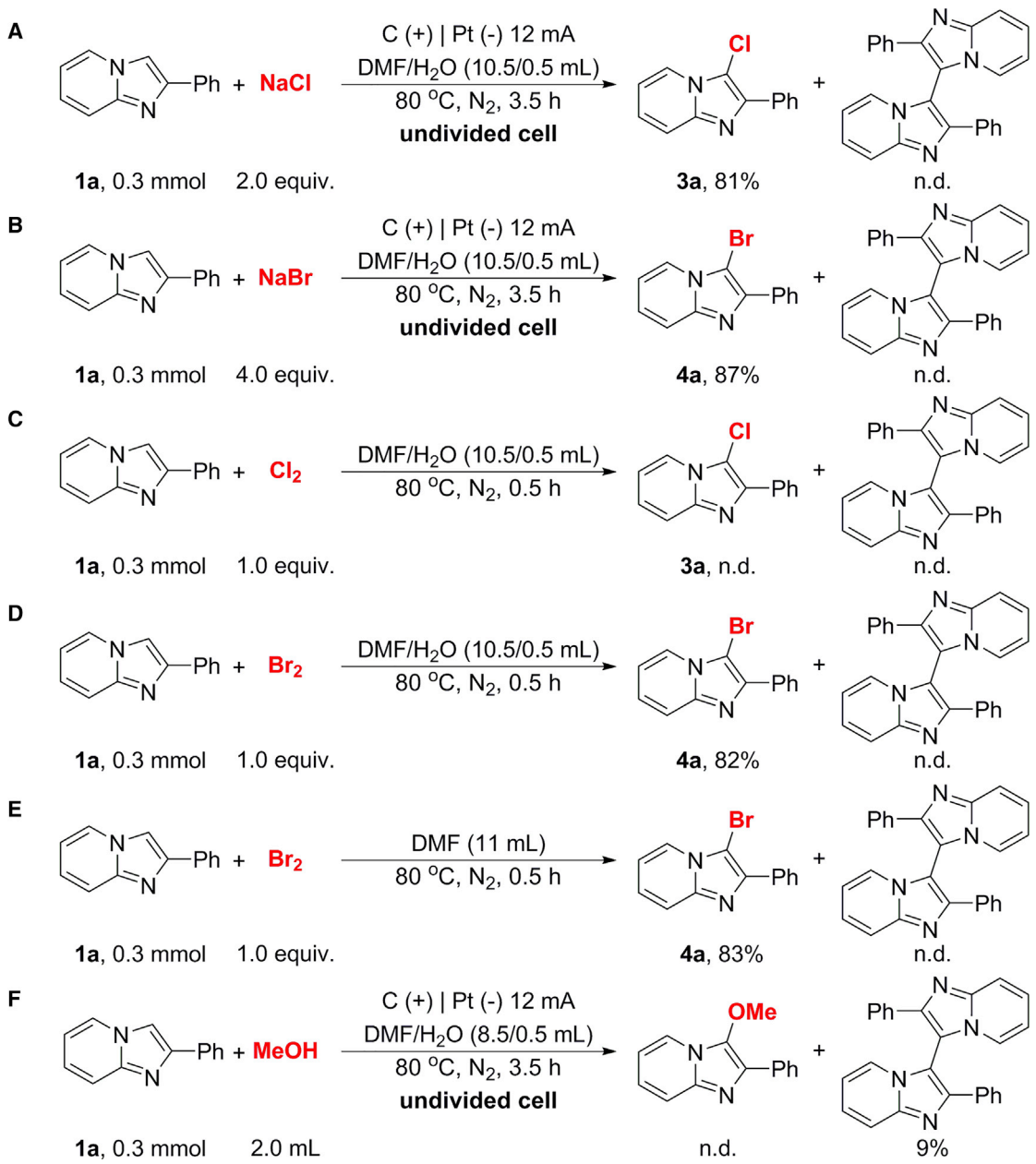

Figure 2. Control Experiments

(Figures 2C–2E). When 1.0 equiv. of molecular Br_2 was added into the reaction system, the desired C-H bromination product could be obtained in high yield and H_2O did not affect the efficiency of this reaction, whereas no chlorination product was detected when molecular Cl_2 was used as the chlorinating agent. These results suggest that molecular Cl_2 might not be involved as the intermediate in C-H chlorination, whereas molecular Br_2 ought to be a key intermediate in C-H bromination. Meanwhile, the pathway in which molecular Br_2 reacted with H_2O yielding the Br^+ (HOBr), then attacked by heteroarenes (**1**) to form the desired product, could be completely ruled out. Last but not least, the reaction of **1a** with MeOH in the absence of sodium halides was carried out (Figure 2F); 9% homo-coupling product of **1a** was isolated from the reaction system, but the product of radical cation intermediate captured by MeOH was not detected. These results suggest that the pathway in which **1a** is oxidized to the corresponding radical cation intermediate and then captured by nucleophile could be ruled out.

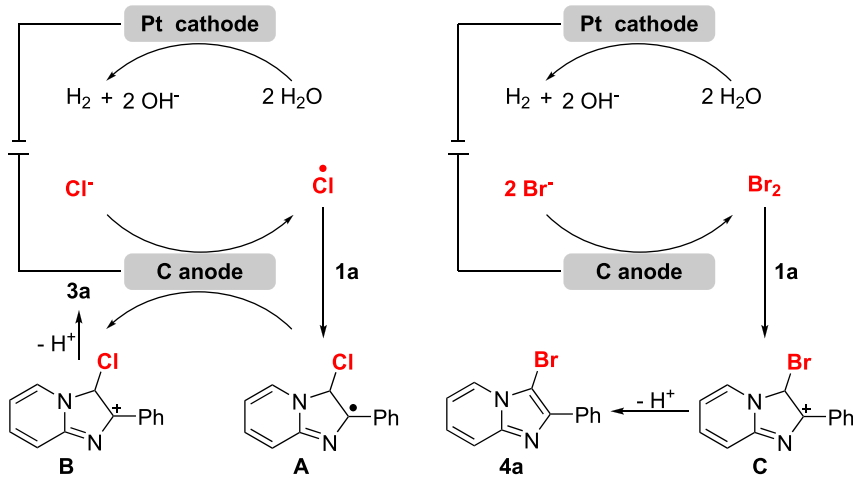

Figure 3. Proposed Mechanism of C-H Halogenation

Based on the above-mentioned experimental results, a plausible reaction mechanism for C-H halogenation is depicted in Figure 3. For the C-H chlorination, the reaction begins with the anodic oxidation of chlorine ion to generate the chlorine radical. The radical intermediate A could then be formed through a radical addition of chlorine radical to **1a**. Finally, further single-electron oxidation and the following deprotonation led to product **3a**. Concomitant cathodic reduction of water leads to hydrogen evolution. Different from the C-H chlorination, in C-H bromination, bromide ion is directly oxidized to molecular Br_2, which then is attacked by **1a** to access the intermediate C. Finally, the following deprotonation led to the product **4a**.

Having successfully demonstrated electrochemical oxidative halogenation of heterocycles/arenes, we subsequently turned our attention to the other type substrates. Indeed, this versatile electrochemical oxidative synthetic protocol was not limited to the heterocycles/arenes; alkenes (**5**) were identified as amenable substrates as well. As shown in Figure 4A, when the ratio of alkenes to HBr (aq.) was 1:2, various styrenes and aliphatic alkenes were compatible with the reaction conditions, providing the desired C-Br double bond forming products in moderate to high yields (Figures 4A, **6a-6x**). Moreover, besides terminal alkenes, internal alkenes were also tolerated in this electrochemical system, and the *trans*-1,2-dibromides were isolated as the sole diastereomeric products (Figures 4A, **6k**, **6r**, **6s**, **6u**). This result suggests that molecular Br_2 might be the key intermediate for this transformation. To evaluate the practicability of this method, we conducted the exogenous-oxidant-free electrochemical oxidative dibromination of 1-decene on a 200-mmol scale and finally obtained 50.9 g pure product (Figure 4B; see Supplemental Information for details), which is hard to access traditionally. This indicates that our protocol could be conveniently scaled up in industry.

To develop a more general method, we also turned our attention to investigate the dibromination of alkynes (Figure 5). Delightfully, when 4-methoxyphenylacetylene (**7a**) and 1-phenyl-1-propyne (**7b**) were employed as the surrogates of alkynes, the desired dibromination products were isolated in 65% and 33% yields (Figure 5), respectively, and *E*-isomers were isolated as the sole diastereomeric products. This result suggests that molecular Br_2 might also be the key intermediate in this dibrominating reaction.

To further affirm that the alkene and alkyne dibromination involved a molecular Br_2 intermediate, the reaction of molecular Br_2 with styrene (**5a**) and 4-methoxyphenylacetylene (**7a**) in the absence of electricity was investigated (Figure 6), respectively. The reaction results indicate that these two transformations indeed involve a molecular Br_2 intermediate.

The success of the heteroarenes, arenes, alkenes, and alkynes led us to extend this method to aliphatic hydrocarbons because alkyl halides are also powerful substrates. To our delight, when ethyl 2-pyridylacetate (**9**) and α-menthylstyrene (**12**) were employed as the surrogates of aliphatic hydrocarbons, the desired alkyl halides **10** and **13** were isolated in 54% and 32% yields (Figure 7), respectively. Moreover, for

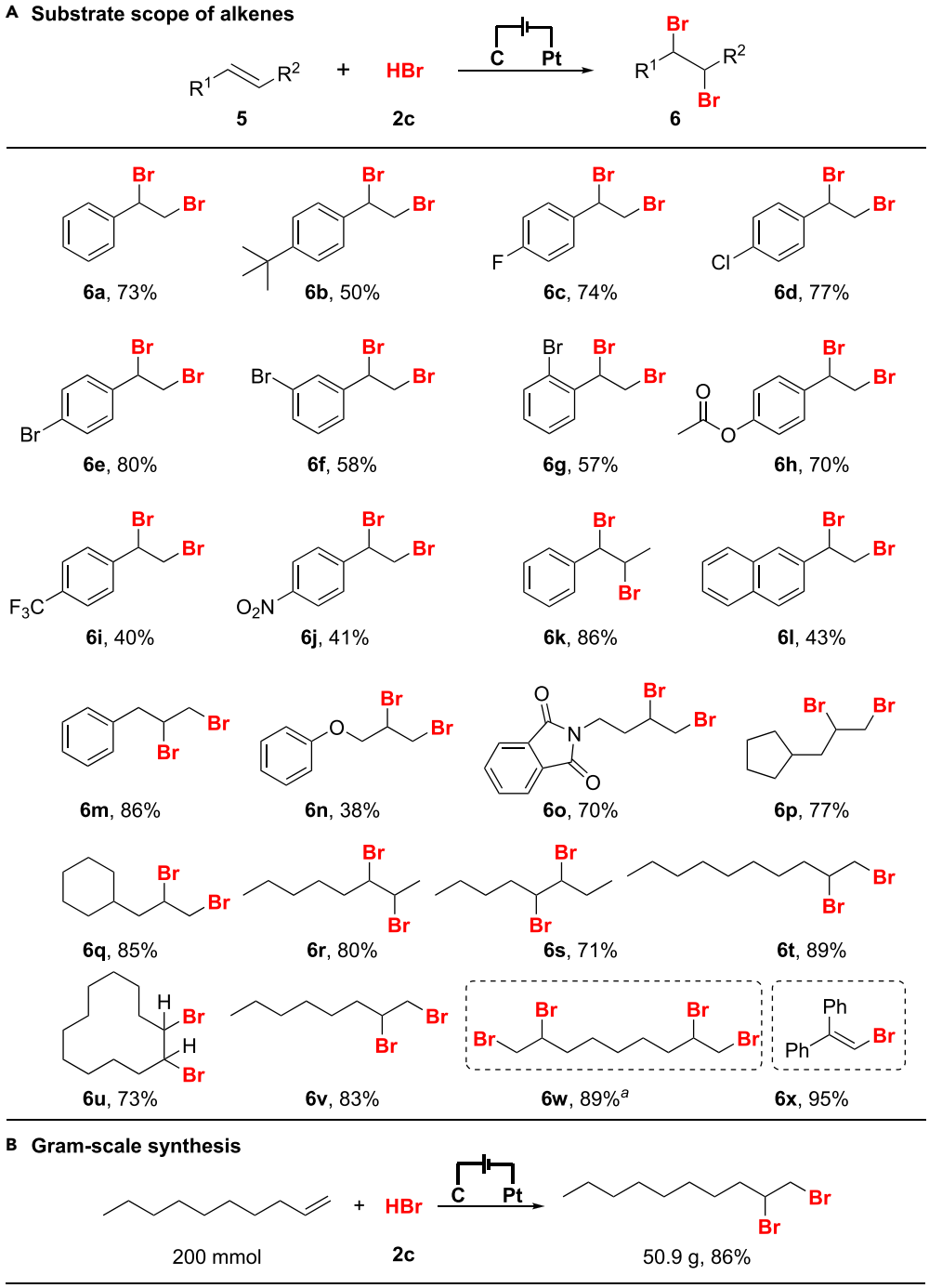

Figure 4. Substrate Scope for Electrochemical Oxidative Dibromination of Alkenes

(A) Substrate scope of alkenes.

(B) Gram-scale synthesis.

Reaction conditions: carbon rod anode, platinum plate cathode, constant current = 12 mA, **5** (0.5 mmol), **2c** (2.0 equiv.), MeCN (10.8 mL), H_2O (0.2 mL), $^nBu_4NBF_4$ (0.1 mmol), RT, N_2, 3.0 h (2.7 F/mol), isolated yields.

[a]**2c** (4.0 equiv.), 6.0 h.

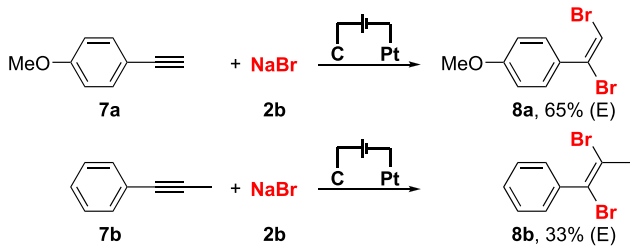

Figure 5. Substrate Scope for Electrochemical Oxidative Dibromination of Alkynes

Reaction conditions: carbon rod anode, platinum plate cathode, constant current = 12 mA, **7** (0.3 mmol), **2b** (4.0 equiv.), MeCN (10.5 mL), H_2O (0.5 mL), 75°C, N_2, 3.5 h, isolated yields.

2-pyridylacetate (**9**), when the amount of sodium bromide (**2b**) was increased to 4.0 equiv. and the reaction time was extended to 3.5 h, the double C-H halogenated product **11** could be isolated in 40% yield.

Limitations of Study

Substrate scope of alkyne dibromination is limited to the electron-rich alkynes.

Conclusion

We have successfully employed constant current for clean halogenation. A series of significant organic halides (R-X) were prepared under a metal-catalyst-free and exogenous-oxidant-free reaction conditions with commercially available, nontoxic, and atom-efficient NaX/HX (aq.). Remarkably, this electrochemical oxidative synthetic protocol has a broad substrate scope. Besides, various heteroarenes/arenes, alkenes, alkynes, and aliphatic hydrocarbons were also suitable. Most importantly, the reaction could also be performed on a 200-mmol scale with the same efficiency (86%, 50.9 g pure product), which further highlighted the synthetic practicability of this electrochemical oxidative strategy.

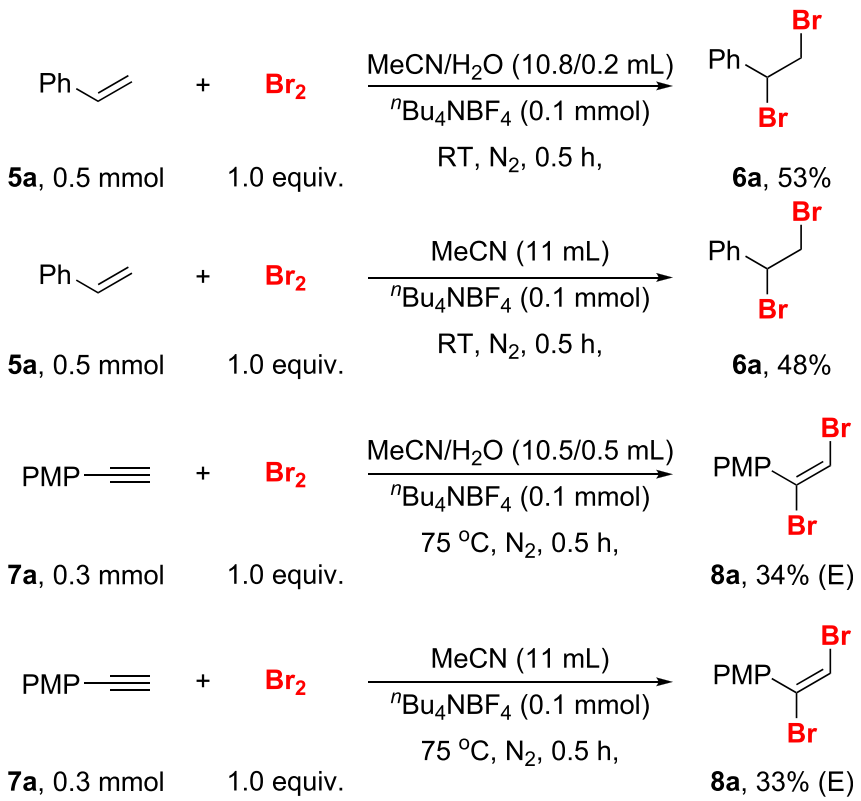

Figure 6. Mechanism Experiments

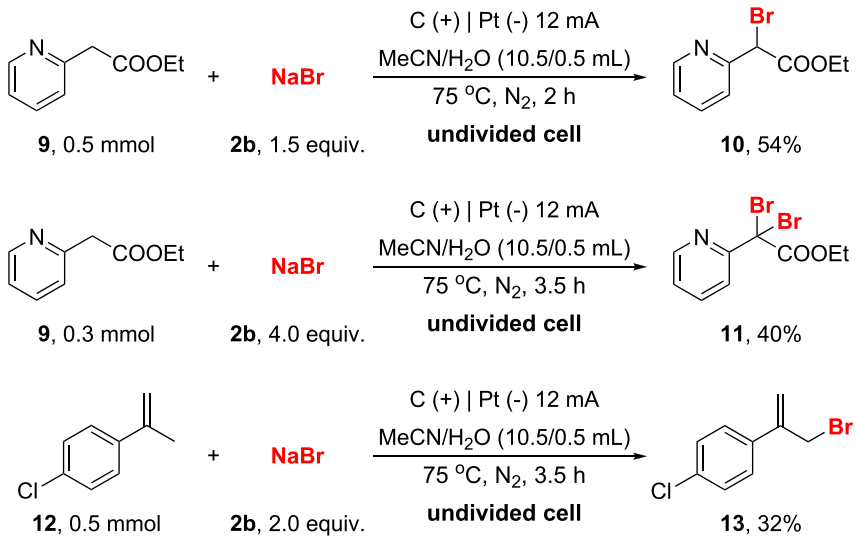

Figure 7. Electrochemical Oxidative C-H Bromination of Aliphatic Hydrocarbons

METHODS

All methods can be found in the accompanying Transparent Methods supplemental file.

SUPPLEMENTAL INFORMATION

Supplemental Information includes Transparent Methods and 160 figures and can be found with this article online at https://doi.org/10.1016/j.isci.2019.01.017.

ACKNOWLEDGMENTS

This work was supported by the National Natural Science Foundation of China (21390402, 21520102003, 21702081, 21702150), the Hubei Province Natural Science Foundation of China (2017CFA010), and the Jiangxi Provincial Education Department Foundation (GJJ160325). The Program of Introducing Talents of Discipline to Universities of China (111 Program) is also appreciated.

AUTHOR CONTRIBUTIONS

A.L. and Y.Y. conceived the project and designed the experiments. Y.Y., A.Y., Y.Z., Z.Z., J.Q., J.H., B.Y., J.Z., and H.W. performed and analyzed the experiments. Y.Y., A.L., and M.G. wrote the manuscript. Y.Y., A.Y., and Y.Z. wrote the Supplemental Information and contributed other related materials. All the authors discussed the results and commented on the manuscript.

DECLARATION OF INTERESTS

The authors declare no competing interests.

Received: October 9, 2018
Revised: December 3, 2018
Accepted: January 9, 2019
Published: February 22, 2019

REFERENCES

Badalyan, A., and Stahl, S.S. (2016). Cooperative electrocatalytic alcohol oxidation with electron-proton-transfer mediators. Nature *535*, 406–410.

Barluenga, J., Alvarez-Gutierrez, J.M., and Ballesteros, A. (2007). Direct ortho iodination of β- and γ-aryl alkylamine derivatives. Angew. Chem. Int. Ed. *46*, 1281–1283.

Bedford, R.B., Haddow, M.F., Mitchell, C.J., and Webster, R.L. (2011). Mild C-H halogenation of anilides and the isolation of an unusual palladium(I)-palladium(II) species. Angew. Chem. Int. Ed. *50*, 5524–5527.

Butler, A., and Sandy, M. (2009). Mechanistic considerations of halogenating enzymes. Nature *460*, 848–854.

David, D.L.M.P.B. (1976). Electrophilic Halogenation Cambridge (University Press).

Depoortere, H., and George, P. (1991). Imidazopyridine for use as an anaesthetic. US 5064836.

Dyminska, L. (2015). Imidazopyridines as a source of biological activity and their pharmacological potentials-Infrared and Raman spectroscopic evidence of their content in pharmaceuticals and plant materials. Bioorg. Med. Chem. *23*, 6087–6099.

Enguehard-Gueiffier, C., and Gueiffier, A. (2007). Recent progress in the pharmacology of imidazo [1,2-a]pyridines. Mini Rev. Med. Chem. *7*, 888–899.

Fairlamb, I.J.S. (2007). Regioselective (site-selective) functionalisation of unsaturated halogenated nitrogen, oxygen and sulfur heterocycles by Pd-catalysed cross-couplings and direct arylation processes. Chem. Soc. Rev. *36*, 1036–1045.

Francke, R., and Little, R.D. (2014). Redox catalysis in organic electrosynthesis: basic principles and recent developments. Chem. Soc. Rev. *43*, 2492–2521.

Fu, N., Sauer, G.S., and Lin, S. (2017a). Electrocatalytic radical dichlorination of alkenes with nucleophilic chlorine sources. J. Am. Chem. Soc. *139*, 15548–15553.

Fu, N., Sauer, G.S., Saha, A., Loo, A., and Lin, S. (2017b). Metal-catalyzed electrochemical diazidation of alkenes. Science *357*, 575–579.

Gao, X., Wang, P., Zeng, L., Tang, S., and Lei, A. (2018). Cobalt(II)-catalyzed electrooxidative C-H amination of arenes with alkylamines. J. Am. Chem. Soc. *140*, 4195–4199.

Gieshoff, T., Kehl, A., Schollmeyer, D., Moeller, K.D., and Waldvogel, S.R. (2017). Insights into the mechanism of anodic N-N bond formation by dehydrogenative coupling. J. Am. Chem. Soc. *139*, 12317–12324.

Hernandez, M., Cavalcanti, S., Moreira, D., Asevedo, W.J., and Leite, A. (2010). Halogen atoms in the modern medicinal chemistry: hints of the drug design. Curr. Drug Targets *11*, 303–315.

Horn, E.J., Rosen, B.R., Chen, Y., Tang, J., Chen, K., Eastgate, M.D., and Baran, P.S. (2016). Scalable and sustainable electrochemical allylic C-H oxidation. Nature *533*, 77–81.

Jeschke, P. (2010). The unique role of halogen substituents in the design of modern agrochemicals. Pest Manage. Sci. *66*, 10–27.

Jiang, Y., Xu, K., and Zeng, C. (2018). Use of electrochemistry in the synthesis of heterocyclic structures. Chem. Rev. *118*, 4485–4540.

Jutand, A. (2008). Contribution of electrochemistry to organometallic catalysis. Chem. Rev. *108*, 2300–2347.

Kakiuchi, F., Kochi, T., Mutsutani, H., Kobayashi, N., Urano, S., Sato, M., Nishiyama, S., and Tanabe, T. (2009). Palladium-catalyzed aromatic C-H halogenation with hydrogen halides by means of electrochemical oxidation. J. Am. Chem. Soc. *131*, 11310–11311.

Kärkäs, M.D. (2018). Electrochemical strategies for C–H functionalization and C–N bond formation. Chem. Soc. Rev. *47*, 5786–5865.

Kulangiappar, K., Ramprakash, M., Vasudevan, D., and Raju, T. (2016). Electrochemical bromination of cyclic and acyclic enes using biphasic electrolysis. Synth. Commun. *46*, 145–153.

Langer, S.Z., Arbilla, S., Benavides, J., and Scatton, B. (1990). Zolpidem and alpidem: two imidazopyridines with selectivity for omega 1- and omega 3-receptor subtypes. Adv. Biochem. Psychopharmacol. *46*, 61–72.

Liu, L., and Groves, G.T. (2010). Manganese porphyrins catalyze selective C-H bond halogenations. J. Am. Chem. Soc. *132*, 12847–12849.

Liu, B., Lim, C.-H., and Miyake, G.M. (2017a). Visible-light-promoted C-S cross-coupling via intermolecular charge transfer. J. Am. Chem. Soc. *139*, 13616–13619.

Liu, W., Yang, X., Gao, Y., and Li, C.-J. (2017b). Simple and efficient generation of aryl radicals from aryl triflates: synthesis of aryl boronates and aryl iodides at room temperature. J. Am. Chem. Soc. *139*, 8621–8627.

Liu, Q., Sun, B., Liu, Z., Kao, Y., Dong, B.-W., Jiang, S.-D., Li, F., Liu, G., Yang, Y., and Mo, F. (2018). A general electrochemical strategy for the Sandmeyer reaction. Chem. Sci. *9*, 8731–8737.

Lyalin, B.V., and Petrosyan, V.A. (2013). Electrochemical halogenation of organic compounds. Russ. J. Electrochem. *49*, 497–529.

Mei, T.-S., Giri, R., Maugel, N., and Yu, J.-Q. (2008). Pd^{II}-catalyzed monoselective ortho halogenation of c-h bonds assisted by counter cations: a complementary method to directed ortho lithiation. Angew. Chem. Int. Ed. *47*, 5215–5219.

Meijere, A.D., and Diederich, F. (2004). Metal Catalyzed Cross-Coupling Reactions (Wiley-VCH Verlag GmbH & Co. KGaA).

Mo, F., Yan, M.J., Qiu, D., Li, F., Zhang, Y., and Wang, J. (2010). Gold-catalyzed halogenation of aromatics by N-Halosuccinimides. Angew. Chem. Int. Ed. *49*, 2028–2032.

Murphy, J.M., Liao, X., and Hartwig, J.F. (2007). Meta halogenation of 1,3-disubstituted arenes via iridium-catalyzed arene borylation. J. Am. Chem. Soc. *129*, 15434–15435.

Nicolaou, K.C., Bulger, P.G., and Sarlah, D. (2005). Palladium-catalyzed cross-coupling reactions in total synthesis. Angew. Chem. Int. Ed. *44*, 4442–4489.

Okubo, T., Yoshikawa, R., Chaki, S., Okuyama, S., and Nakazato, A. (2004). Design, synthesis and structure-affinity relationships of aryloxyanilide derivatives as novel peripheral benzodiazepine receptor ligands. Bioorg. Med. Chem. *12*, 423–438.

Petrone, D.A., Ye, J., and Lautens, M. (2016). Modern transition-metal-catalyzed carbon–halogen bond formation. Chem. Rev. *116*, 8003–8104.

Pletcher, D., Green, R.A., and Brown, R.C.D. (2018). Flow electrolysis cells for the synthetic organic chemistry laboratory. Chem. Rev. *118*, 4573–4591.

Prakash, G.K., Mathew, T., Hoole, D., Esteves, P.M., Wang, Q., Rasul, G., and Olah, G.A. (2004). N-halosuccinimide/BF_3-H_2O, efficient electrophilic halogenating systems for aromatics. J. Am. Chem. Soc. *126*, 15770–15776.

Qiu, Y., Kong, W.-J., Struwe, J., Sauermann, N., Rogge, T., Scheremetjew, A., and Ackermann, L. (2018). Electrooxidative rhodium-catalyzed C-H/C-H activation: electricity as oxidant for cross-dehydrogenative alkenylation. Angew. Chem. Int. Ed. *57*, 5828–5832.

Rafiee, M., Wang, F., Hruszkewycz, D.P., and Stahl, S.S. (2018). N-Hydroxyphthalimide-mediated electrochemical iodination of methylarenes and comparison to electron-transfer-initiated C−H functionalization. J. Am. Chem. Soc. *140*, 22–25.

Raju, T., Kulangiappar, K., Kulandainathan, M.A., Uma, U., Malini, R., and Muthukumaran, A. (2006). Site directed nuclear bromination of aromatic compounds by an electrochemical method. Tetrahedron Lett. *47*, 4581–4584.

Sanger, D.J. (1995). Behavioural effects of novel benzodiazepine (ω) receptor agonists and partial agonists: increases in punished responding and antagonism of the pentylenetetrazole cue. Behav. Pharmacol. *6*, 116–126.

Schröder, N., Wencel-Delord, J., and Glorius, F. (2012). High-Yielding, versatile, and practical [Rh(III)Cp*]-catalyzed ortho bromination and iodination of arenes. J. Am. Chem. Soc. *134*, 8298–8301.

Schröder, N., Lied, F., and Glorius, F. (2015). Dual role of Rh(III) catalyst enables regioselective halogenation of (electron-rich) heterocycles. J. Am. Chem. Soc. *137*, 1448–1451.

Smith, M.B., Guo, L., Okeyo, S., Stenzel, J., Yanella, J., and LaChapelle, E. (2002). Regioselective one-pot bromination of aromatic amines. Org. Lett. *4*, 2321–2323.

Sperry, J.B., and Wright, D.L. (2006). The application of cathodic reductions and anodic oxidations in the synthesis of complex molecules. Chem. Soc. Rev. *35*, 605–621.

Tan, Z., Liu, Y., Helmy, R., Rivera, N.R., Hesk, D., Tyagarajan, S., Yang, L., and Su, J. (2017). Electrochemical bromination of late stage intermediates and drug molecules. Tetrahedron Lett. *58*, 3014–3018.

Tang, S., Liu, Y., and Lei, A. (2018a). Electrochemical oxidative cross-coupling with hydrogen evolution: a green and sustainable way for bond formation. Chem *4*, 27–45.

Tang, S., Wang, S., Liu, Y., Cong, H., and Lei, A. (2018b). Electrochemical oxidative C-H amination of phenols: access to triarylamine derivatives. Angew. Chem. Int. Ed. *57*, 4737–4741.

Teskey, C.J., Lui, A.Y.W., and Greaney, M.F. (2015). Ruthenium-catalyzed meta-selective C-H bromination. Angew. Chem. Int. Ed. *54*, 11677–11680.

Wallentin, C.-J., Nguyen, J.D., Finkbeiner, P., and Stephenson, C.R.J. (2012). Visible light-mediated atom transfer radical addition via oxidative and reductive quenching of photocatalysts. J. Am. Chem. Soc. *134*, 8875–8884.

Wan, X.-B. (2006). Highly selective C-H functionalization/halogenation of acetanilide. J. Am. Chem. Soc. *128*, 7416–7417.

Wang, Z., Zhu, L., Yin, F., Su, Z., Li, Z., and Li, C. (2012). Silver-catalyzed decarboxylative chlorination of aliphatic carboxylic acids. J. Am. Chem. Soc. *134*, 4258–4263.

Whitfield, S.R., and Sanford, M.S. (2007). Reactivity of Pd(II) complexes with electrophilic chlorinating reagents: isolation of Pd(IV) products and observation of C-Cl bond-forming reductive elimination. J. Am. Chem. Soc. *129*, 15142–15143.

Xiong, P., Xu, H.-H., and Xu, H.-C. (2017). Metal- and reagent-free intramolecular oxidative amination of tri- and tetrasubstituted alkenes. J. Am. Chem. Soc. *139*, 2956–2959.

Yan, M., Kawamata, Y., and Baran, P.S. (2017). Synthetic organic electrochemical methods since 2000: on the verge of a renaissance. Chem. Rev. *117*, 13230–13319.

Yang, Q.-L., Li, Y.-Q., Ma, C., Fang, P., Zhang, X.-J., and Mei, T.-S. (2017). Palladium-catalyzed C(sp3)-H oxygenation via electrochemical oxidation. J. Am. Chem. Soc. *139*, 3293–3298.

Ye, K.-Y., Pombar, G., Fu, N., Sauer, G.S., Keresztes, I., and Lin, S. (2018). Anodically coupled electrolysis for the heterodifunctionalization of alkenes. J. Am. Chem. Soc. *140*, 2438–2441.

Yoshida, J.-I., Shimizu, A., and Hayashi, R. (2018). Electrogenerated cationic reactive intermediates: the pool method and further advances. Chem. Rev. *118*, 4702–4730.

Yuan, Y., Chen, Y., Tang, S., Huang, Z., and Lei, A. (2018a). Electrochemical oxidative oxysulfenylation and aminosulfenylation of alkenes with hydrogen evolution. Sci. Adv. *4*, eaat5312.

Yuan, Y., Cao, Y., Lin, Y., Li, Y., Huang, Z., and Lei, A. (2018b). Electrochemical oxidative alkoxysulfonylation of alkenes using sulfonyl hydrazines and alcohols with hydrogen evolution. ACS Catal. *8*, 10871–10875.

Yuan, Y., Yu, Y., Qiao, J., Liu, P., Yu, B., Zhang, W., Liu, H., He, M., Huang, Z., and Lei, A. (2018c). Exogenous-oxidant-free electrochemical oxidative C-H sulfonylation of arenes/heteroarenes with hydrogen evolution. Chem. Commun. (Camb). *54*, 11471–11474.

Yuan, Y., Cao, Y., Qiao, J., Lin, Y., Jiang, X., Weng, Y., Tang, S., and Lei, A. (2019). Electrochemical oxidative C-H sulfenylation of imidazopyridines with hydrogen evolution. Chin. J. Chem. *37*, 49–52.

Yue, H.F., Zhu, C., and Rueping, M. (2018). Cross-coupling of sodium sulfinates with aryl, heteroaryl, and vinyl halides by nickel/photoredox dual catalysis. Angew. Chem. Int. Ed. *57*, 1371–1375.

ISCI, Volume *12*

Supplemental Information

Electrochemical Oxidative Clean Halogenation Using HX/NaX with Hydrogen Evolution

Yong Yuan, Anjin Yao, Yongfu Zheng, Meng Gao, Zhilin Zhou, Jin Qiao, Jiajia Hu, Baoqin Ye, Jing Zhao, Huilai Wen, and Aiwen Lei

Supplemental Information

Electrochemical Oxidative Clean Halogenation Using HX/NaX with Hydrogen Evolution

Yong Yuan,[1,2,3] Anjin Yao,[1,3] Yongfu Zheng,[1,3] Meng Gao,[1] Zhilin Zhou,[1] Jin Qiao,[1] Jiajia Hu,[1] Baoqin Ye,[1] Jing Zhao,[1] Huilai Wen,[1] and Aiwen Lei[1,2,4,*]

[1]National Research Center for Carbohydrate Synthesis, Jiangxi Normal University, Nanchang, Jiangxi 330022, P. R. China.

[2]College of Chemistry and Molecular Sciences, the Institute for Advanced Studies (IAS), Wuhan University, Wuhan, Hubei 430072, P. R. China.

[3]These authors contributed equally to this work

[4]Lead Contact

[*]Correspondence: aiwenlei@whu.edu.cn

Copies of product NMR spectra

Figure S1. ^{1}H NMR (400 MHz, $CDCl_3$) spectrum of compound **3a**, related to **Figure 1**

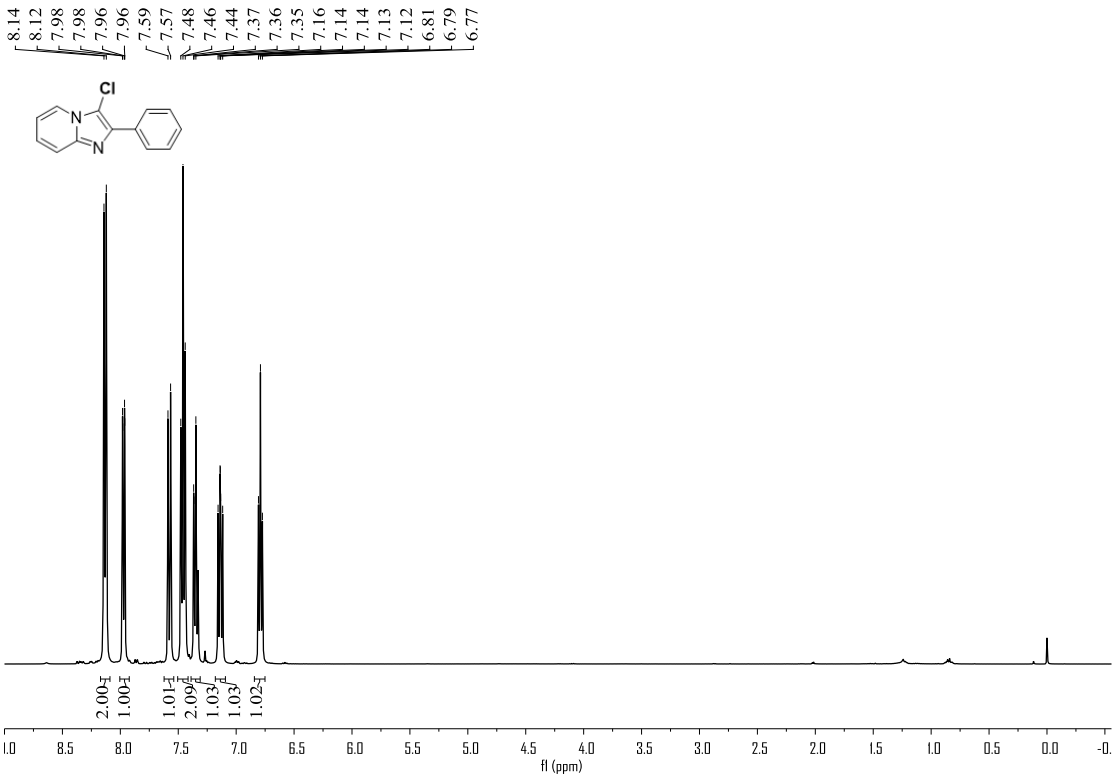

Figure S2. ^{13}C NMR (100 MHz, $CDCl_3$) spectrum of compound **3a**, related to **Figure 1**

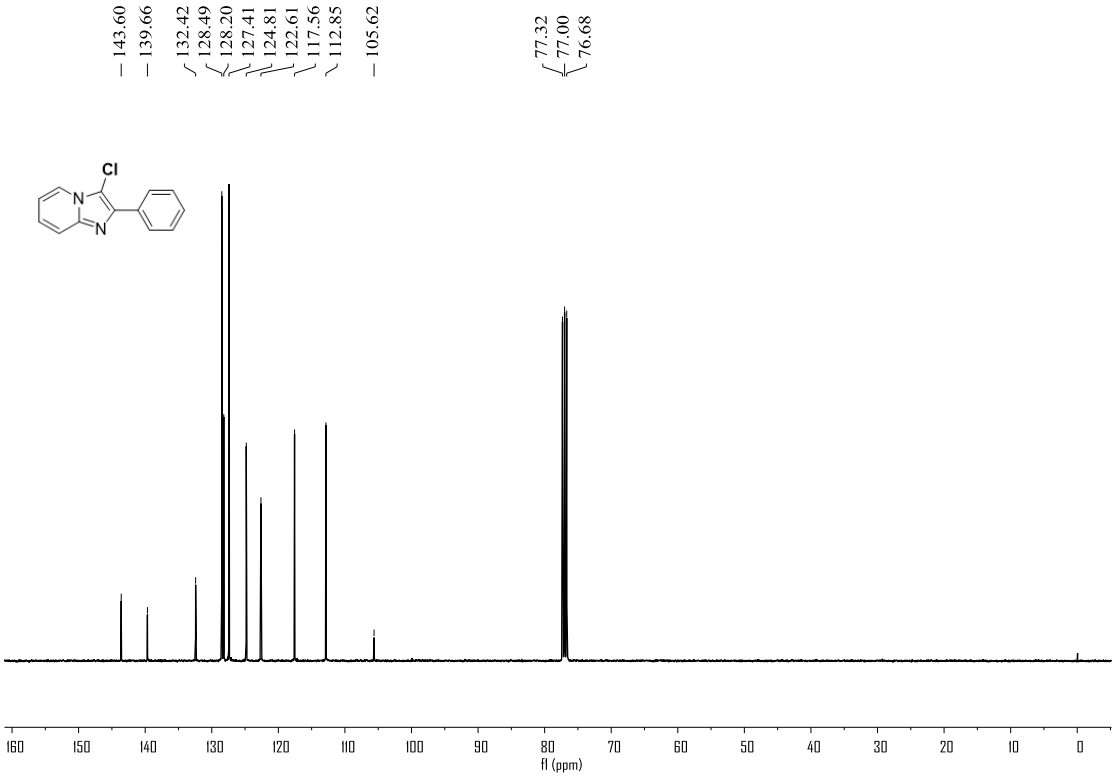

Figure S3. ^{1}H NMR (400 MHz, DMSO-d_6) spectrum of compound **3b**, related to **Figure 1**

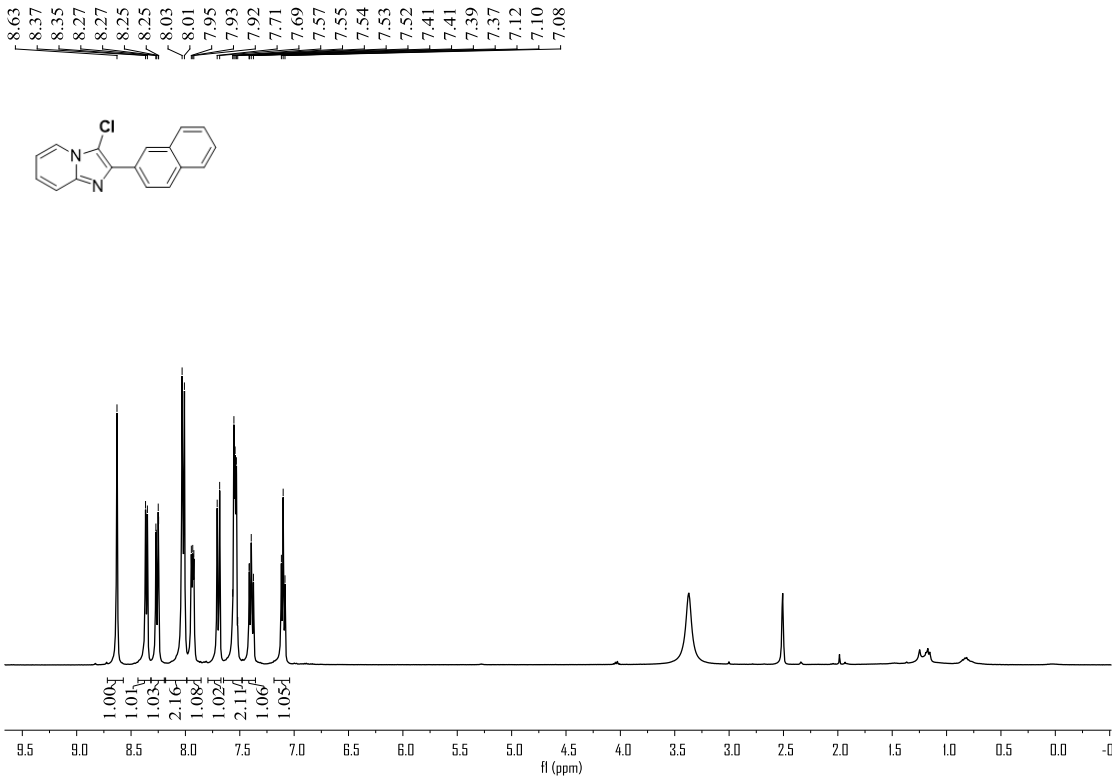

Figure S4. ^{13}C NMR(100 MHz, $CDCl_3$) spectrum of compound **3b**, related to **Figure 1**

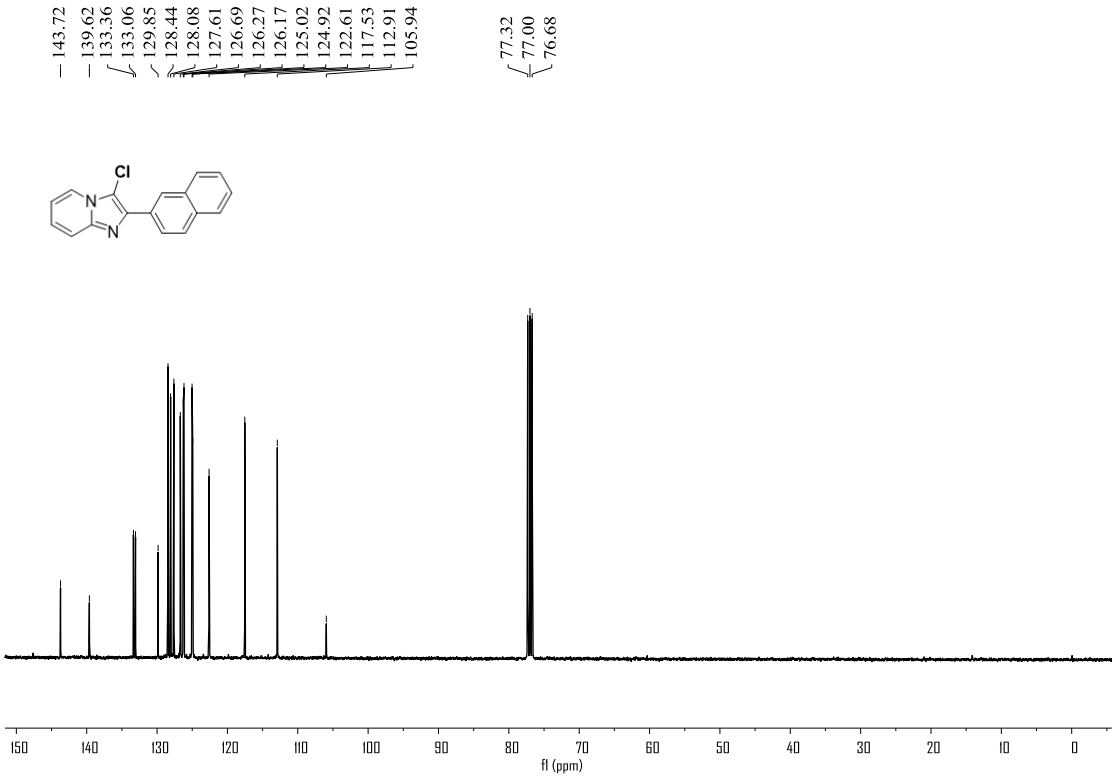

Figure S5. ^{1}H NMR (400 MHz, $CDCl_3$) spectrum of compound **3c**, related to **Figure 1**

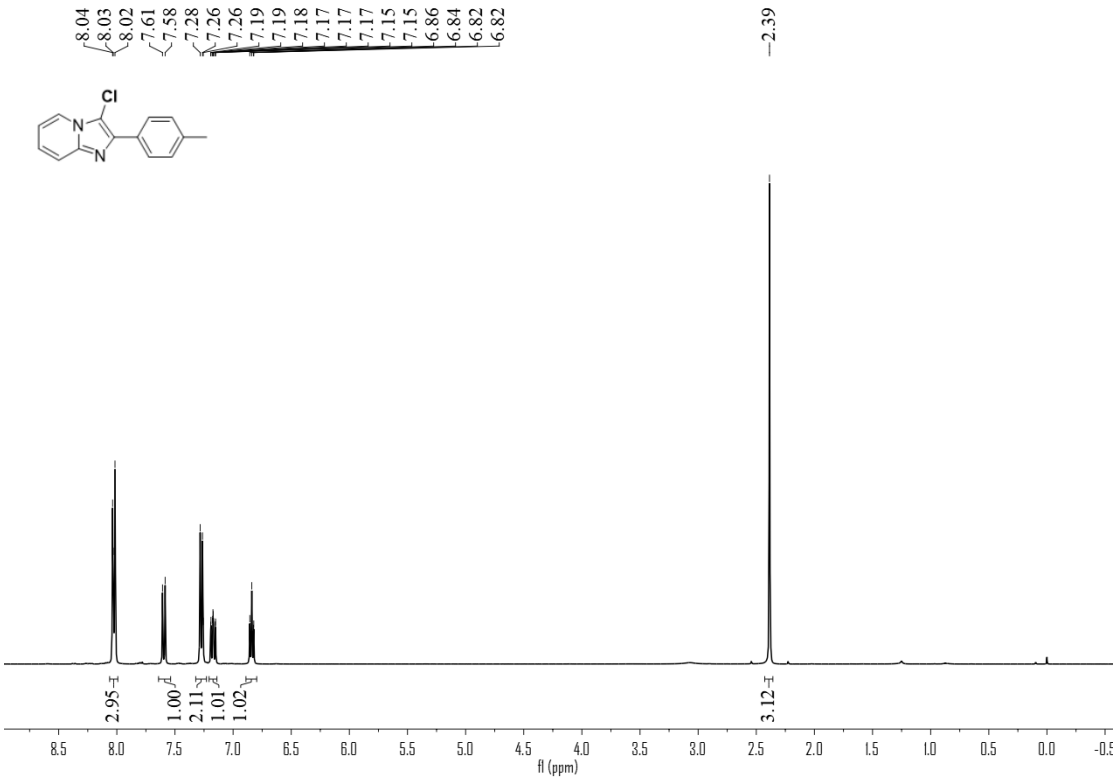

Figure S6. ^{13}C NMR (100 MHz, $CDCl_3$) spectrum of compound **3c**, related to **Figure 1**

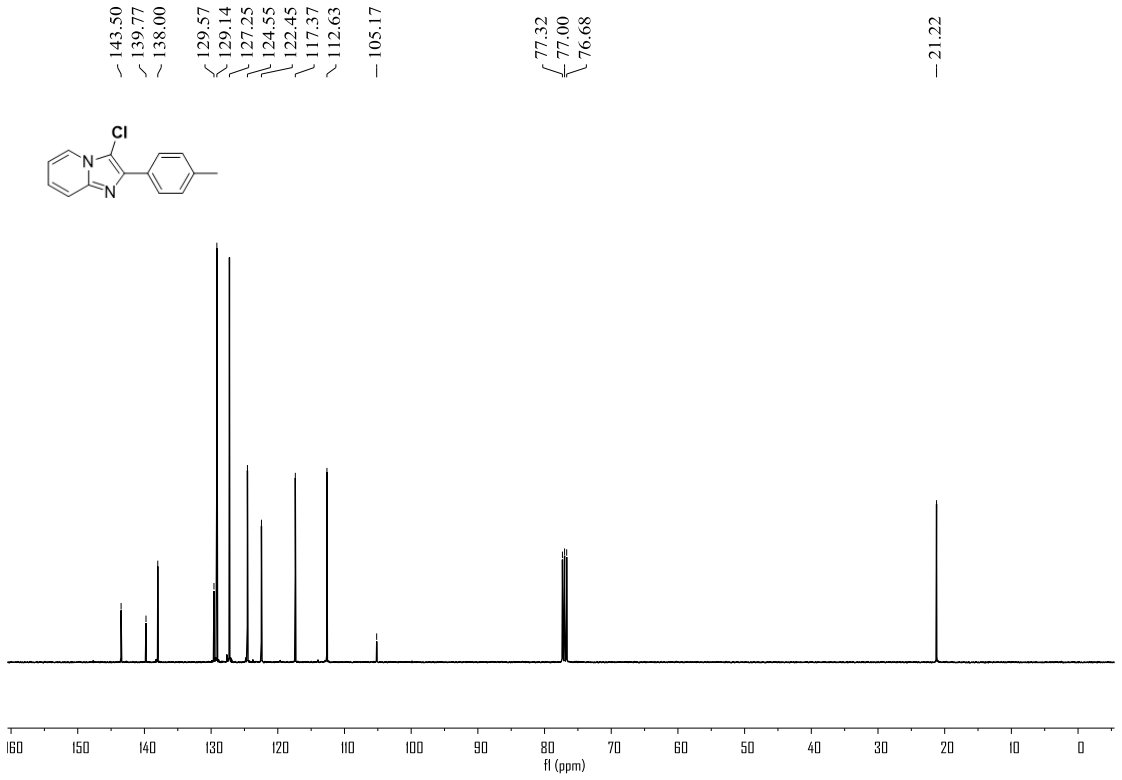

Figure S7. ^{1}H NMR (400 MHz, $CDCl_3$) spectrum of compound **3d**, related to **Figure 1**

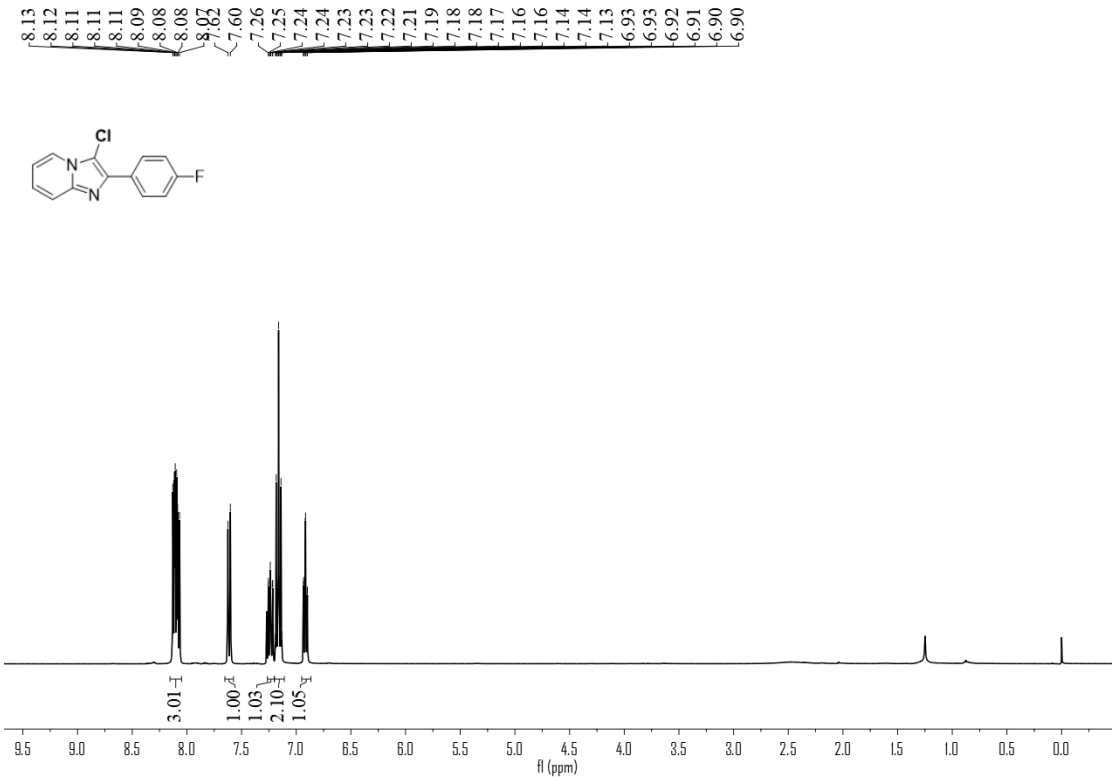

Figure S8. ^{13}C NMR (100 MHz, $CDCl_3$) spectrum of compound **3d**, related to **Figure 1**

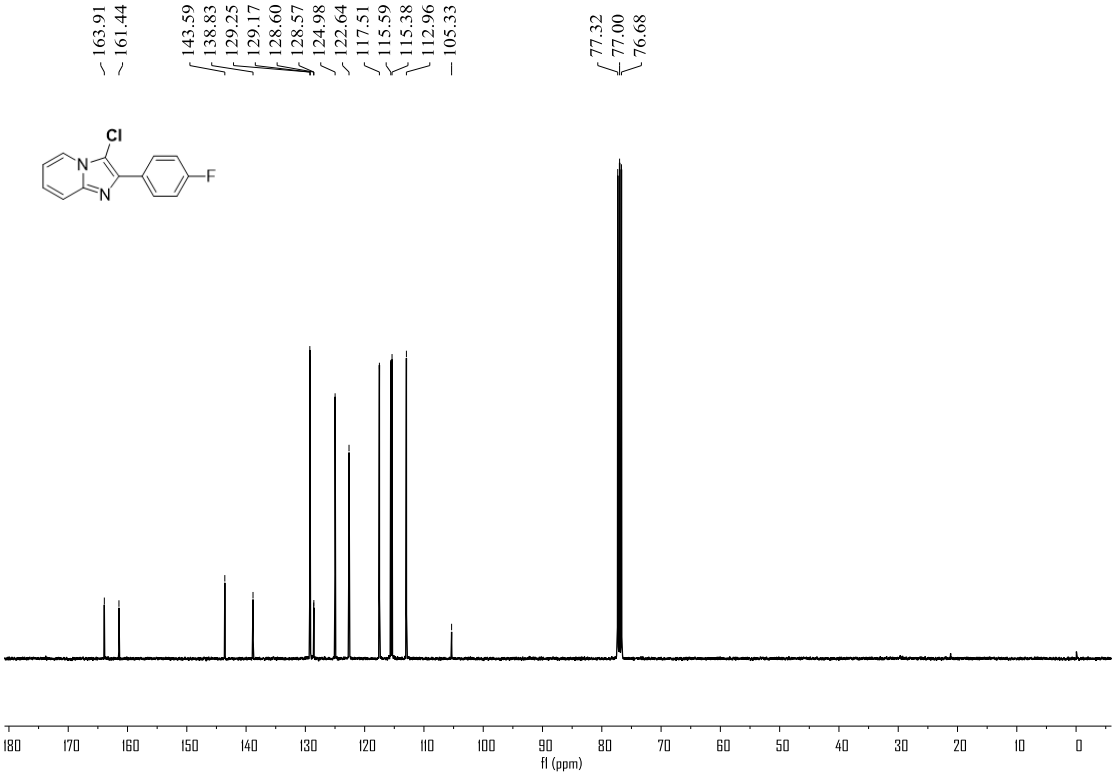

Figure S9. ^{19}F NMR (376 MHz, $CDCl_3$) spectrum of compound **3d**, related to **Figure 1**

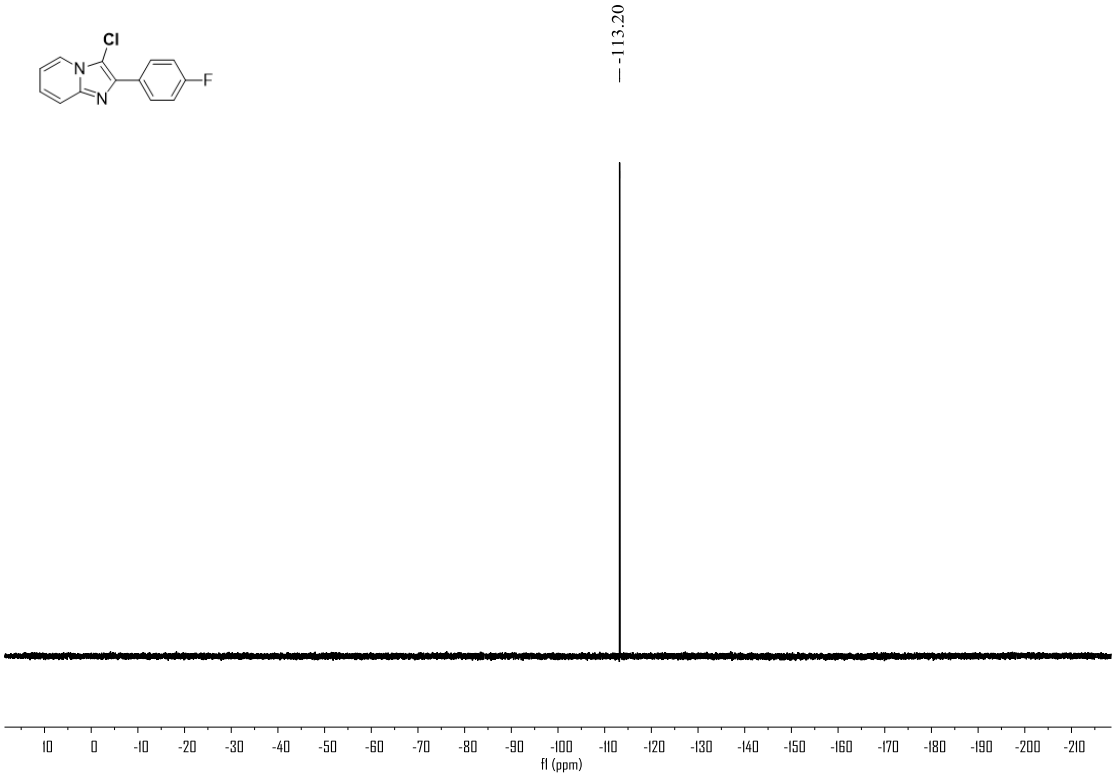

Figure S10. ^{1}H NMR (400 MHz, $CDCl_3$) spectrum of compound **3e**, related to **Figure 1**

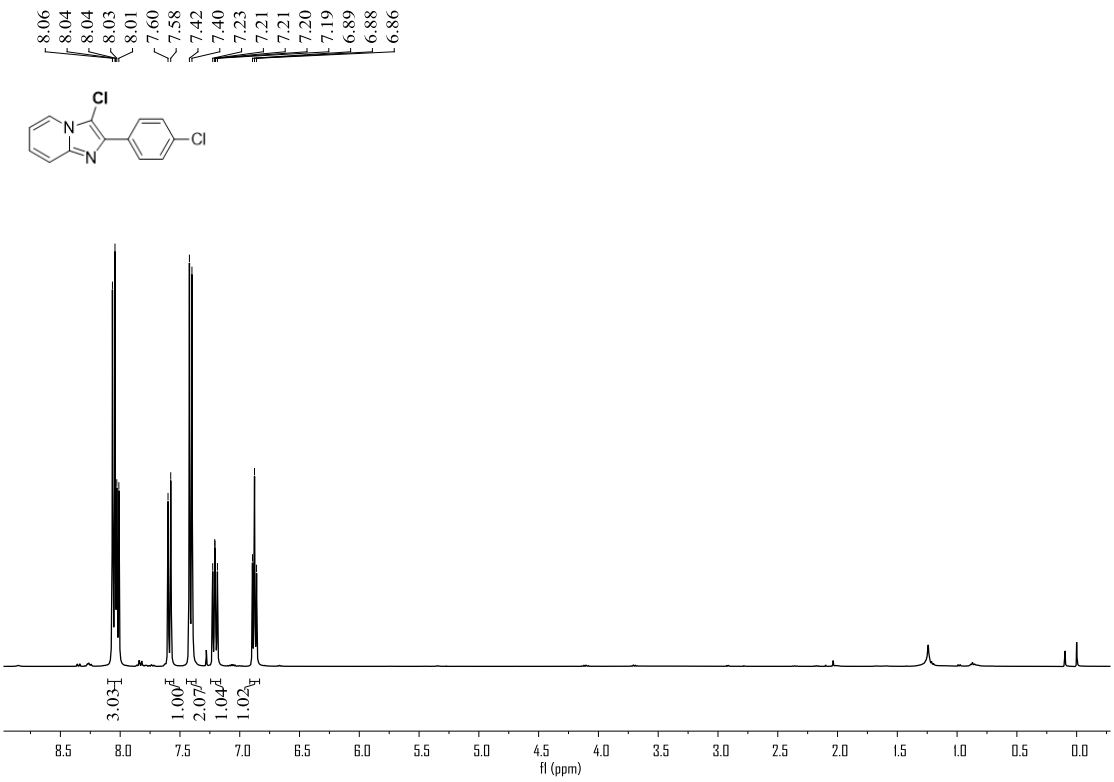

Figure S11. ^{13}C NMR (100 MHz, $CDCl_3$) spectrum of compound **3e**, related to **Figure 1**

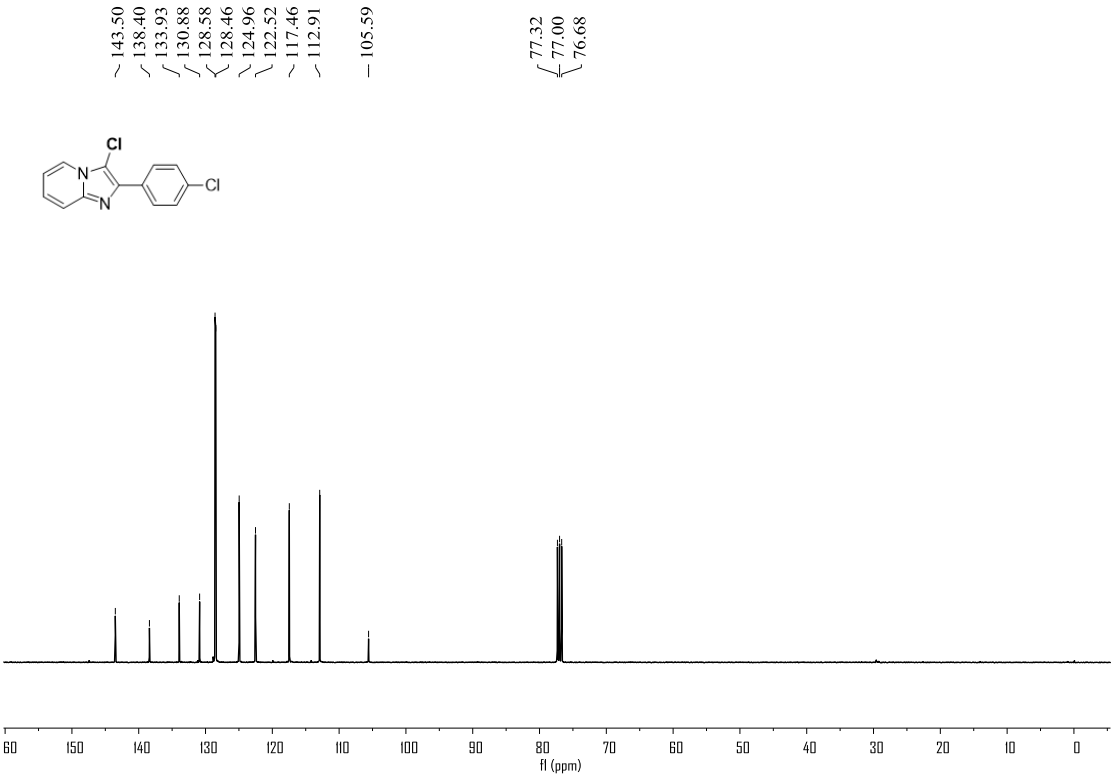

Figure S12. ^{1}H NMR (400 MHz, DMSO-d_6) spectrum of compound **3f**, related to **Figure 1**

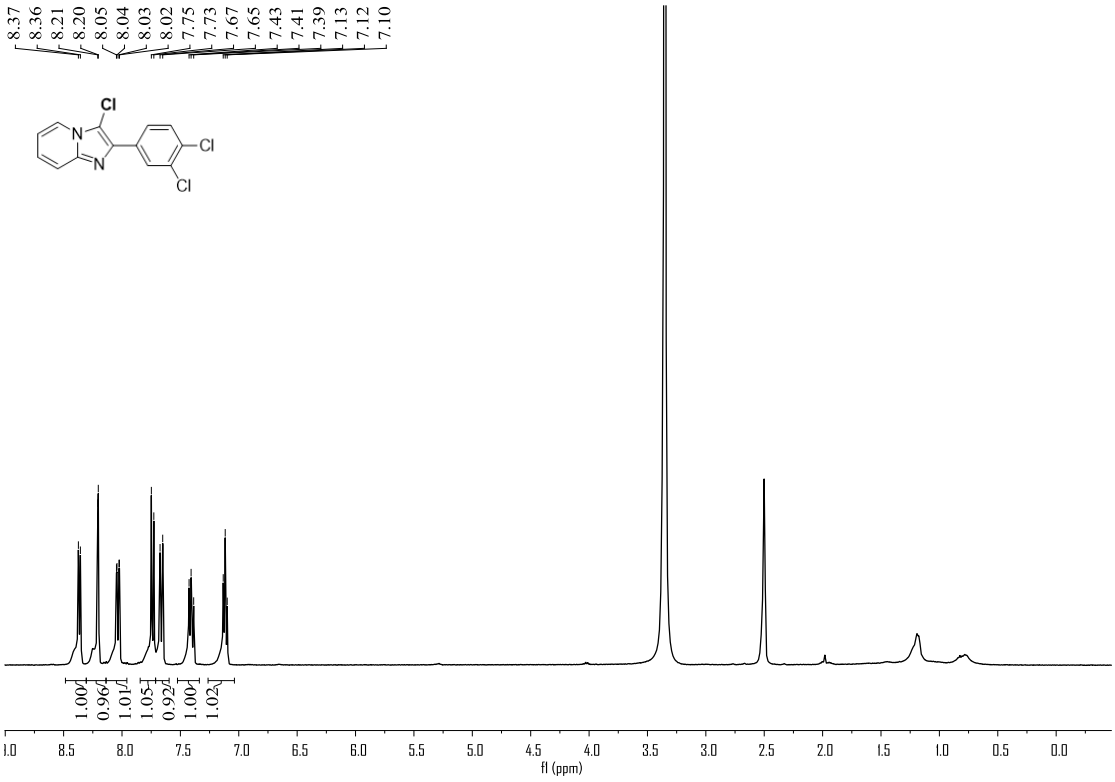

Figure S13. ^{13}C NMR (100 MHz, $CDCl_3$) spectrum of compound **3f**, related to **Figure 1**

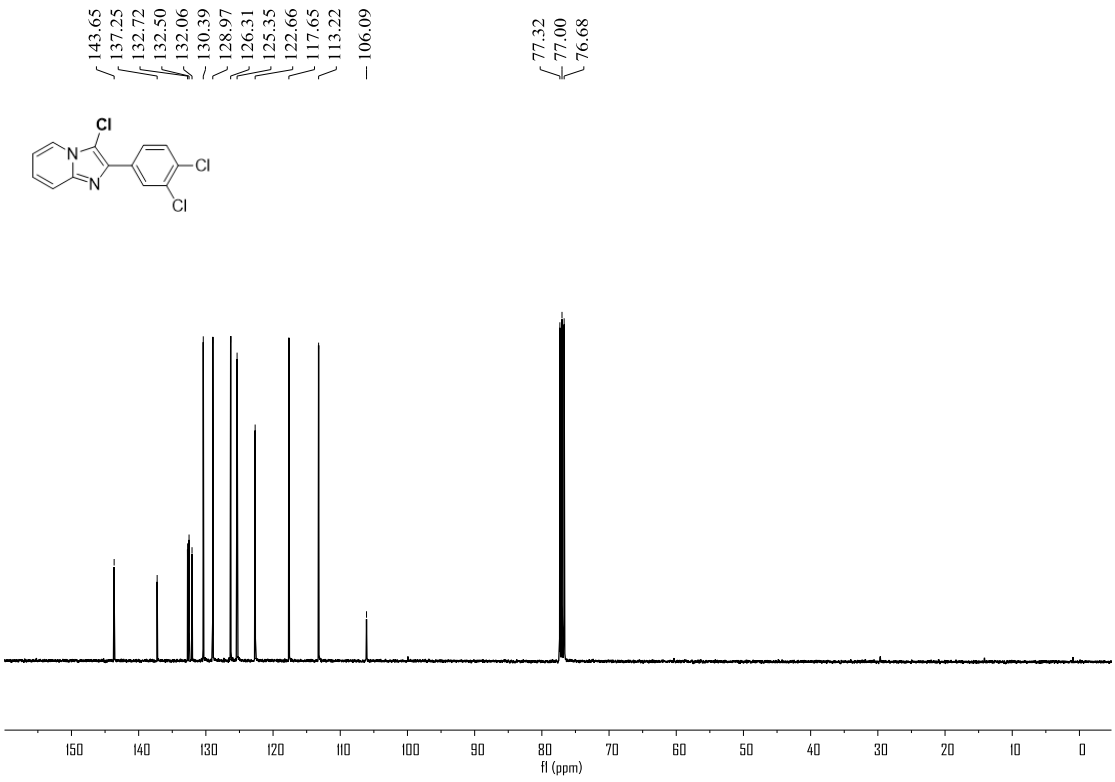

Figure S14. ^{1}H NMR (400 MHz, DMSO-d_6) spectrum of compound **3g**, related to **Figure 1**

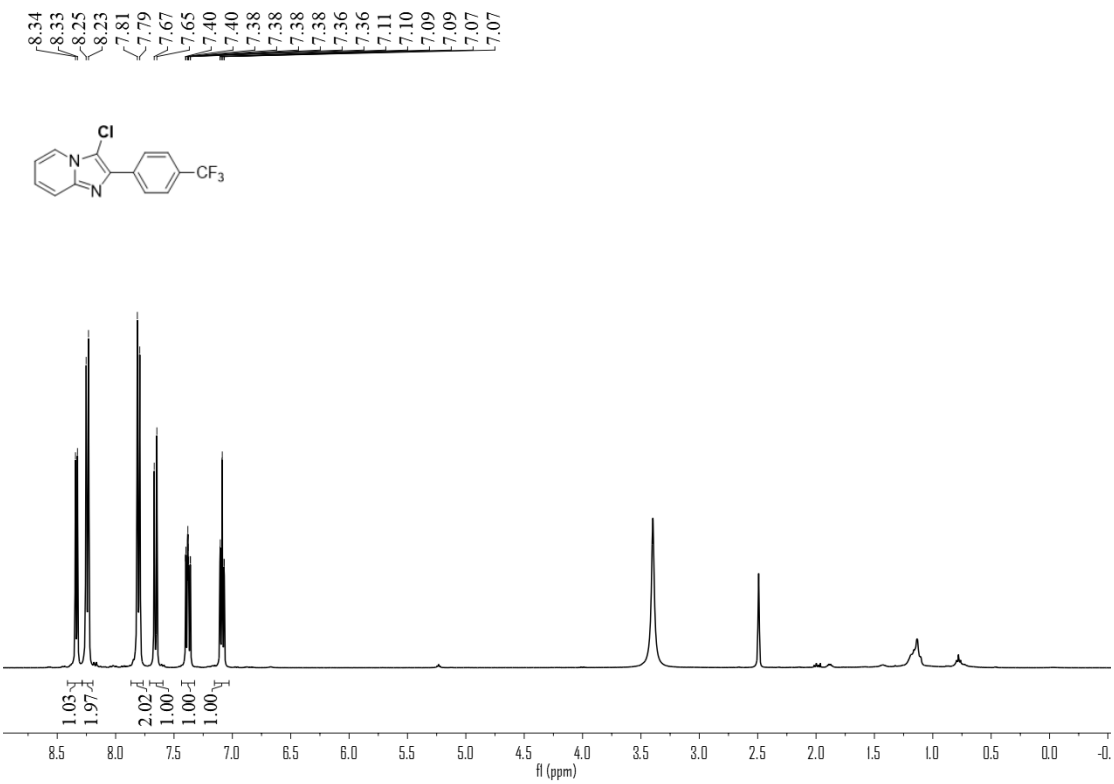

Figure S15. ^{13}C NMR (100 MHz, $CDCl_3$) spectrum of compound **3g**, related to **Figure 1**

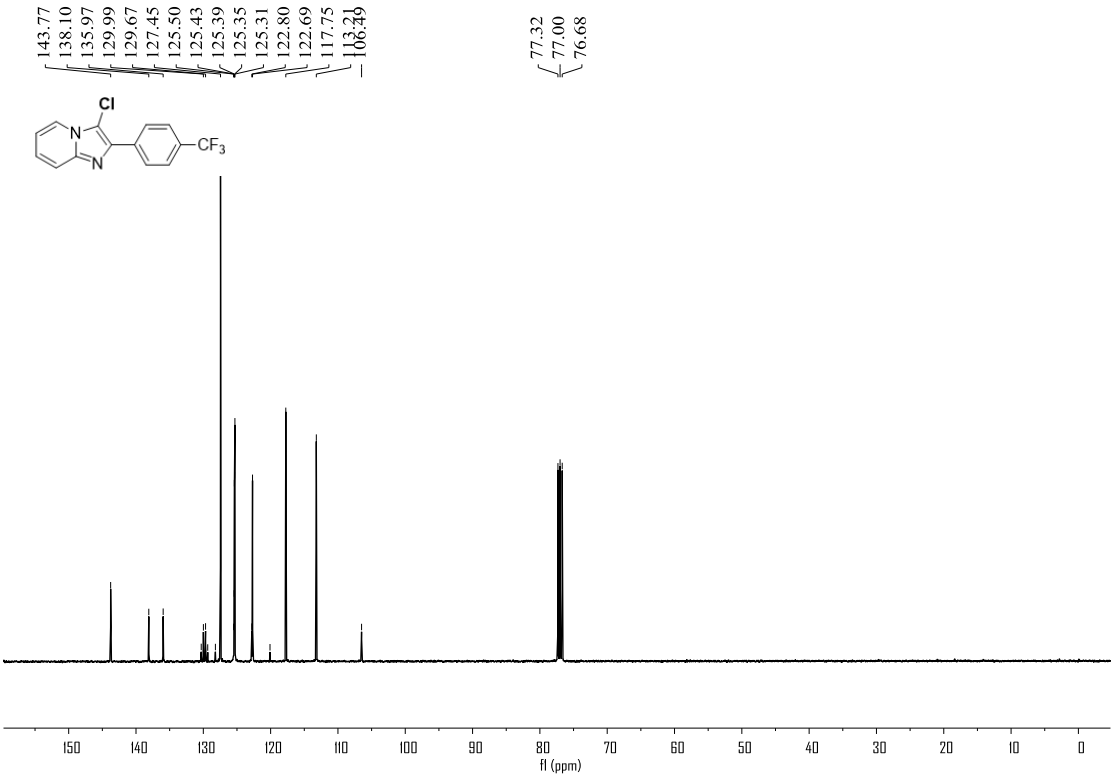

Figure S16. ^{19}F NMR (376 MHz, $CDCl_3$) spectrum of compound **3g**, related to **Figure 1**

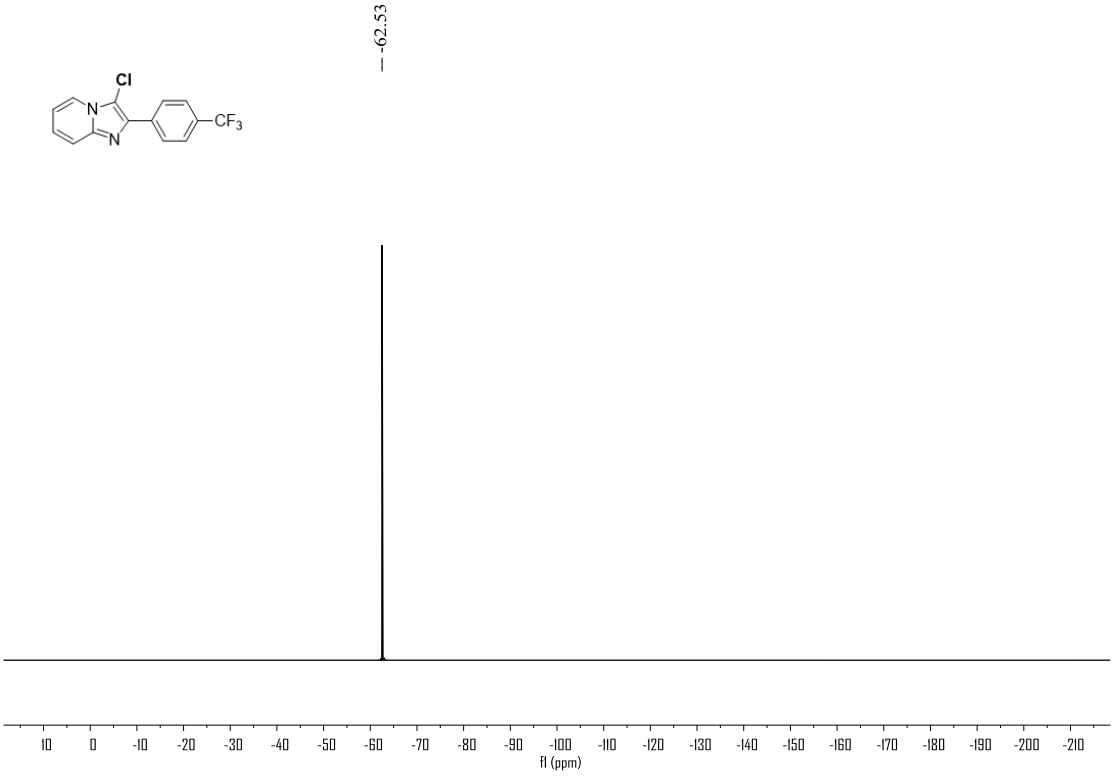

Figure S17. ^{1}H NMR (400 MHz, $CDCl_3$) spectrum of compound **3h**, related to **Figure 1**

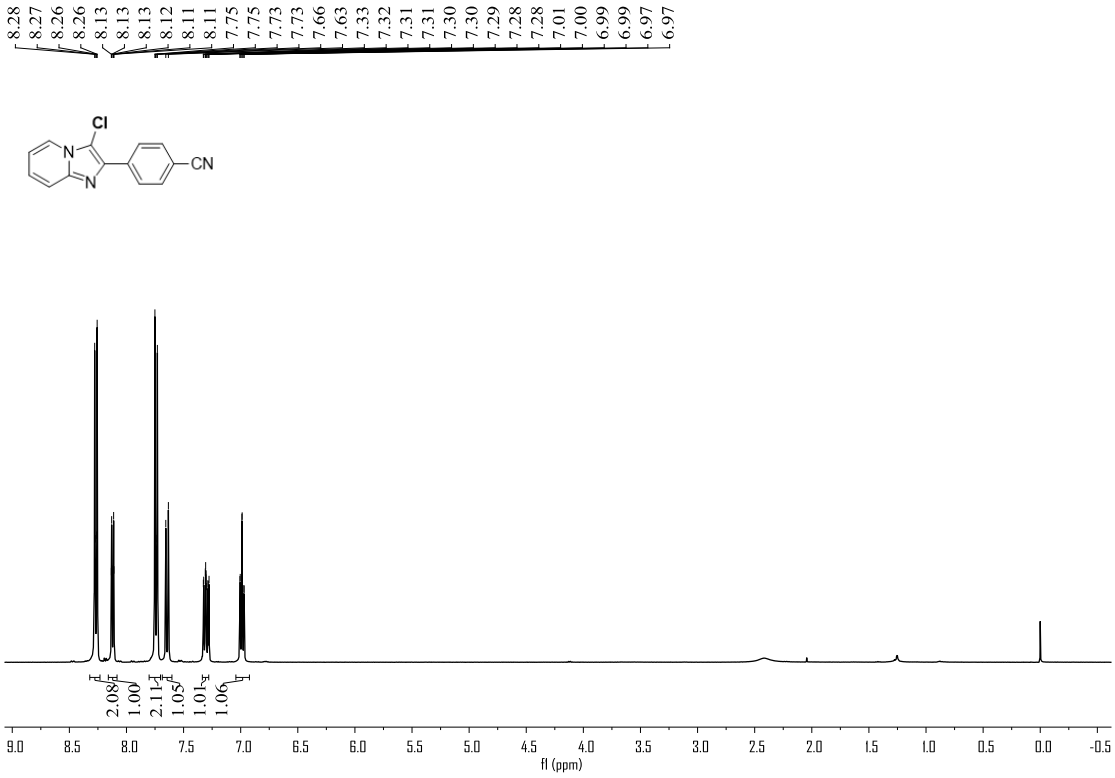

Figure S18. ^{13}C NMR (100 MHz, $CDCl_3$) spectrum of compound **3h**, related to **Figure 1**

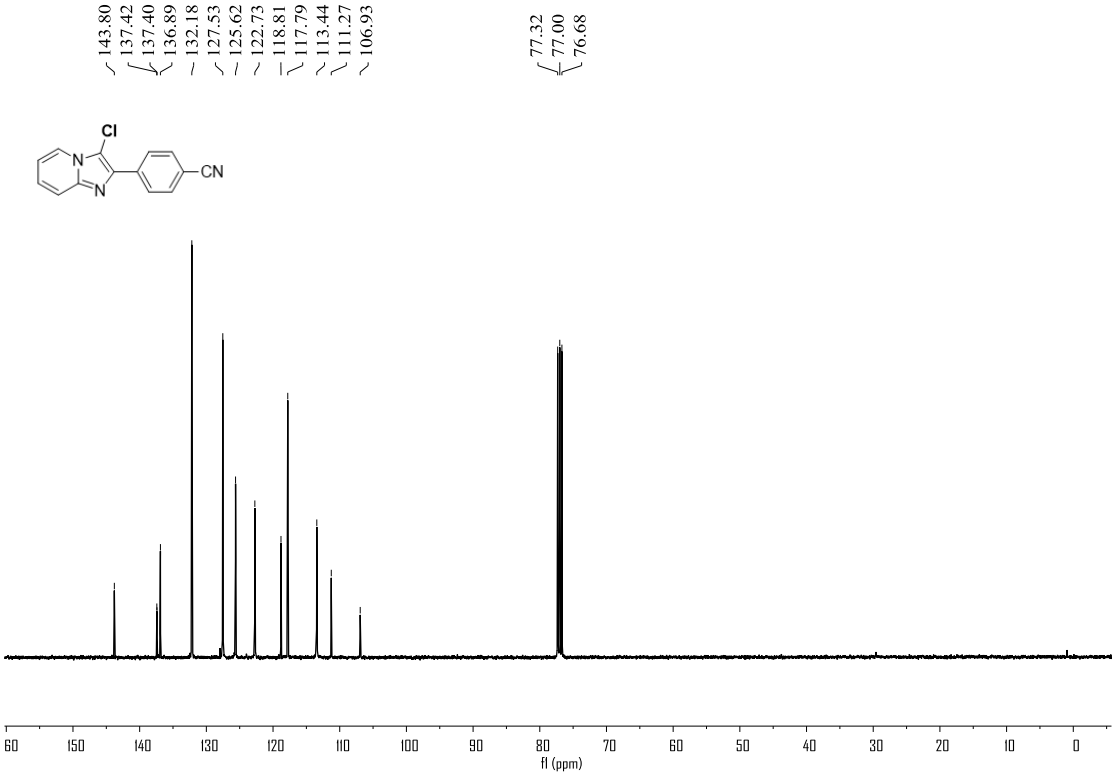

Figure S19. ^{1}H NMR (400 MHz, $CDCl_3$) spectrum of compound **3i**, related to **Figure 1**

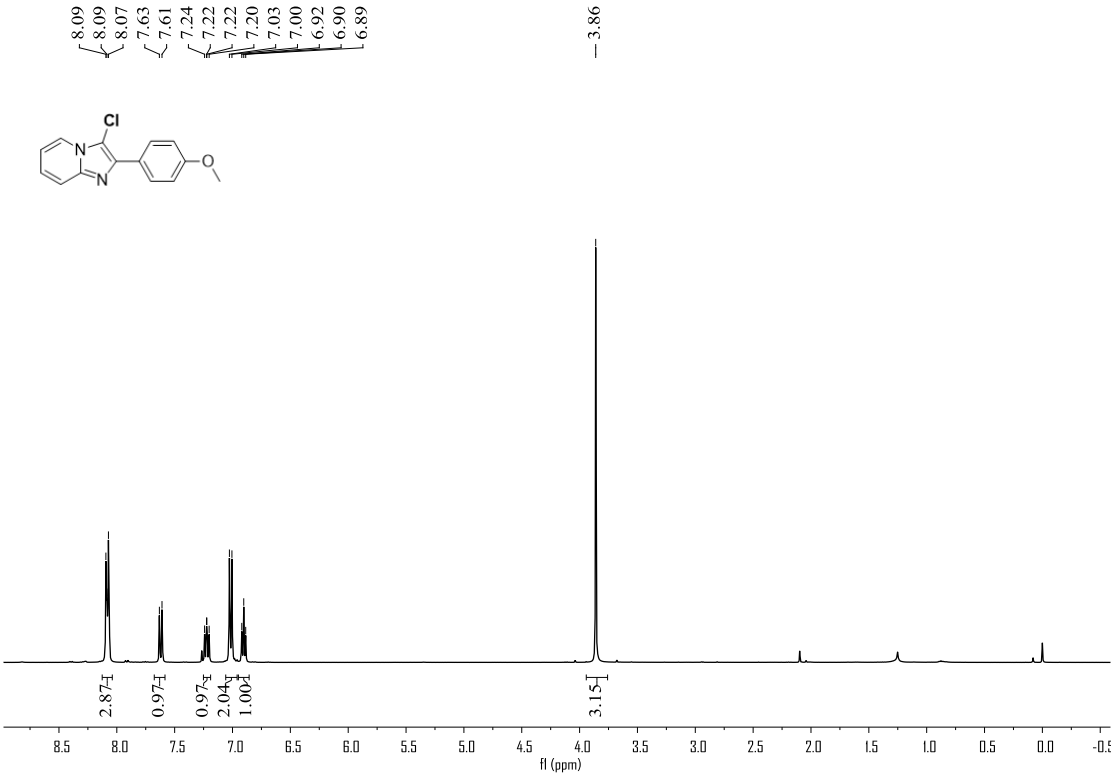

Figure S20. ^{13}C NMR (100 MHz, $CDCl_3$) spectrum of compound **3i**, related to **Figure 1**

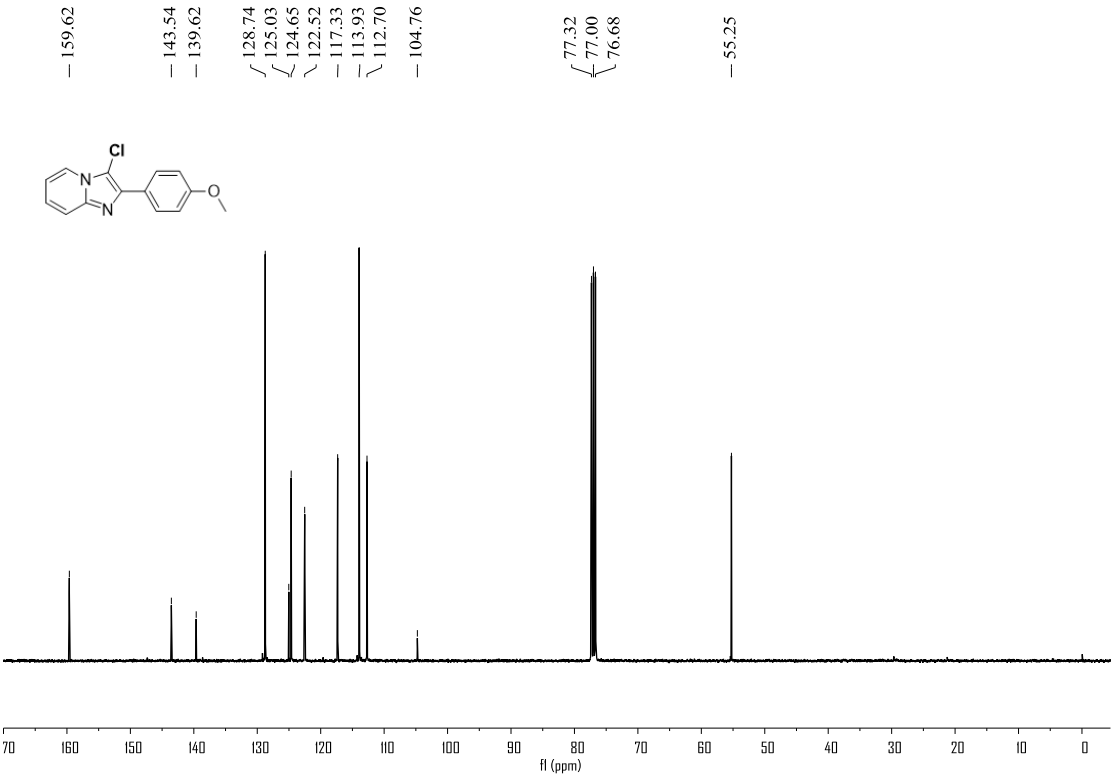

Figure S21. ^{1}H NMR (400 MHz, $CDCl_3$) spectrum of compound **3j**, related to **Figure 1**

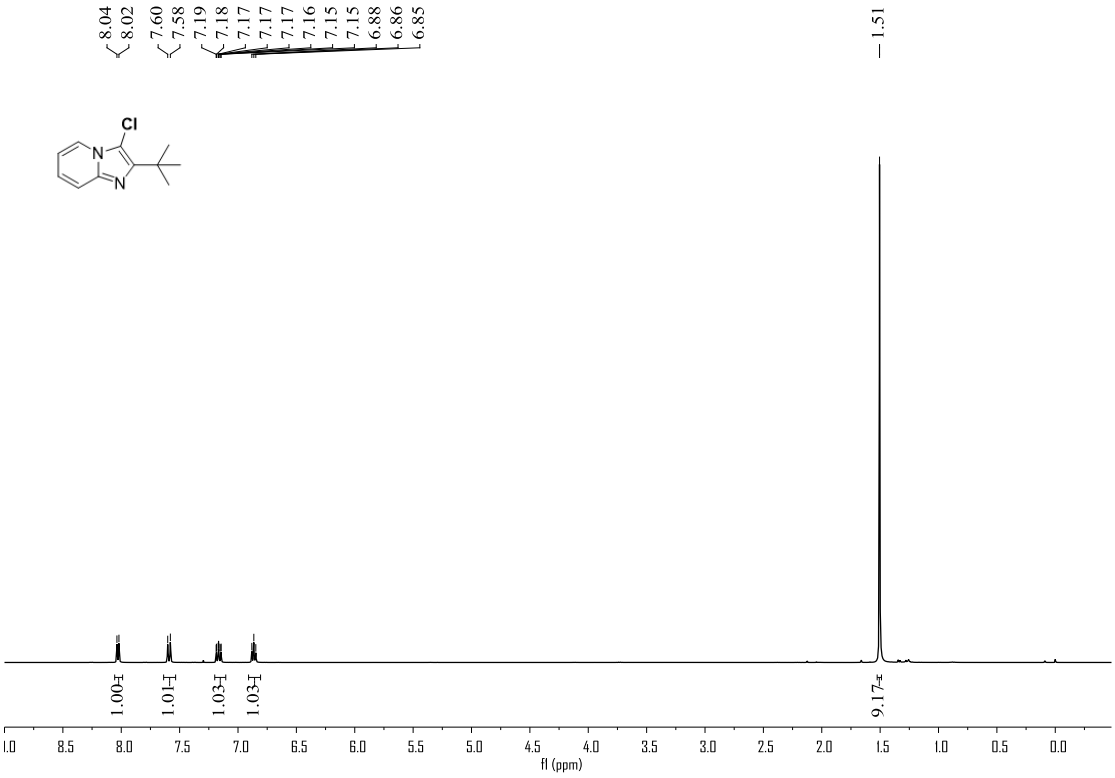

Figure S22. ^{13}C NMR (100 MHz, $CDCl_3$) spectrum of compound **3j**, related to **Figure 1**

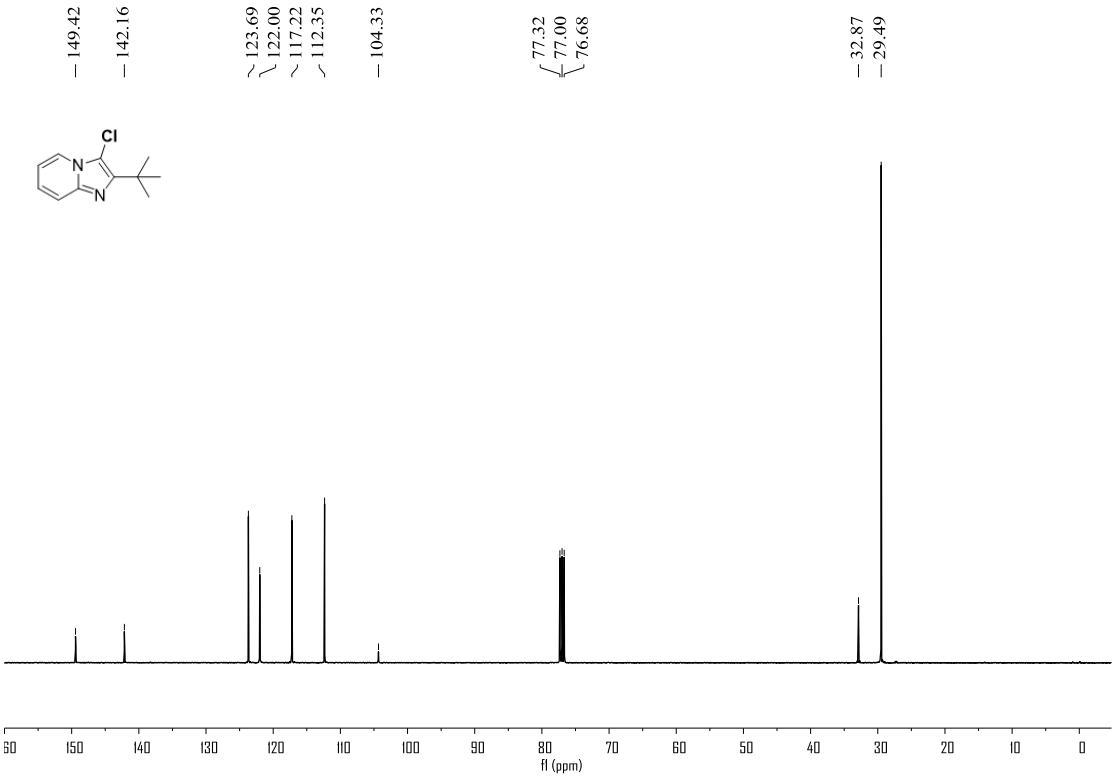

Figure S23. ^{1}H NMR (400 MHz, DMSO-d_6) spectrum of compound **3k**, related to **Figure 1**

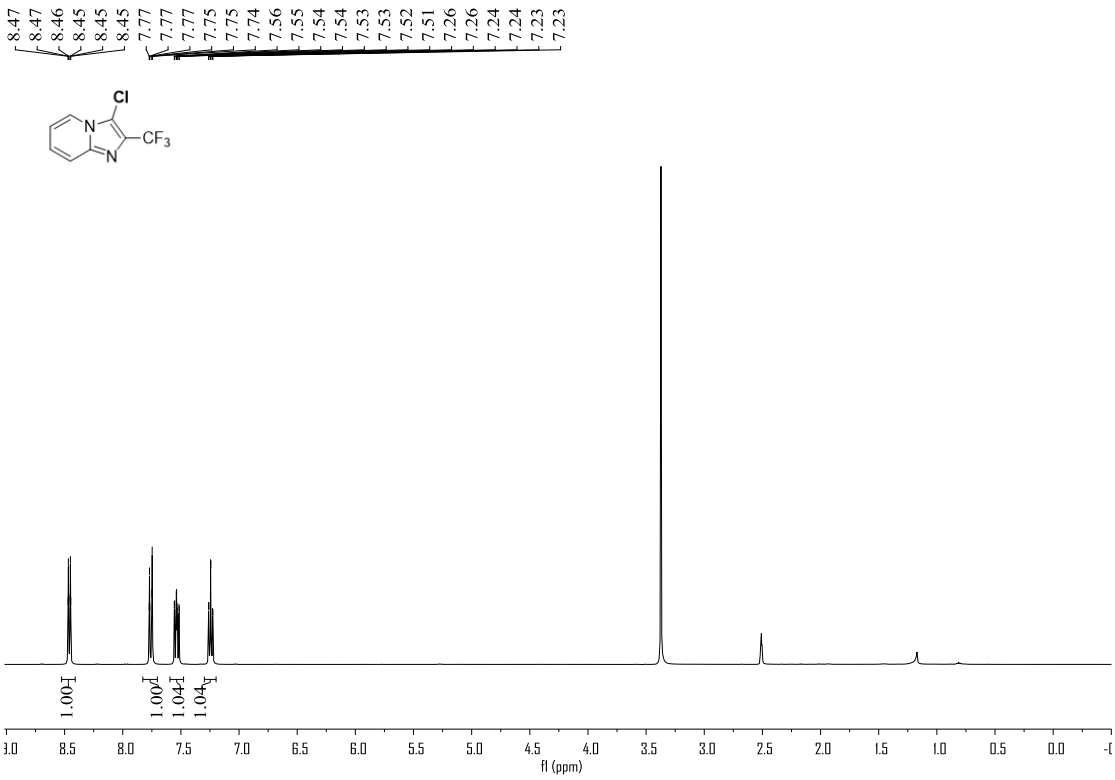

Figure S24. ^{13}C NMR (100 MHz, $CDCl_3$) spectrum of compound **3k**, related to **Figure 1**

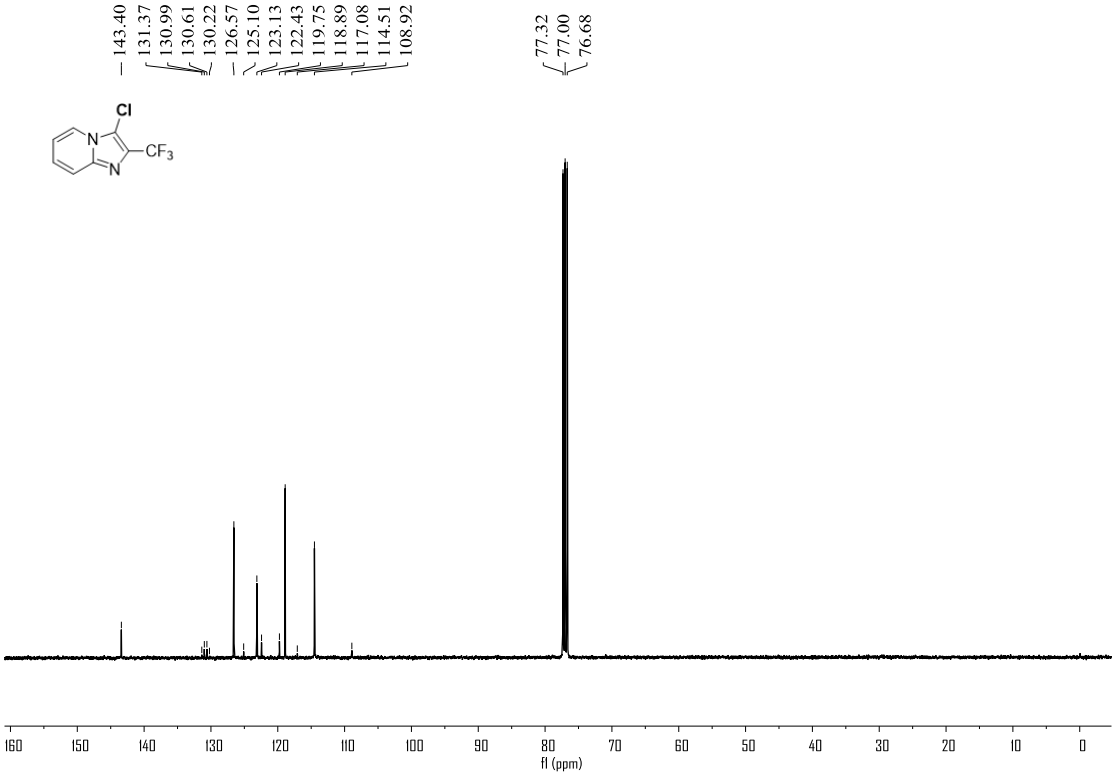

Figure S25. ^{19}F NMR (376 MHz, $CDCl_3$) spectrum of compound **3k**, related to **Figure 1**

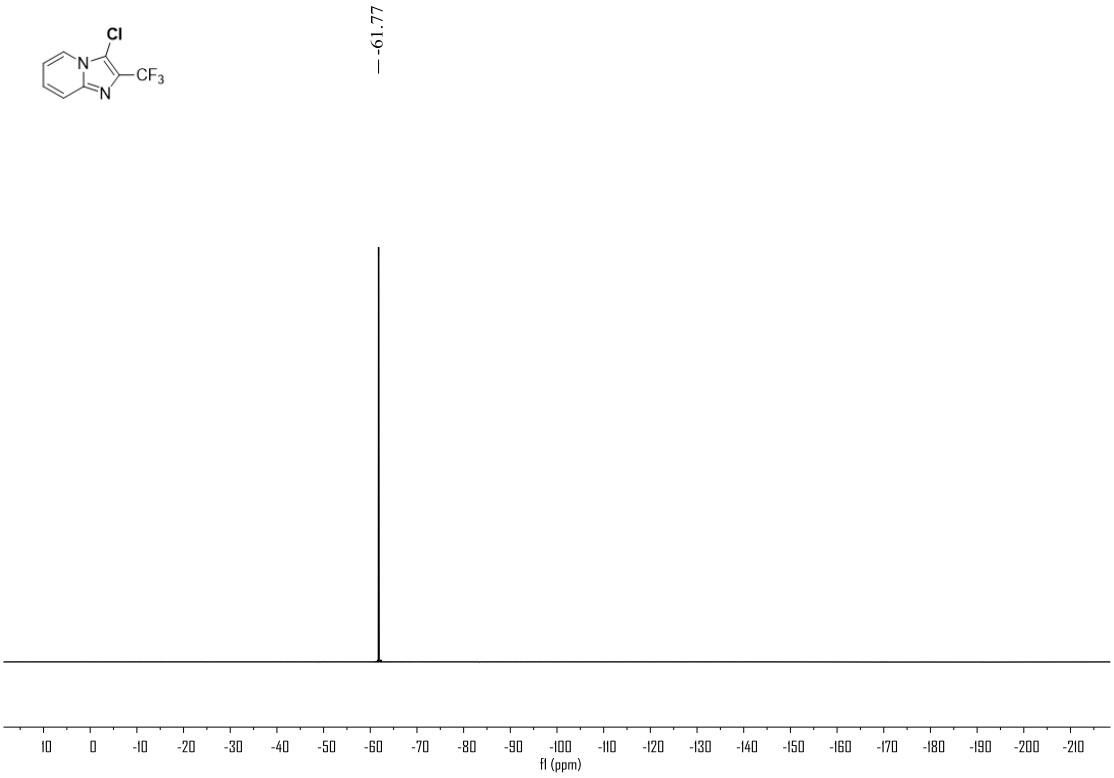

Figure S26. ^{1}H NMR (400 MHz, $CDCl_3$) spectrum of compound **3l**, related to **Figure 1**

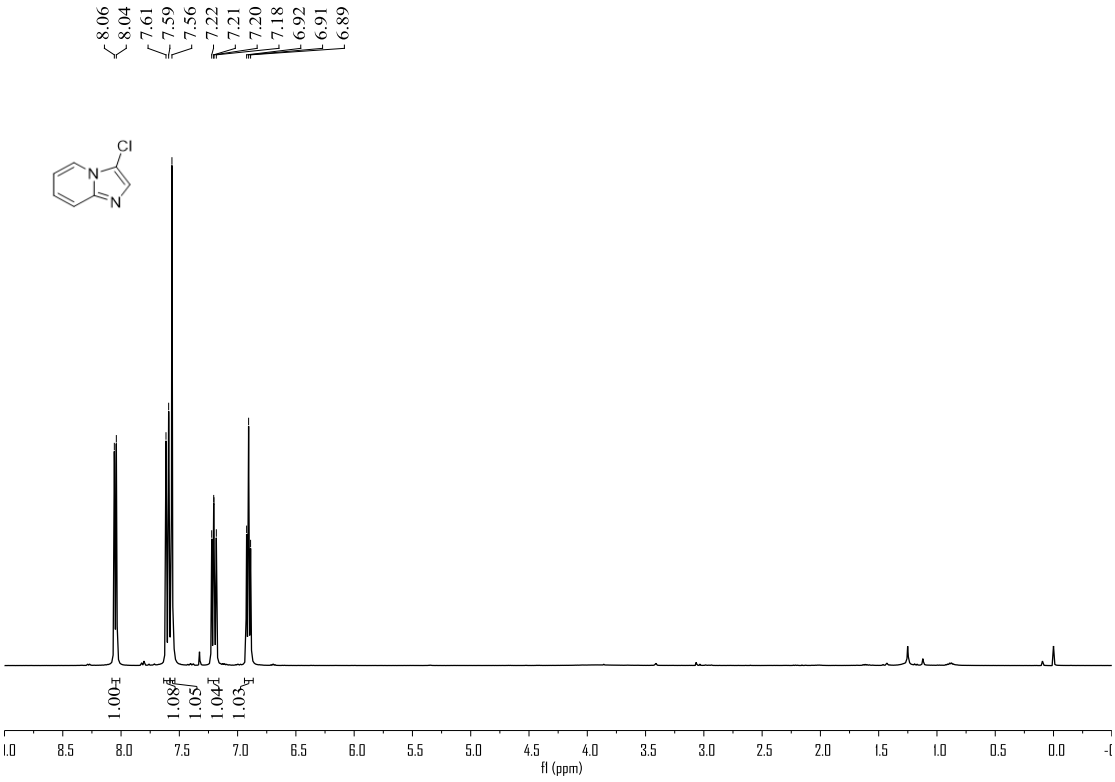

Figure S27. ^{13}C NMR (100 MHz, $CDCl_3$) spectrum of compound **3l**, related to **Figure 1**

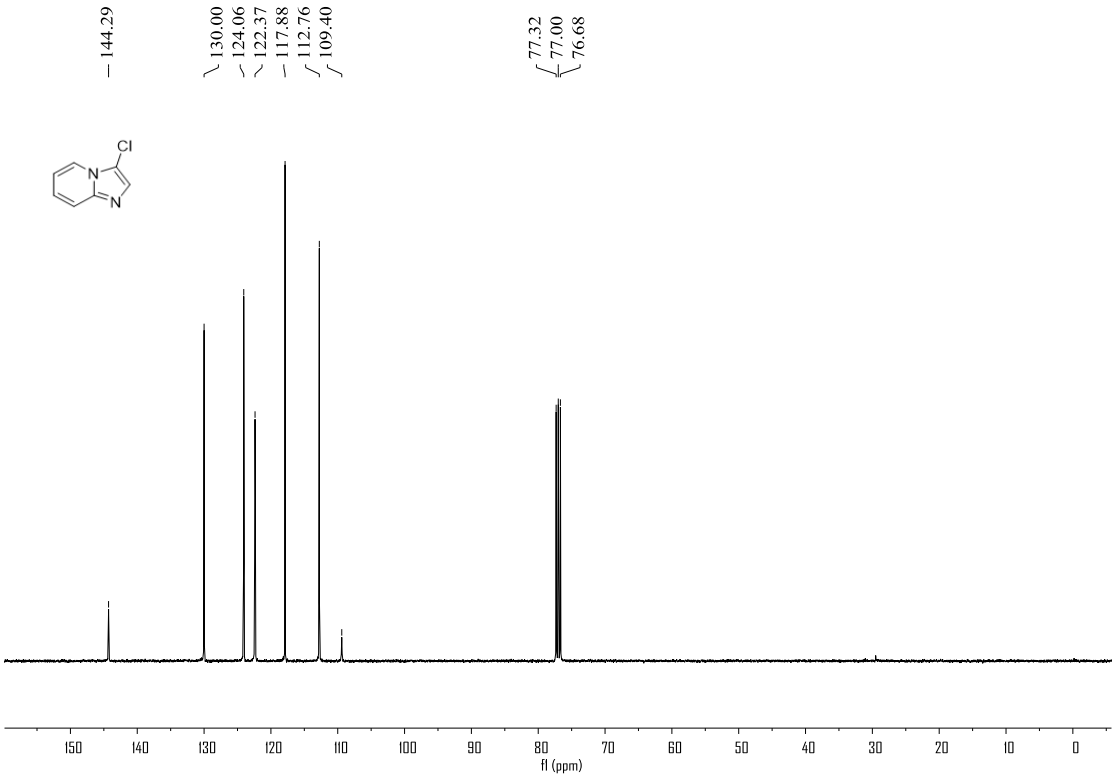

Figure S28. ^{1}H NMR (400 MHz, $CDCl_3$) spectrum of compound **3m**, related to **Figure 1**

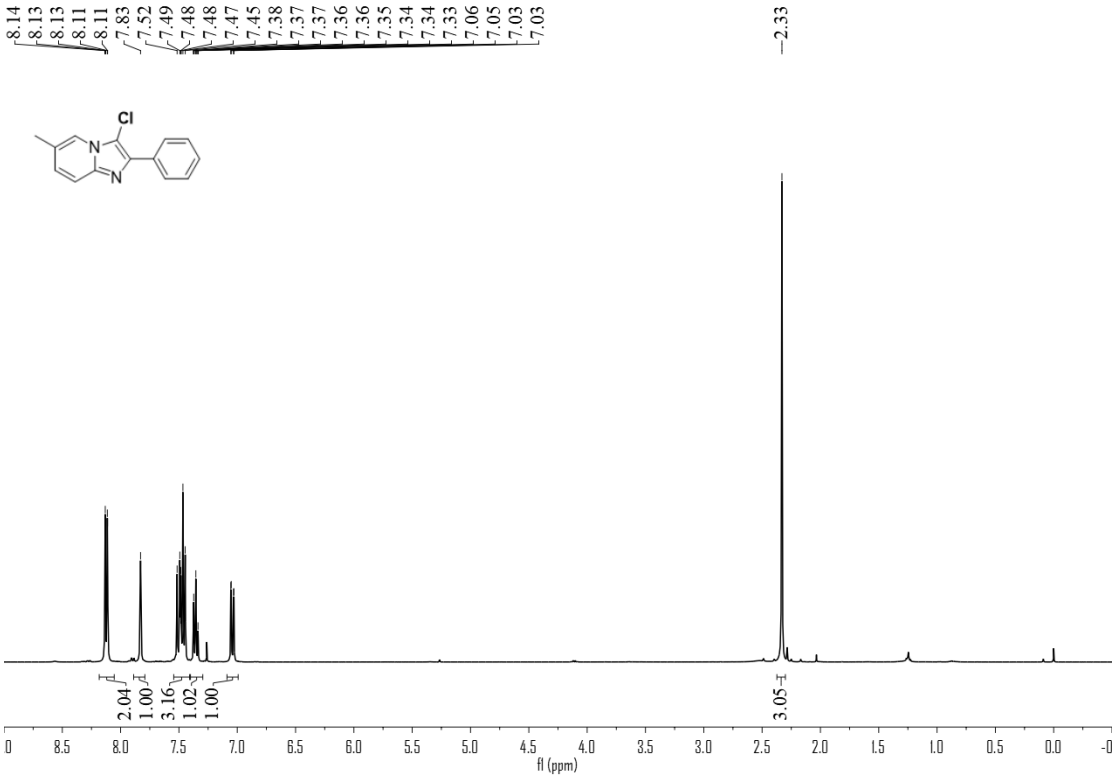

Figure S29. ^{13}C NMR (100 MHz, $CDCl_3$) spectrum of compound **3m**, related to **Figure 1**

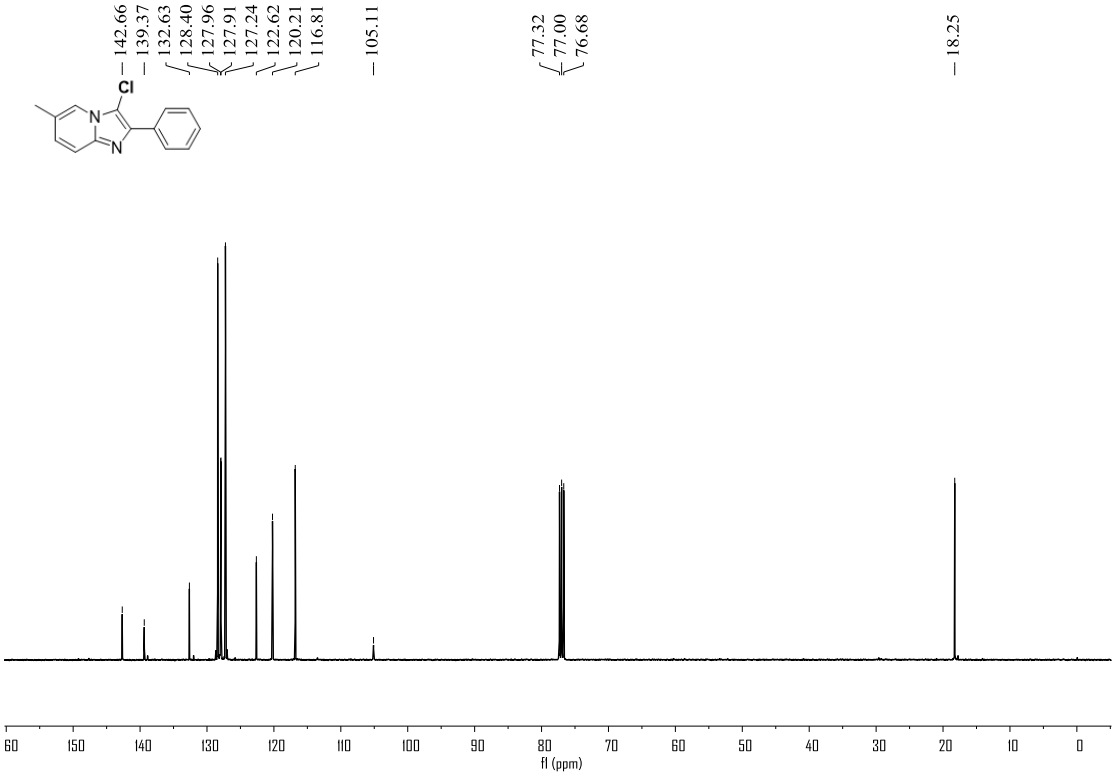

Figure S30. ^{1}H NMR (400 MHz, DMSO-d_6) spectrum of compound **3n**, related to **Figure 1**

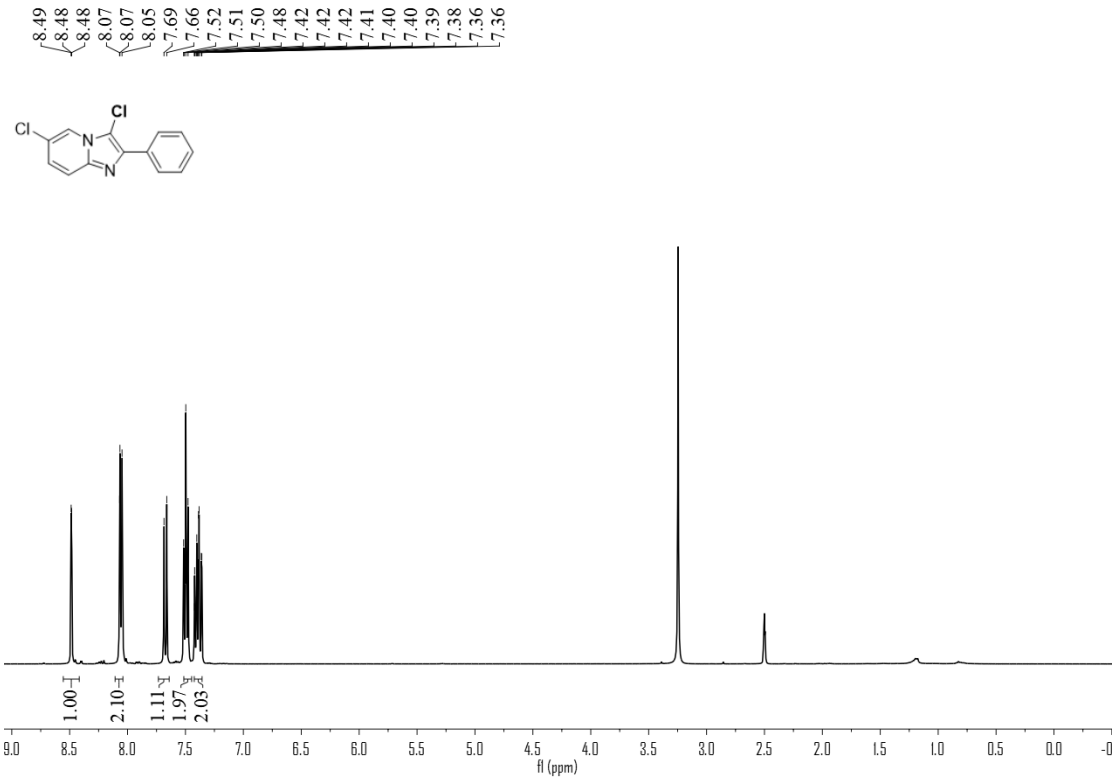

Figure S31. ^{13}C NMR (100 MHz, $CDCl_3$) spectrum of compound **3n**, related to **Figure 1**

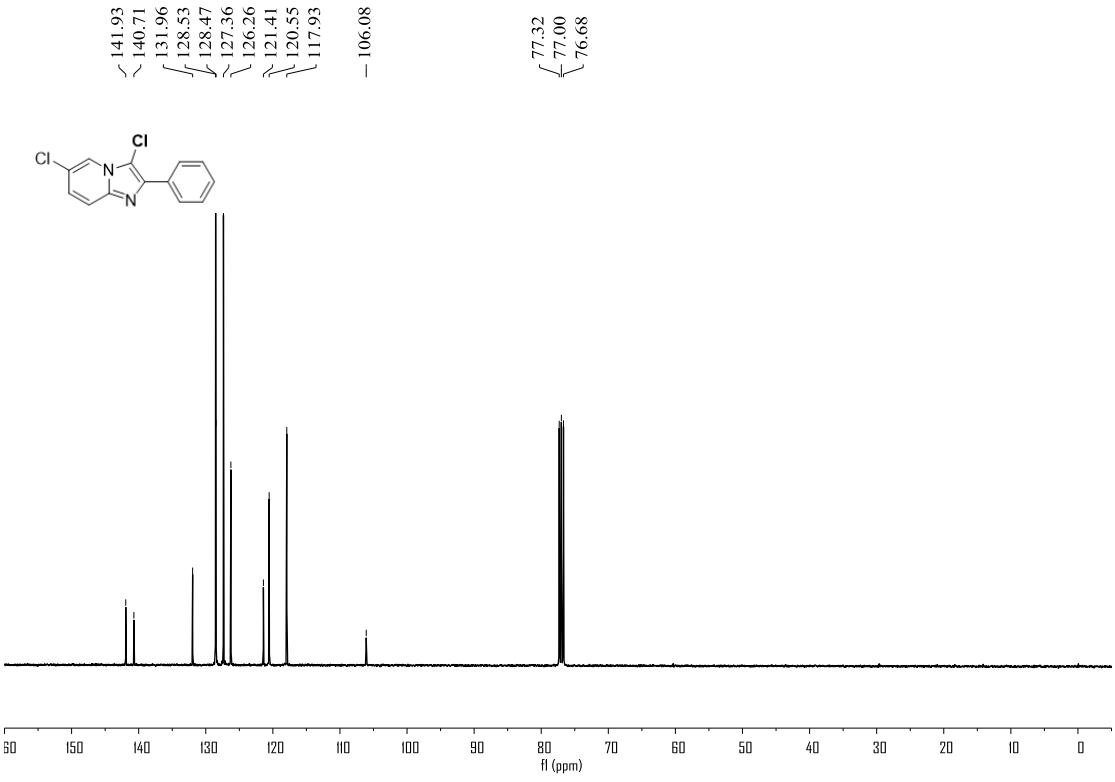

Figure S32. ^{1}H NMR (400 MHz, DMSO-d_6) spectrum of compound **3o**, related to **Figure 1**

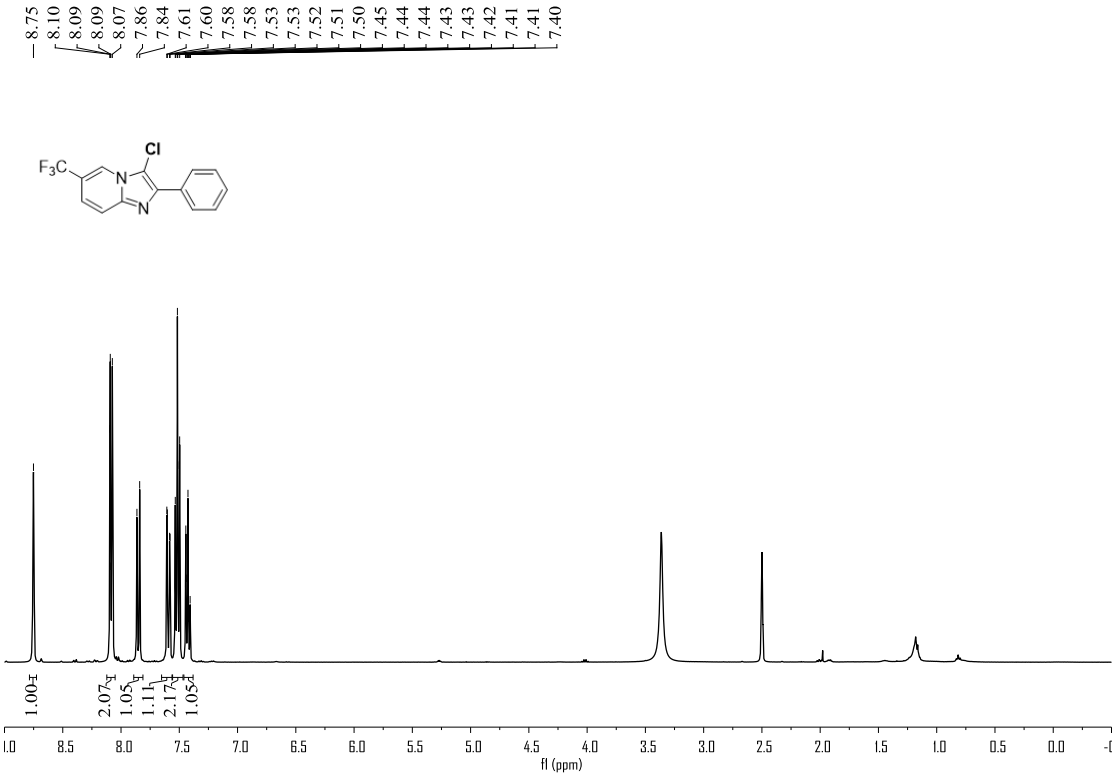

Figure S33. ^{13}C NMR (100 MHz, $CDCl_3$) spectrum of compound **3o**, related to **Figure 1**

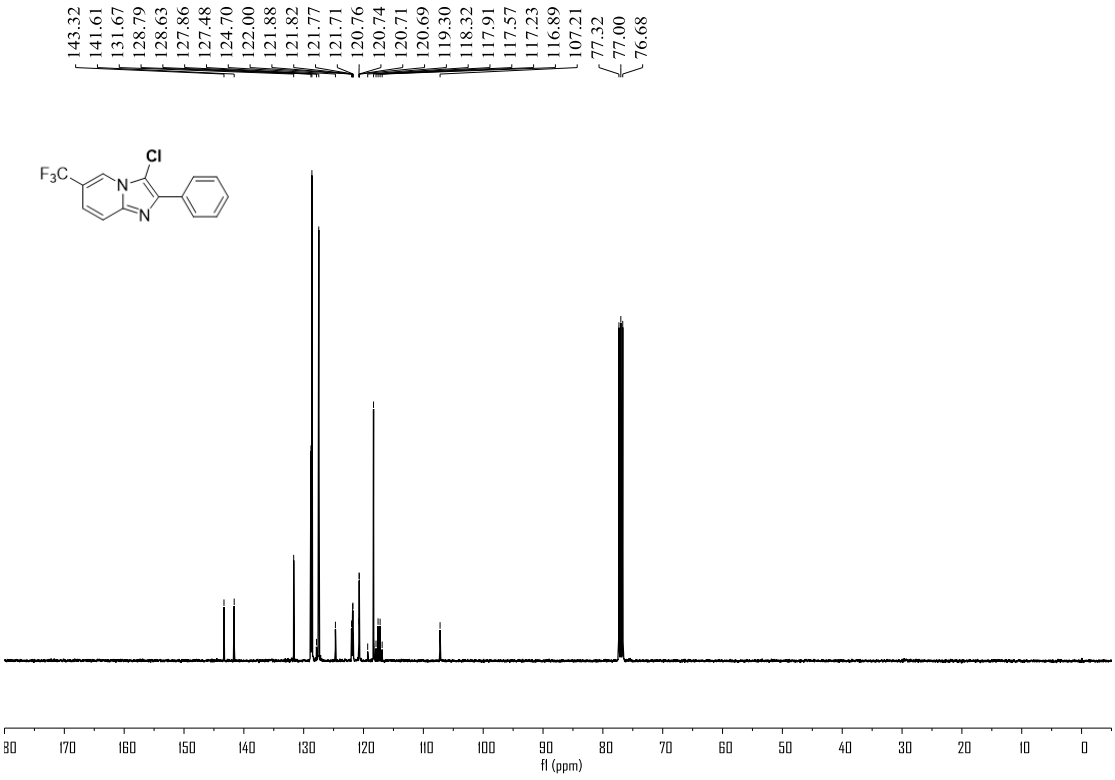

Figure S34. ^{19}F NMR (376 MHz, $CDCl_3$) spectrum of compound **3o**, related to **Figure 1**

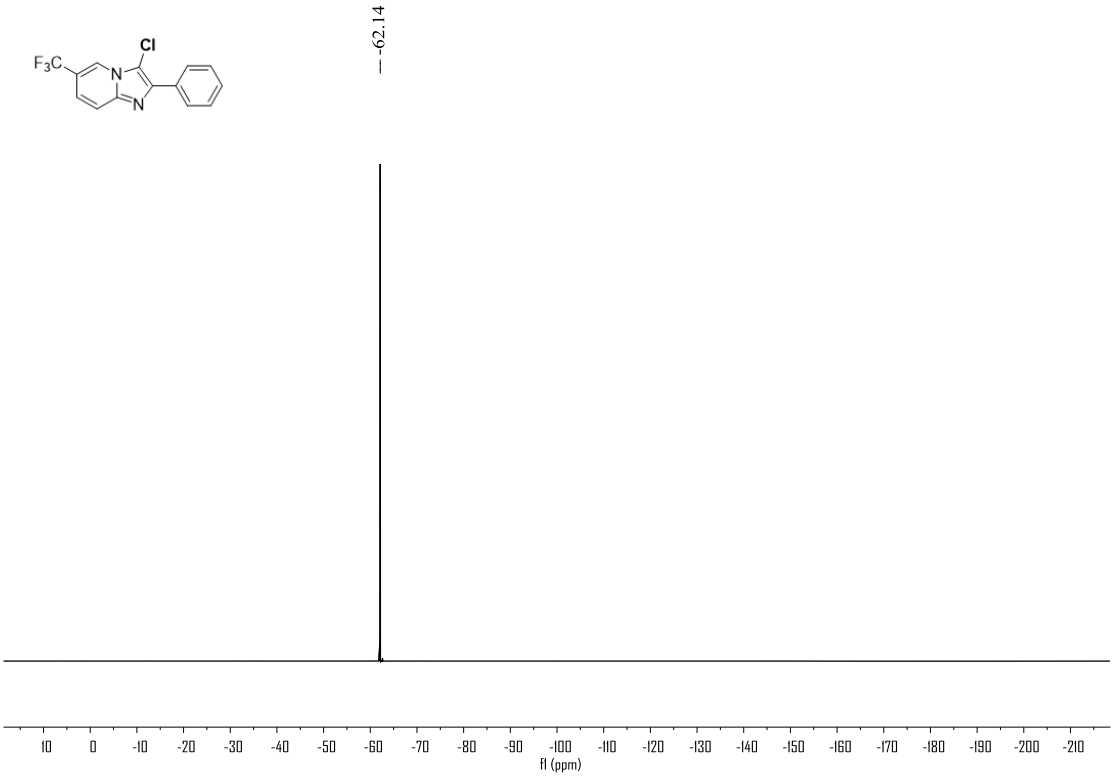

Figure S35. ^{1}H NMR (400 MHz, $CDCl_3$) spectrum of compound **3p**, related to **Figure 1**

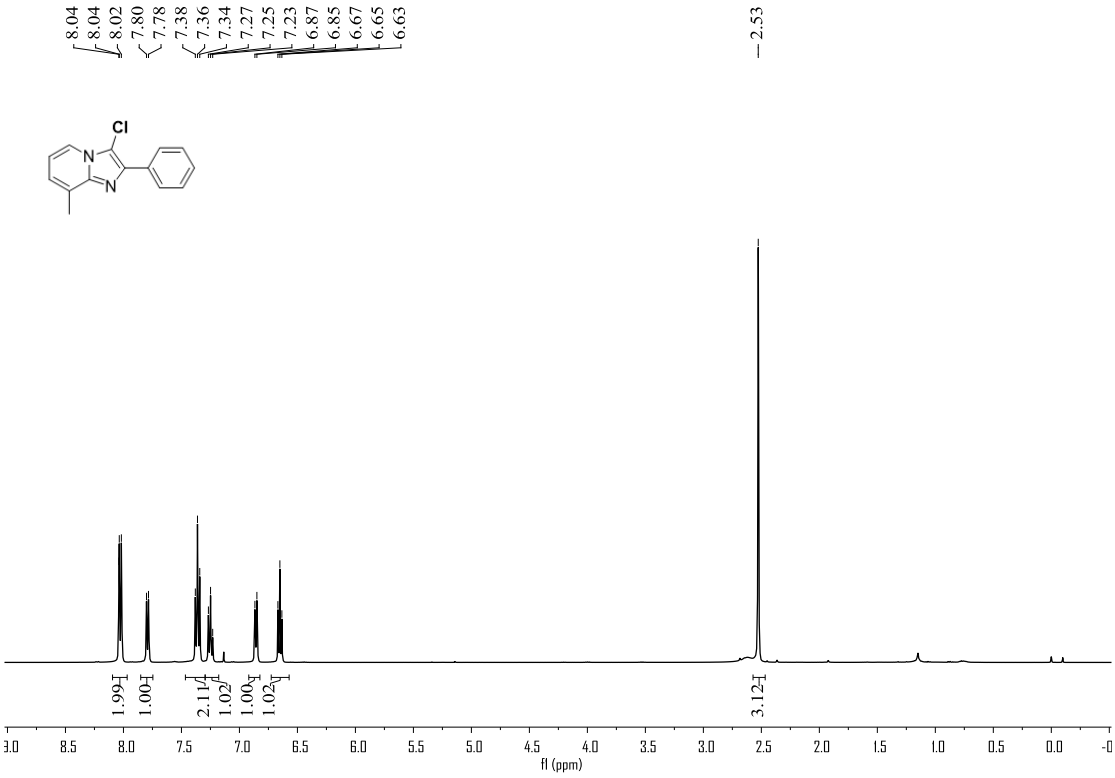

Figure S36. ^{13}C NMR (100 MHz, $CDCl_3$) spectrum of compound **3p**, related to **Figure 1**

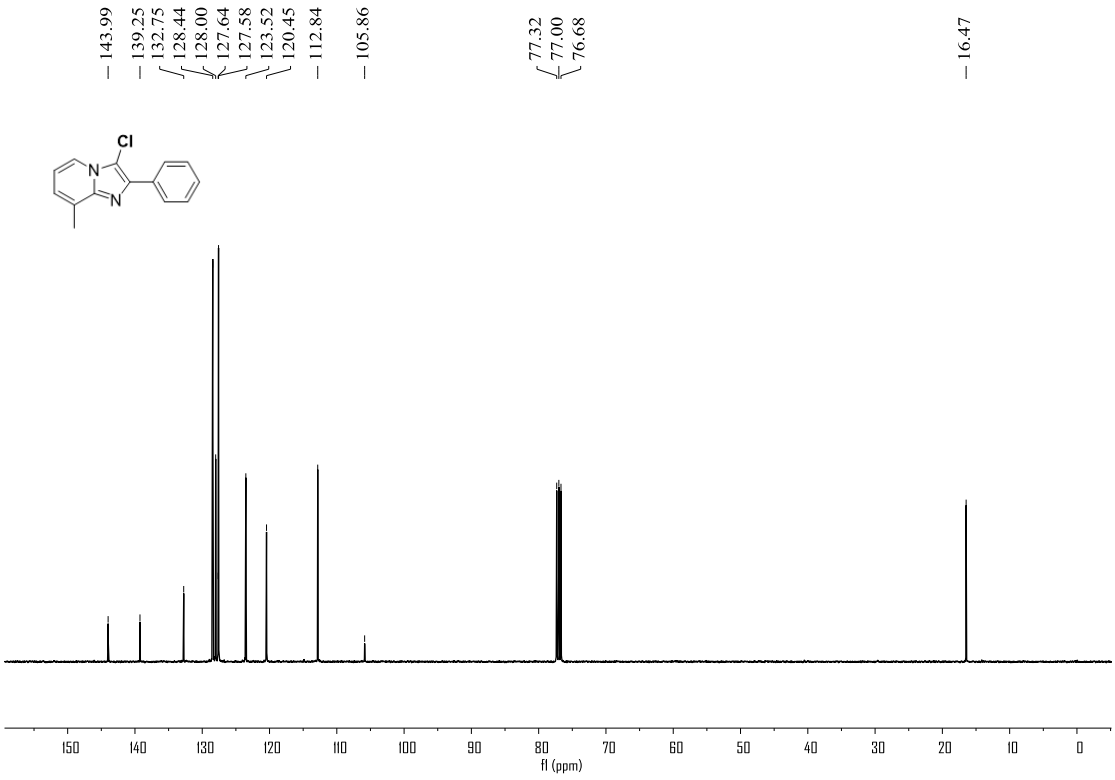

Figure S37. ^{1}H NMR (400 MHz, $CDCl_3$) spectrum of compound **3q**, related to **Figure 1**

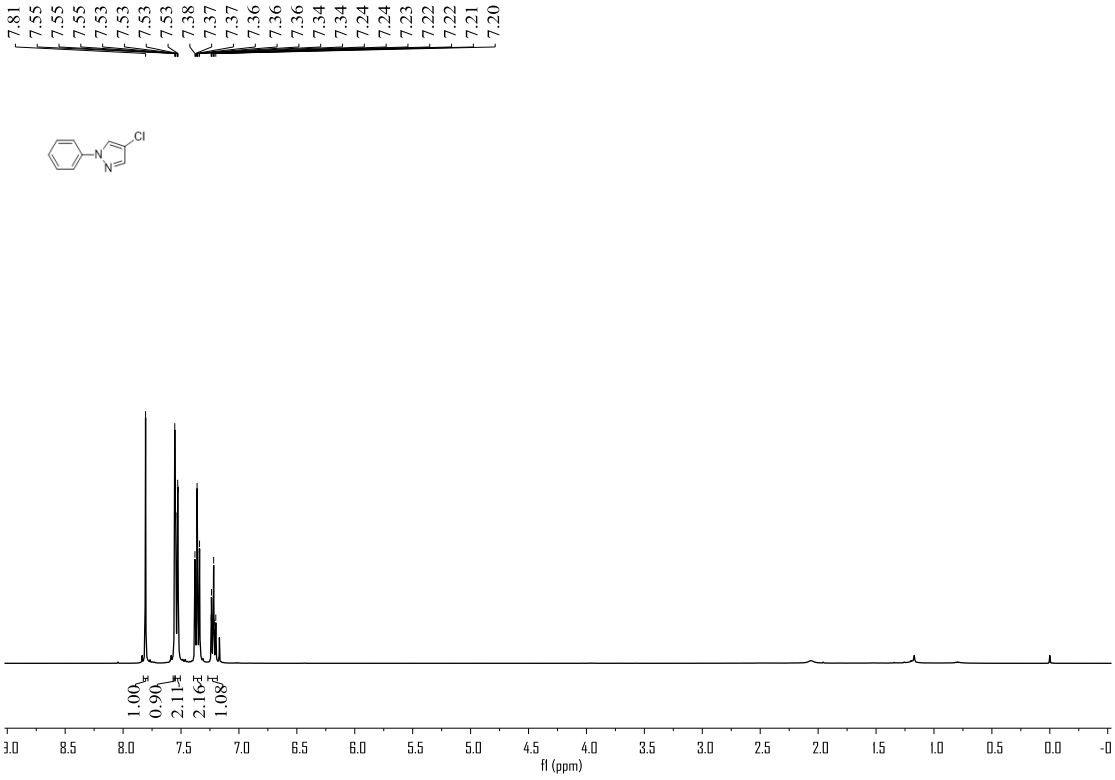

Figure S38. ^{13}C NMR (100 MHz, $CDCl_3$) spectrum of compound **3q**, related to **Figure 1**

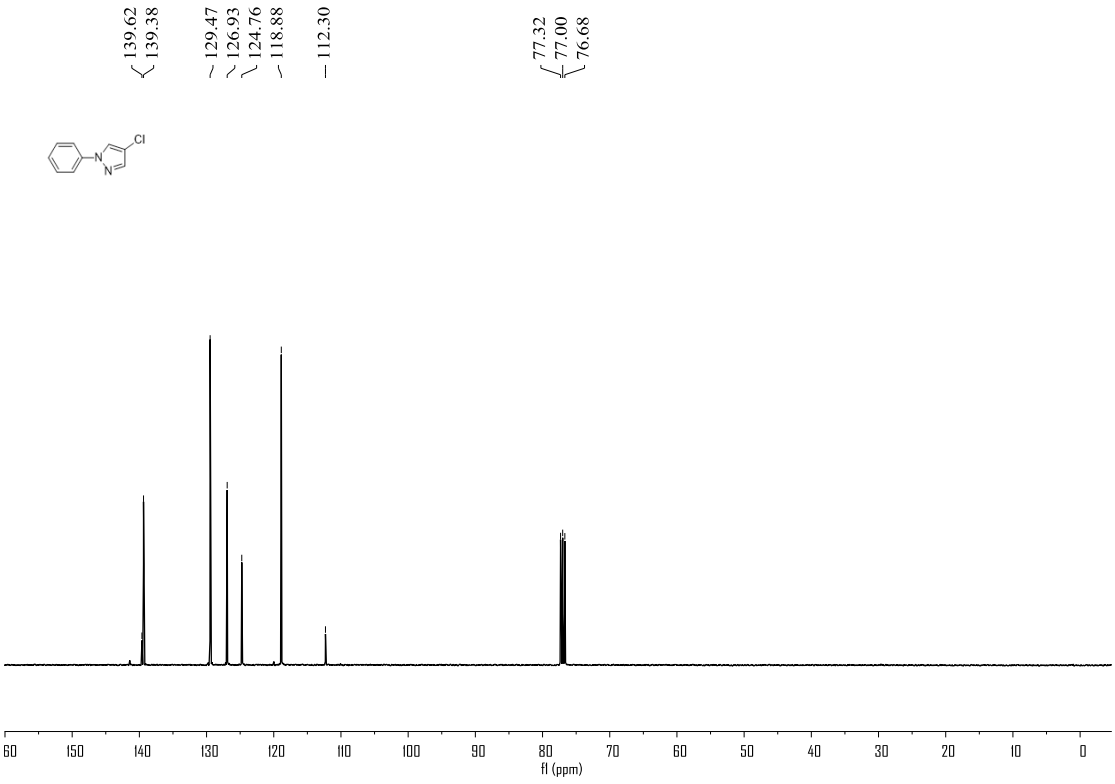

Figure S39. ^{1}H NMR (400 MHz, $CDCl_3$) spectrum of compound **3r**, related to **Figure 1**

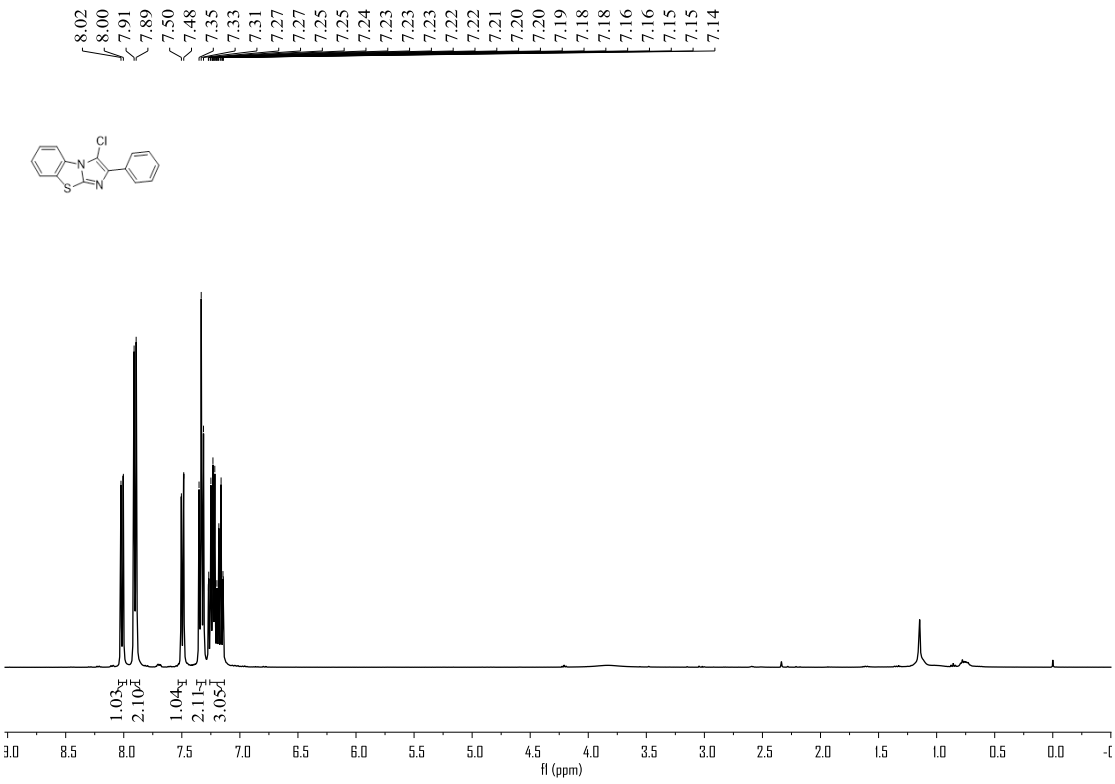

Figure S40. ^{13}C NMR (100 MHz, $CDCl_3$) spectrum of compound **3r**, related to **Figure 1**

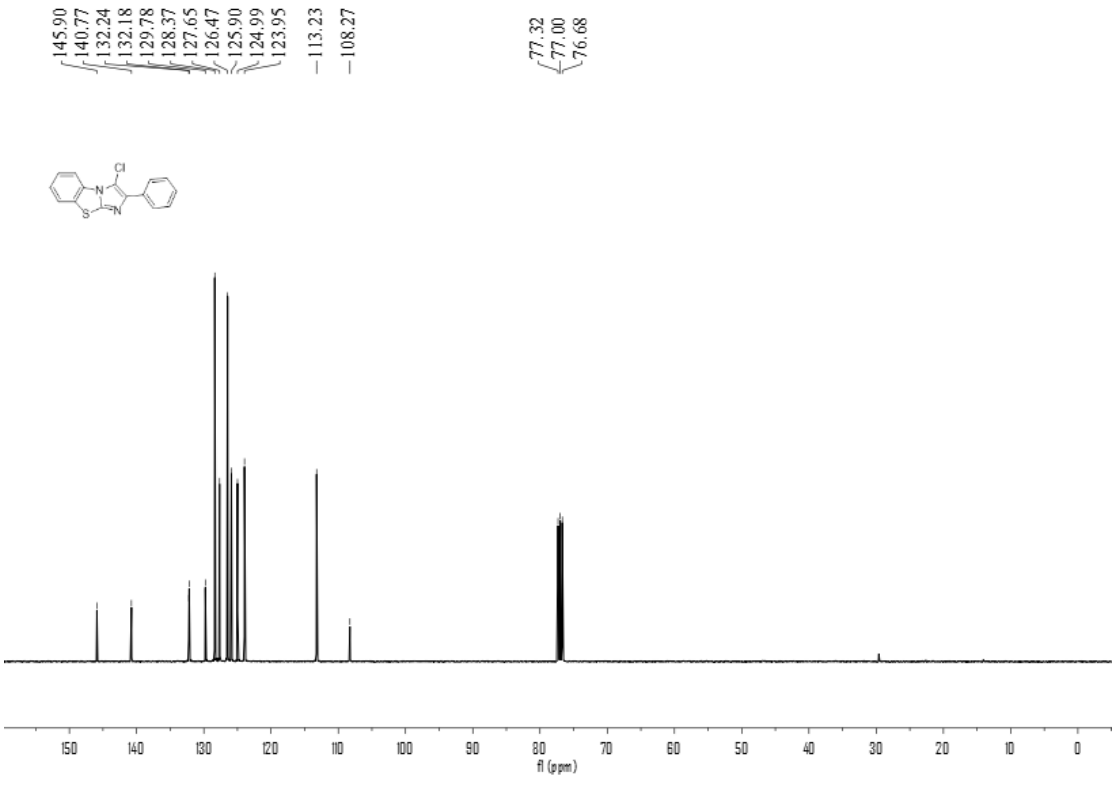

Figure S41. ^{1}H NMR (400 MHz, $CDCl_3$) spectrum of compound **3s**, related to **Figure 1**

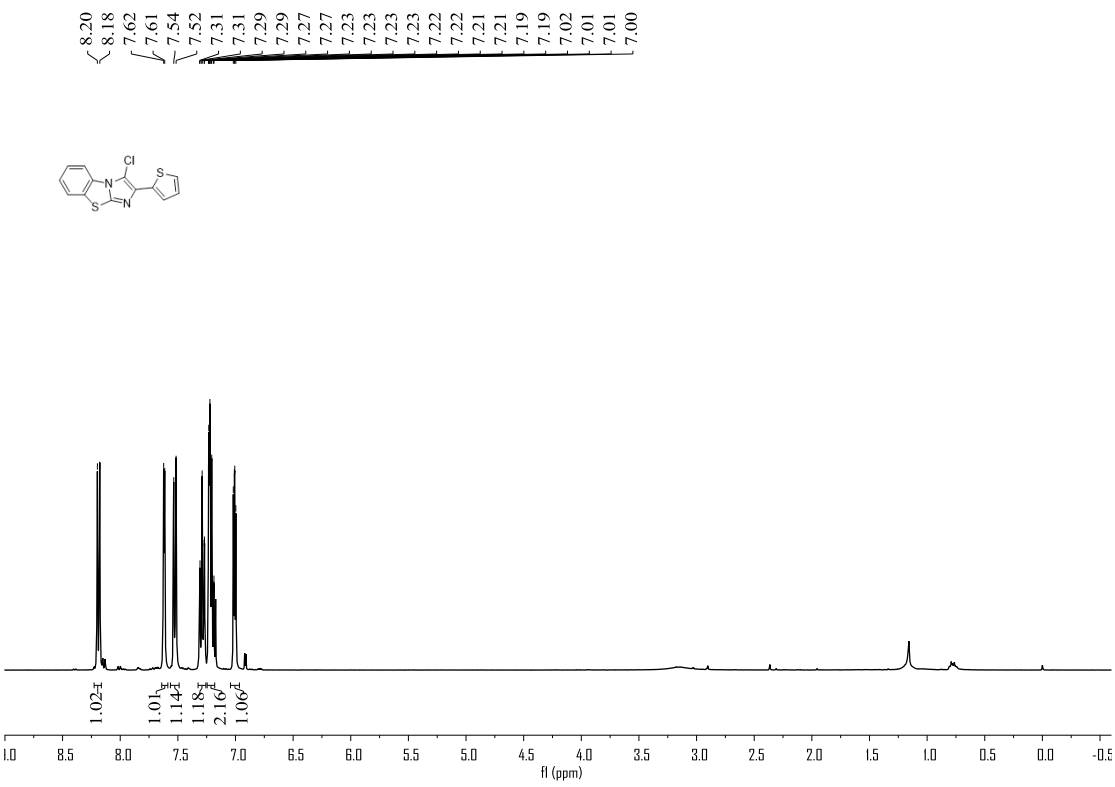

Figure S42. ^{13}C NMR (100 MHz, $CDCl_3$) spectrum of compound **3s**, related to **Figure 1**

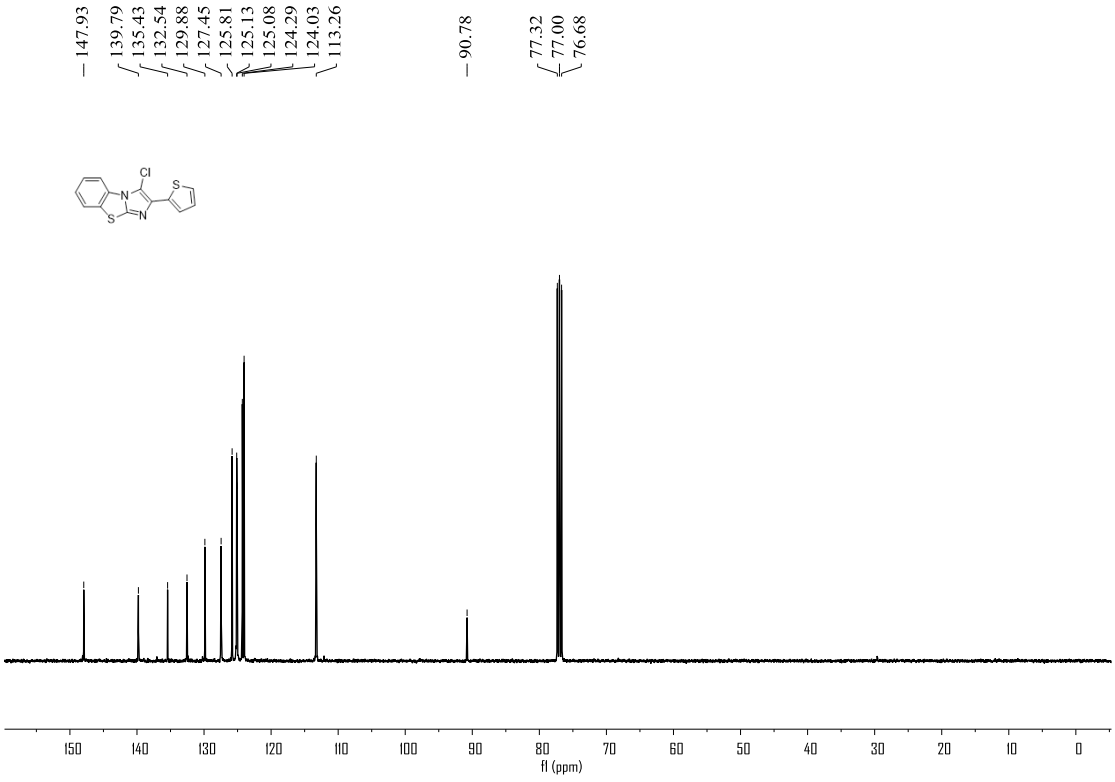

Figure S43. ^{1}H NMR (400 MHz, $CDCl_3$) spectrum of compound **3t**, related to **Figure 1**

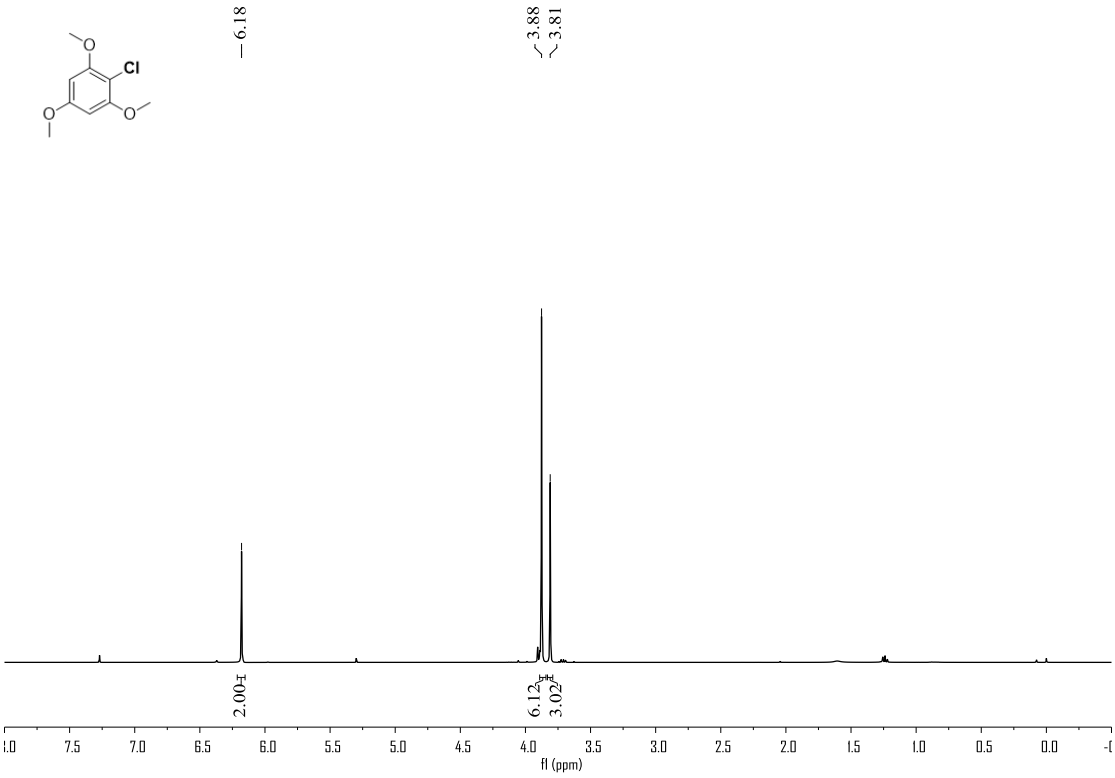

Figure S44. ^{13}C NMR (100 MHz, $CDCl_3$) spectrum of compound **3t**, related to **Figure 1**

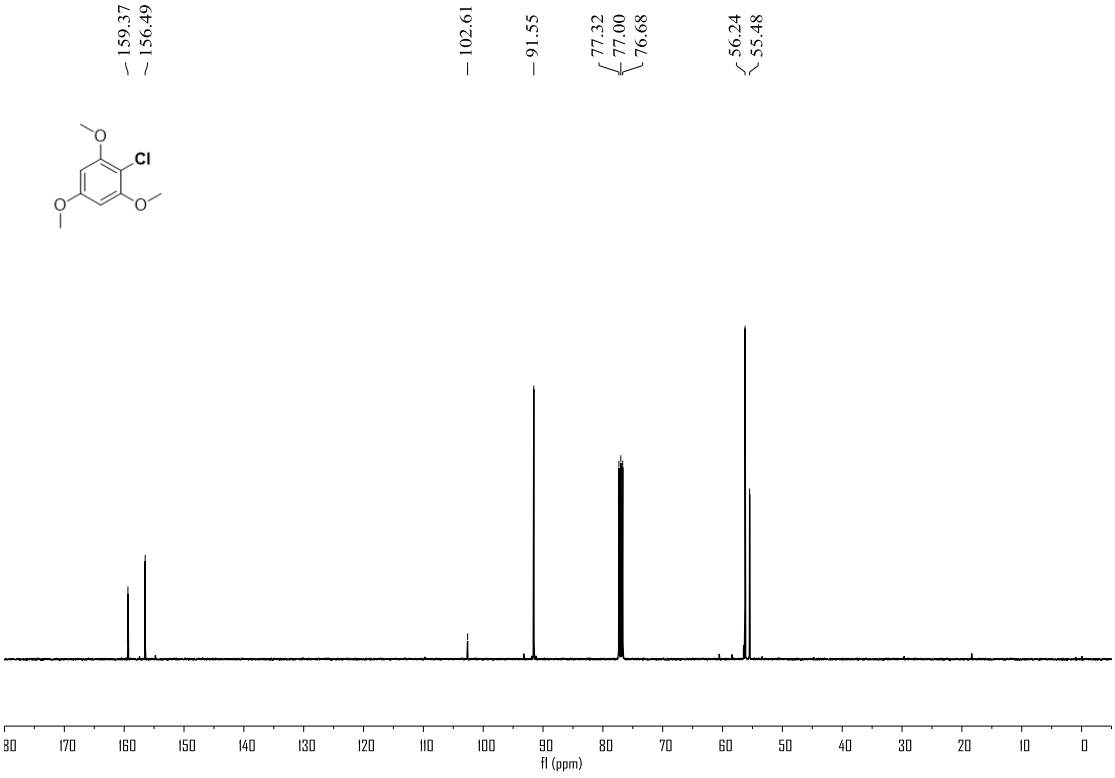

Figure S45. ^{1}H NMR (400 MHz, DMSO-d_6) spectrum of compound **4a**, related to **Figure 1**

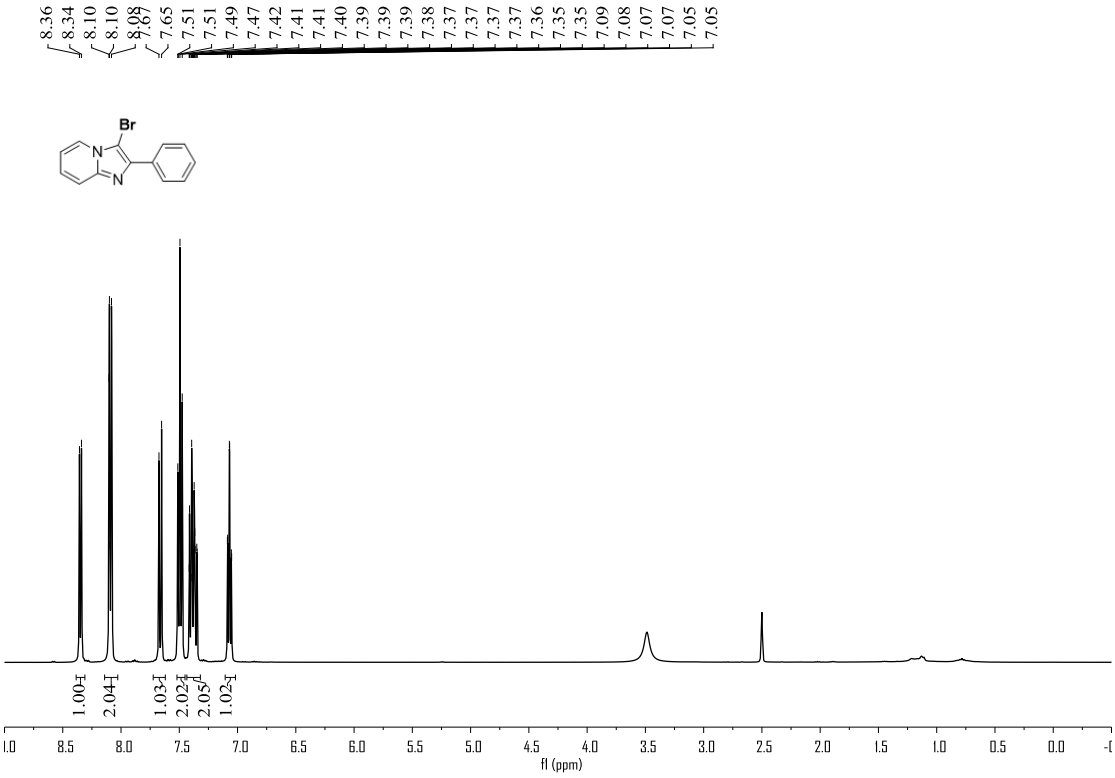

Figure S46. ^{13}C NMR (100 MHz, DMSO-d_6) spectrum of compound **4a**, related to **Figure 1**

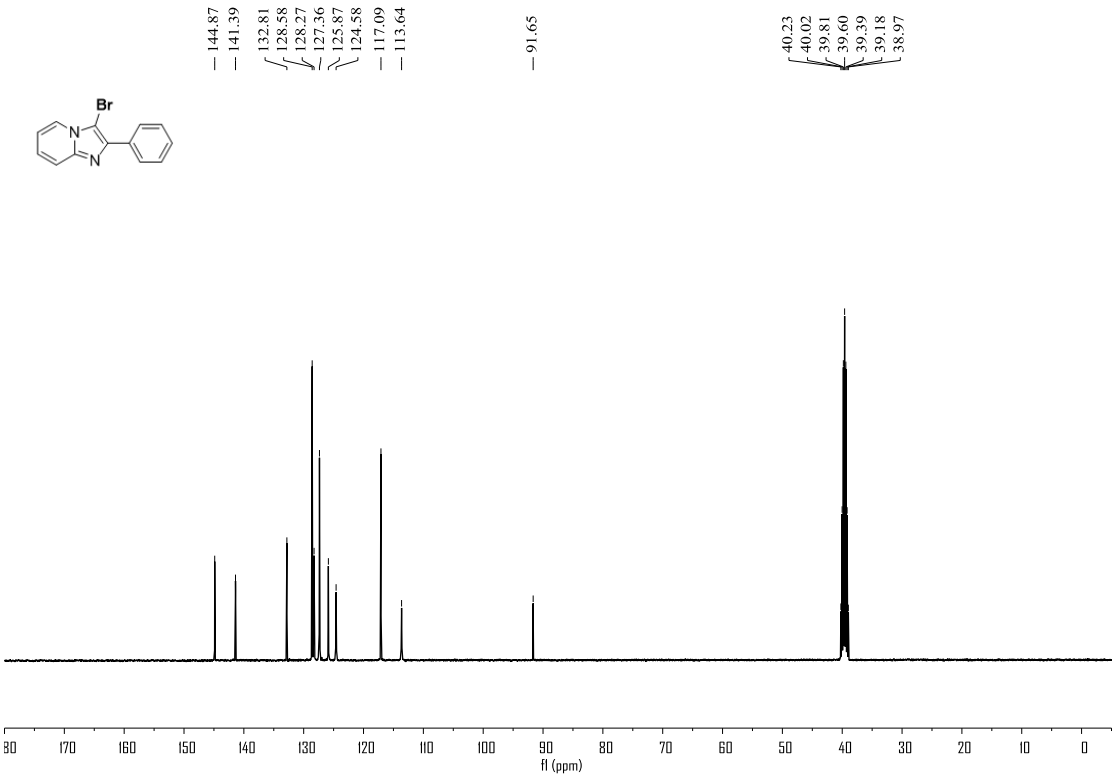

Figure S47. ^{1}H NMR (400 MHz, DMSO-d_6) spectrum of compound **4b**, related to **Figure 1**

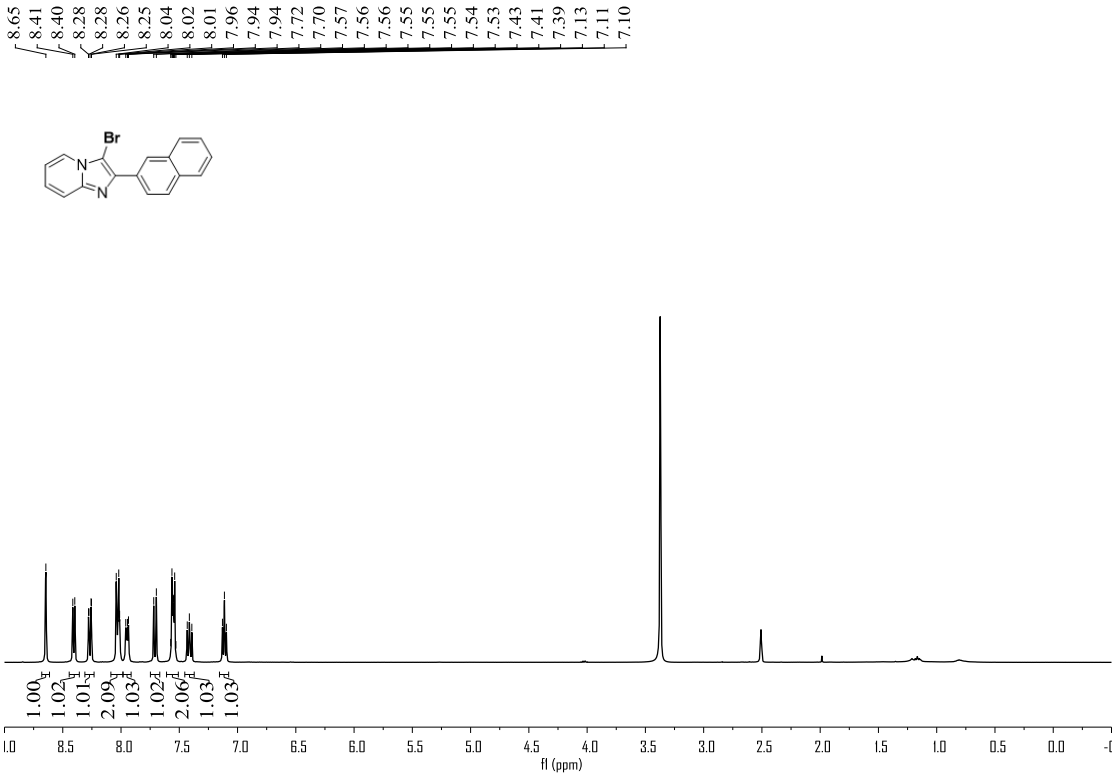

Figure S48. ^{13}C NMR (100 MHz, $CDCl_3$) spectrum of compound **4b**, related to **Figure 1**

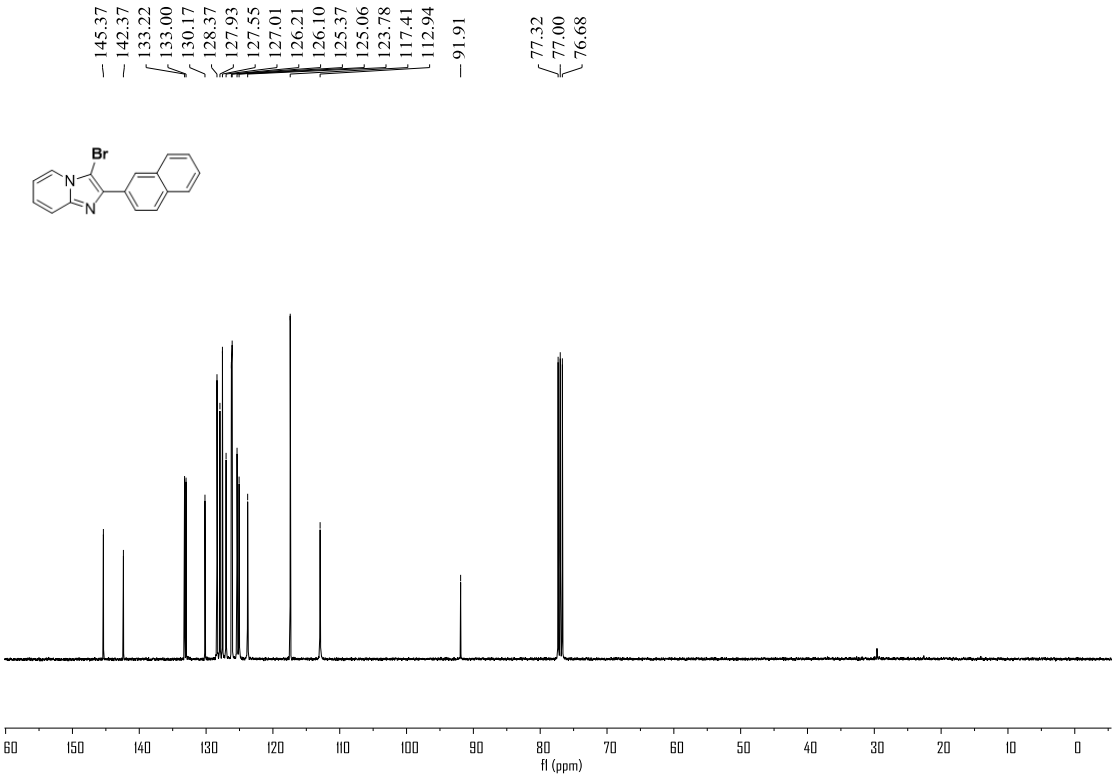

Figure S49. ^{1}H NMR (400 MHz, $CDCl_3$) spectrum of compound **4c**, related to **Figure 1**

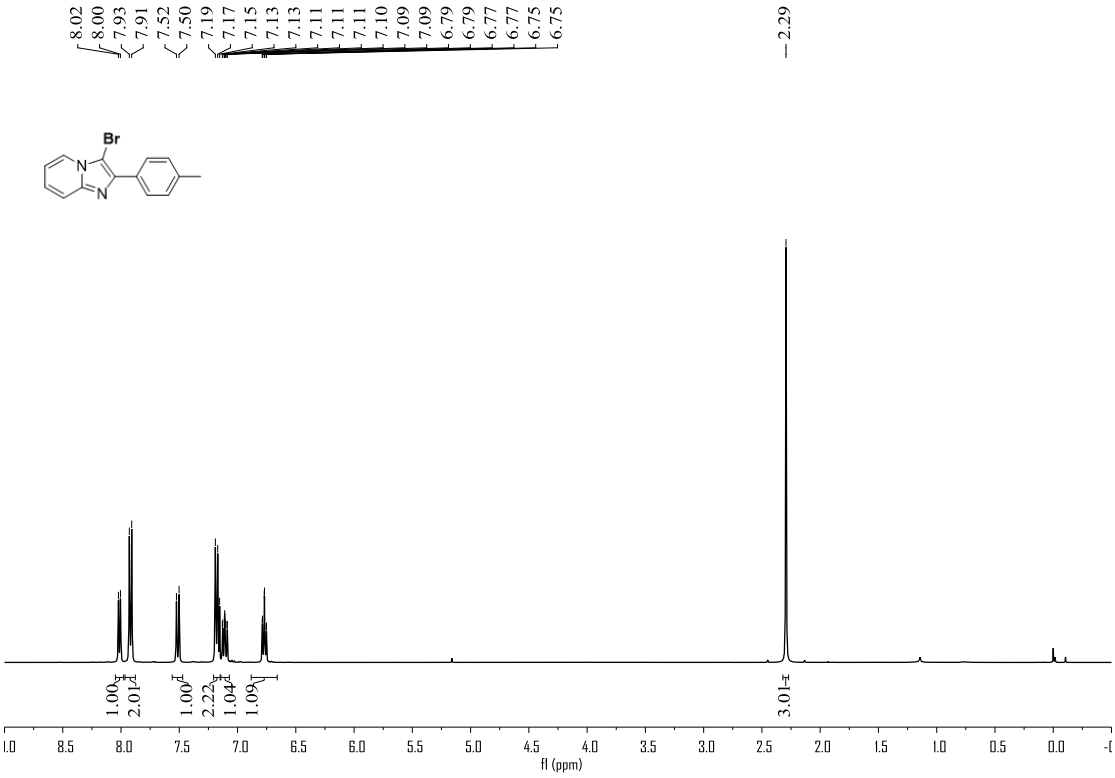

Figure S50. ^{13}C NMR (100 MHz, $CDCl_3$) spectrum of compound **4c**, related to **Figure 1**

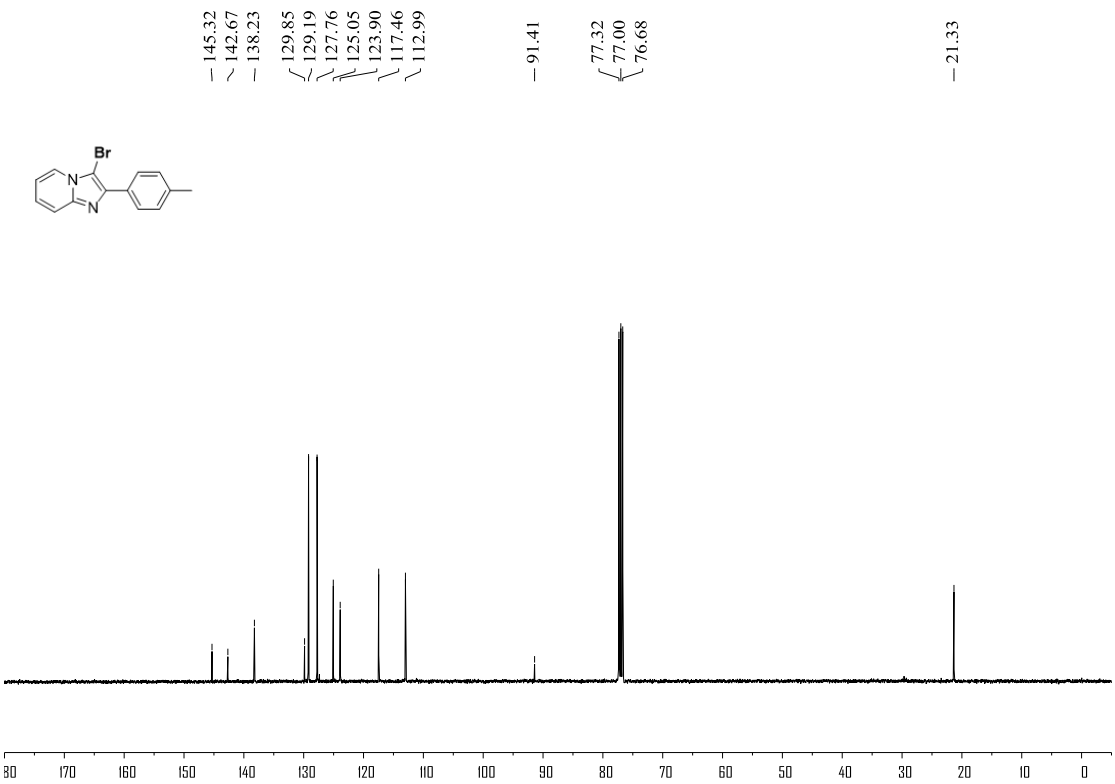

Figure S51. ^{1}H NMR (400 MHz, $CDCl_3$) spectrum of compound **4d**, related to **Figure 1**

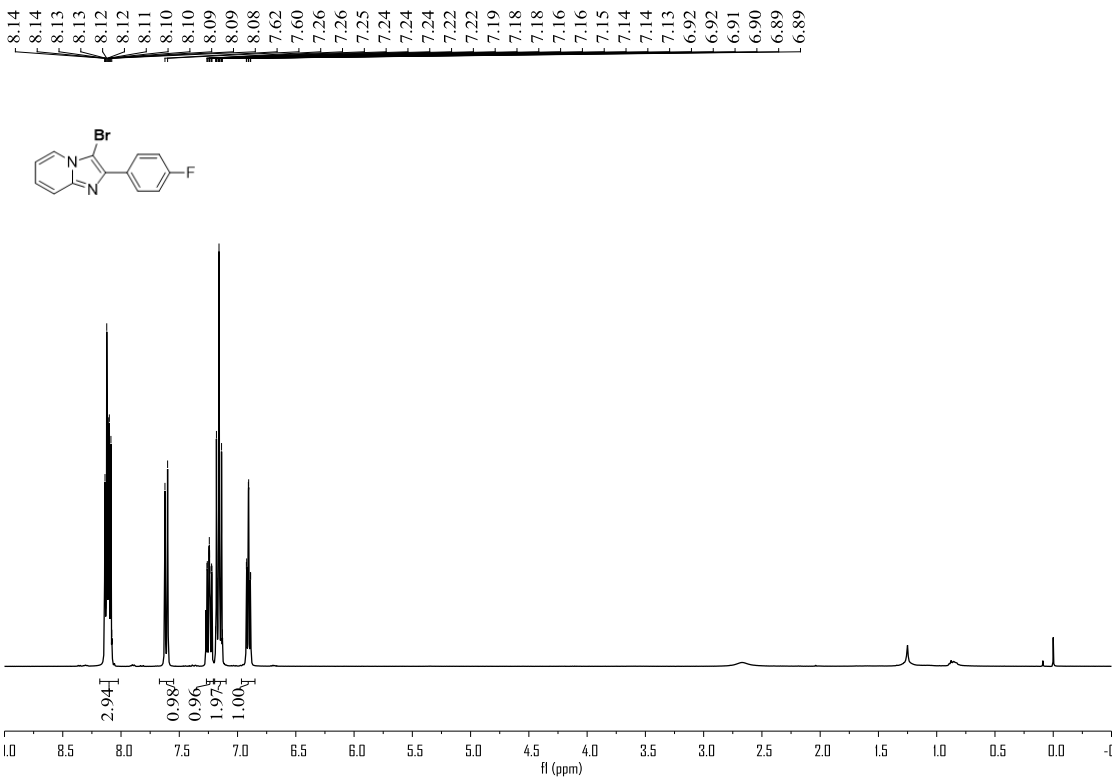

Figure S52. ^{13}C NMR (100 MHz, $CDCl_3$) spectrum of compound **4d**, related to **Figure 1**

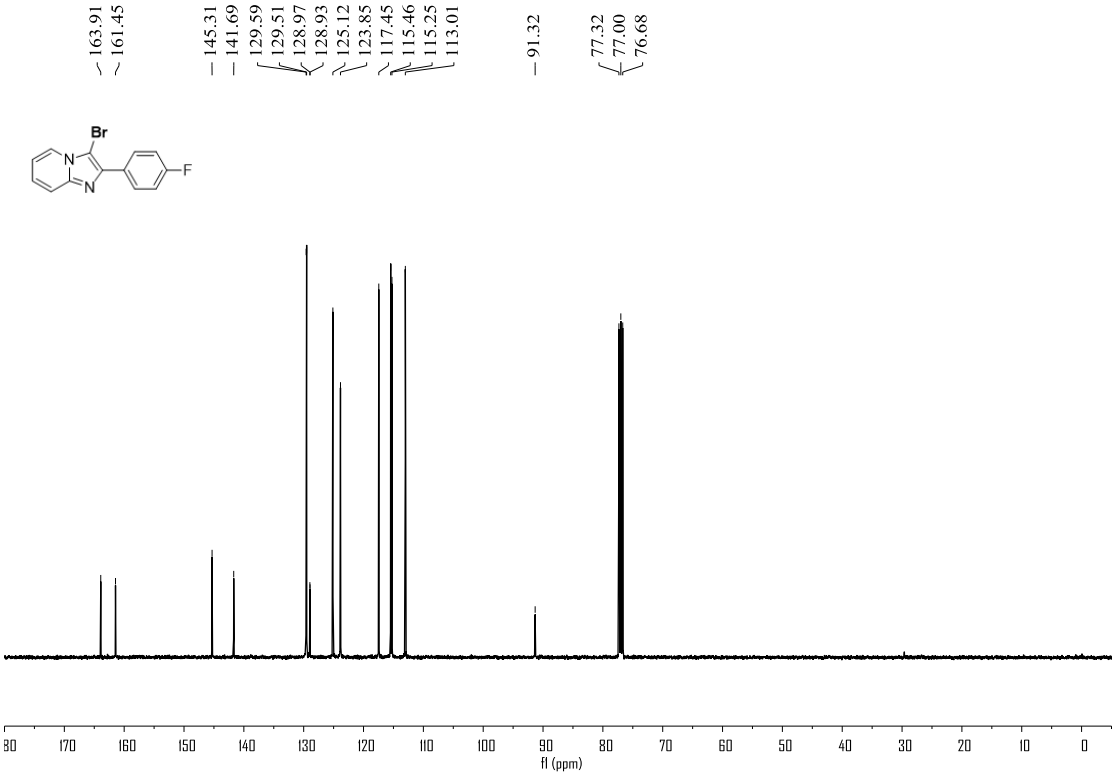

Figure S53. ^{19}F NMR (376 MHz, $CDCl_3$) spectrum of compound **4d**, related to **Figure 1**

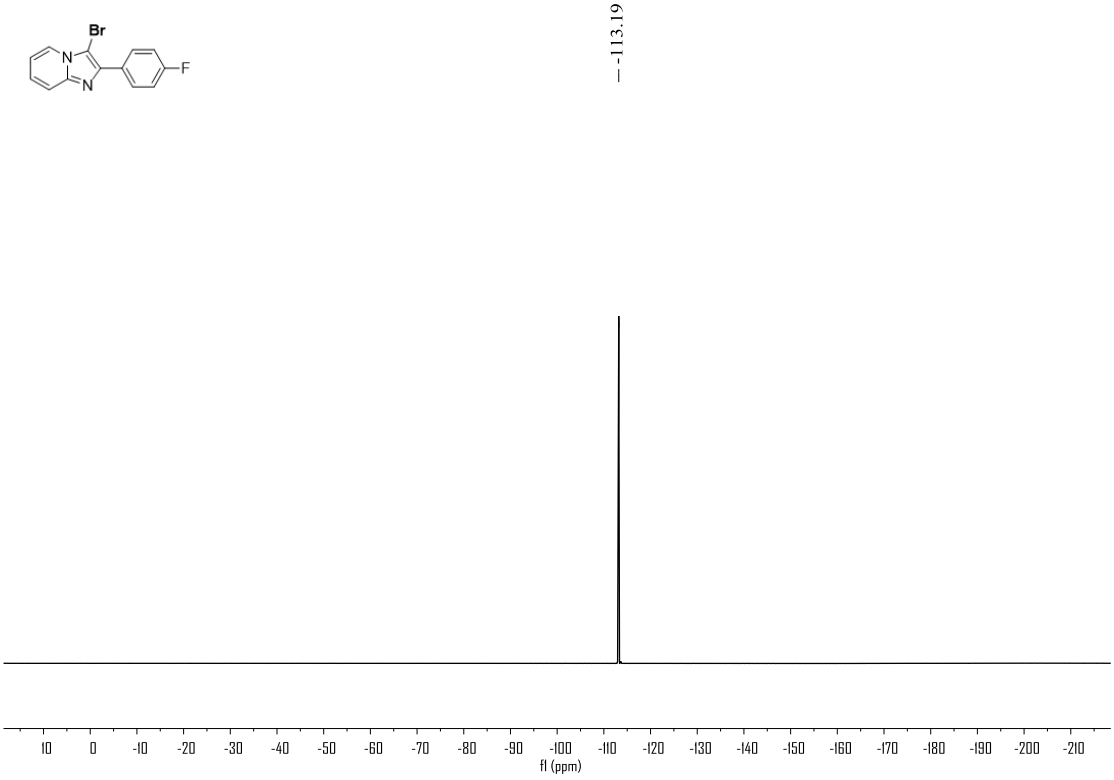

Figure S54. ^{1}H NMR (400 MHz, $CDCl_3$) spectrum of compound **4e**, related to **Figure 1**

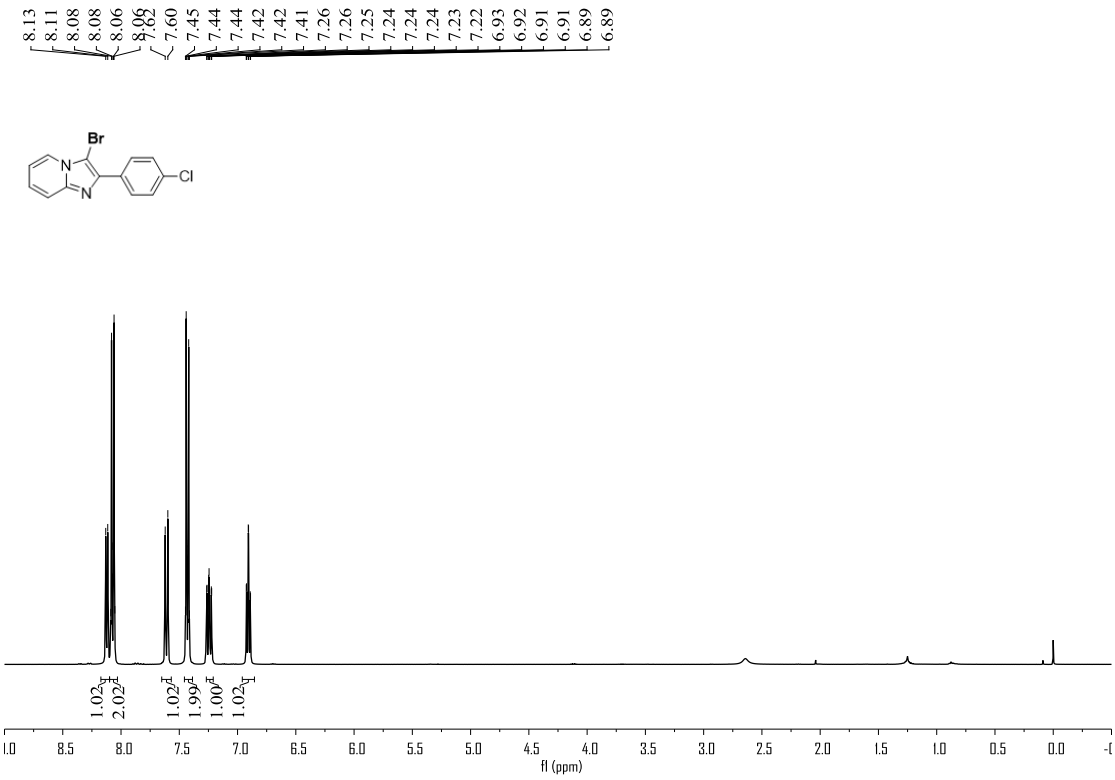

Figure S55. ^{13}C NMR (100 MHz, $CDCl_3$) spectrum of compound **4e**, related to **Figure 1**

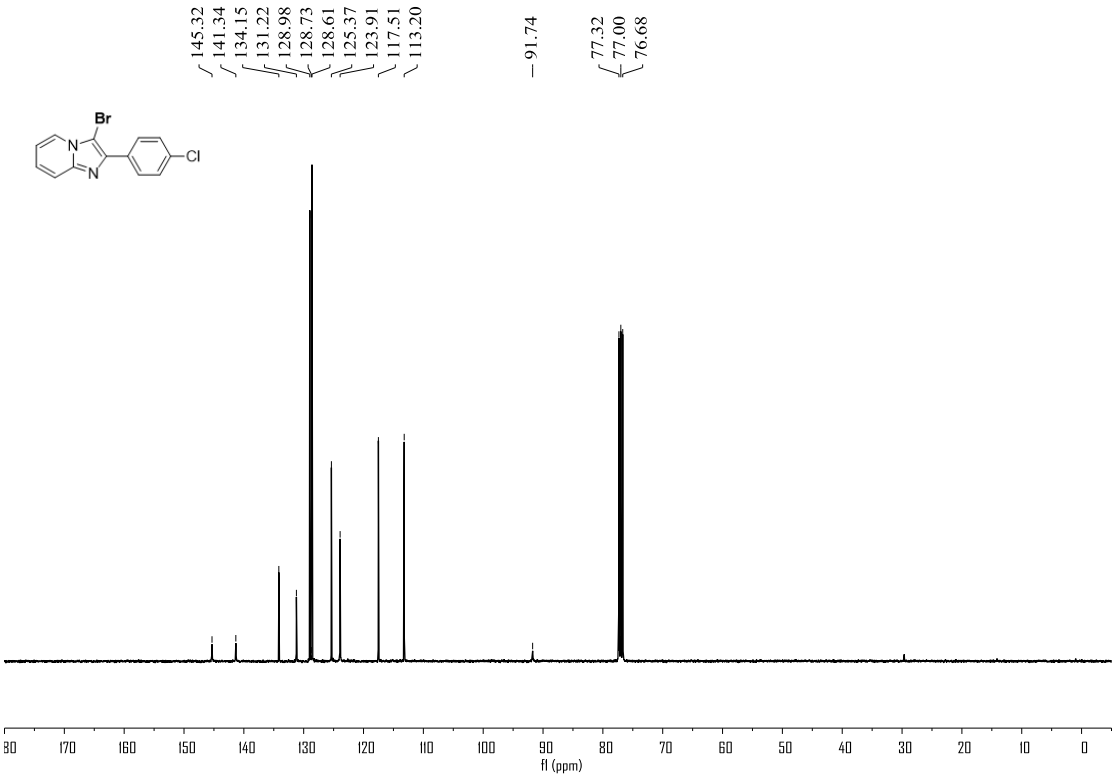

Figure S56. ^{1}H NMR (400 MHz, DMSO-d_6) spectrum of compound **4f**, related to **Figure 1**

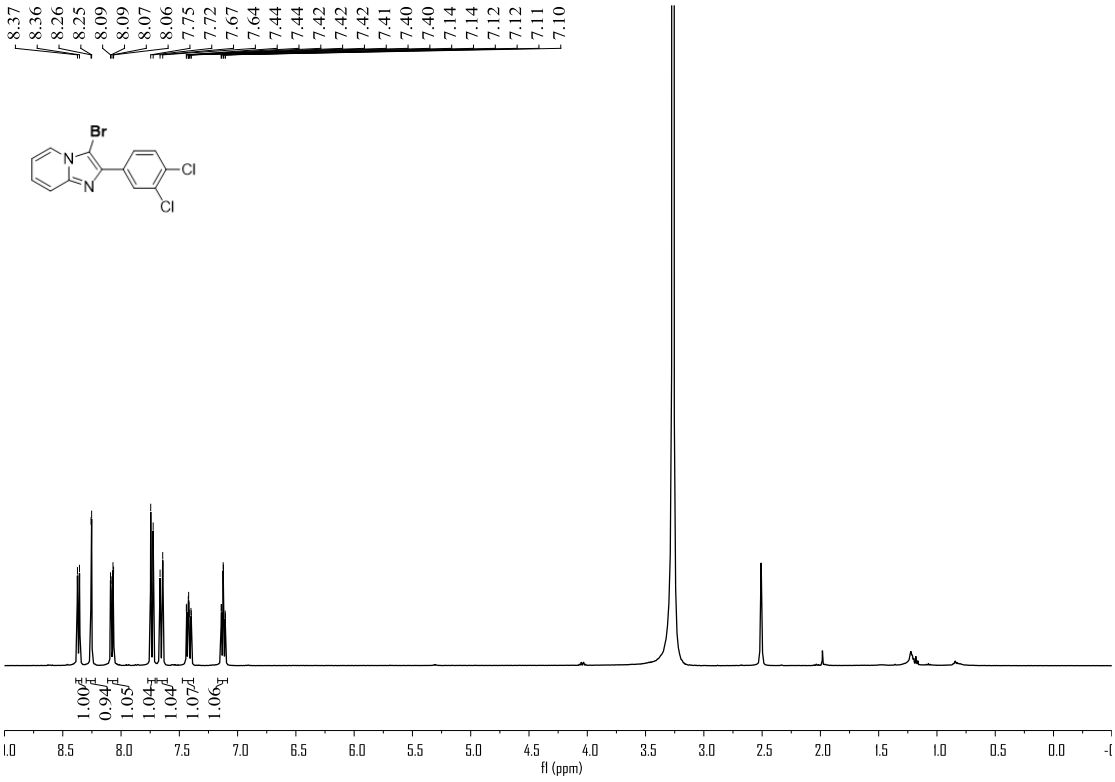

Figure S57. ^{13}C NMR (100 MHz, $CDCl_3$) spectrum of compound **4f**, related to **Figure 1**

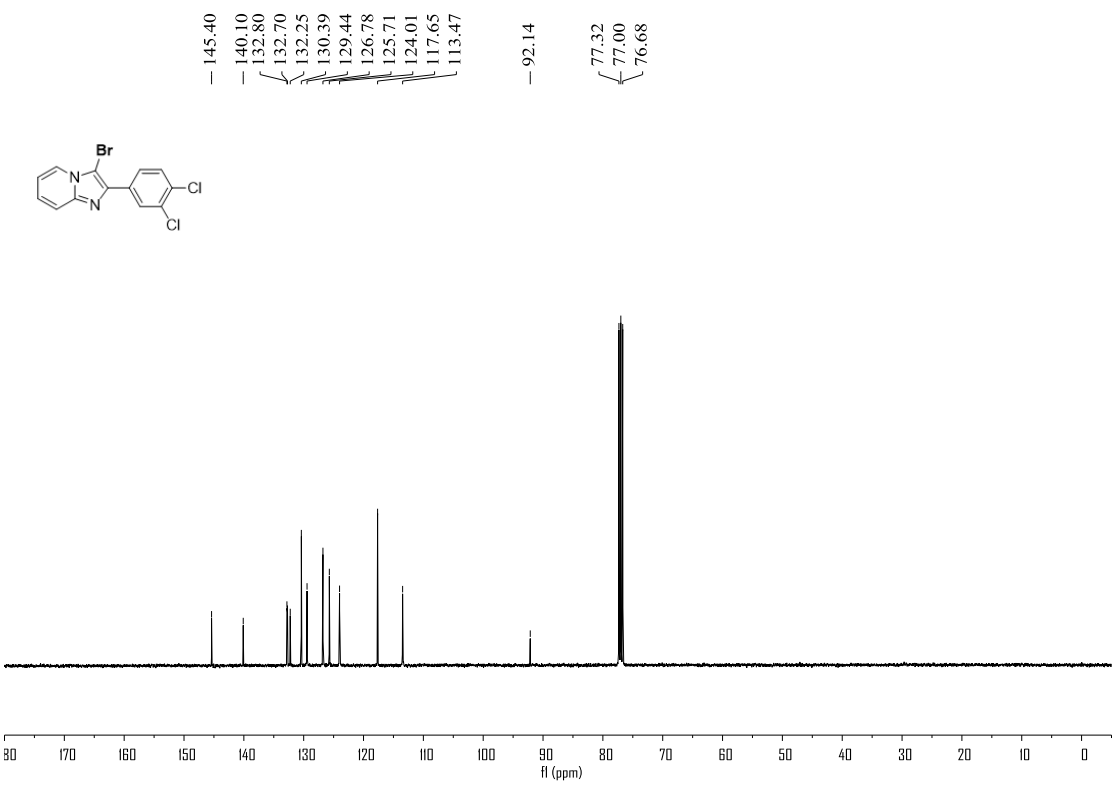

Figure S58. ^{1}H NMR (400 MHz, DMSO-d_6) spectrum of compound **4g**, related to **Figure 1**

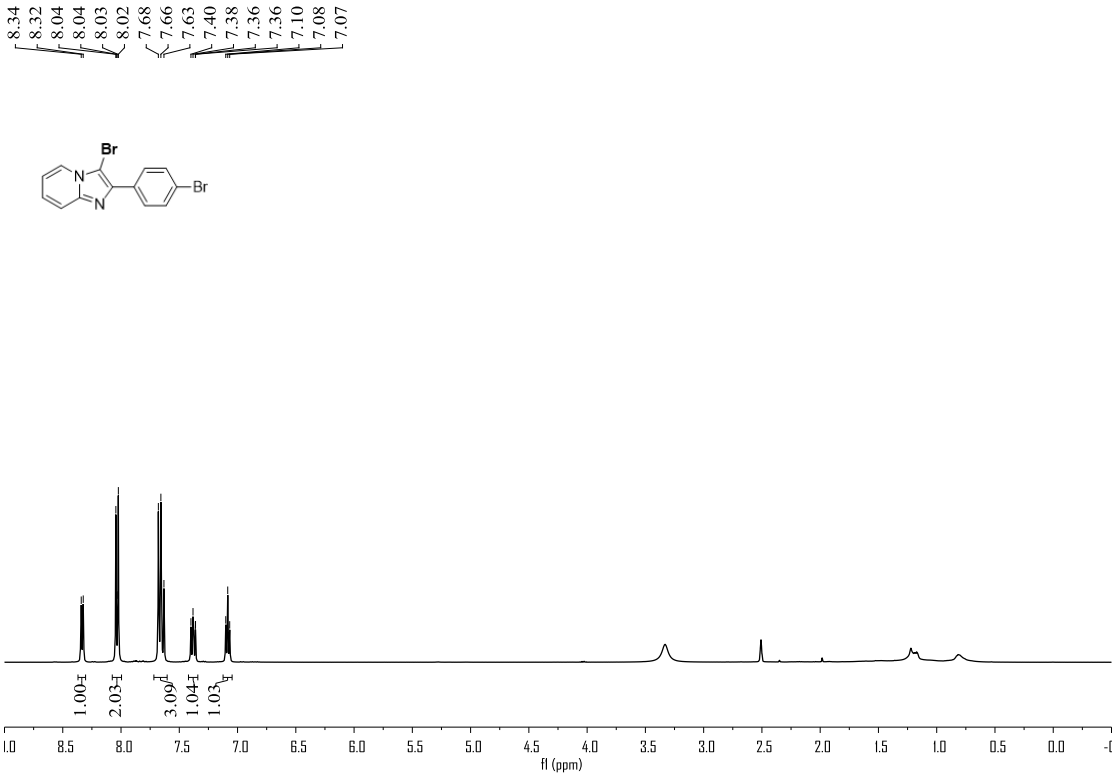

Figure S59. ^{13}C NMR (100 MHz, DMSO-d_6) spectrum of compound **4g**, related to **Figure 1**

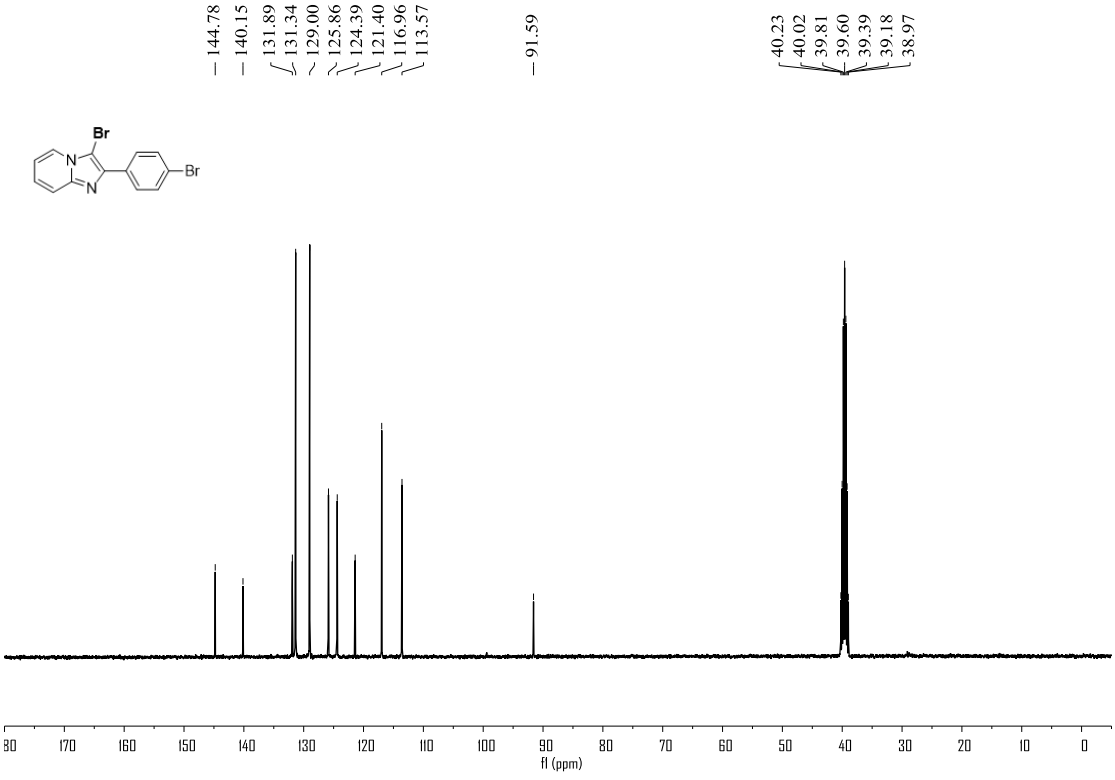

Figure S60. ^{1}H NMR (400 MHz, DMSO-d_6) spectrum of compound **4h**, related to **Figure 1**

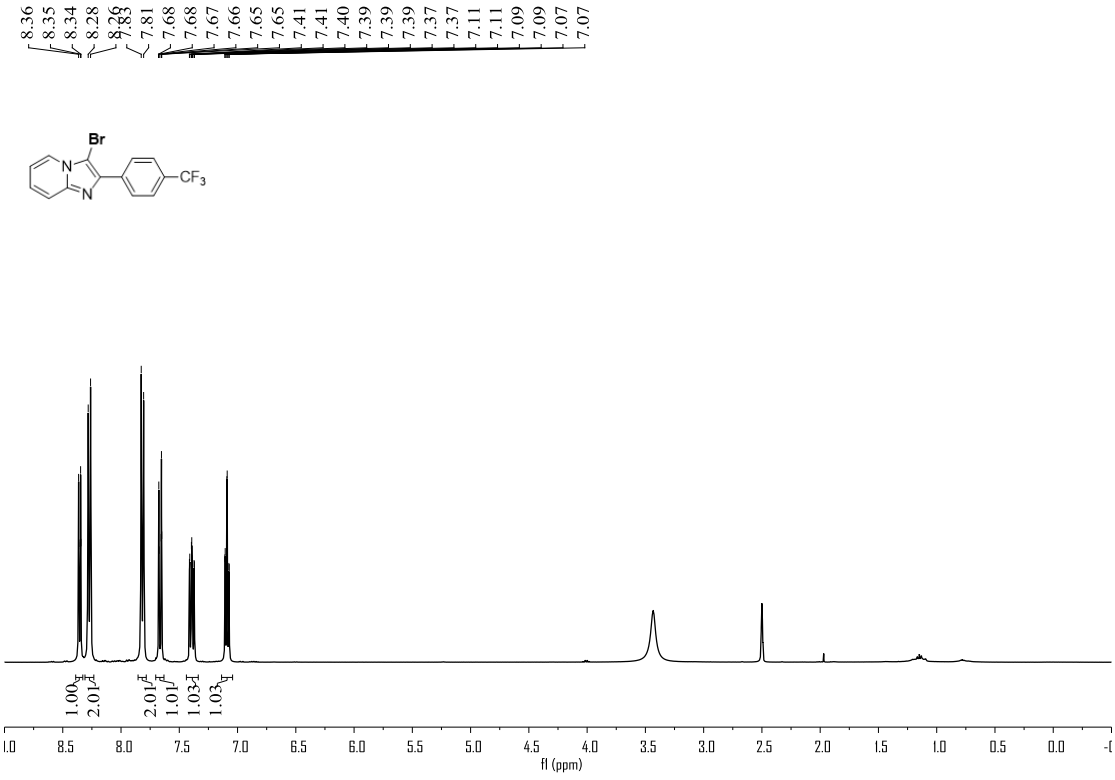

Figure S61. ^{13}C NMR (100 MHz, DMSO-d_6) spectrum of compound **4h**, related to **Figure 1**

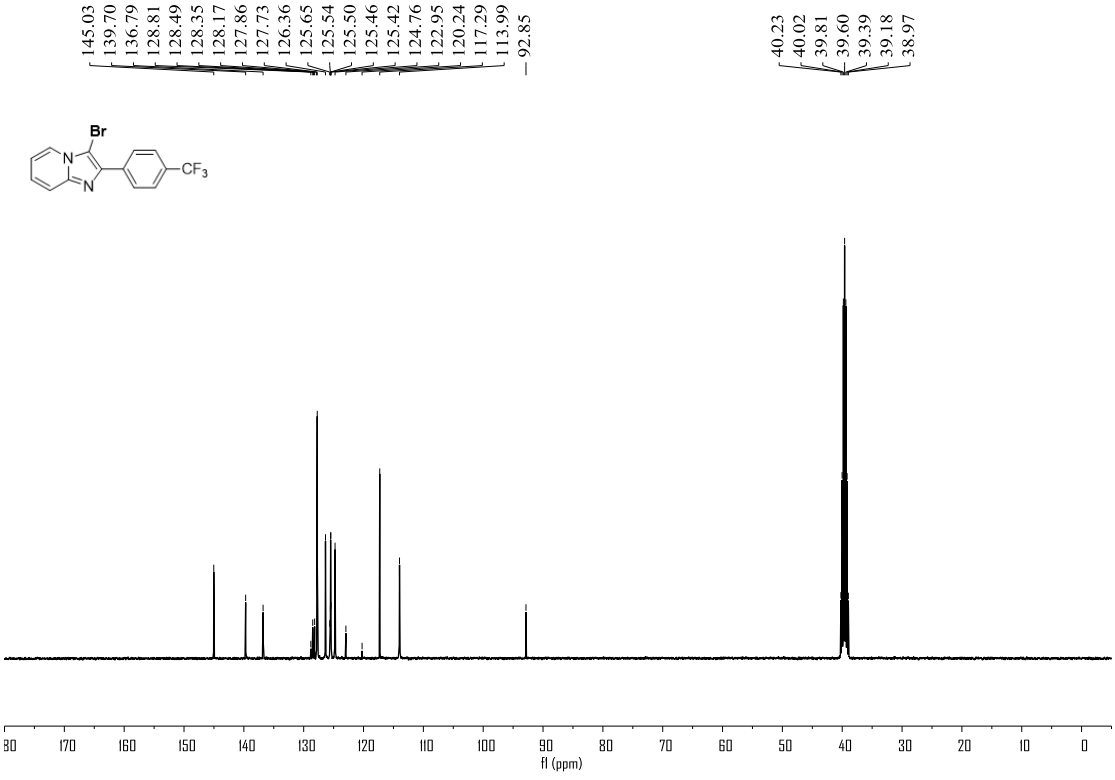

Figure S62. ^{19}F NMR (376 MHz, $CDCl_3$) spectrum of compound **4h**, related to **Figure 1**

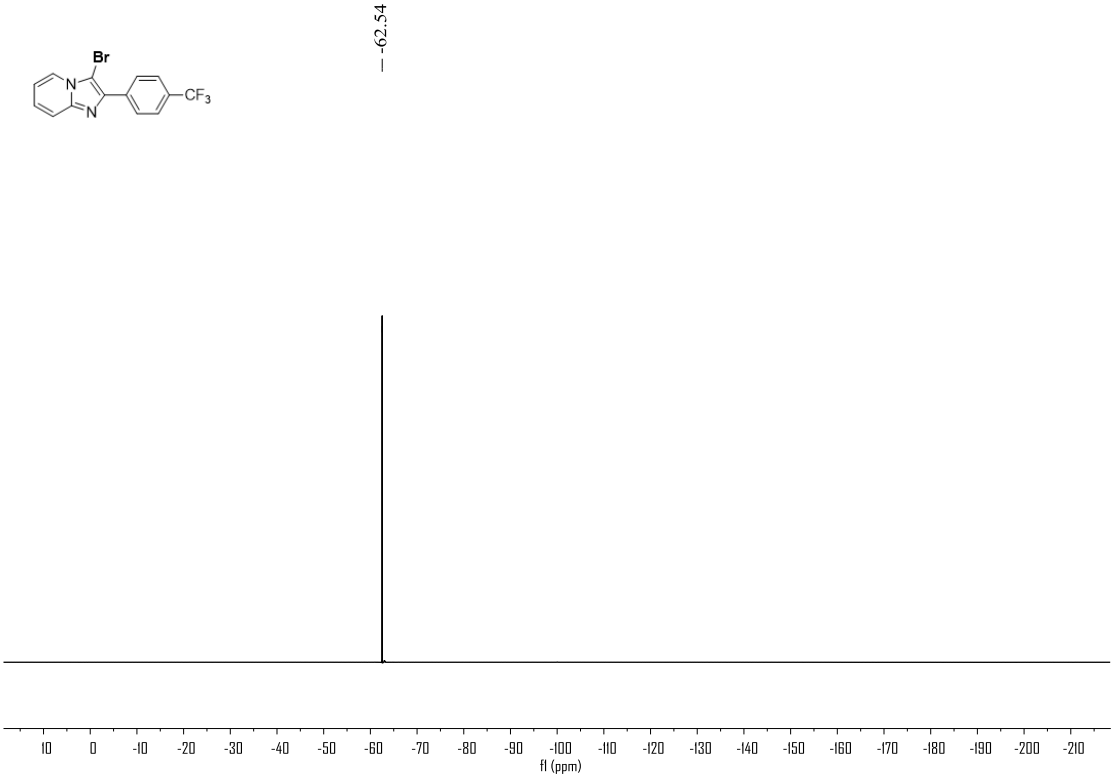

Figure S63. ^{1}H NMR (400 MHz, DMSO-d_6) spectrum of compound **4i**, related to **Figure 1**

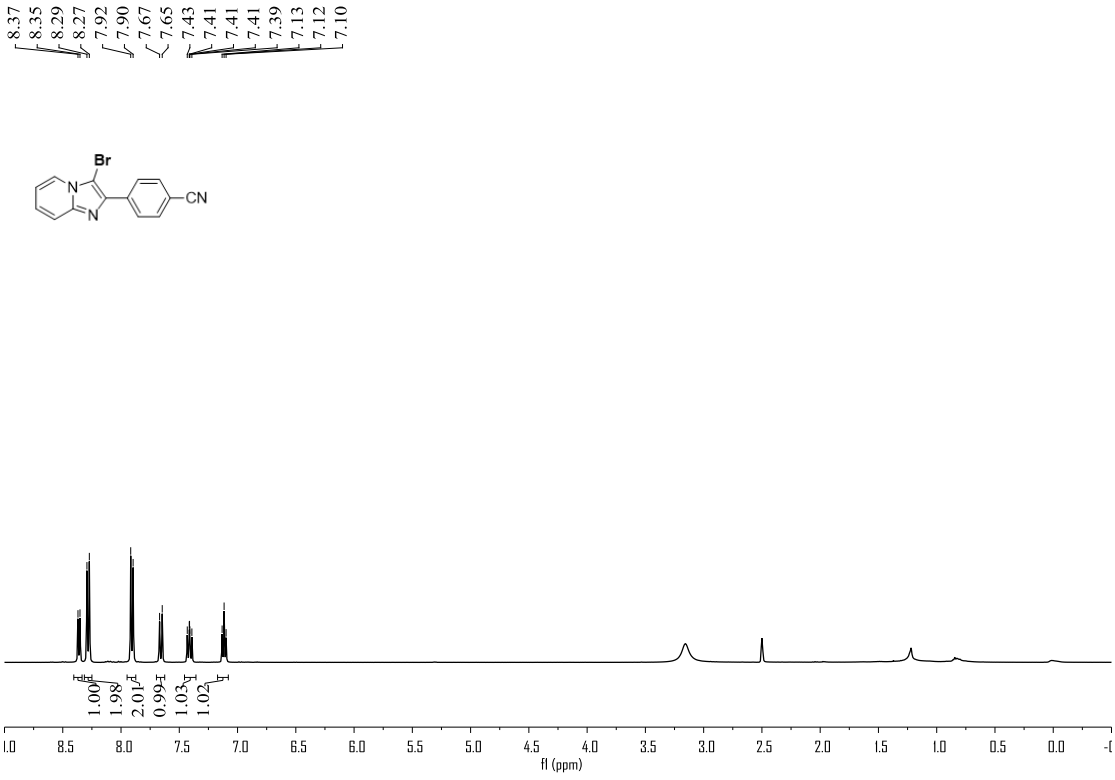

Figure S64. ^{13}C NMR (100 MHz, DMSO-d_6) spectrum of compound **4i**, related to **Figure 1**

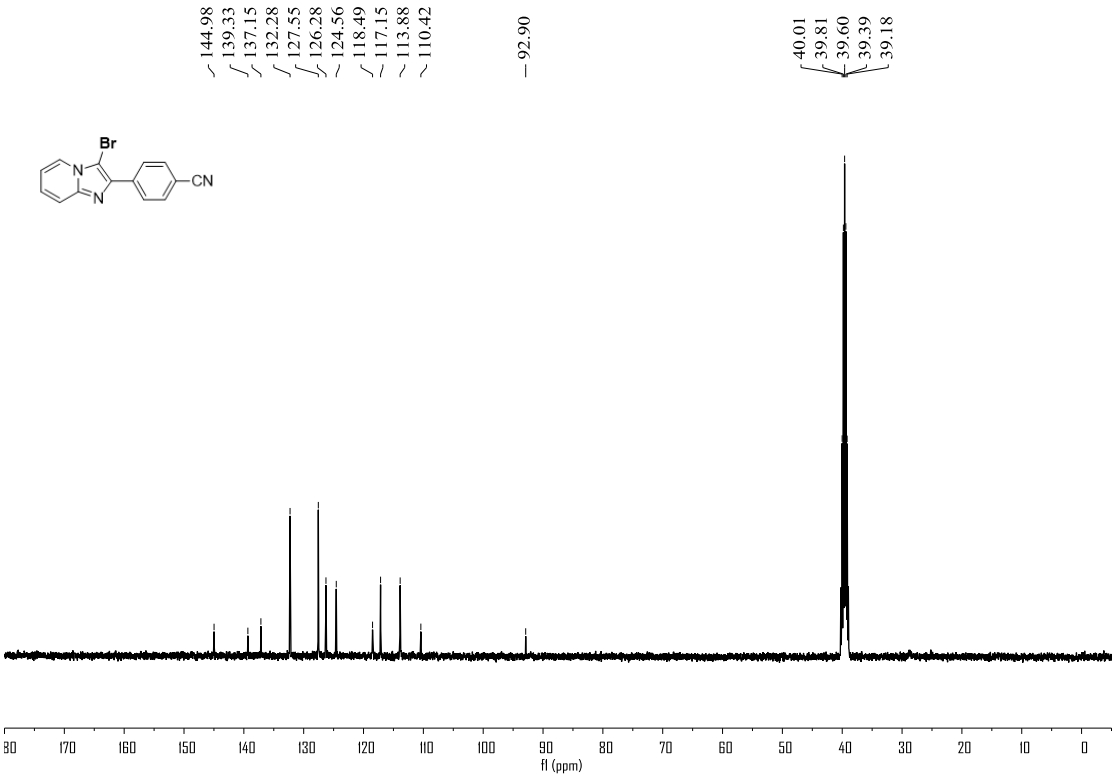

Figure S65. ^{1}H NMR (400 MHz, DMSO-d_6) spectrum of compound **4j**, related to **Figure 1**

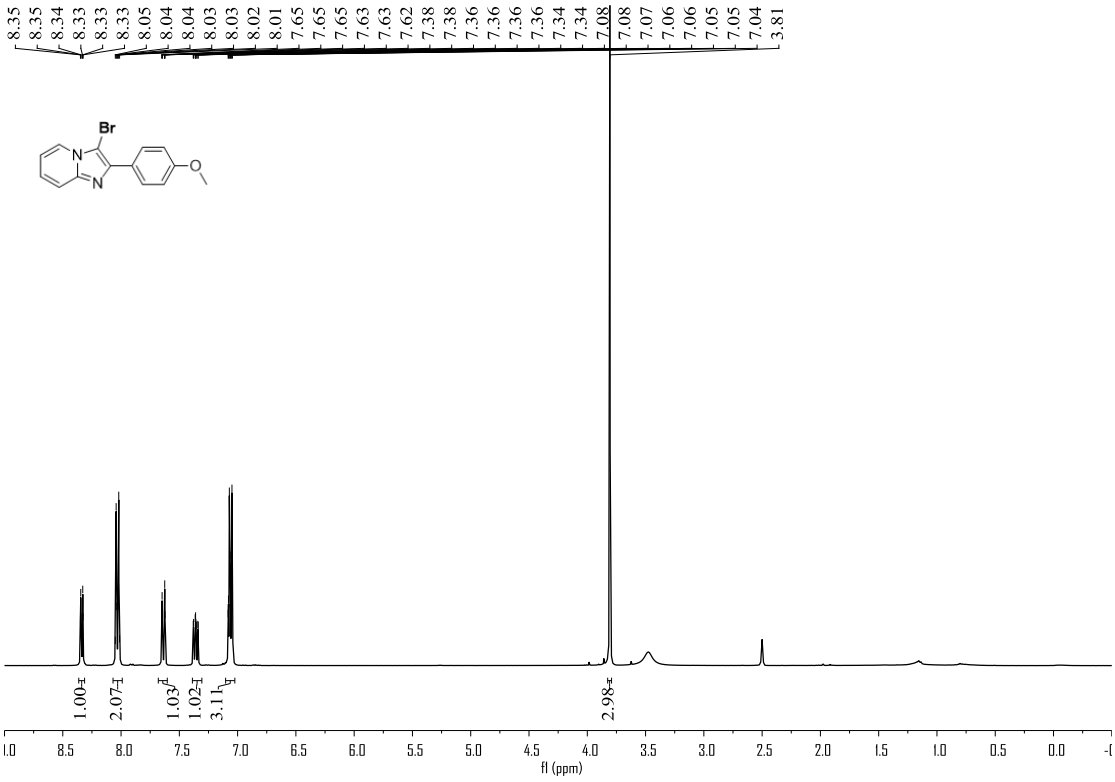

Figure S66. ^{13}C NMR (100 MHz, DMSO-d_6) spectrum of compound **4j**, related to **Figure 1**

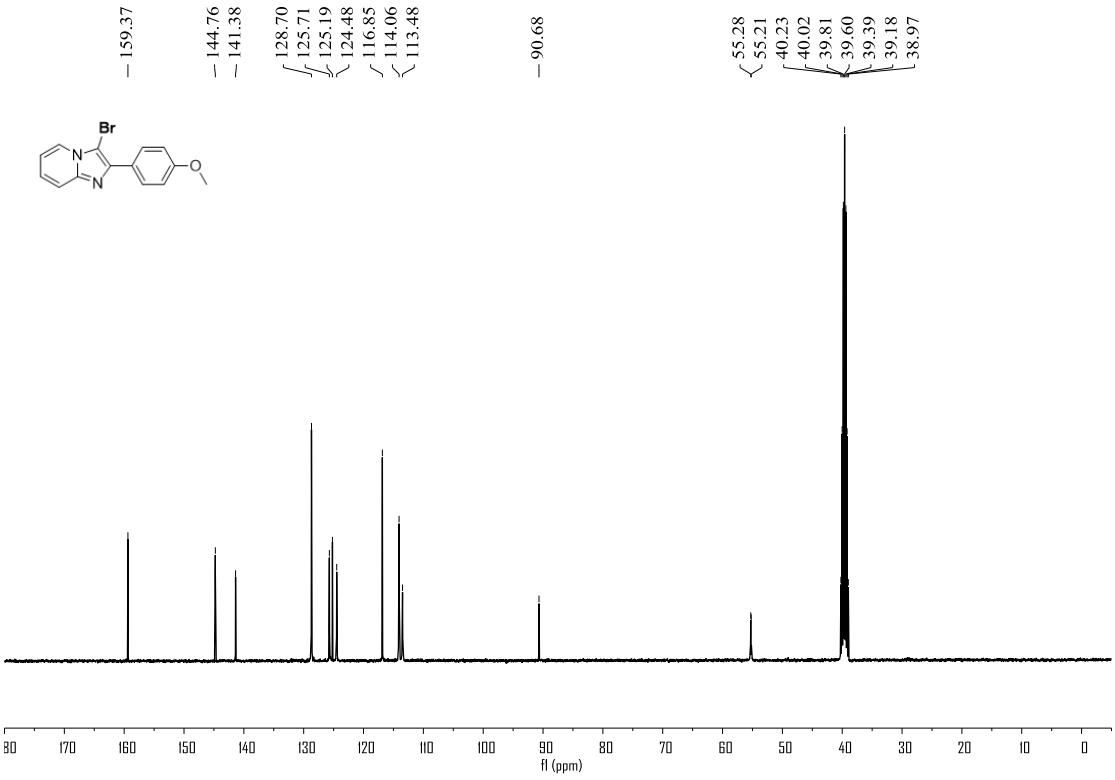

Figure S67. ^{1}H NMR (400 MHz, $CDCl_3$) spectrum of compound **4k**, related to **Figure 1**

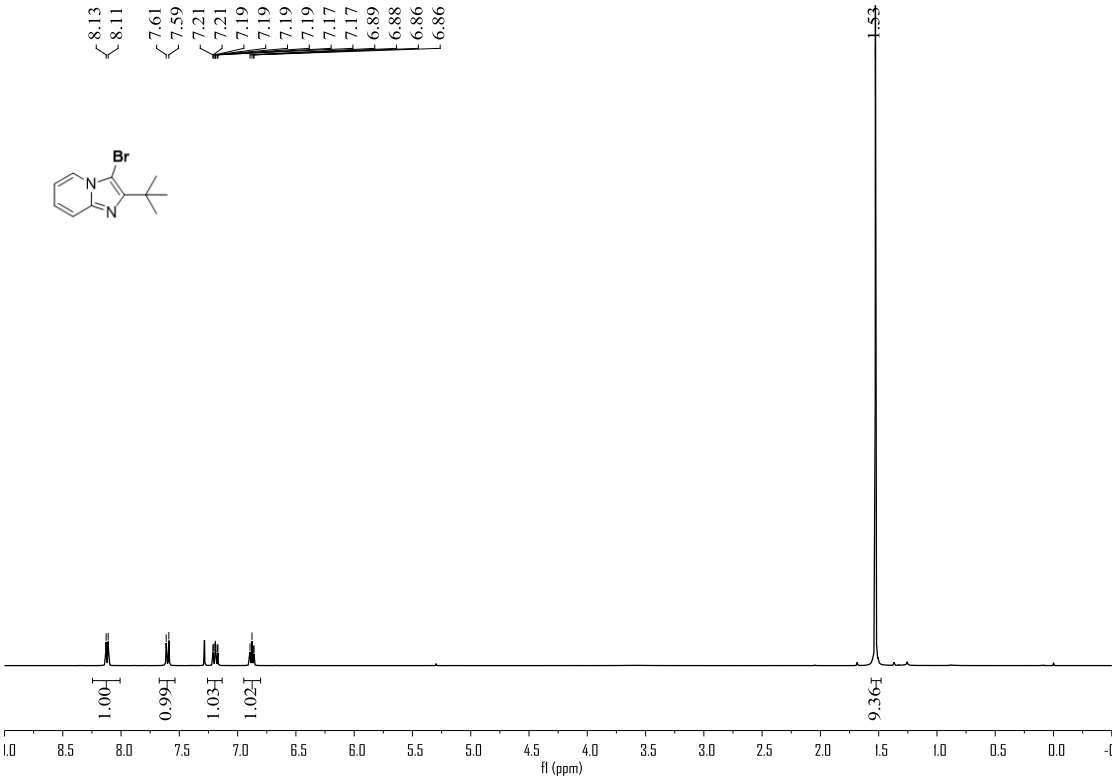

Figure S68. ^{13}C NMR (100 MHz, $CDCl_3$) spectrum of compound **4k**, related to **Figure 1**

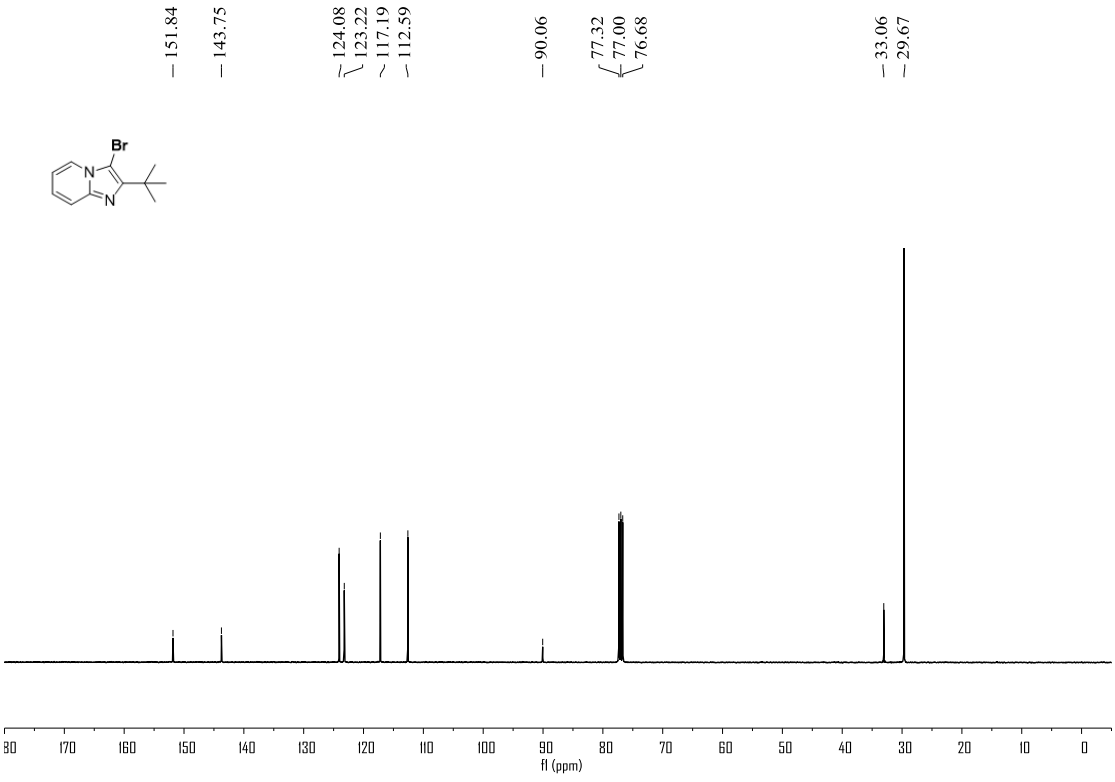

Figure S69. ^{1}H NMR (400 MHz, $CDCl_3$) spectrum of compound **4l**, related to **Figure 1**

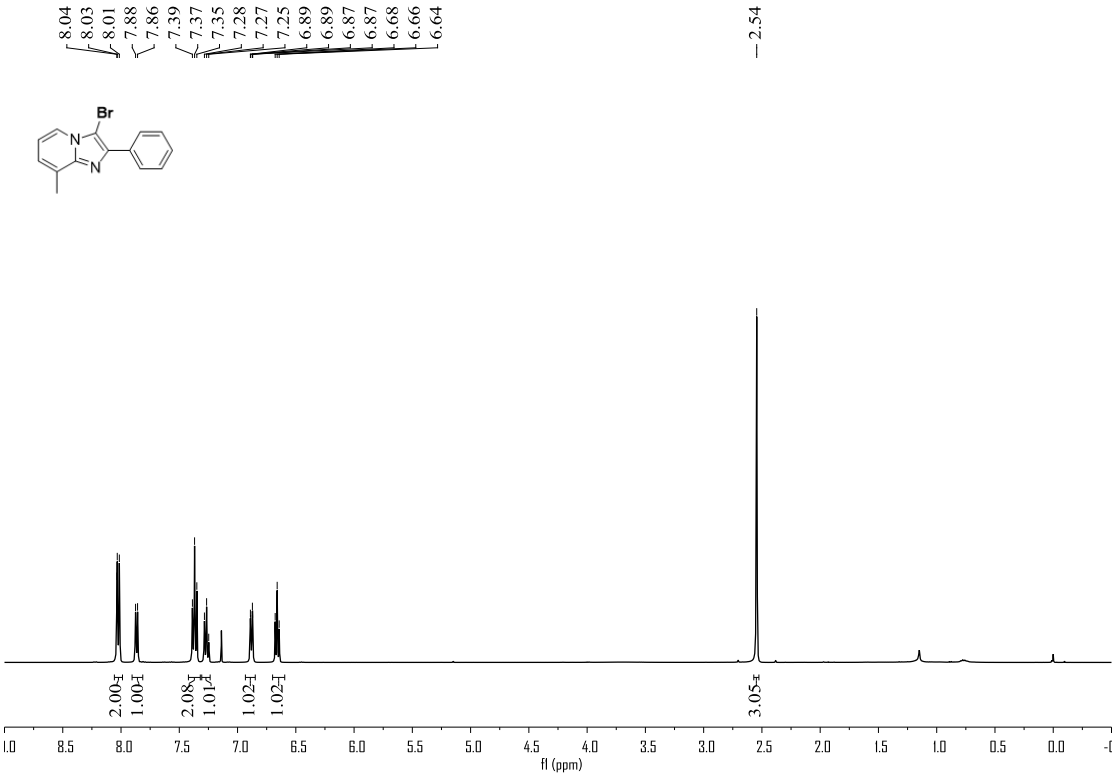

Figure S70. ^{13}C NMR (100 MHz, $CDCl_3$) spectrum of compound **4l**, related to **Figure 1**

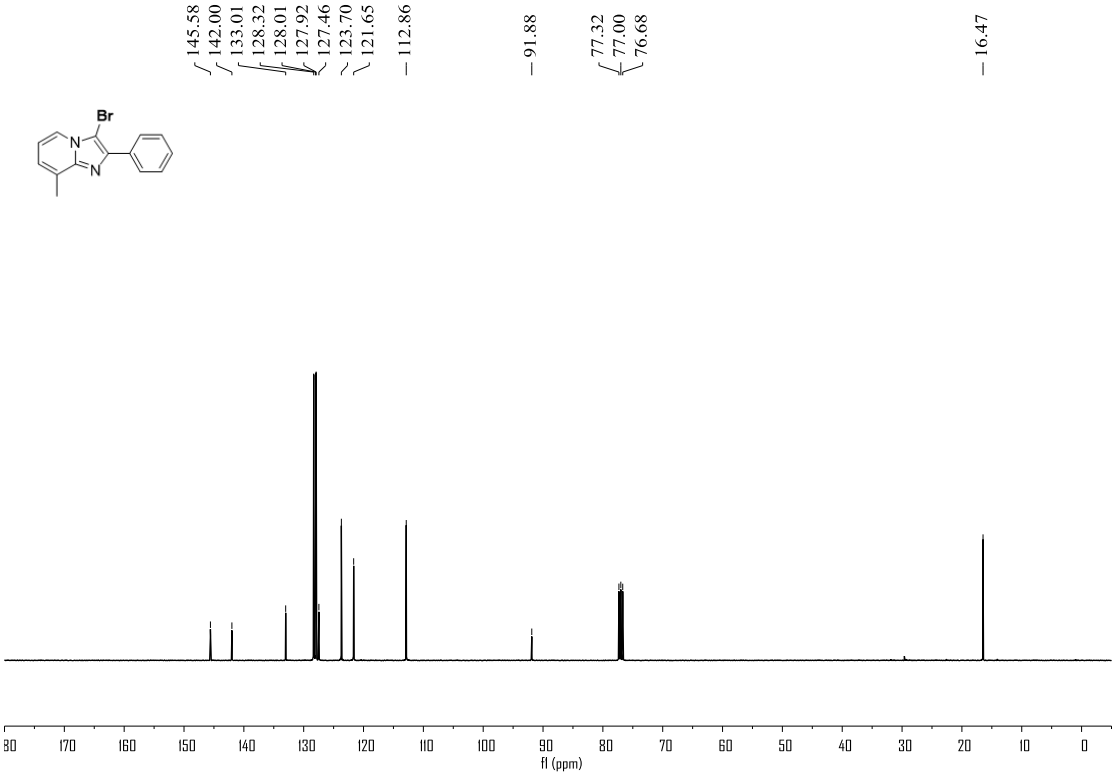

Figure S71. ^{1}H NMR (400 MHz, DMSO-d_6) spectrum of compound **4m**, related to **Figure 1**

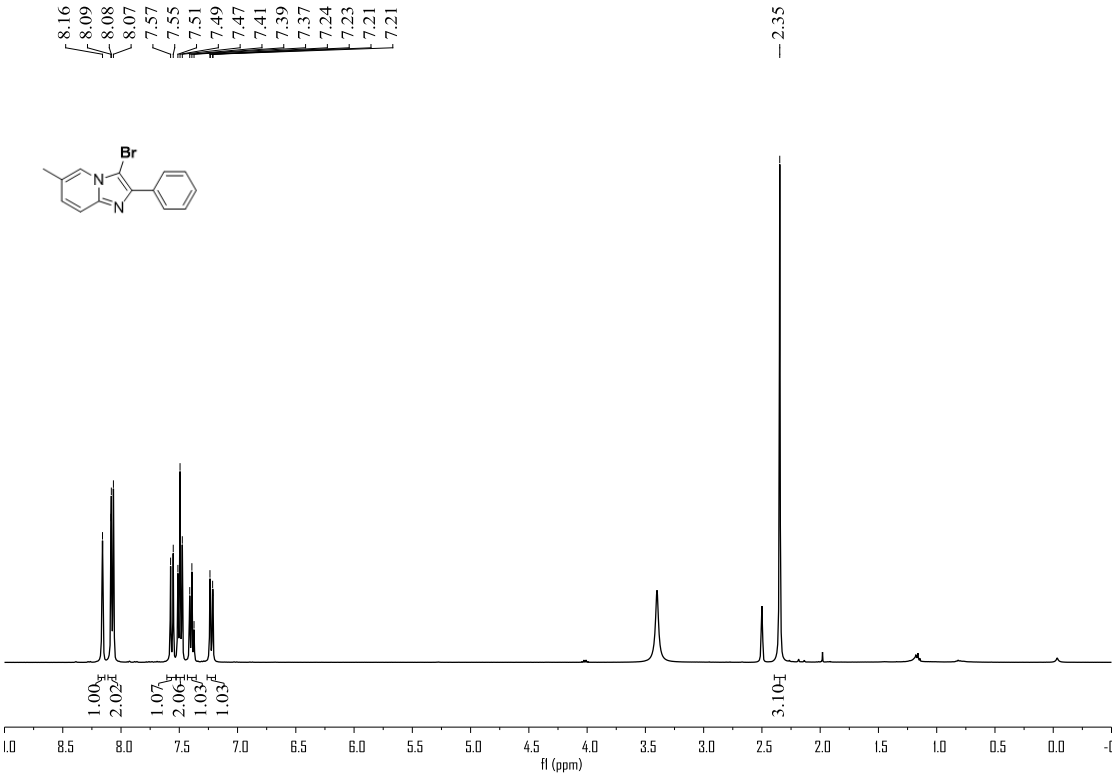

Figure S72. ^{13}C NMR (100 MHz, $CDCl_3$) spectrum of compound **4m**, related to **Figure 1**

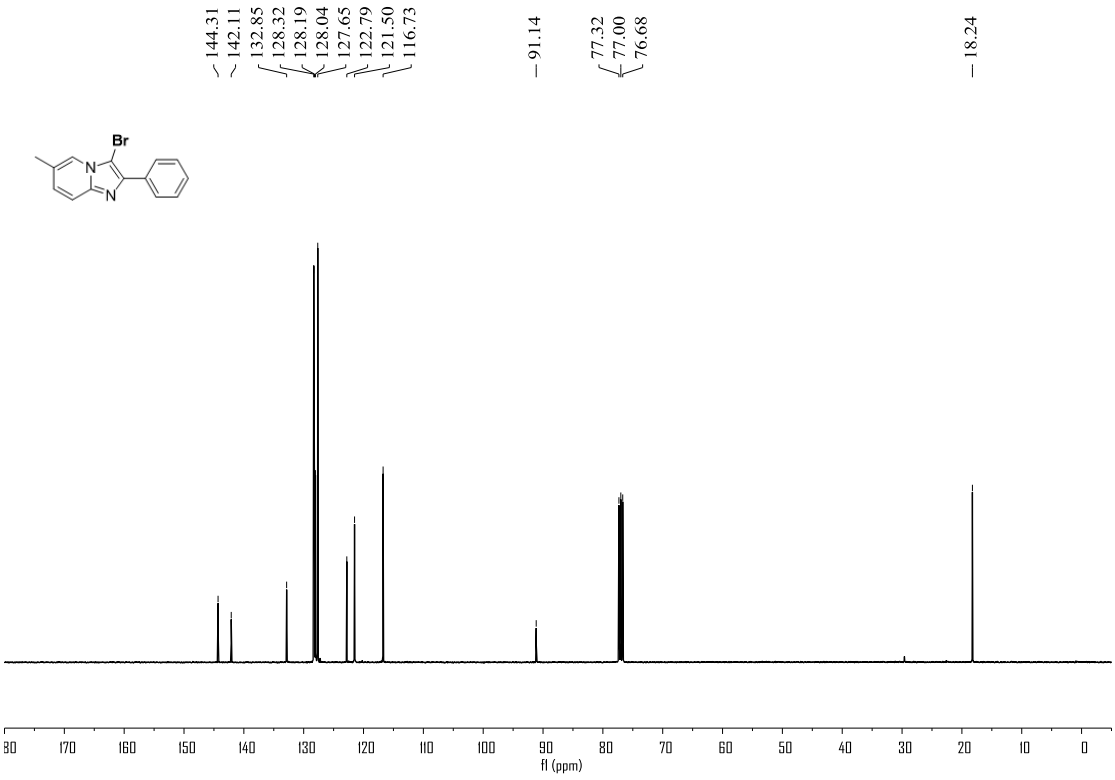

Figure S73. ^{1}H NMR (400 MHz, $CDCl_3$) spectrum of compound **4n**, related to **Figure 1**

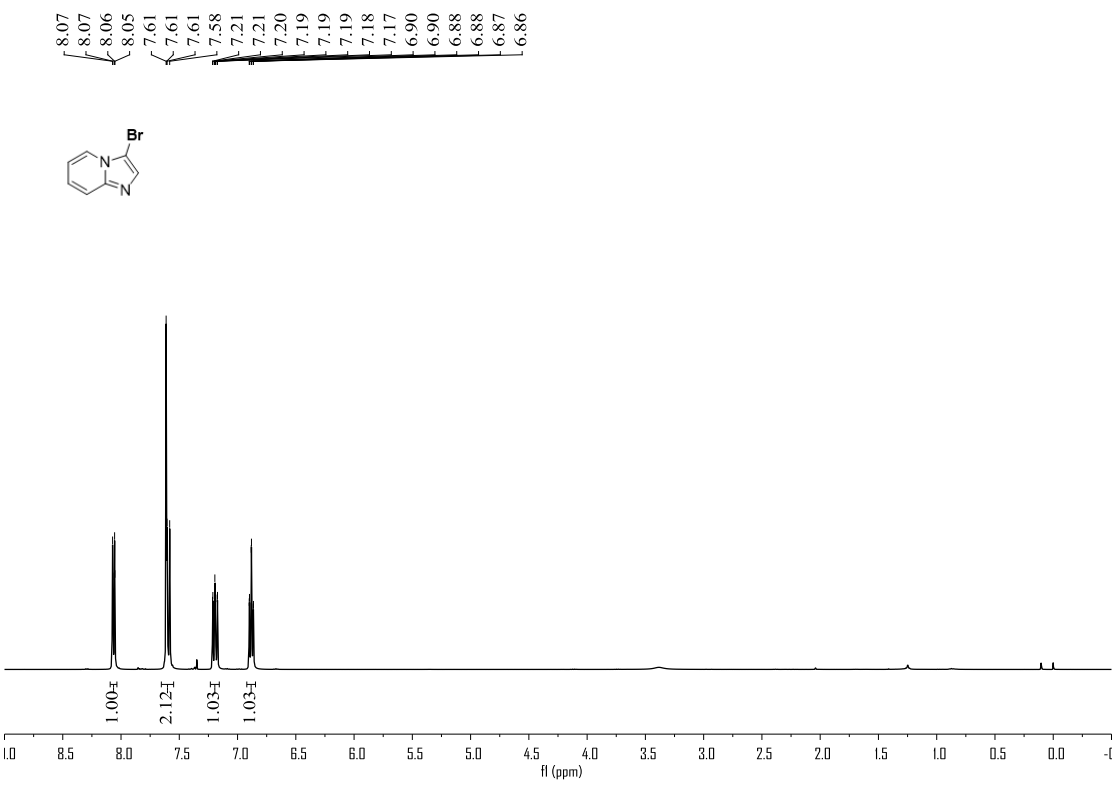

Figure S74. ^{13}C NMR (100 MHz, $CDCl_3$) spectrum of compound **4n**, related to **Figure 1**

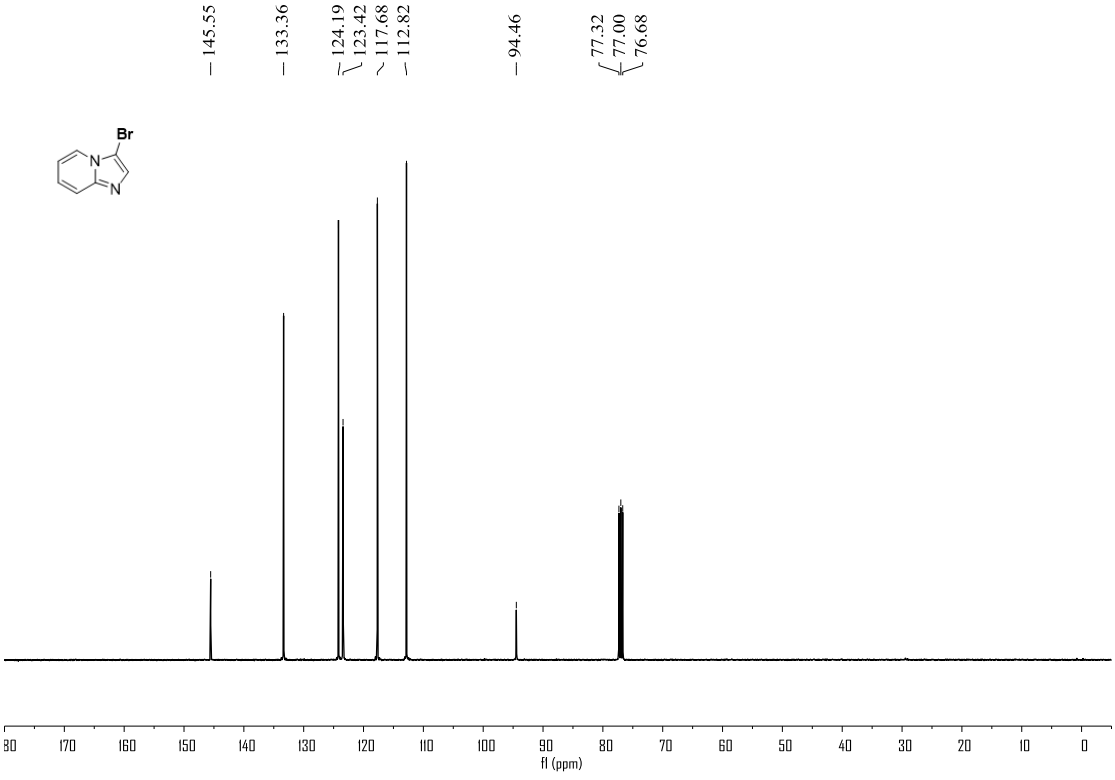

Figure S75. ^{1}H NMR (400 MHz, DMSO-d_6) spectrum of compound **4o**, related to **Figure 1**

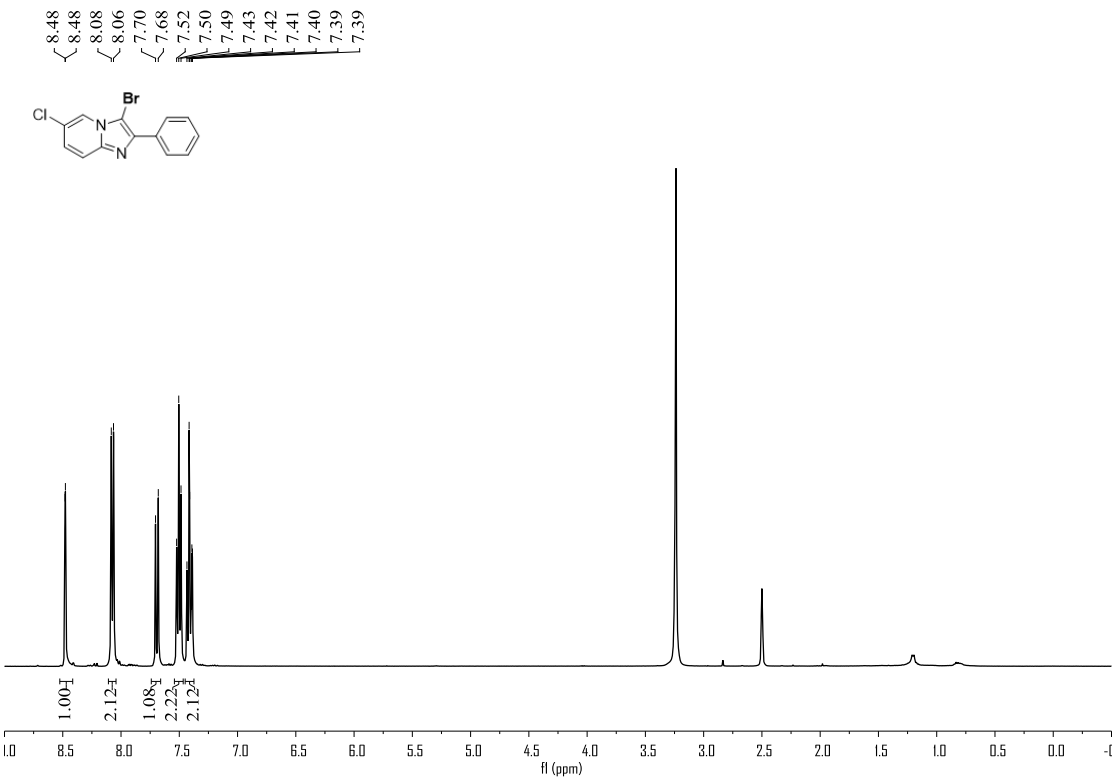

Figure S76. ^{13}C NMR (100 MHz, $CDCl_3$) spectrum of compound **4o**, related to **Figure 1**

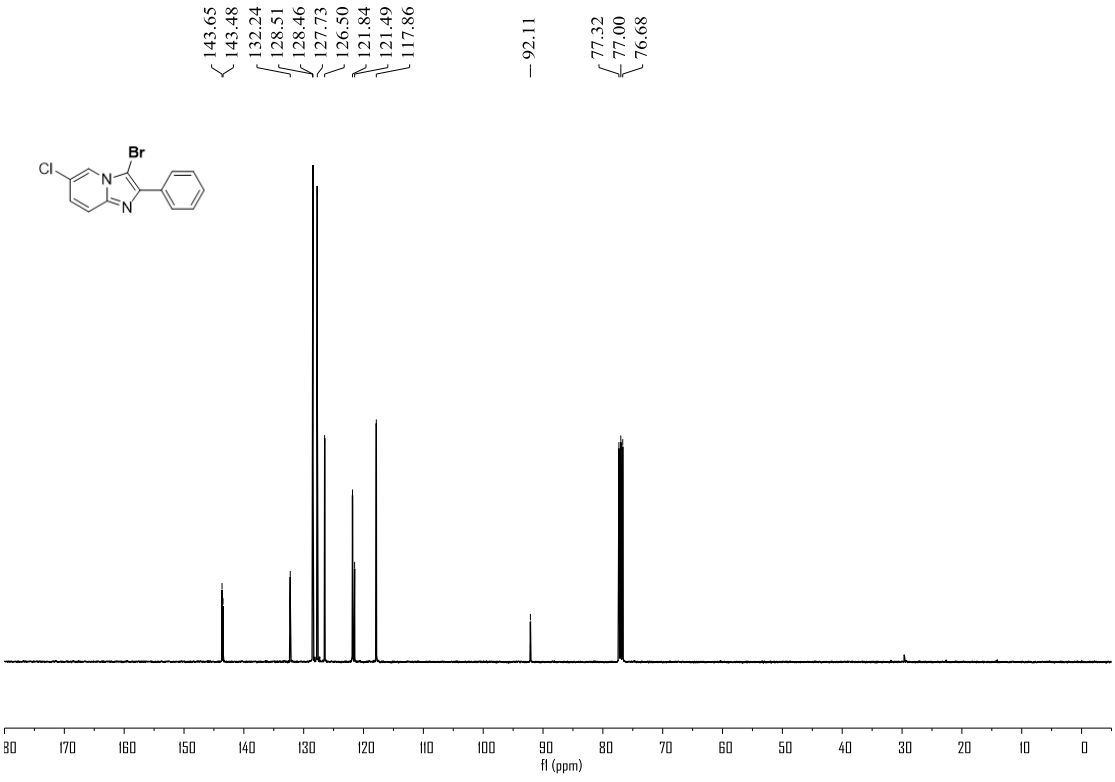

Figure S77. ^{1}H NMR (400 MHz, $CDCl_3$) spectrum of compound **4p**, related to **Figure 1**

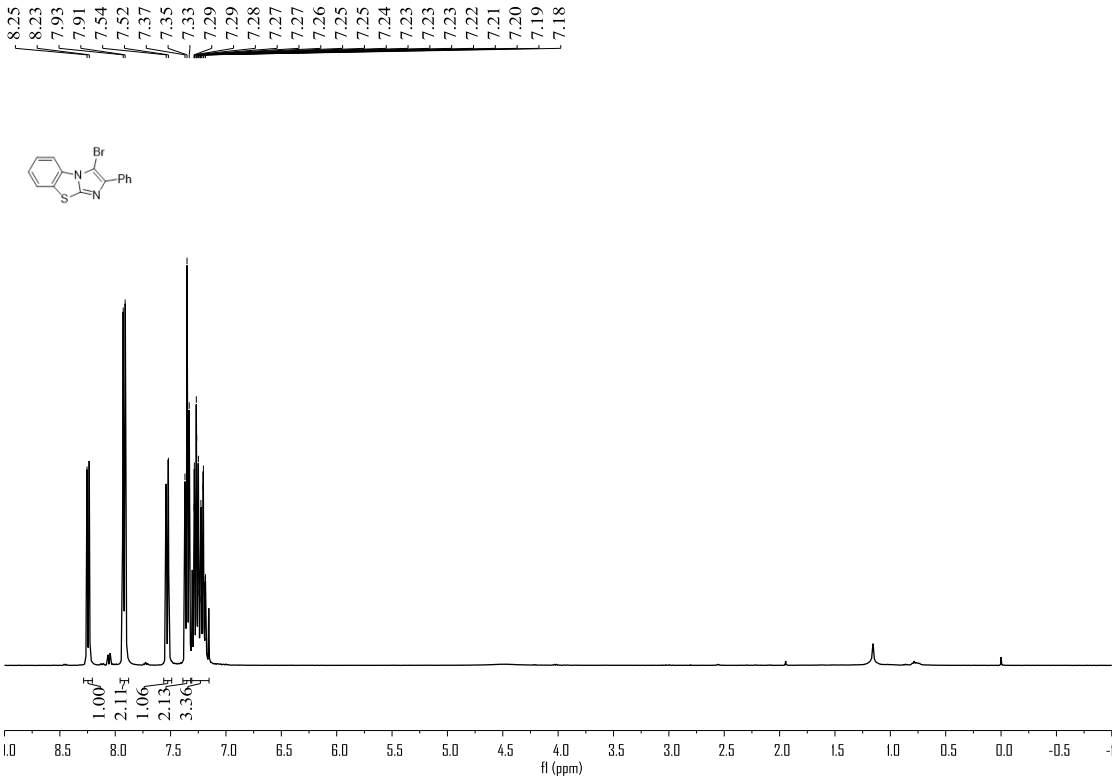

Figure S78. ^{13}C NMR (100 MHz, $CDCl_3$) spectrum of compound **4p**, related to **Figure 1**

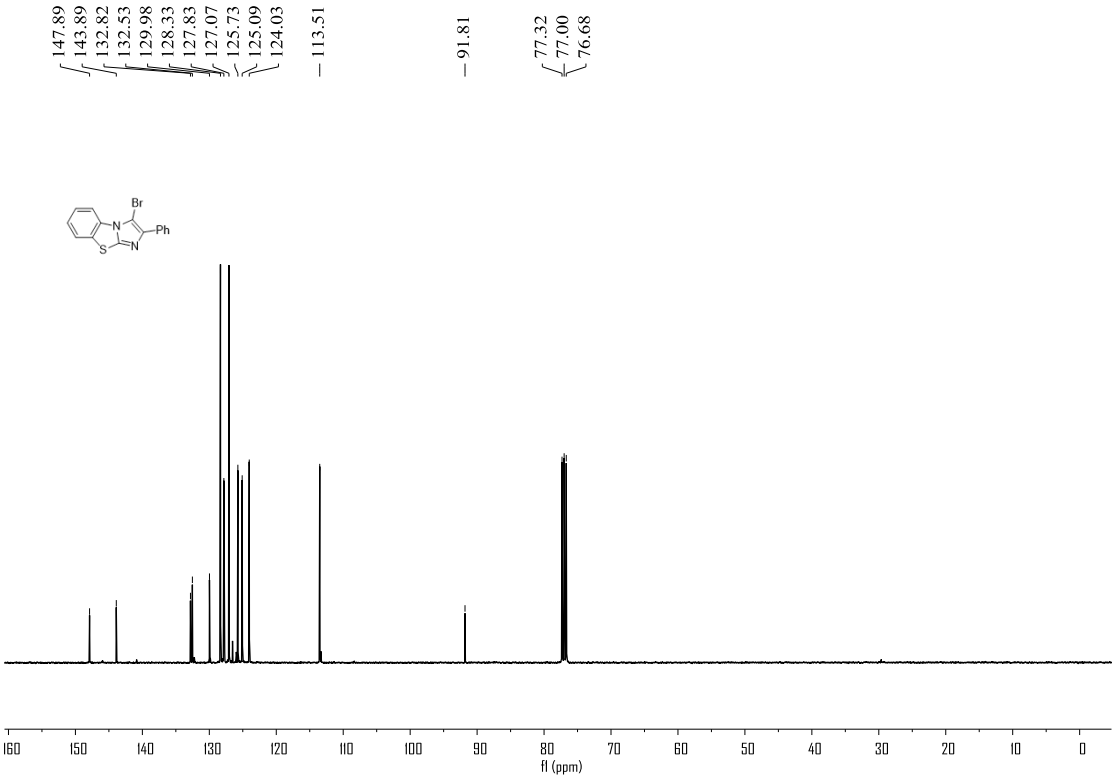

Figure S79. ^{1}H NMR (400 MHz, $CDCl_3$) spectrum of compound **4q**, related to **Figure 1**

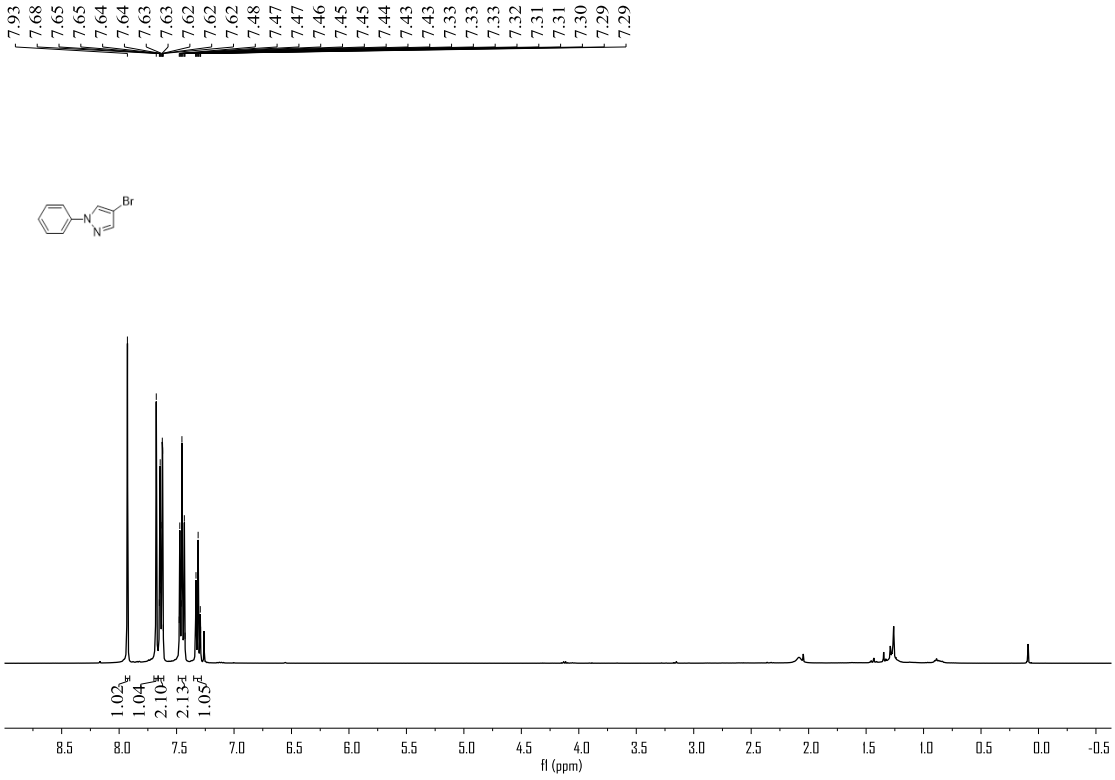

Figure S80. ^{13}C NMR (100 MHz, $CDCl_3$) spectrum of compound **4q**, related to **Figure 1**

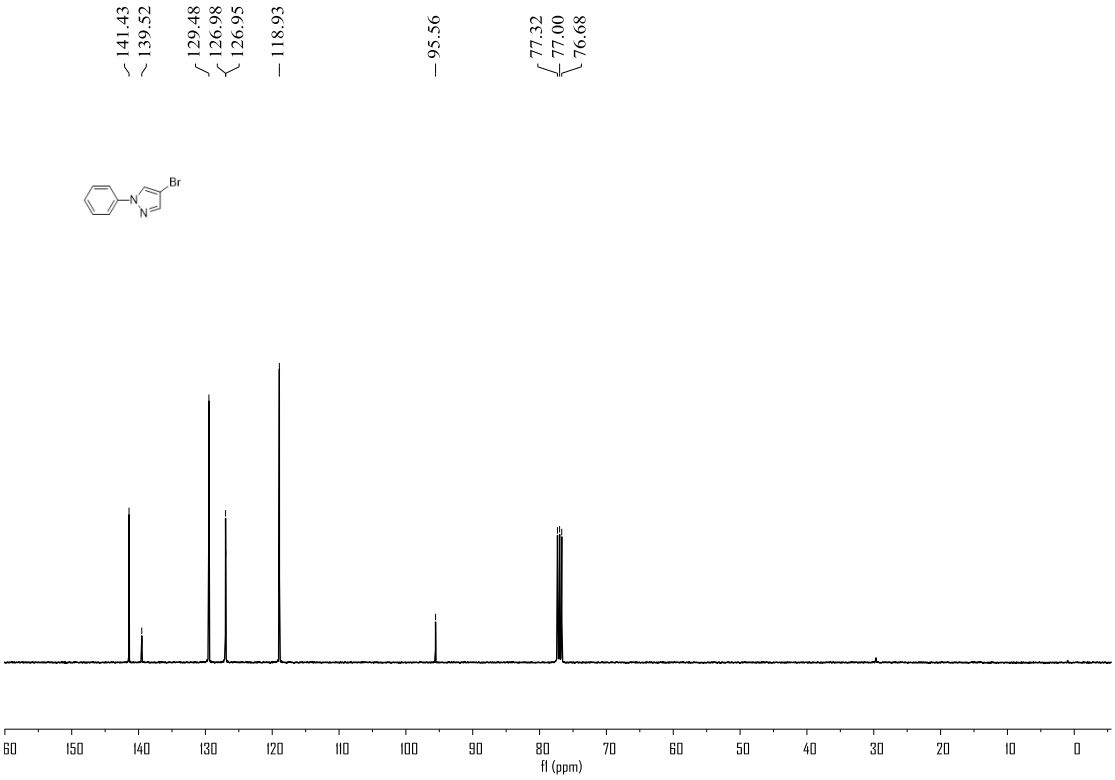

Figure S81. ^{1}H NMR (400 MHz, $CDCl_3$) spectrum of compound **4r**, related to **Figure 1**

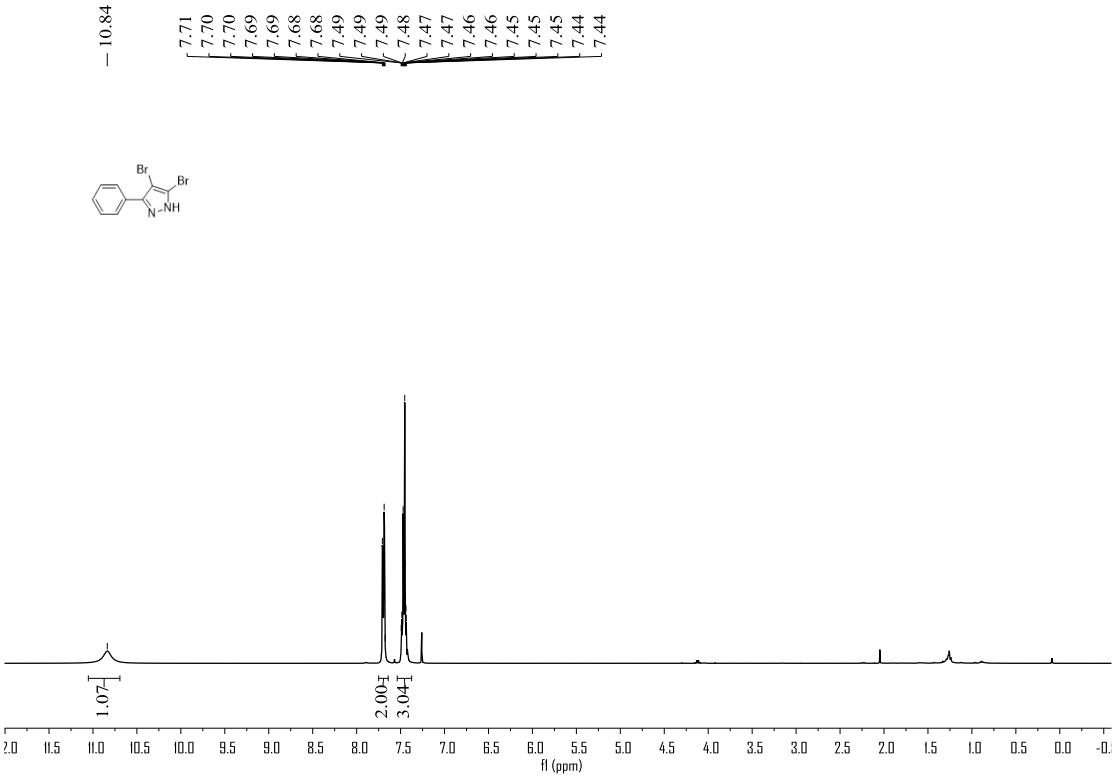

Figure S82. ^{13}C NMR (100 MHz, $CDCl_3$) spectrum of compound **4r**, related to **Figure 1**

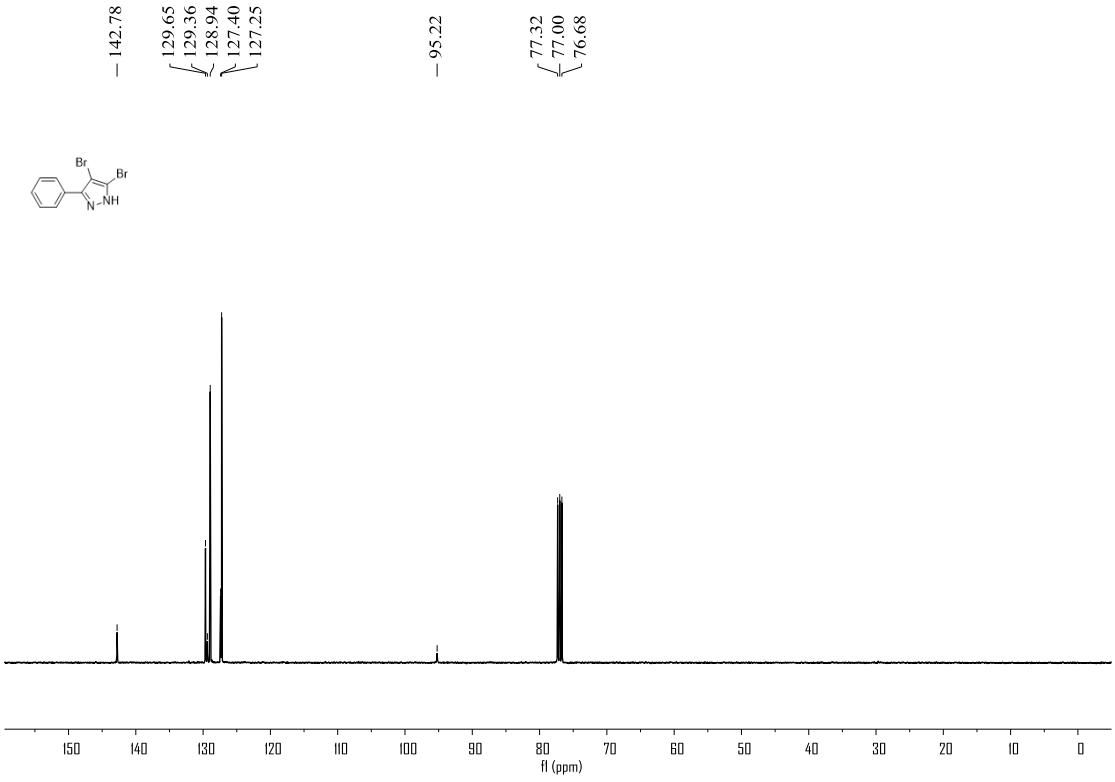

Figure S83. ^{1}H NMR (400 MHz, $CDCl_3$) spectrum of compound **4s**, related to **Figure 1**

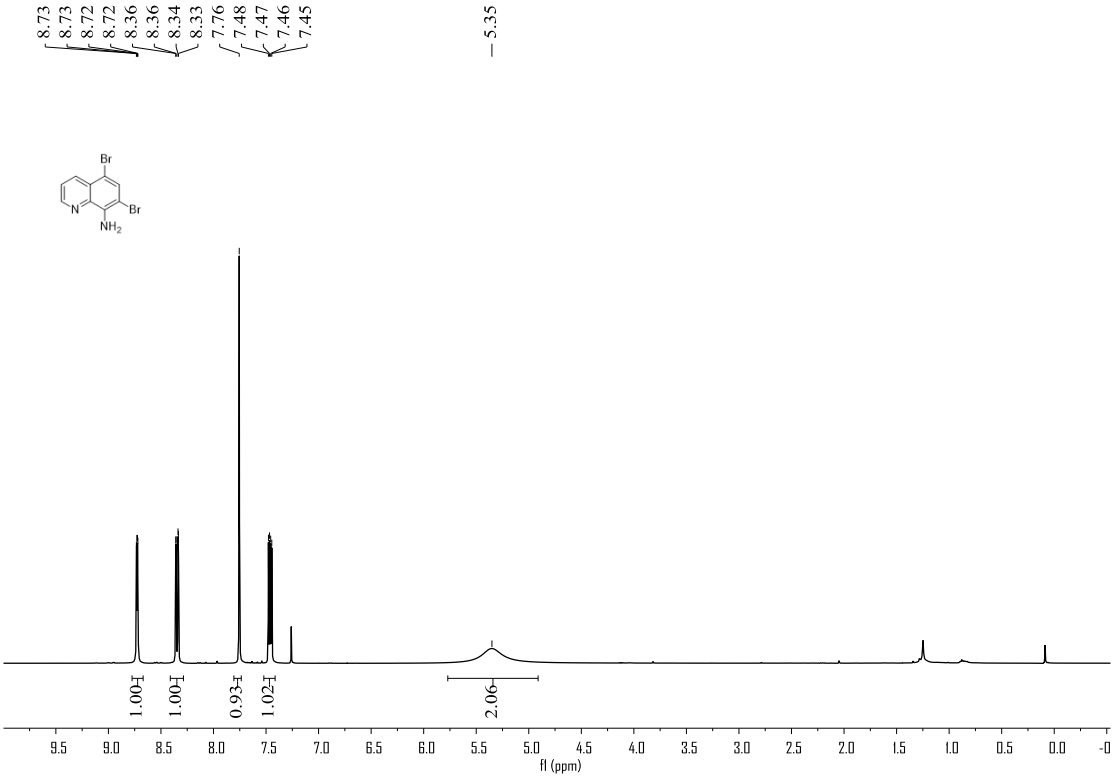

Figure S84. ^{13}C NMR (100 MHz, $CDCl_3$) spectrum of compound **4s**, related to **Figure 1**

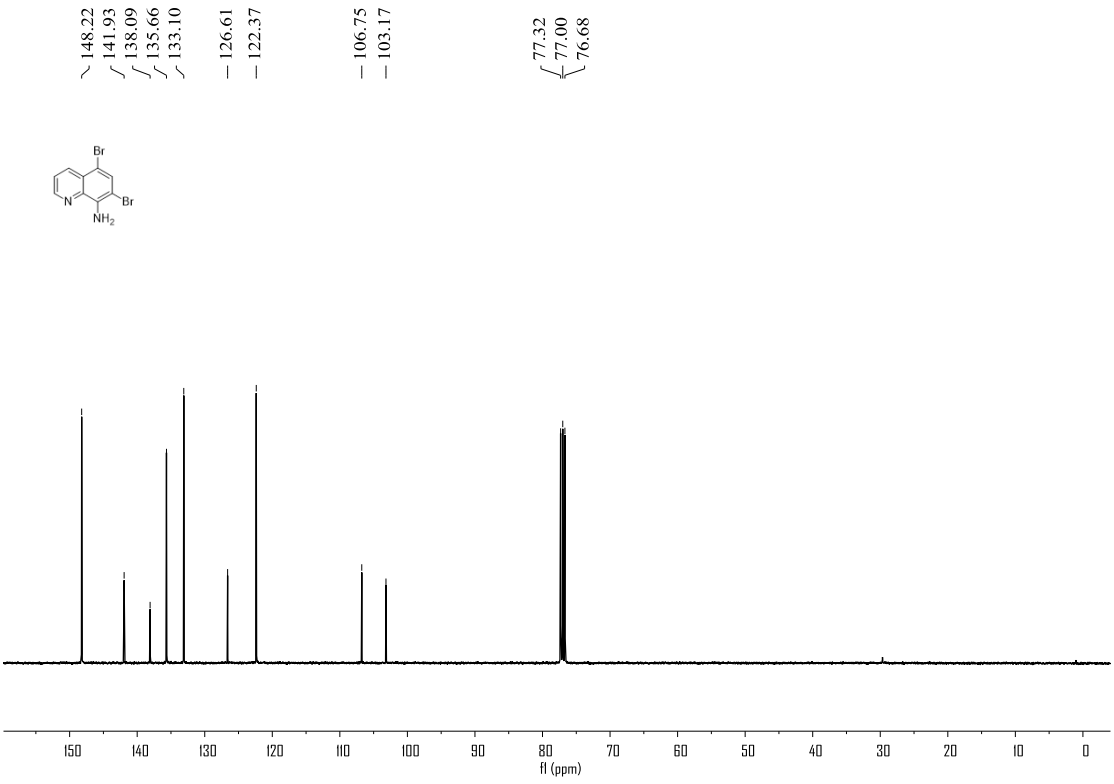

Figure S85. ^{1}H NMR (400 MHz, DMSO-d_6) spectrum of compound **4t**, related to **Figure 1**

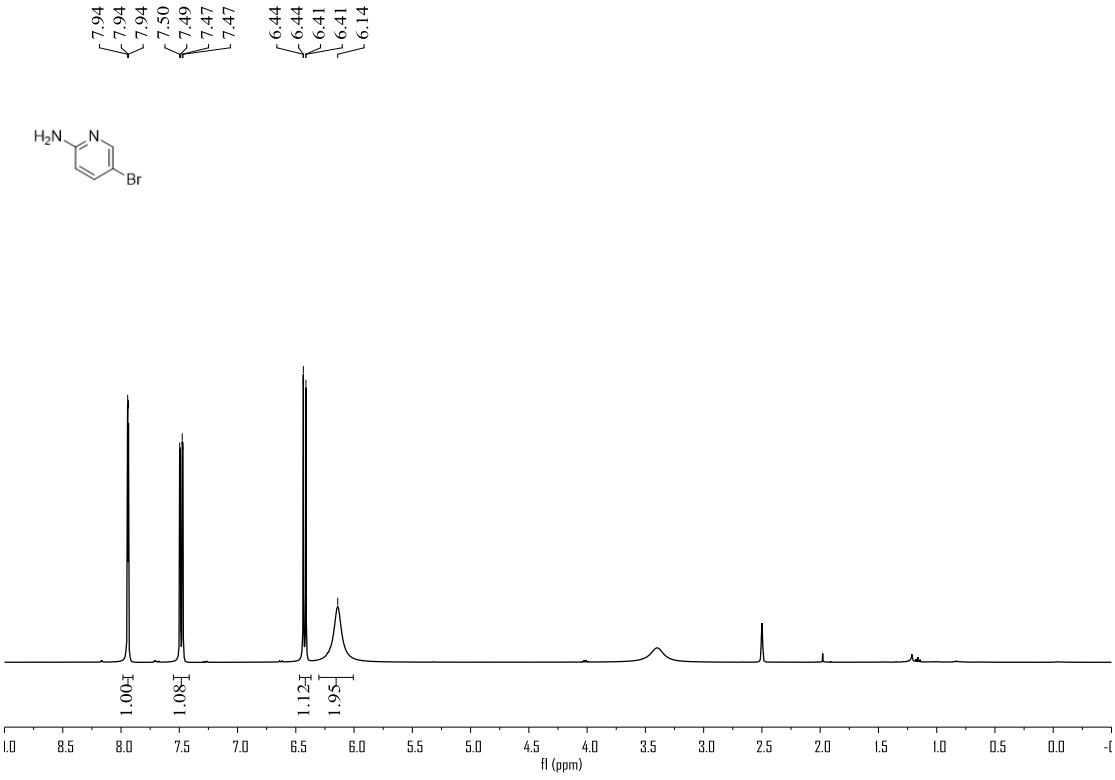

Figure S86. ^{13}C NMR (100 MHz, $CDCl_3$) spectrum of compound **4t**, related to **Figure 1**

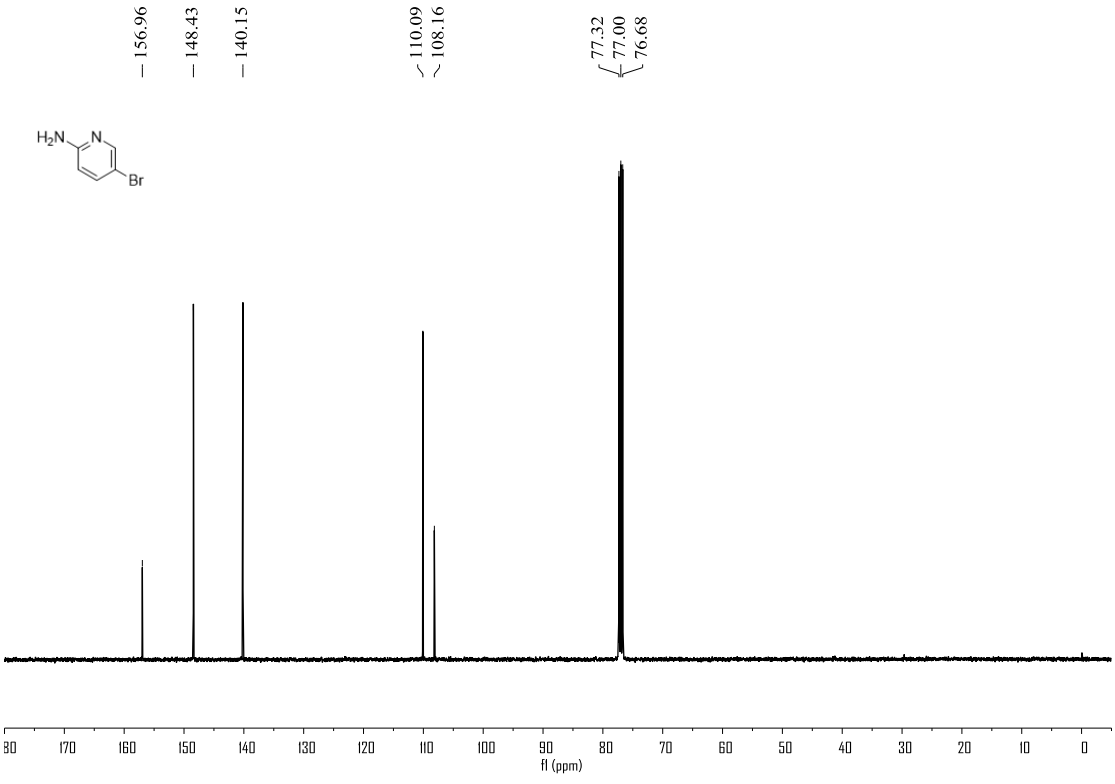

Figure S87. ^{1}H NMR (400 MHz, $CDCl_3$) spectrum of compound **4u**, related to **Figure 1**

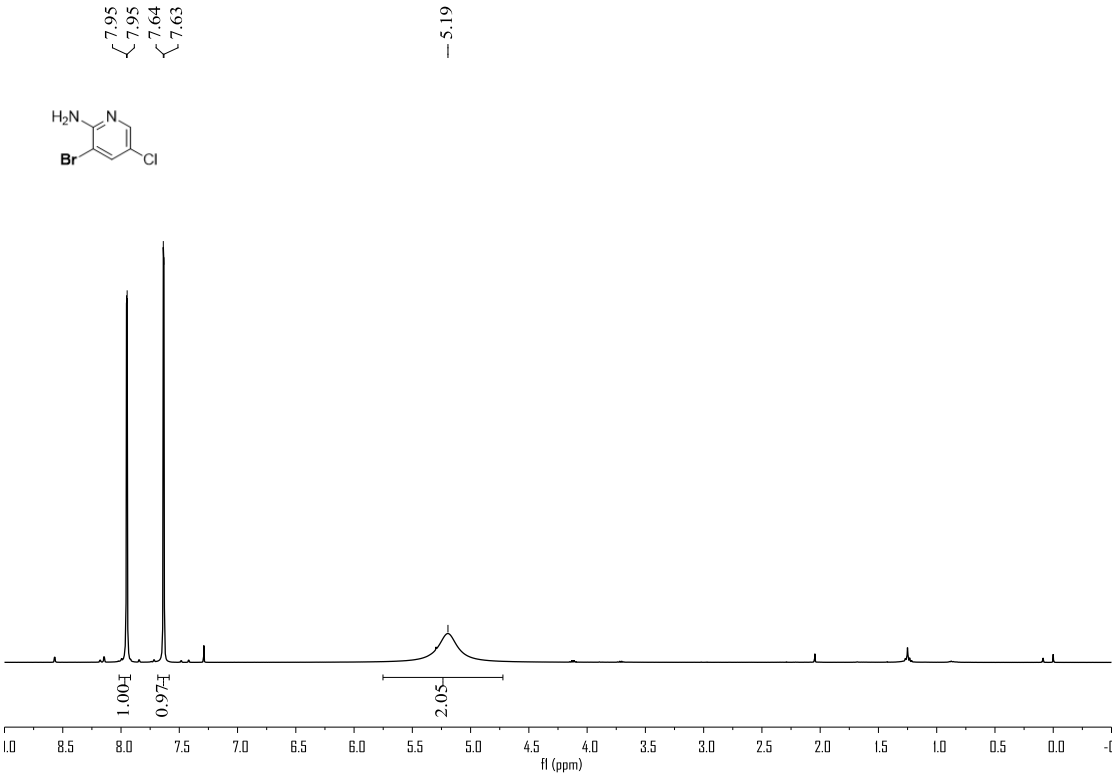

Figure S88. ^{13}C NMR (100 MHz, $CDCl_3$) spectrum of compound **4u**, related to **Figure 1**

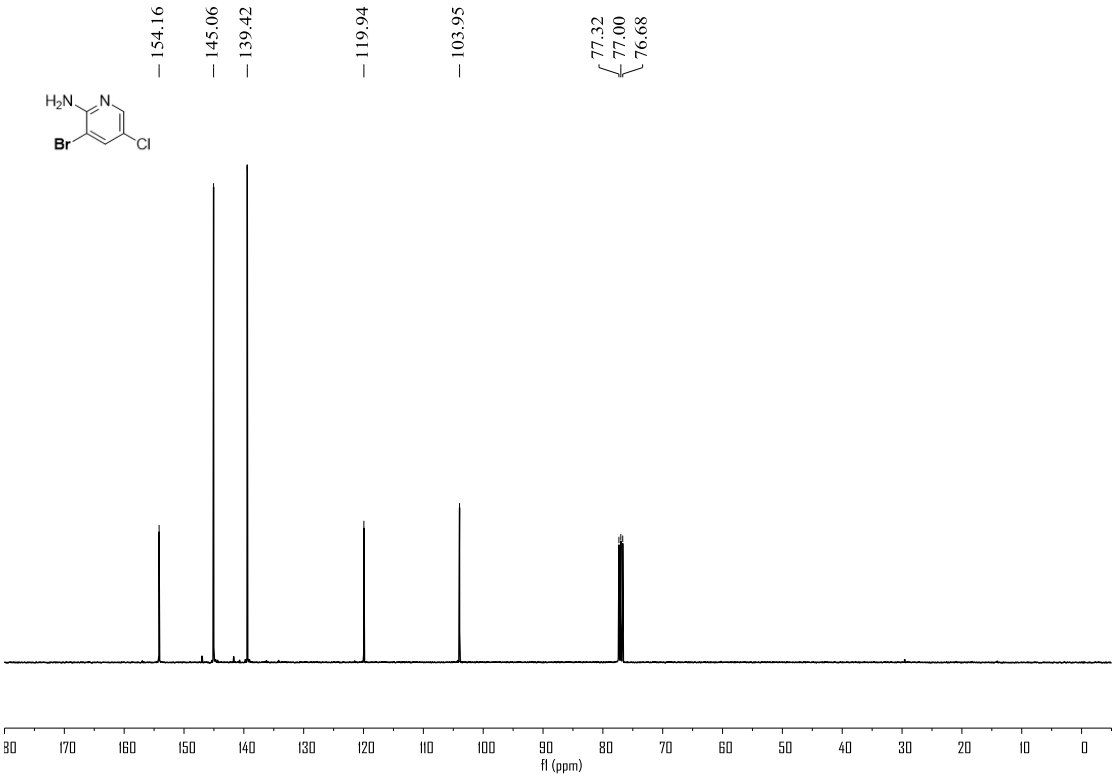

Figure S89. ^{1}H NMR (400 MHz, DMSO-d_6) spectrum of compound **4v**, related to **Figure 1**

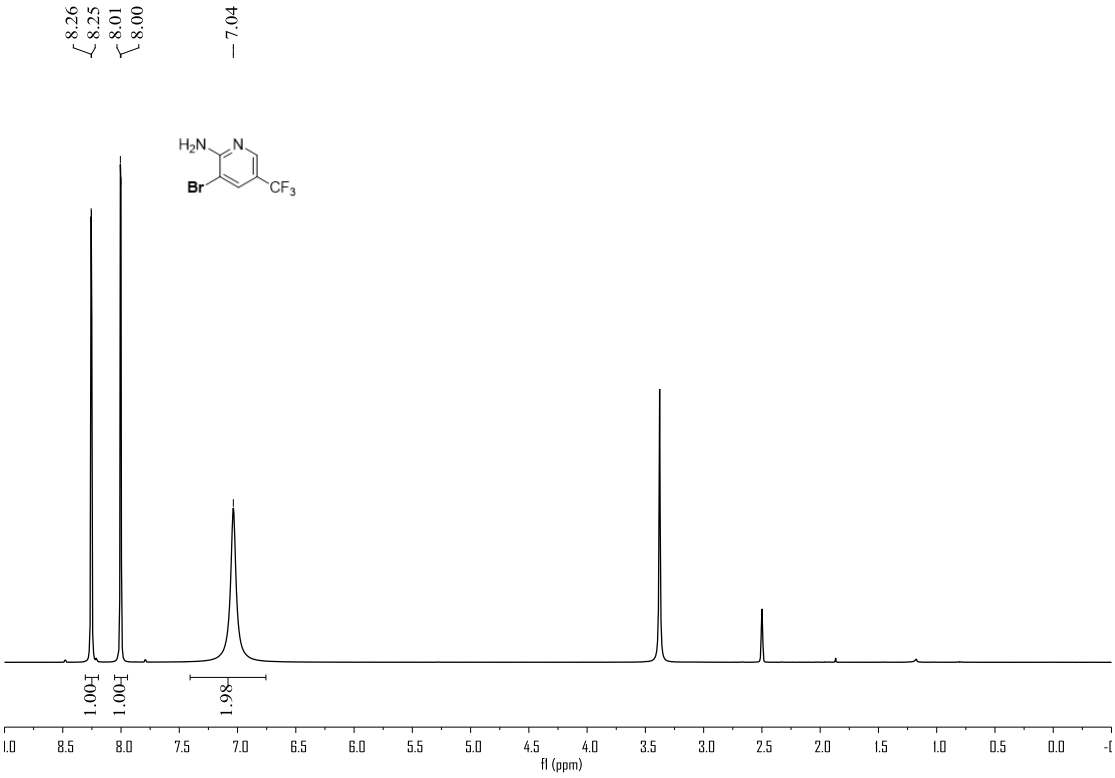

Figure S90. ^{13}C NMR (100 MHz, $CDCl_3$) spectrum of compound **4v**, related to **Figure 1**

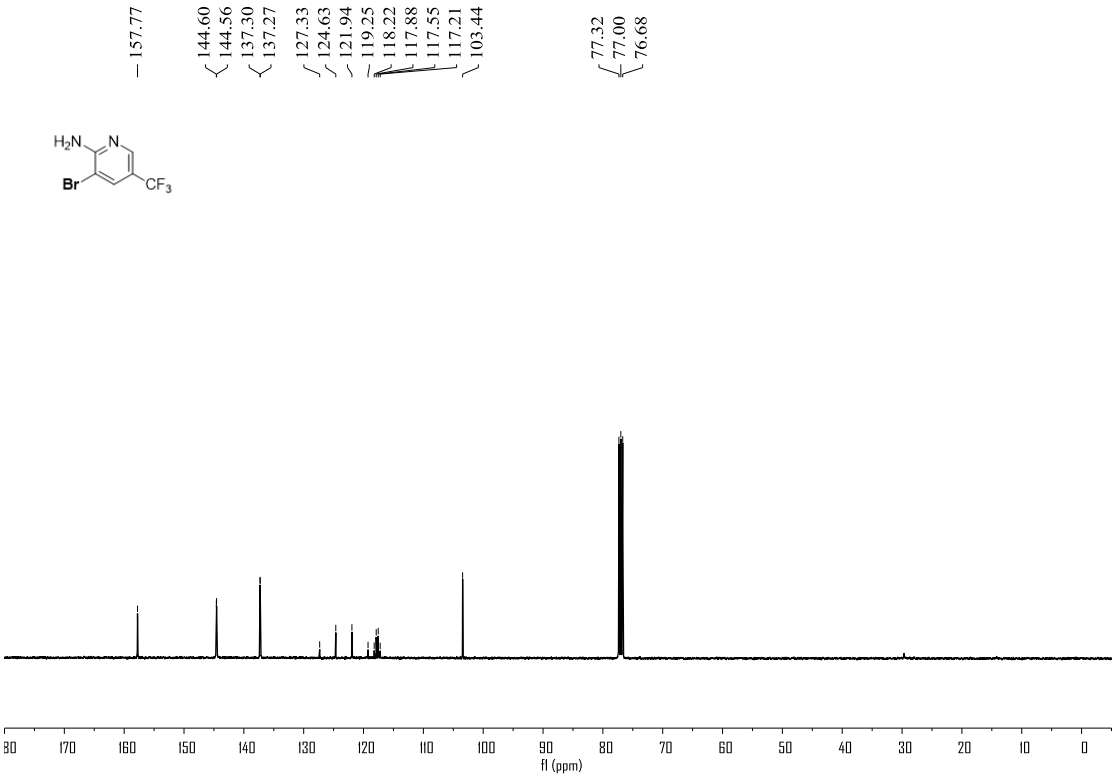

Figure S91. ^{19}F NMR (376 MHz, $CDCl_3$) spectrum of compound **4v**, related to **Figure 1**

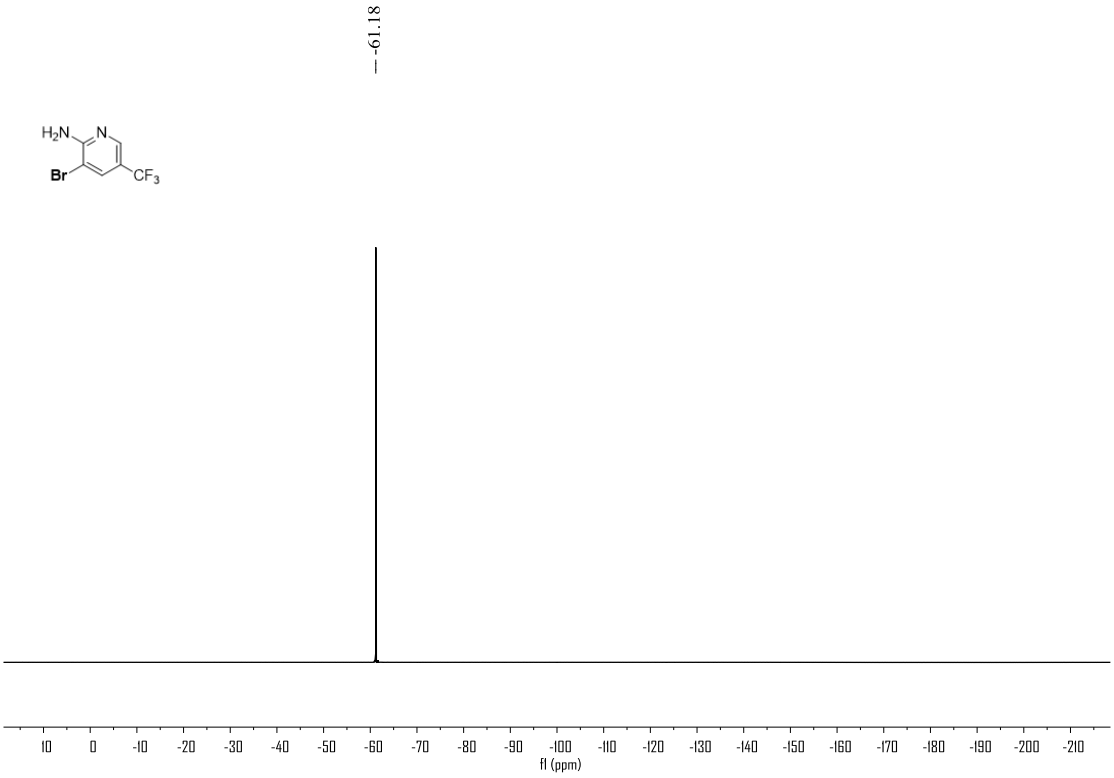

Figure S92. ^{1}H NMR (400 MHz, $CDCl_3$) spectrum of compound **4w**, related to **Figure 1**

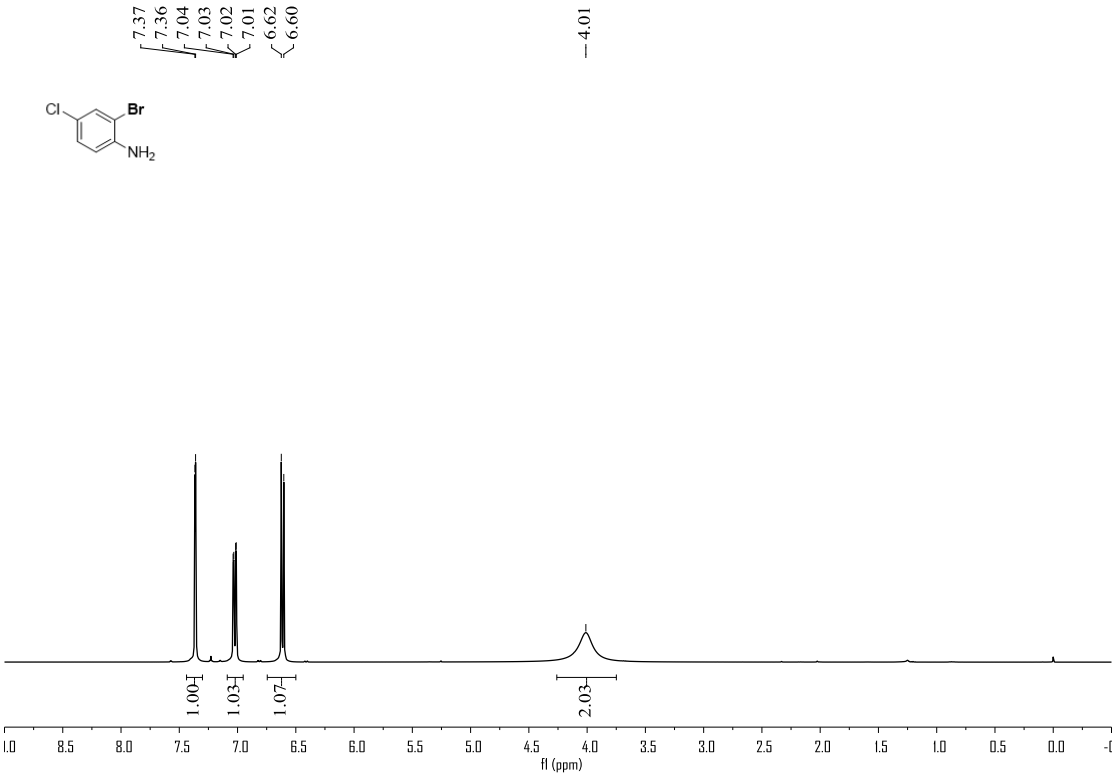

Figure S93. ^{13}C NMR (100 MHz, $CDCl_3$) spectrum of compound **4w**, related to **Figure 1**

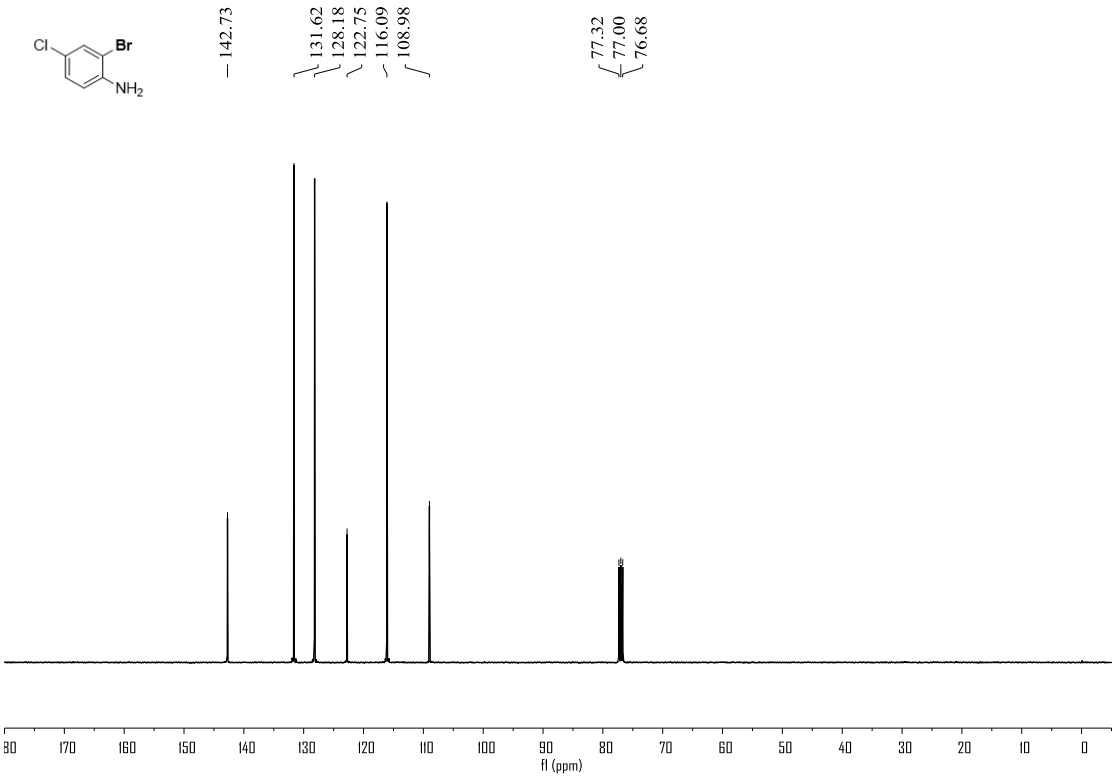

Figure S94. ^{1}H NMR (400 MHz, $CDCl_3$) spectrum of compound **4x**, related to **Figure 1**

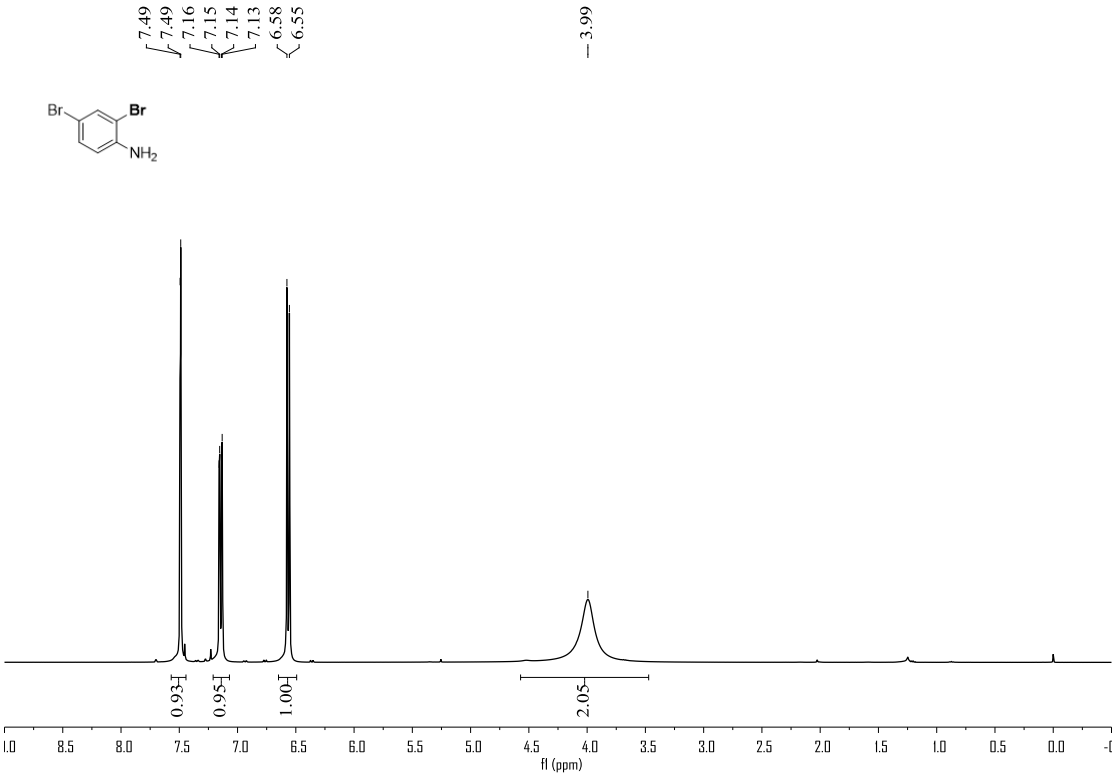

Figure S95. ^{13}C NMR (100 MHz, $CDCl_3$) spectrum of compound **4x**, related to **Figure 1**

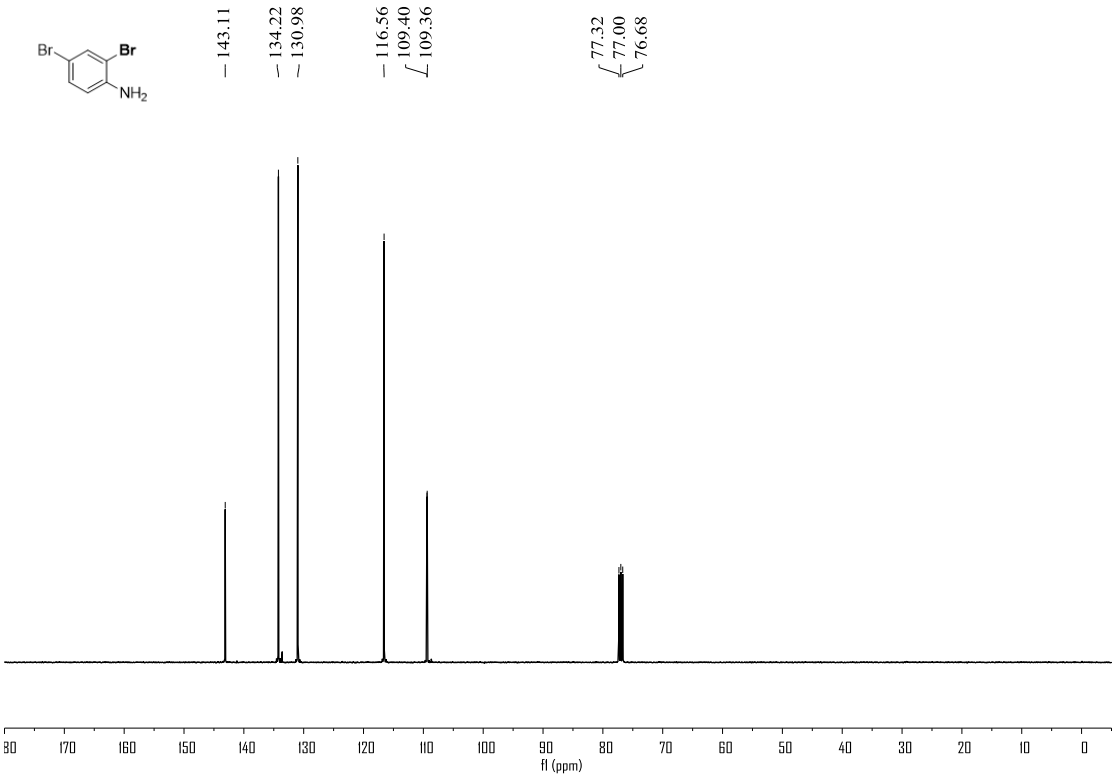

Figure S96. ^{1}H NMR (400 MHz, $CDCl_3$) spectrum of compound **4y**, related to **Figure 1**

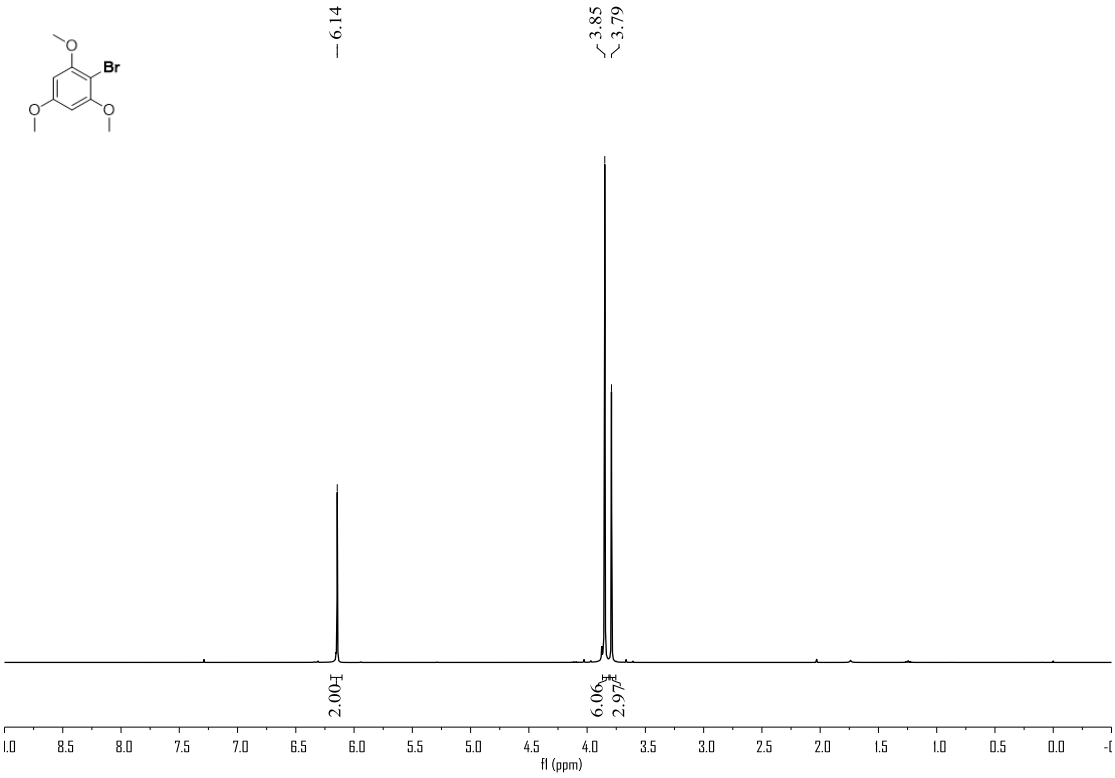

Figure S97. ^{13}C NMR (100 MHz, $CDCl_3$) spectrum of compound **4y**, related to **Figure 1**

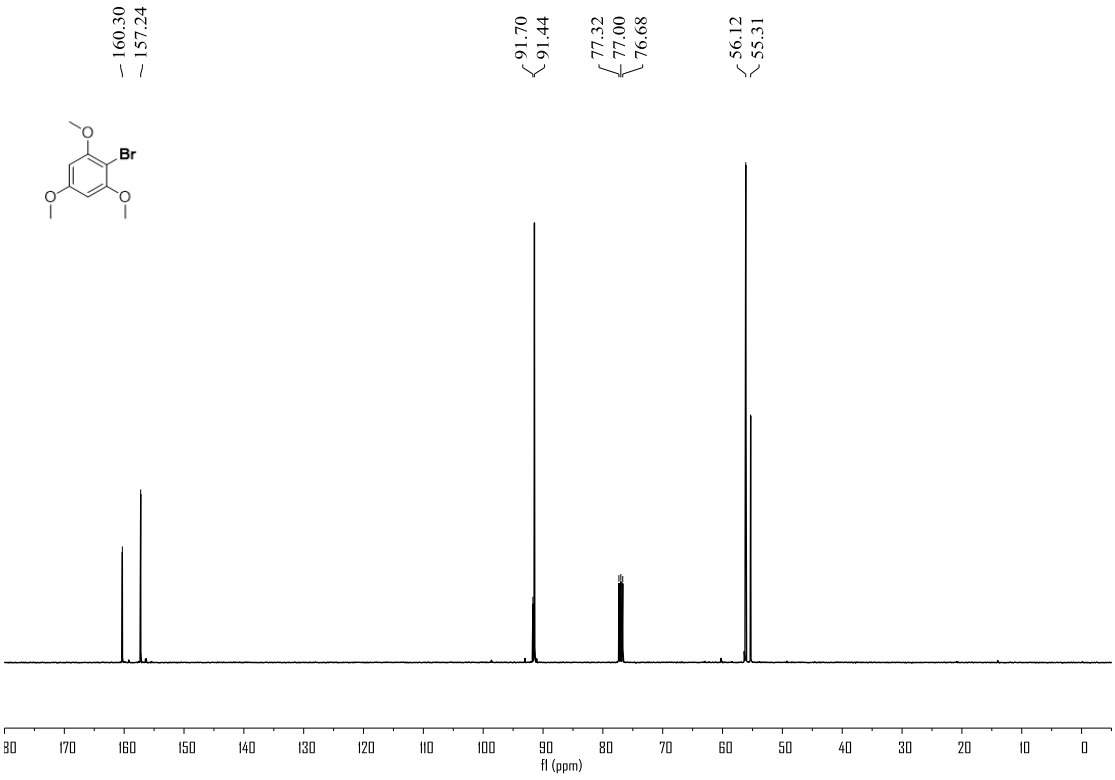

Figure S98. ^{1}H NMR (400 MHz, $CDCl_3$) spectrum of compound **4z**, related to **Figure 1**

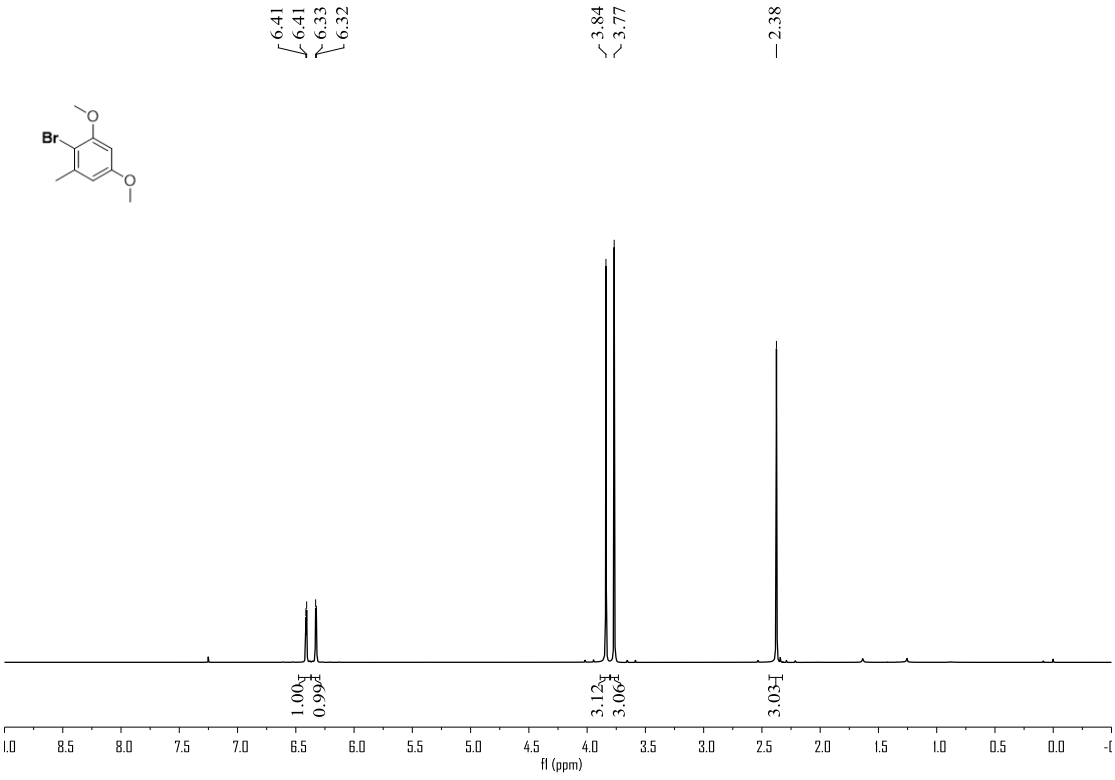

Figure S99. ^{13}C NMR (100 MHz, $CDCl_3$) spectrum of compound **4z**, related to **Figure 1**

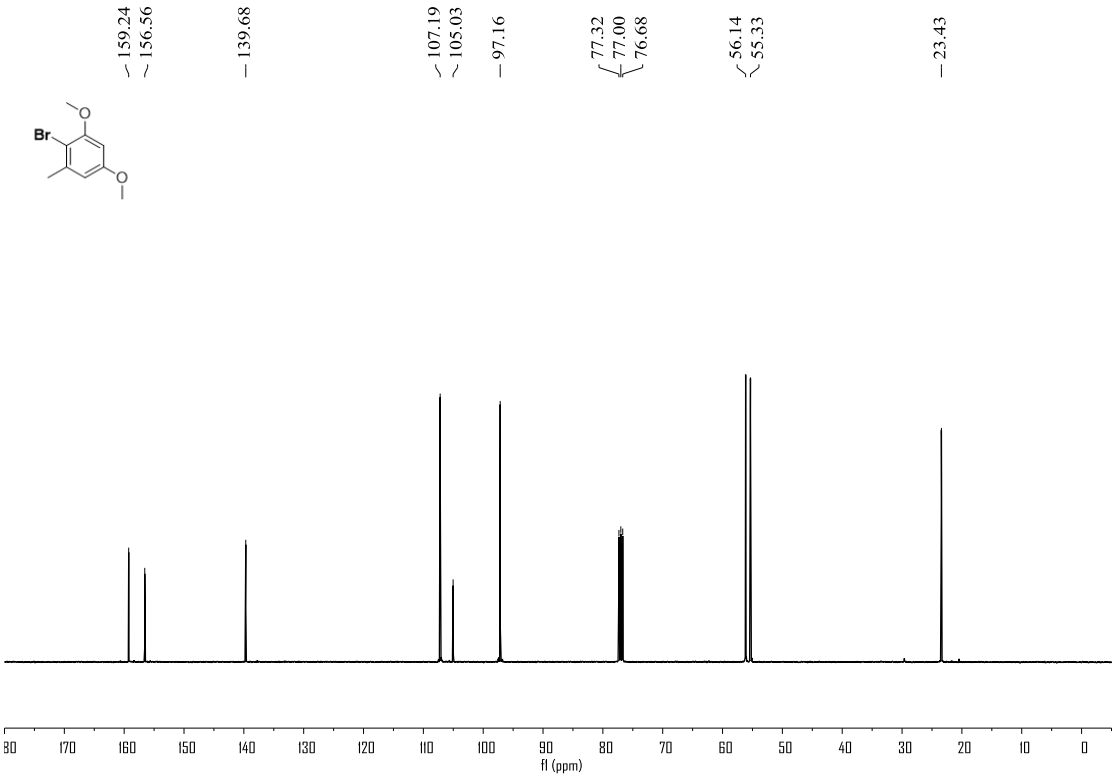

Figure S100. ^{1}H NMR (400 MHz, $CDCl_3$) spectrum of compound **6a**, related to **Figure 4**

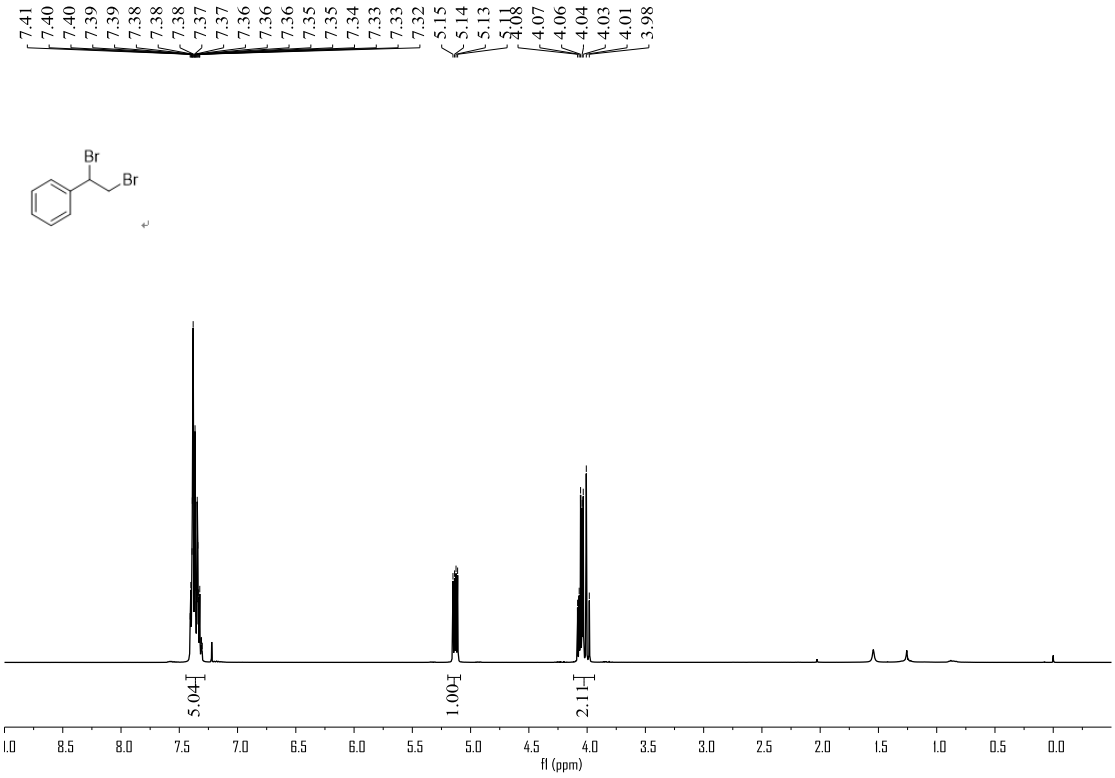

Figure S101. ^{13}C NMR (100 MHz, $CDCl_3$) spectrum of compound **6a**, related to **Figure 4**

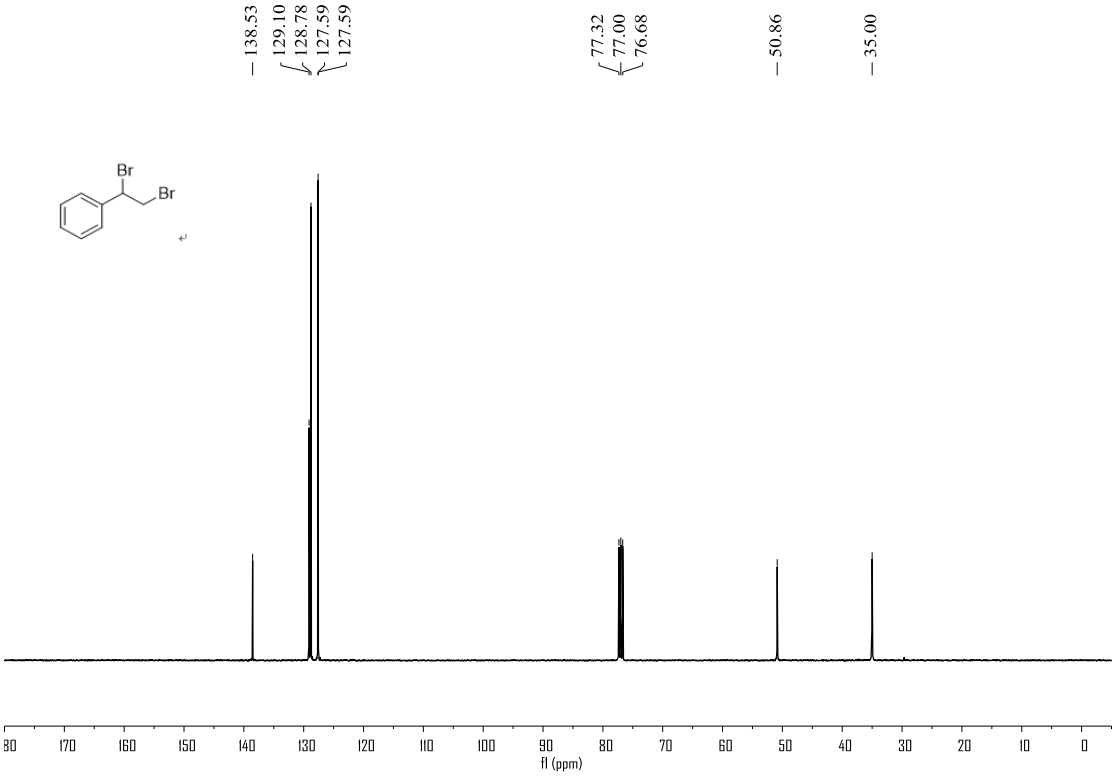

Figure S102. ^{1}H NMR (400 MHz, $CDCl_3$) spectrum of compound **6b**, related to **Figure 4**

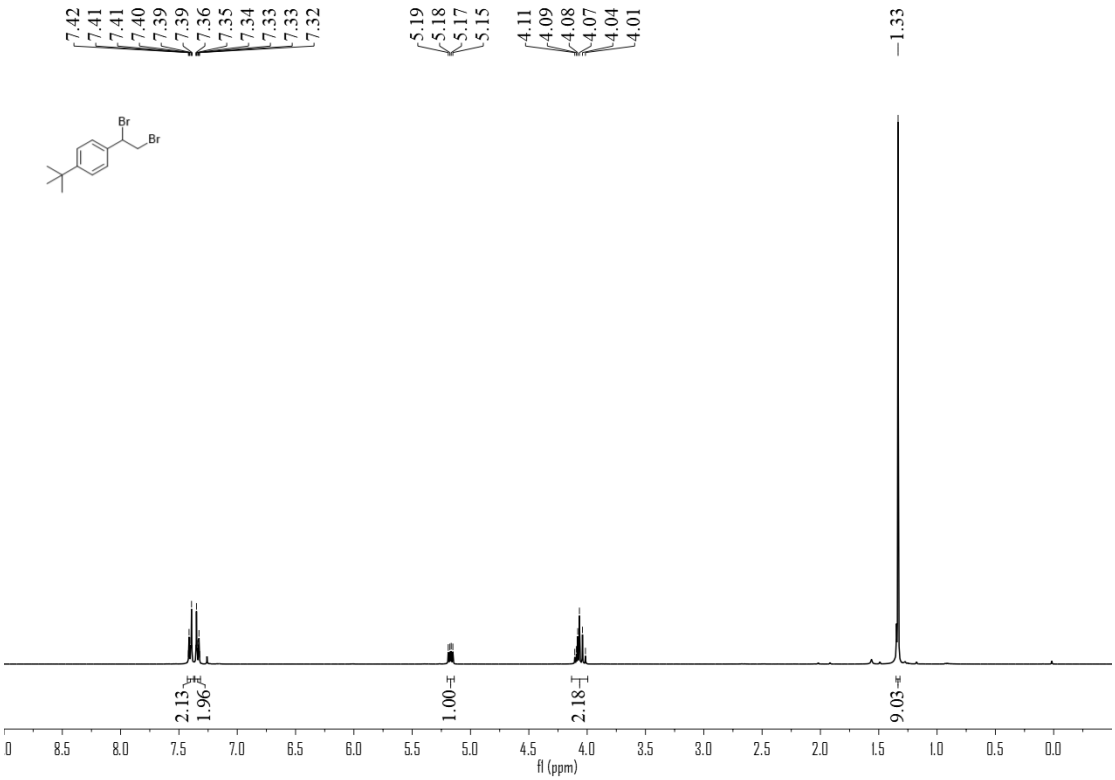

Figure S103. ^{13}C NMR (100 MHz, $CDCl_3$) spectrum of compound **6b**, related to **Figure 4**

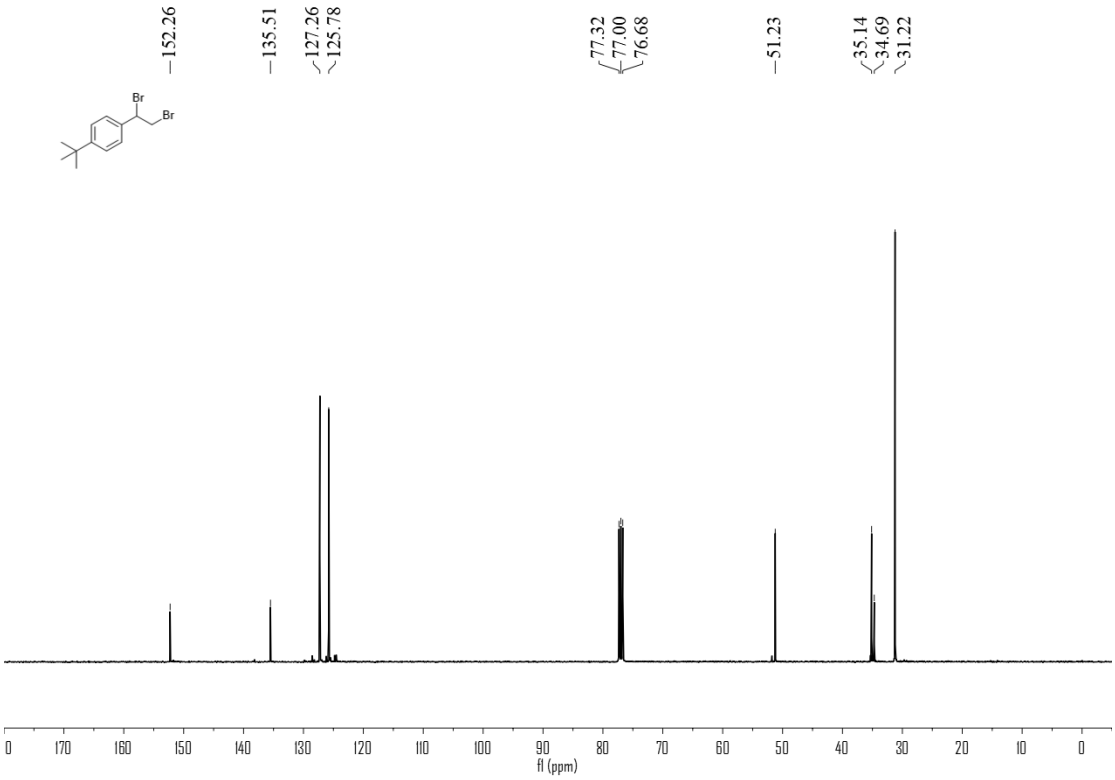

Figure S104. ^{1}H NMR (400 MHz, $CDCl_3$) spectrum of compound **6c**, related to **Figure 4**

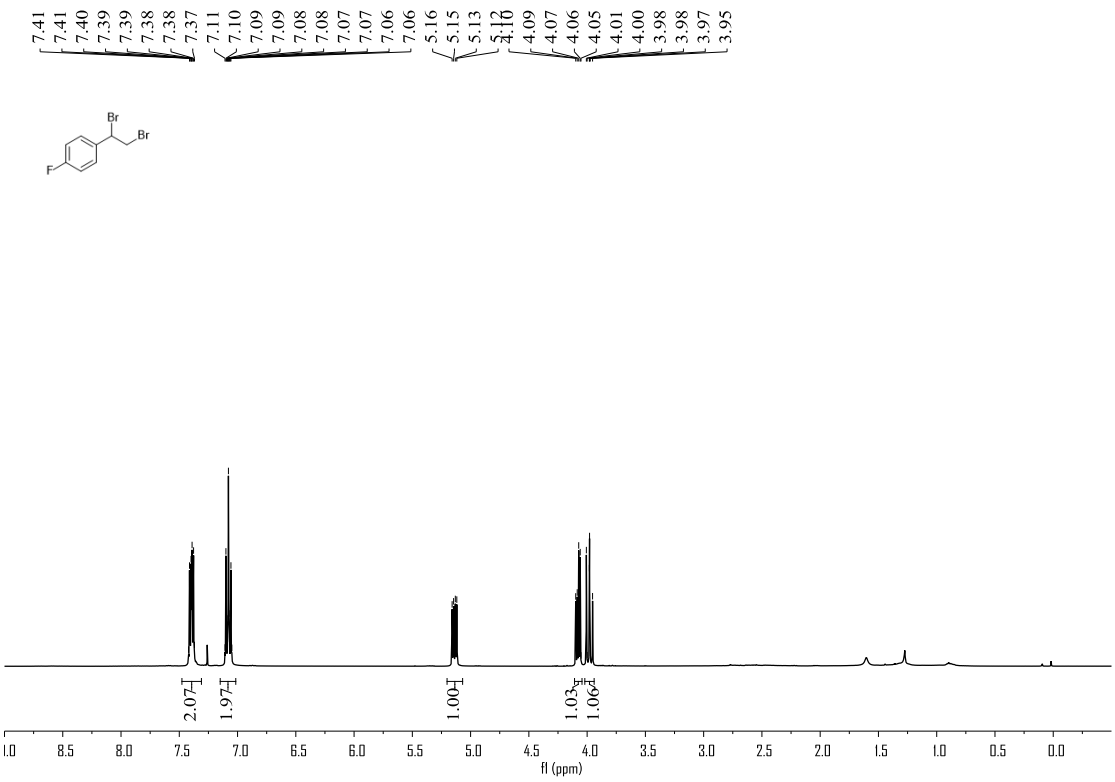

Figure S105. ^{13}C NMR (100 MHz, $CDCl_3$) spectrum of compound **6c**, related to **Figure 4**

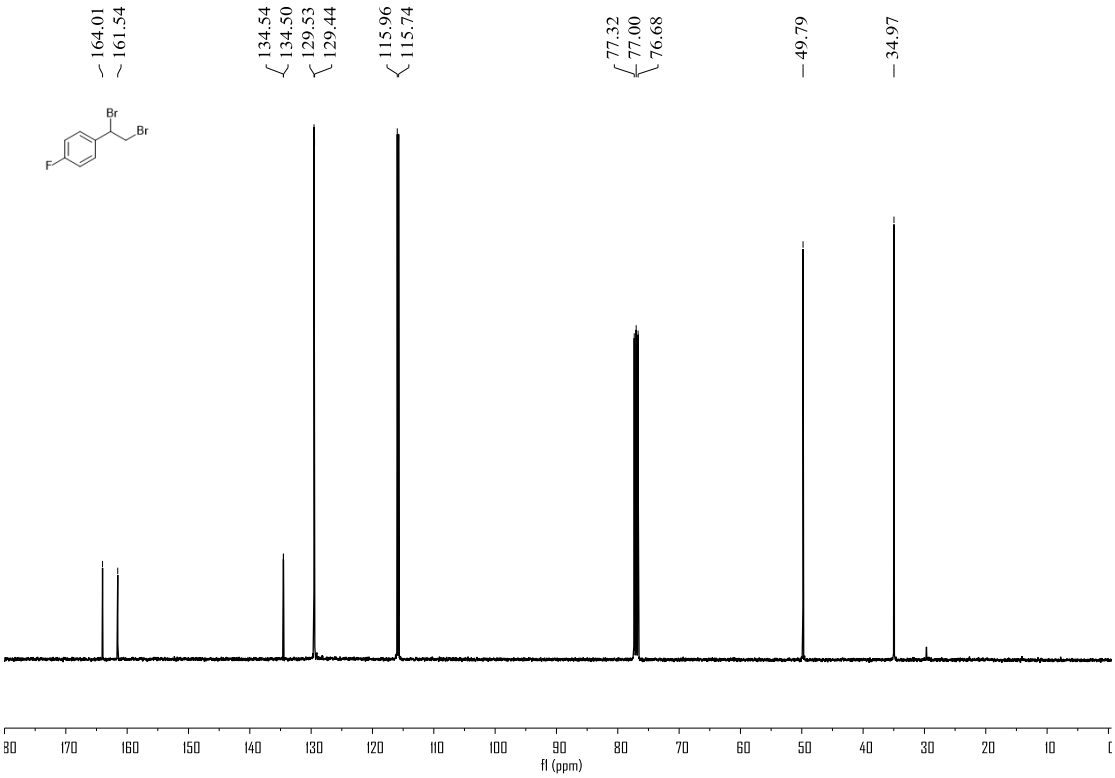

Figure S106. ^{19}F NMR (376 MHz, $CDCl_3$) spectrum of compound **6c**, related to **Figure 4**

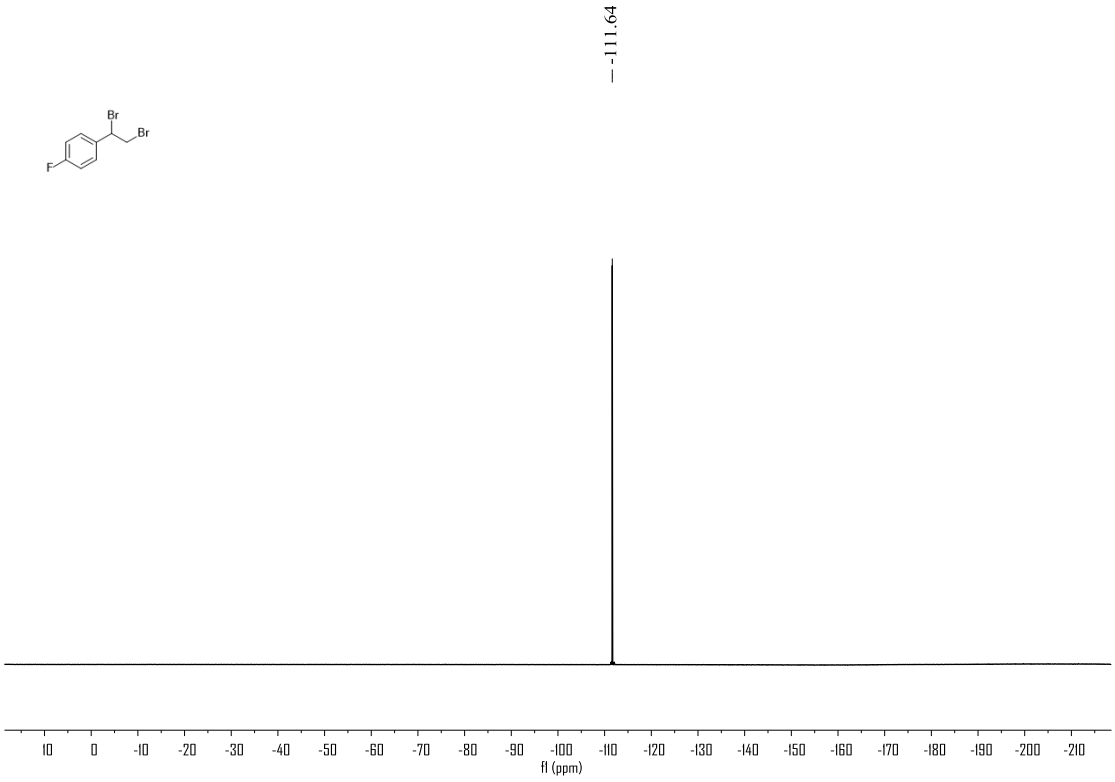

Figure S107. ^{1}H NMR (400 MHz, $CDCl_3$) spectrum of compound **6d**, related to **Figure 4**

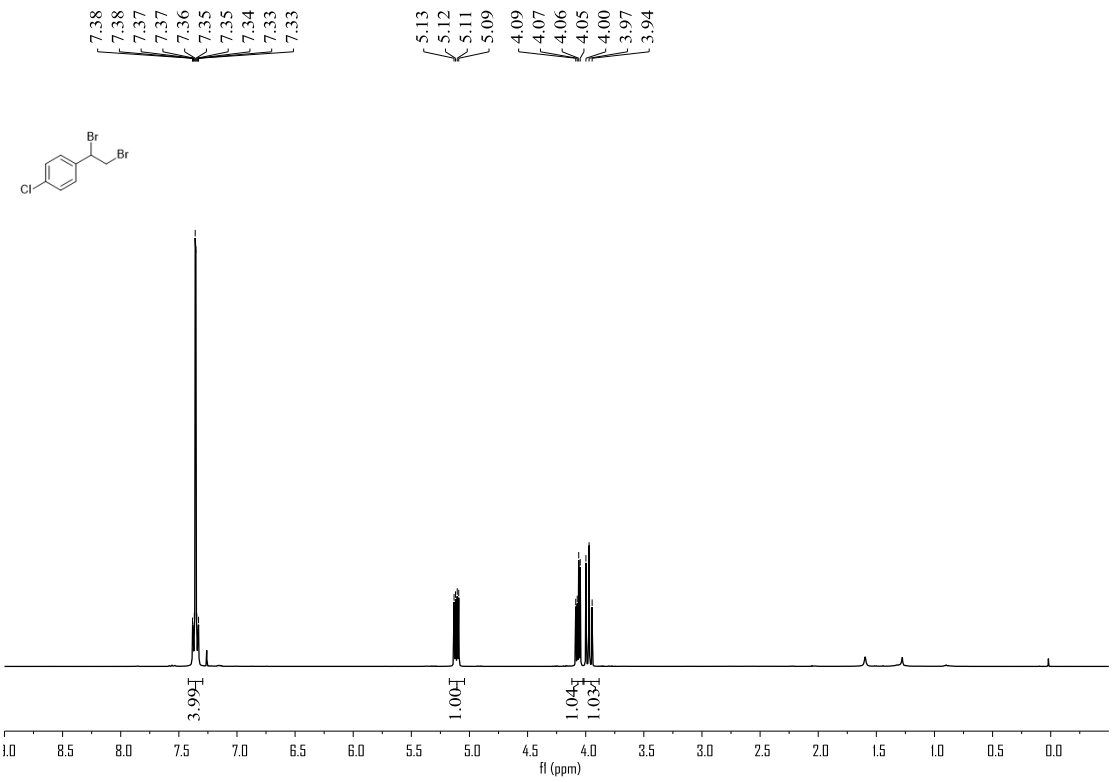

Figure S108. ^{13}C NMR (100 MHz, $CDCl_3$) spectrum of compound **6d**, related to **Figure 4**

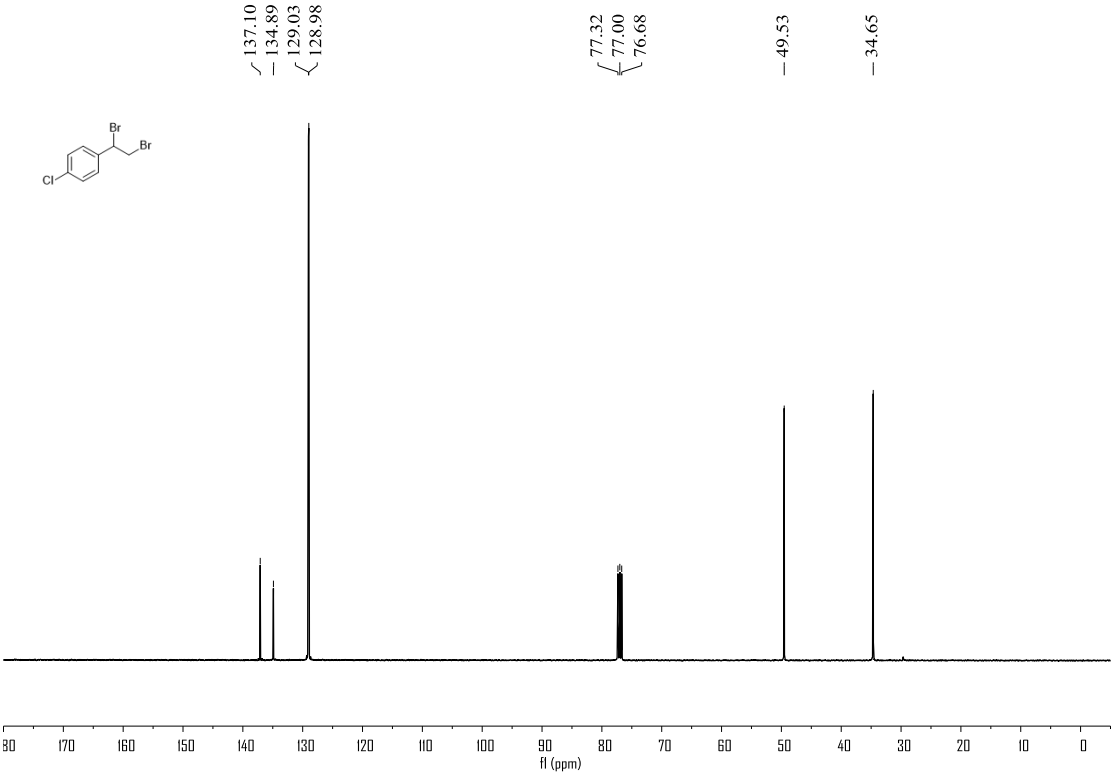

Figure S109. ^{1}H NMR (400 MHz, $CDCl_3$) spectrum of compound **6e**, related to **Figure 4**

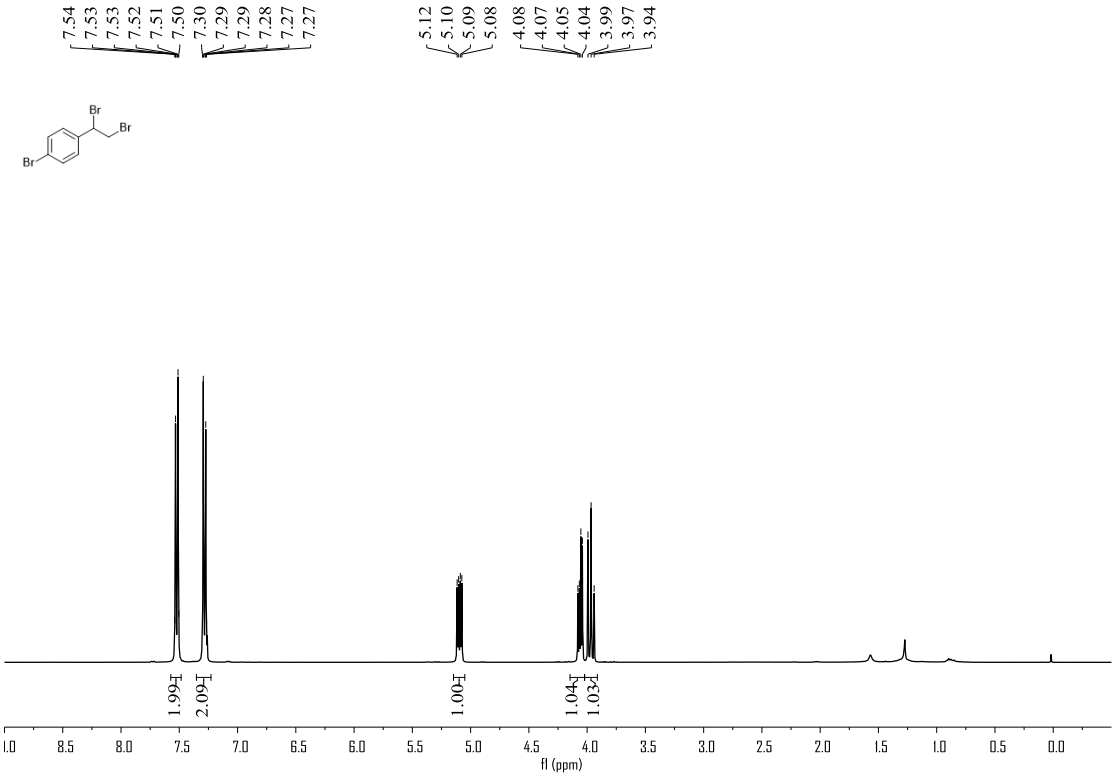

Figure S110. ^{13}C NMR (100 MHz, $CDCl_3$) spectrum of compound **6e**, related to **Figure 4**

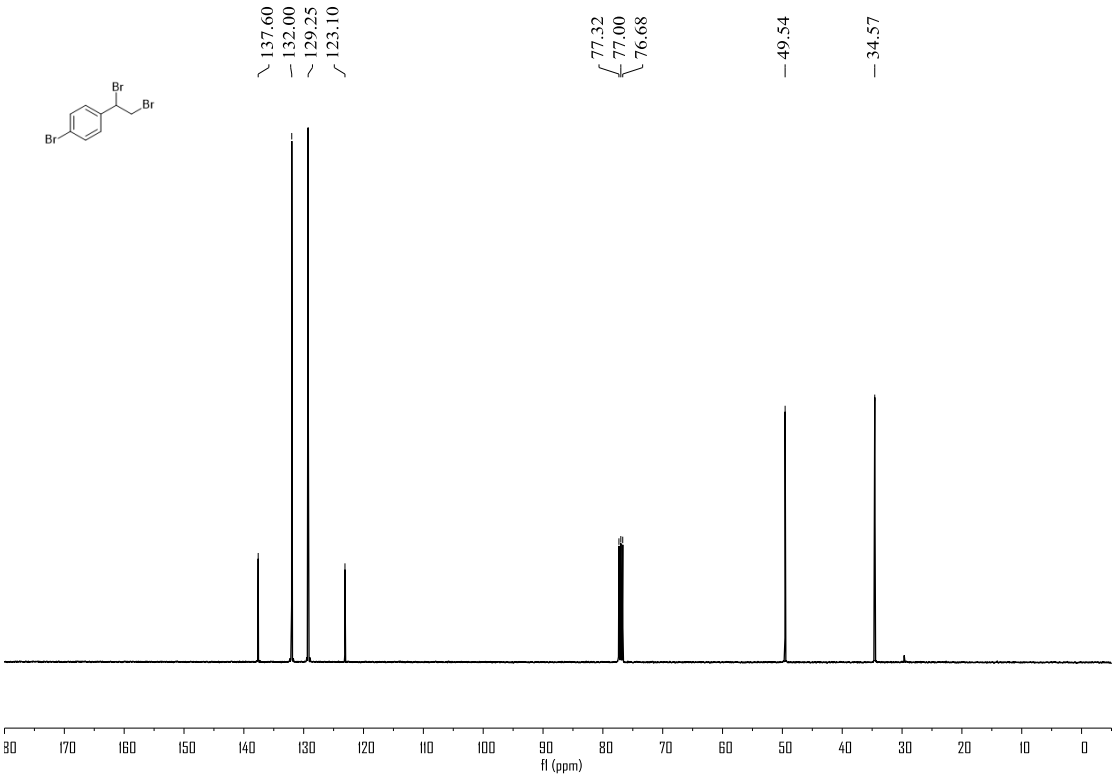

Figure S111. ^{1}H NMR (400 MHz, $CDCl_3$) spectrum of compound **6f**, related to **Figure 4**

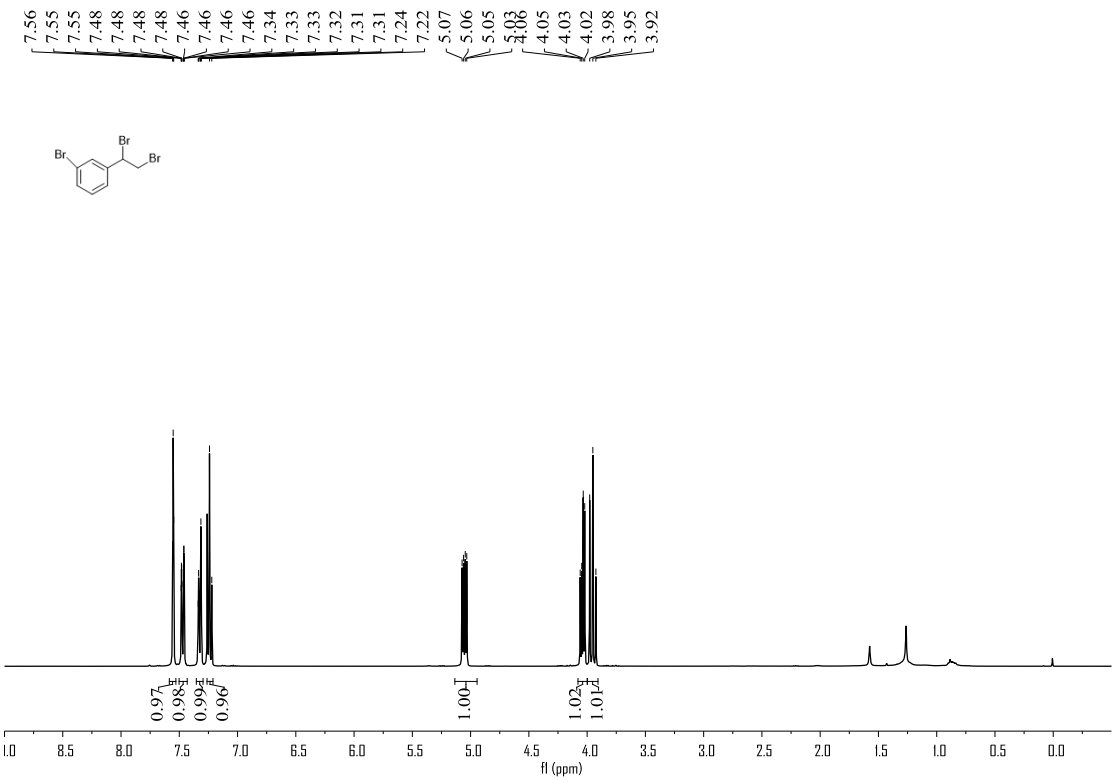

Figure S112. ^{13}C NMR (100 MHz, $CDCl_3$) spectrum of compound **6f**, related to **Figure 4**

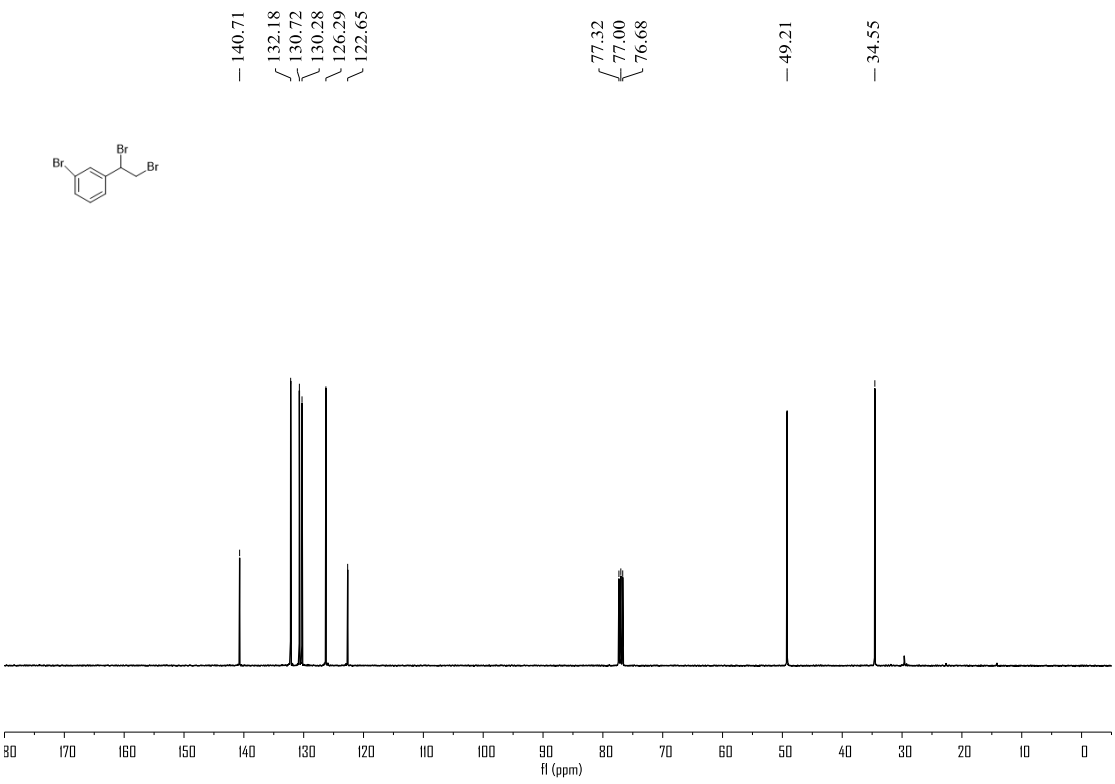

Figure S113. ^{1}H NMR (400 MHz, $CDCl_3$) spectrum of compound **6g**, related to **Figure 4**

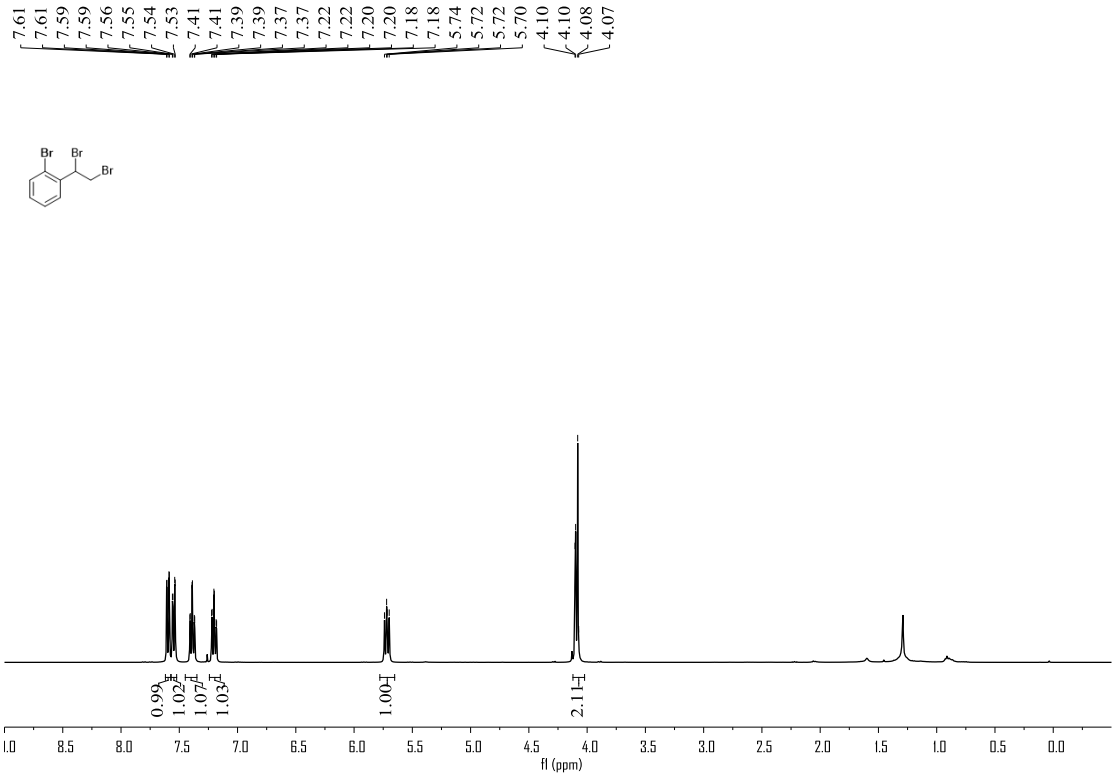

Figure S114. ^{13}C NMR (100 MHz, $CDCl_3$) spectrum of compound **6g**, related to **Figure 4**

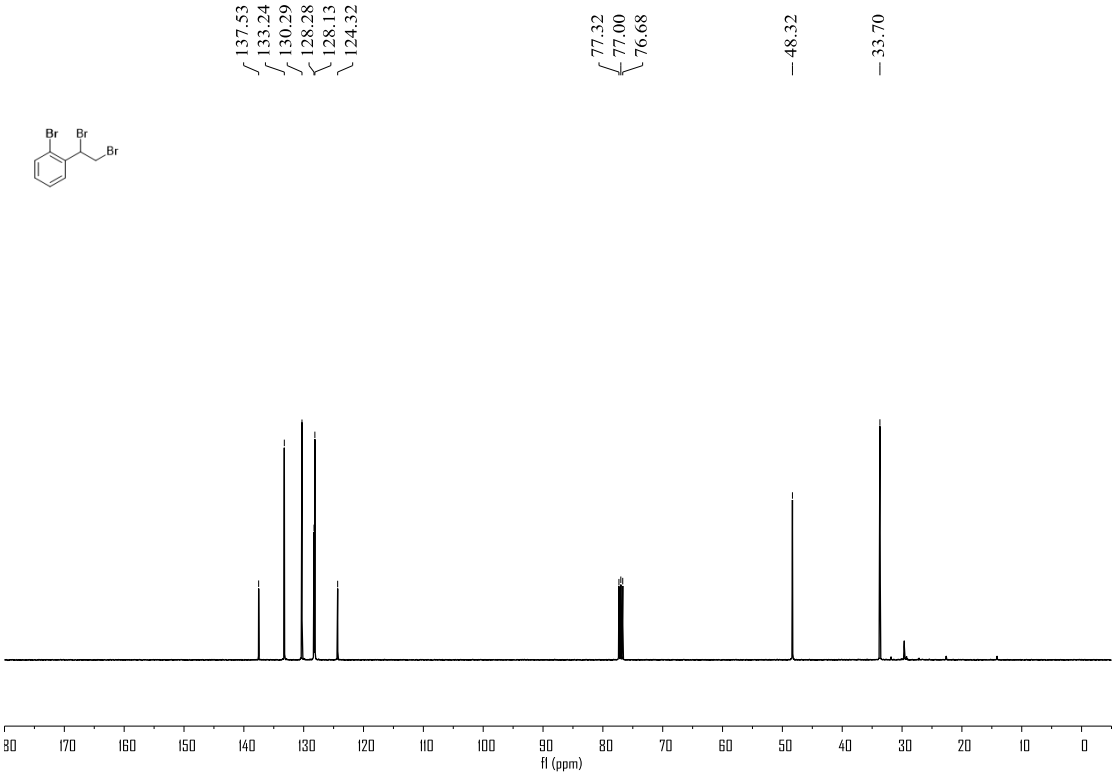

Figure S115. ^{1}H NMR (400 MHz, $CDCl_3$) spectrum of compound **6h**, related to **Figure 4**

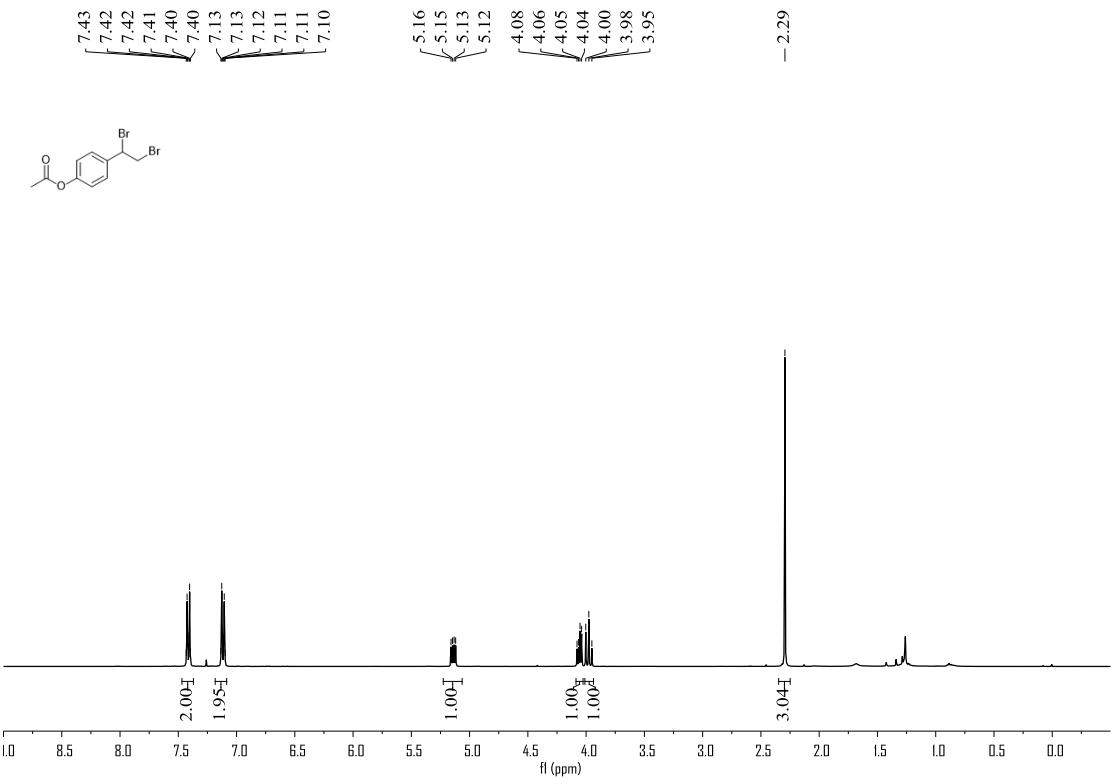

Figure S116. ^{13}C NMR (100 MHz, $CDCl_3$) spectrum of compound **6h**, related to **Figure 4**

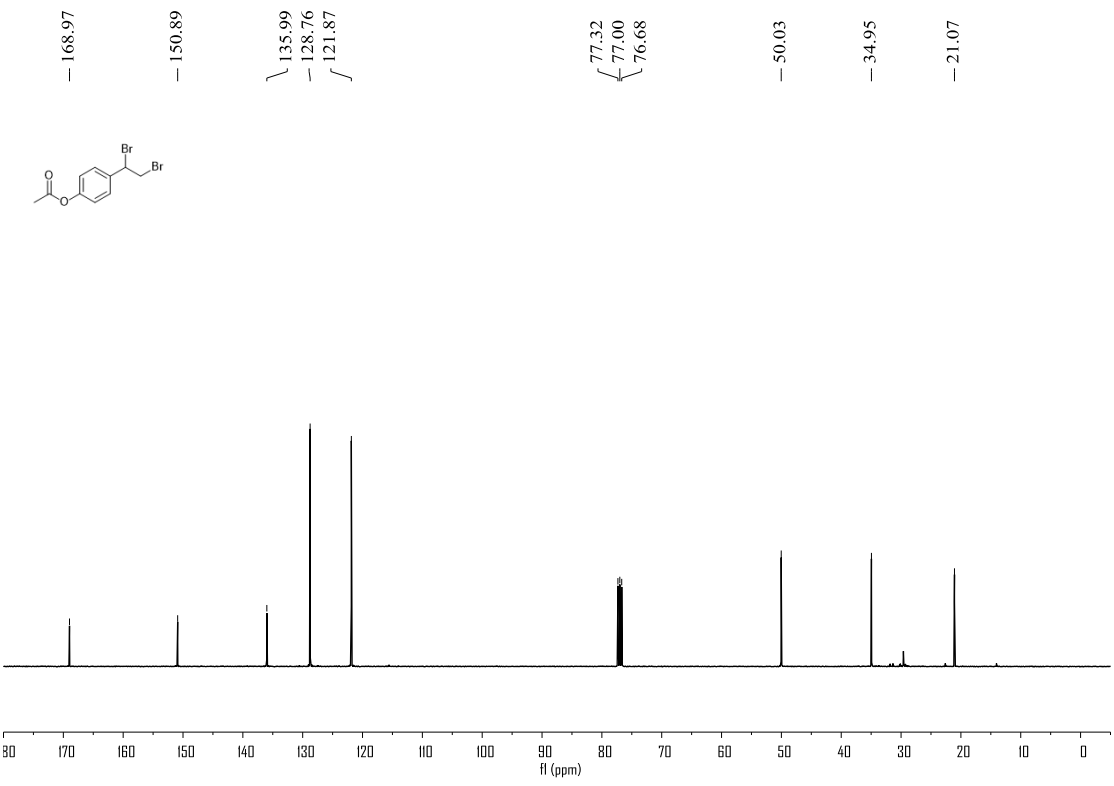

Figure S117. ^{1}H NMR (400 MHz, $CDCl_3$) spectrum of compound **6i**, related to **Figure 4**

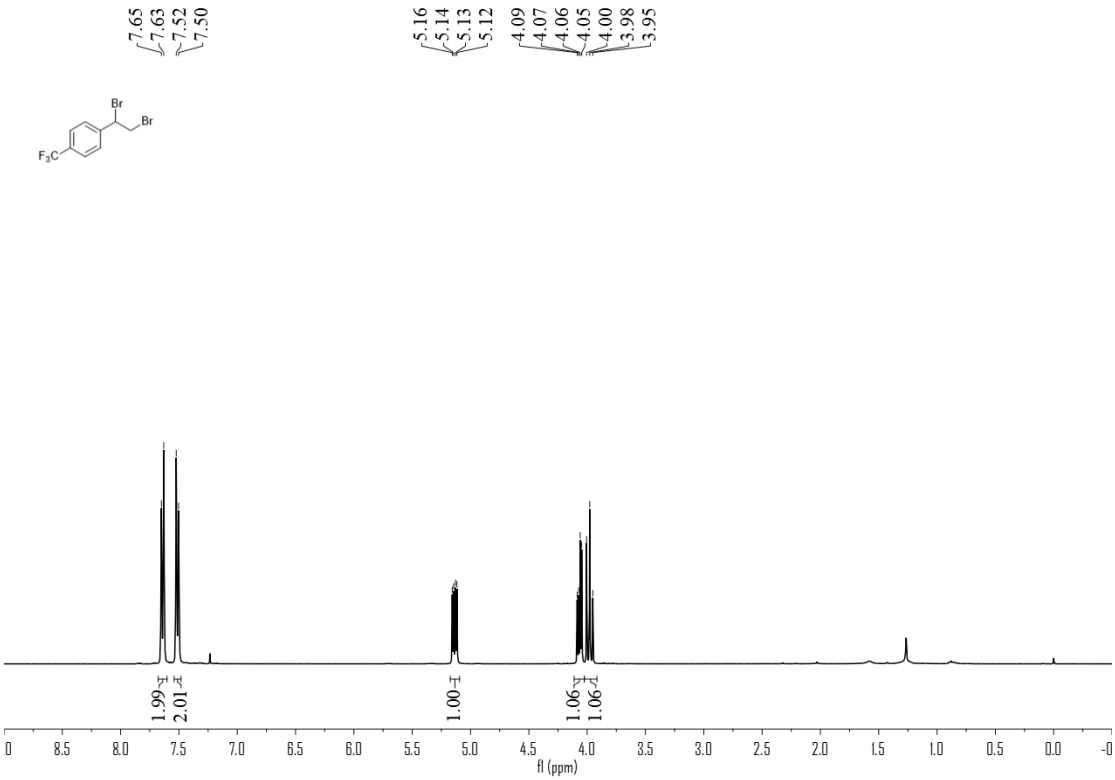

Figure S118. ^{13}C NMR (100 MHz, $CDCl_3$) spectrum of compound **6i**, related to **Figure 4**

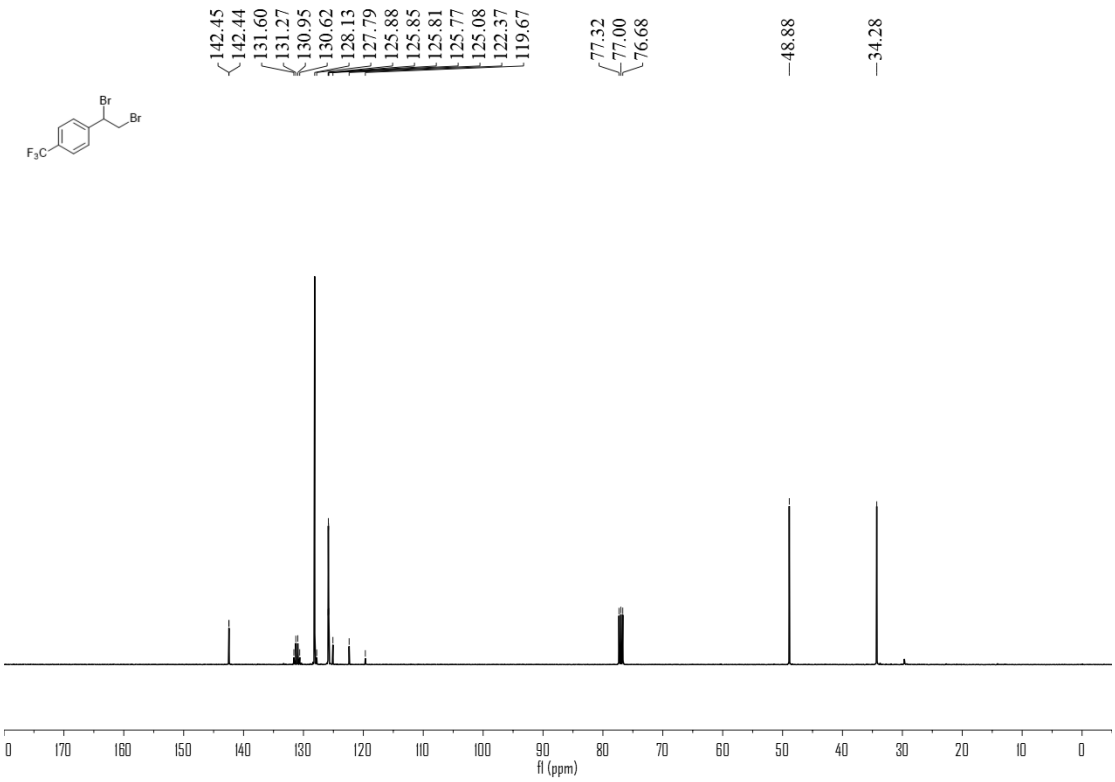

Figure S119. ^{19}F NMR (376 MHz, $CDCl_3$) spectrum of compound **6i**, related to **Figure 4**

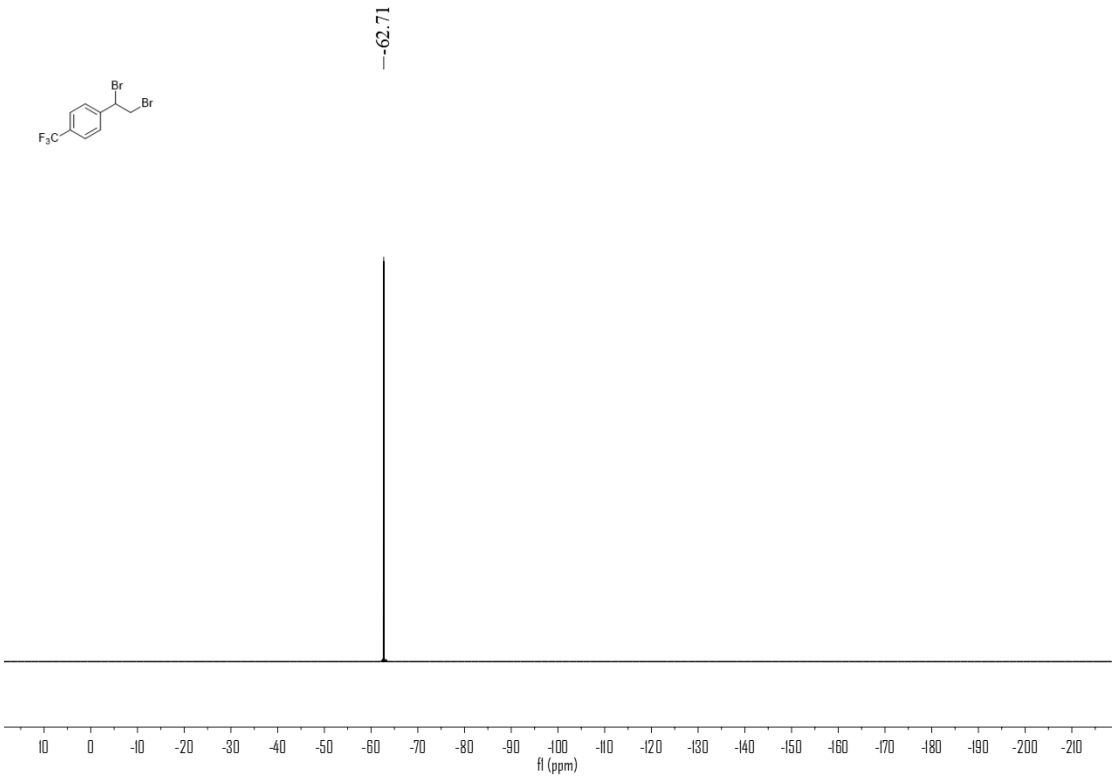

Figure S120. ^{1}H NMR (400 MHz, $CDCl_3$) spectrum of compound **6j**, related to **Figure 4**

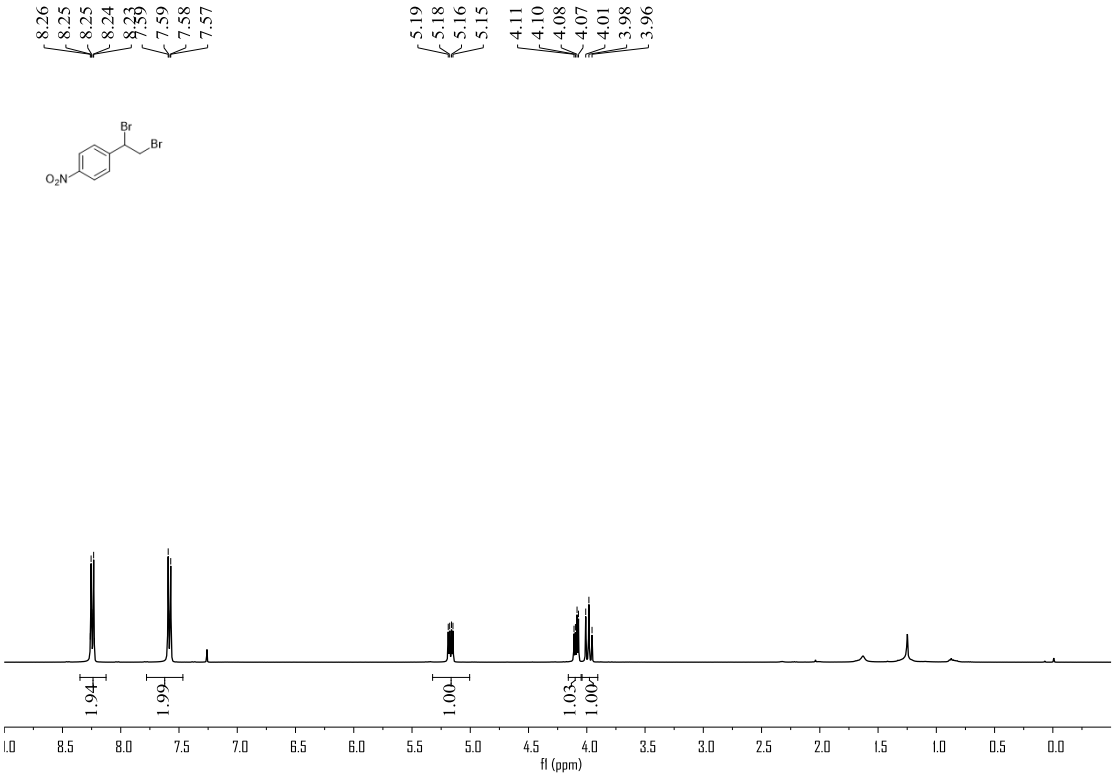

Figure S121. ^{13}C NMR (100 MHz, $CDCl_3$) spectrum of compound **6j**, related to **Figure 4**

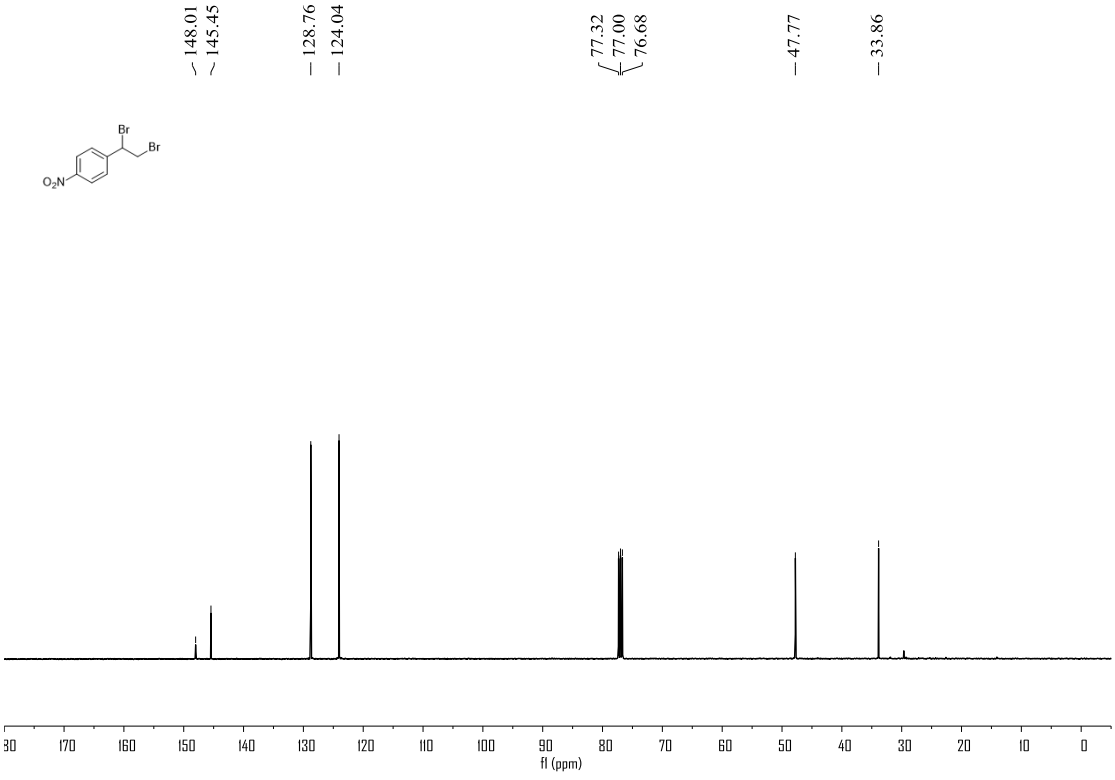

Figure S122. ^{1}H NMR (400 MHz, $CDCl_3$) spectrum of compound **6k**, related to **Figure 4**

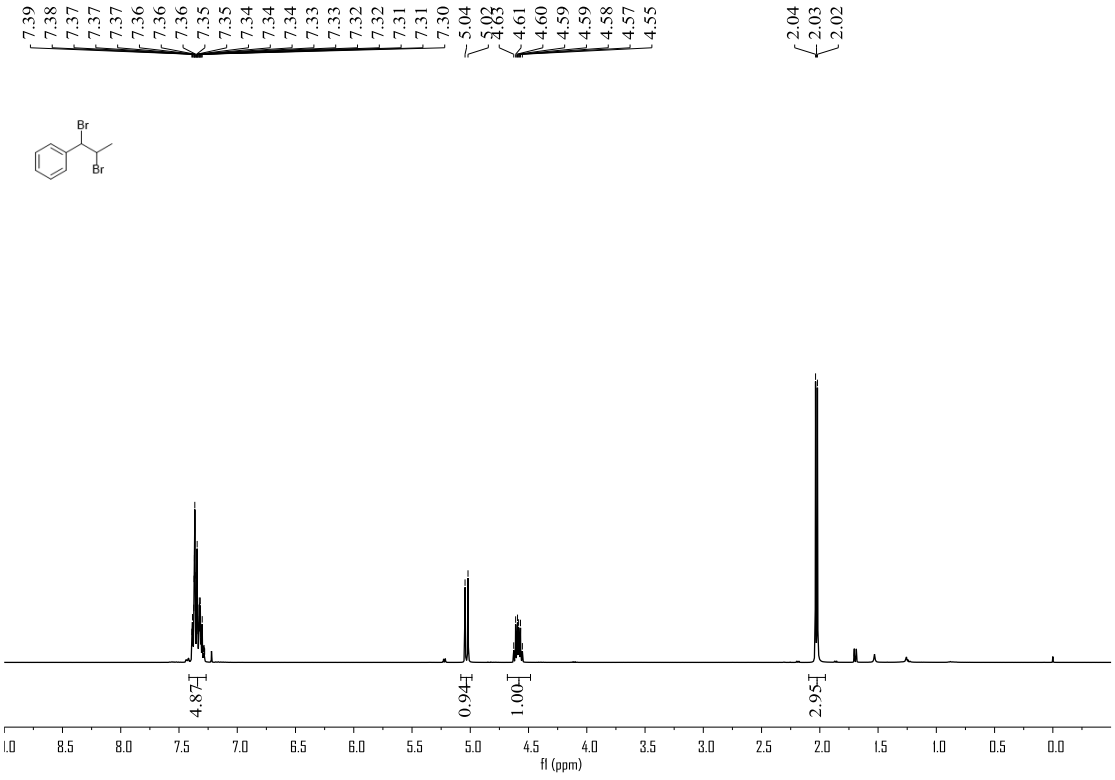

Figure S123. ^{13}C NMR (100 MHz, $CDCl_3$) spectrum of compound **6k**, related to **Figure 4**

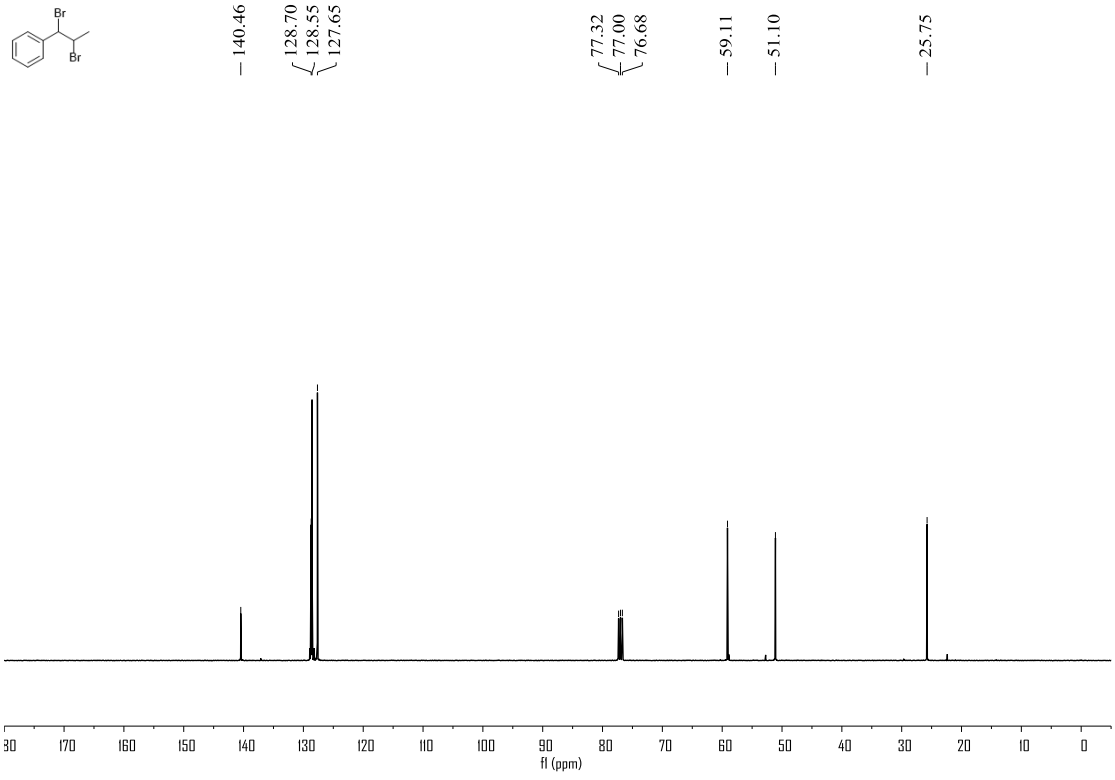

Figure S124. ^{1}H NMR (400 MHz, $CDCl_3$) spectrum of compound **6l**, related to **Figure 4**

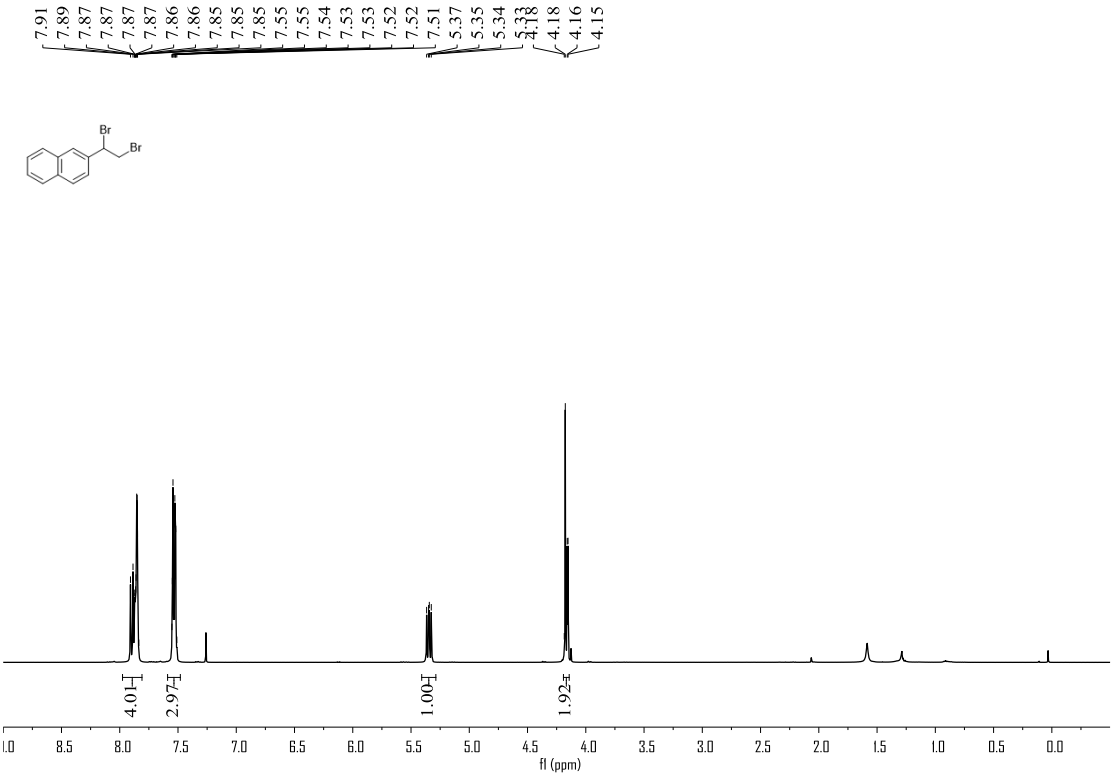

Figure S125. ^{13}C NMR (100 MHz, $CDCl_3$) spectrum of compound **6l**, related to **Figure 4**

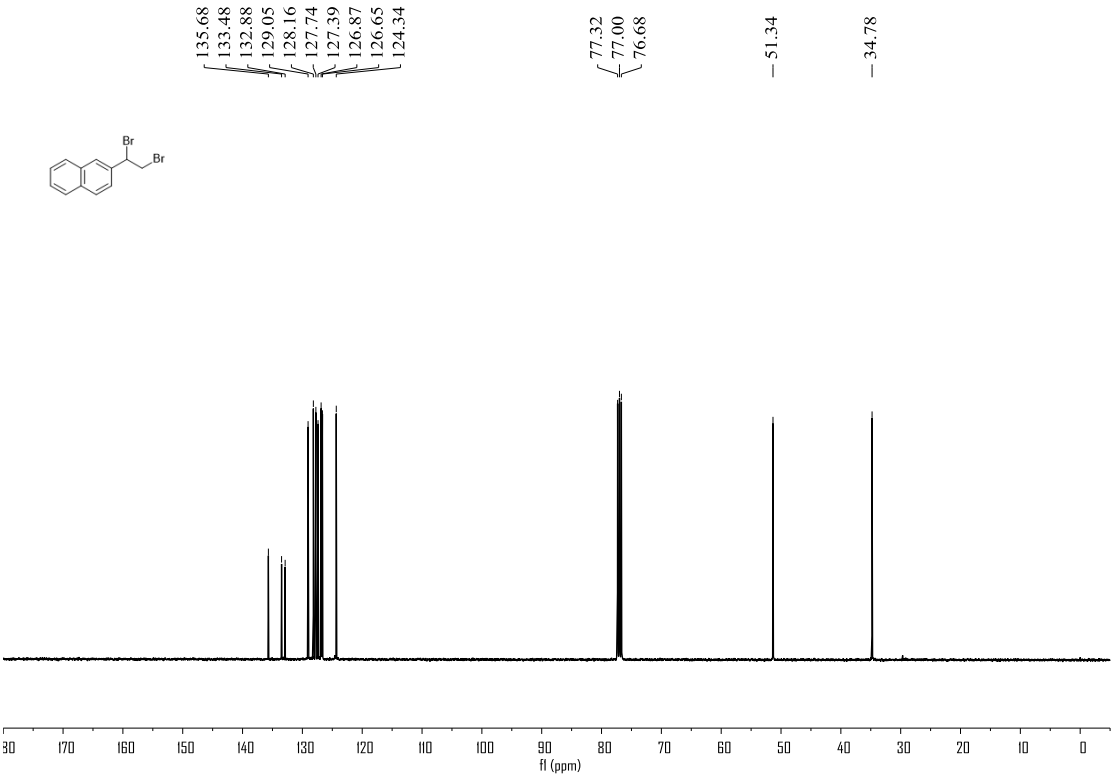

Figure S126. ^{1}H NMR (400 MHz, $CDCl_3$) spectrum of compound **6m**, related to **Figure 4**

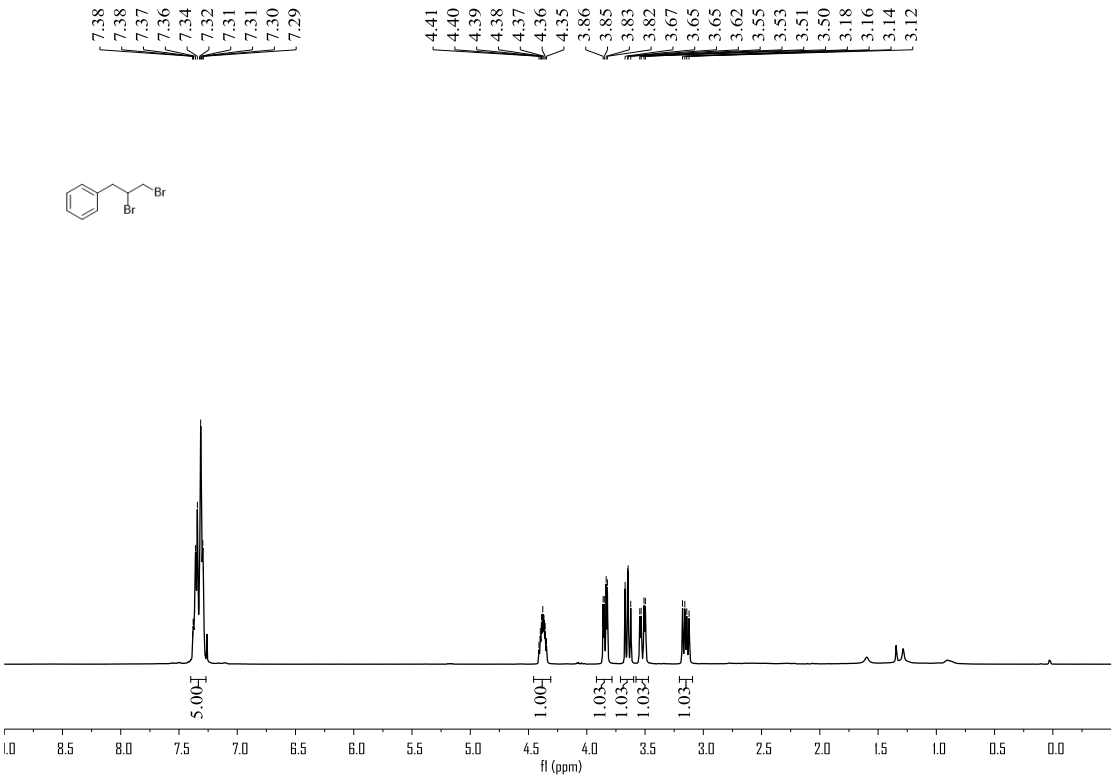

Figure S127. ^{13}C NMR (100 MHz, $CDCl_3$) spectrum of compound **6m**, related to **Figure 4**

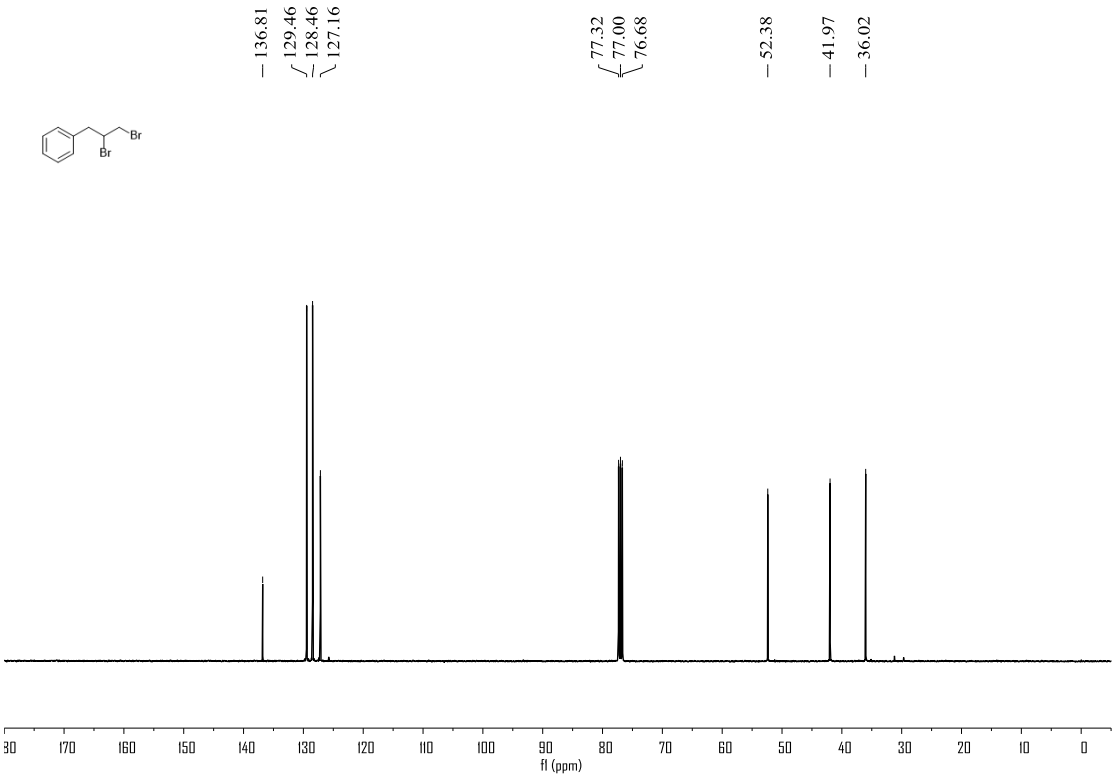

Figure S128. ^{1}H NMR (400 MHz, $CDCl_3$) spectrum of compound **6n**, related to **Figure 4**

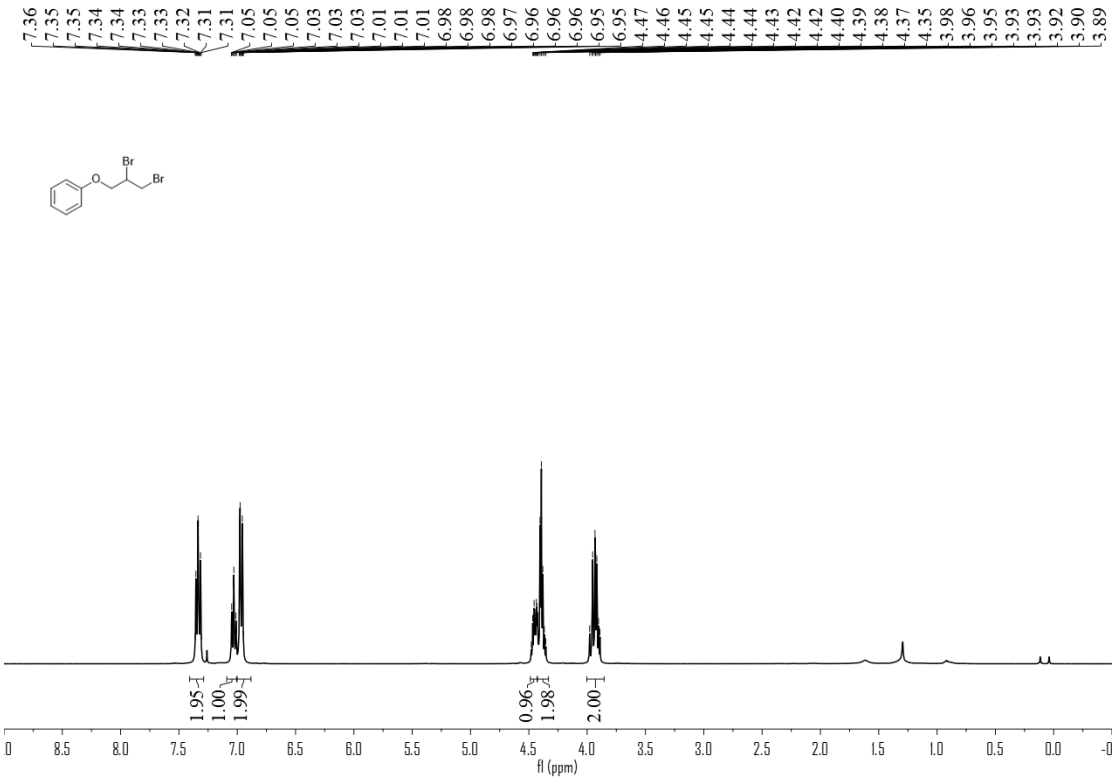

Figure S129. ^{13}C NMR (100 MHz, $CDCl_3$) spectrum of compound **6n**, related to **Figure 4**

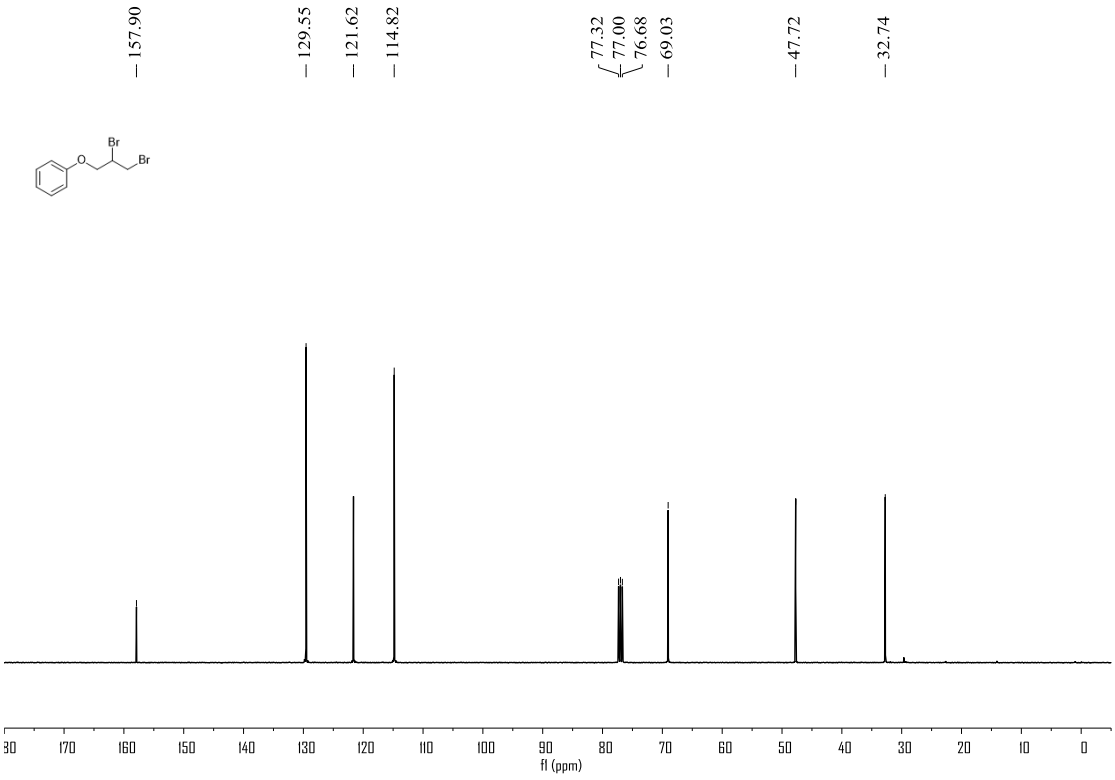

Figure S130. ^{1}H NMR (400 MHz, DMSO-d_6) spectrum of compound **6o**, related to **Figure 4**

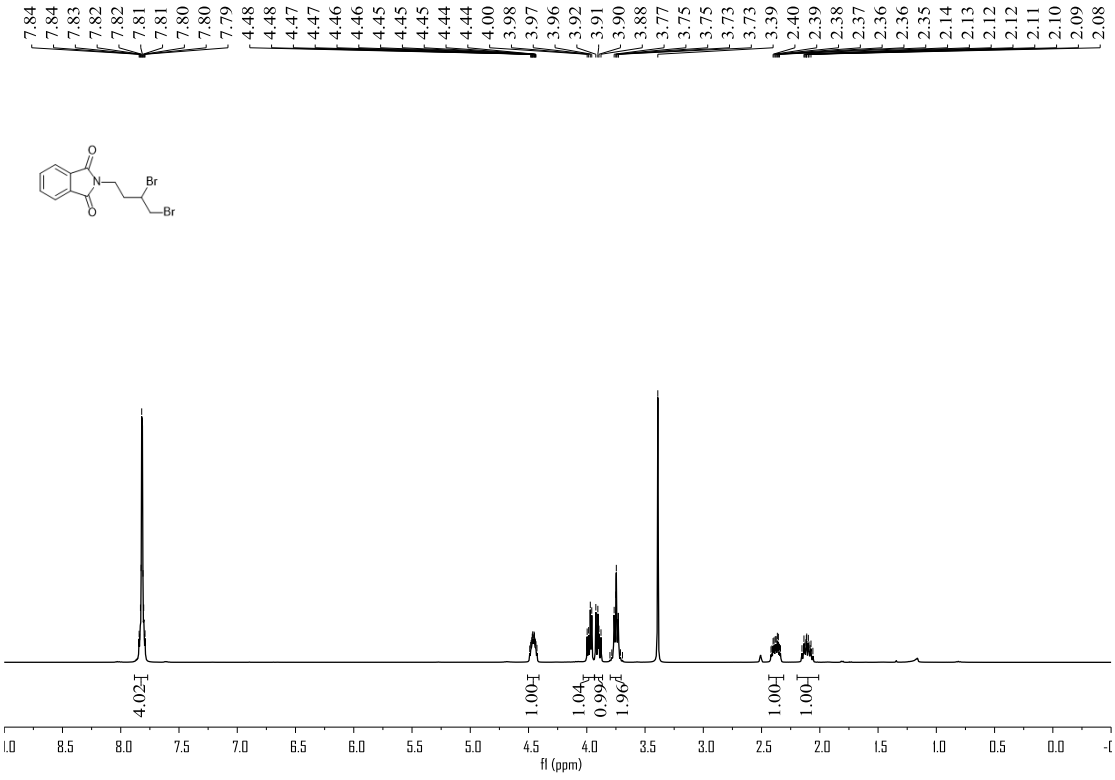

Figure S131. ^{13}C NMR (100 MHz, DMSO-d_6) spectrum of compound **6o**, related to **Figure 4**

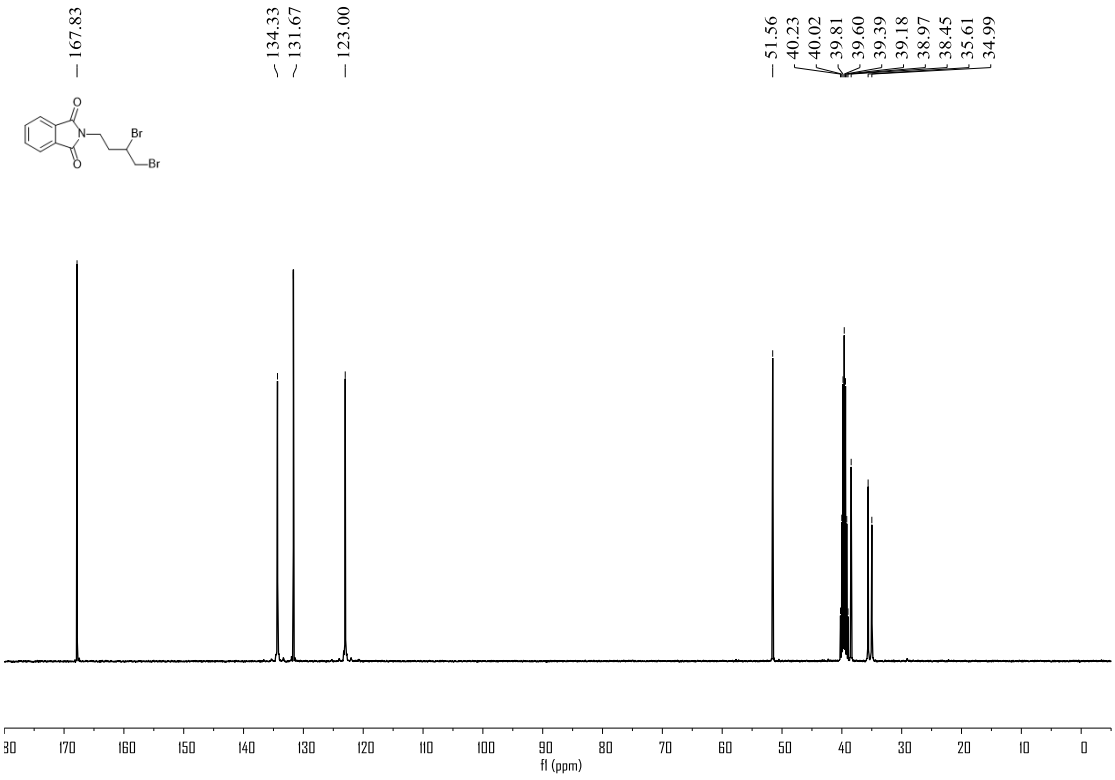

Figure S132. ^{1}H NMR (400 MHz, $CDCl_3$) spectrum of compound **6p**, related to **Figure 4**

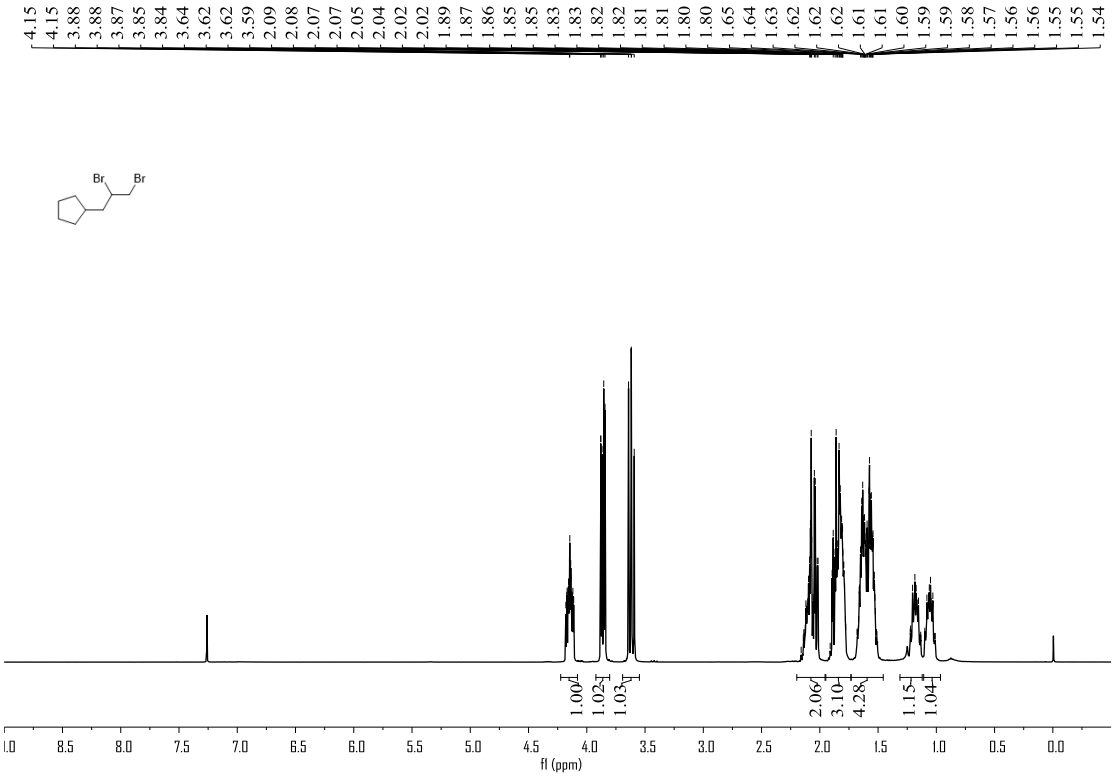

Figure S133. ^{13}C NMR (100 MHz, $CDCl_3$) spectrum of compound **6p**, related to **Figure 4**

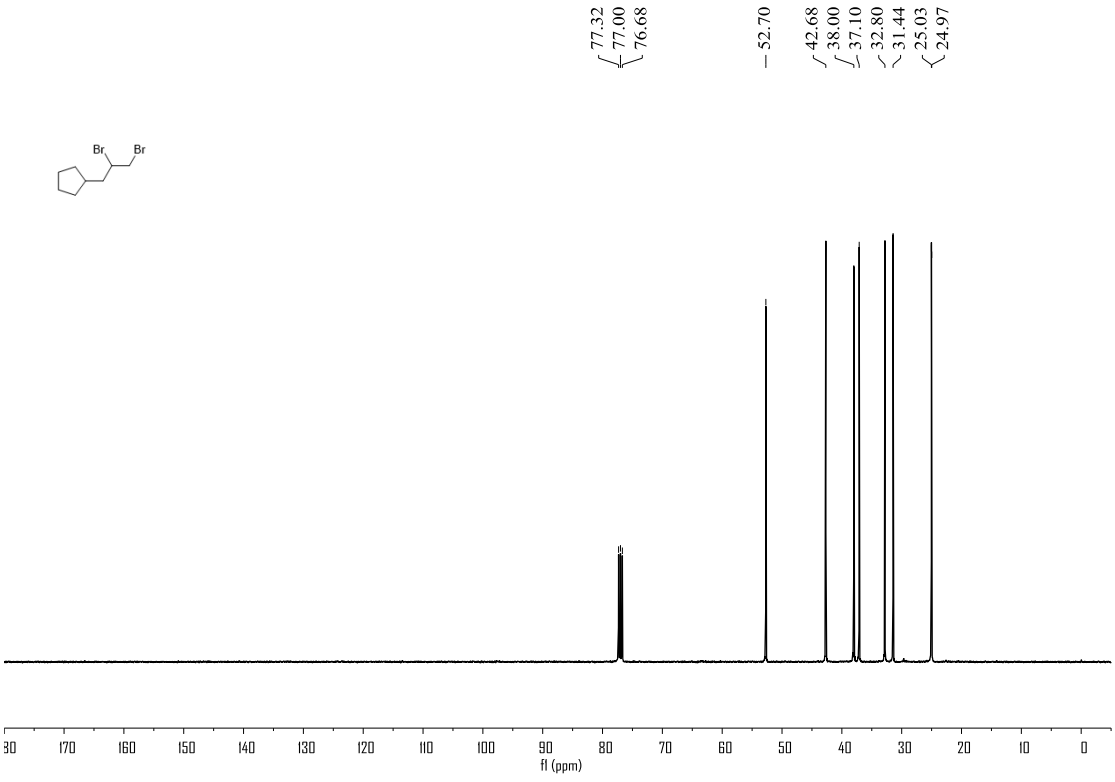

Figure S134. ^{1}H NMR (400 MHz, $CDCl_3$) spectrum of compound **6q**, related to **Figure 4**

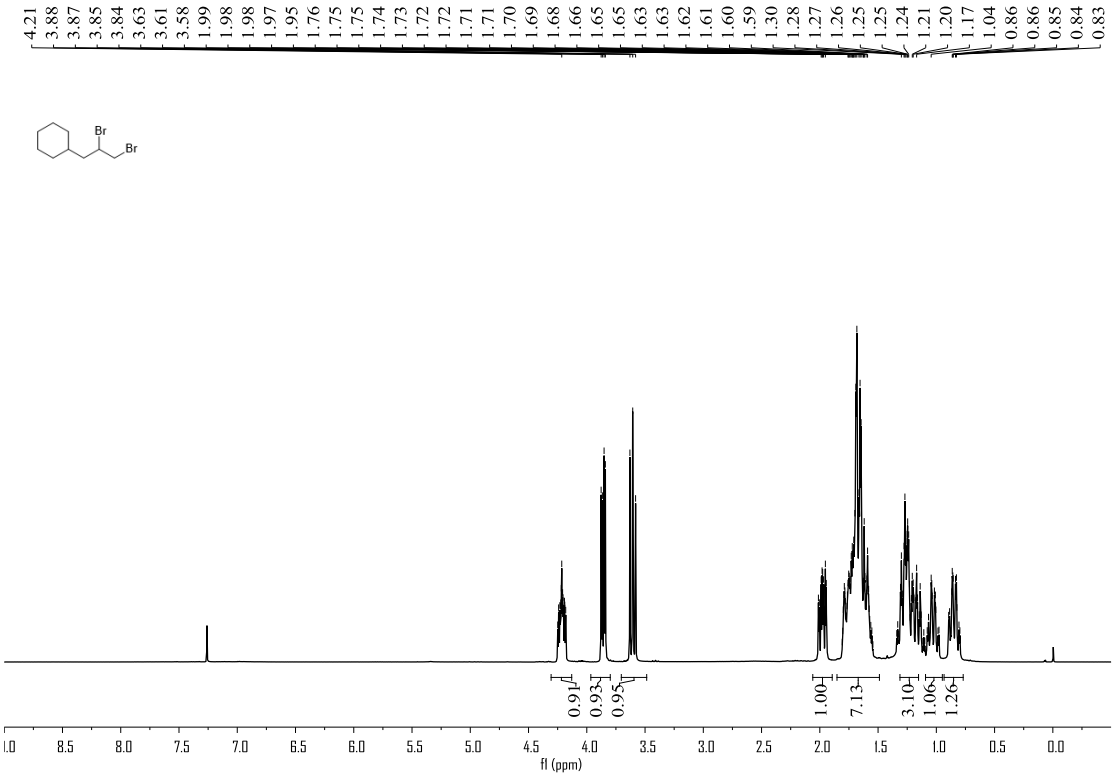

Figure S135. ^{13}C NMR (100 MHz, $CDCl_3$) spectrum of compound **6q**, related to **Figure 4**

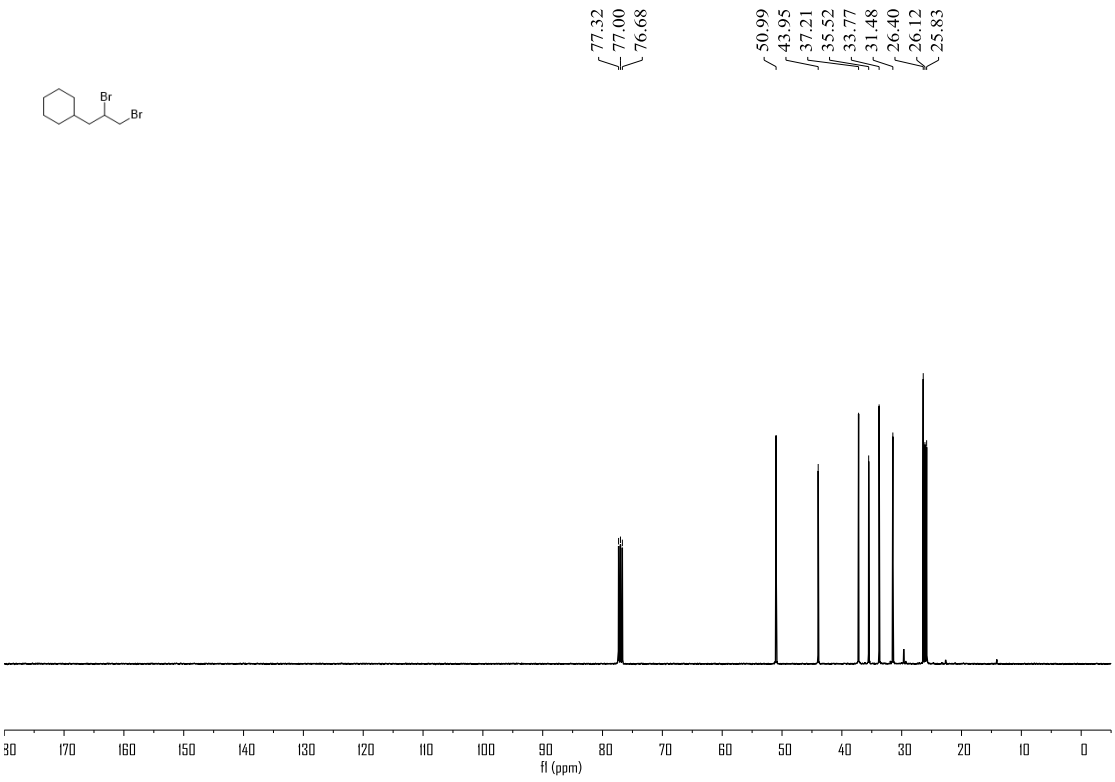

Figure S136. ^{1}H NMR (400 MHz, $CDCl_3$) spectrum of compound **6r**, related to **Figure 4**

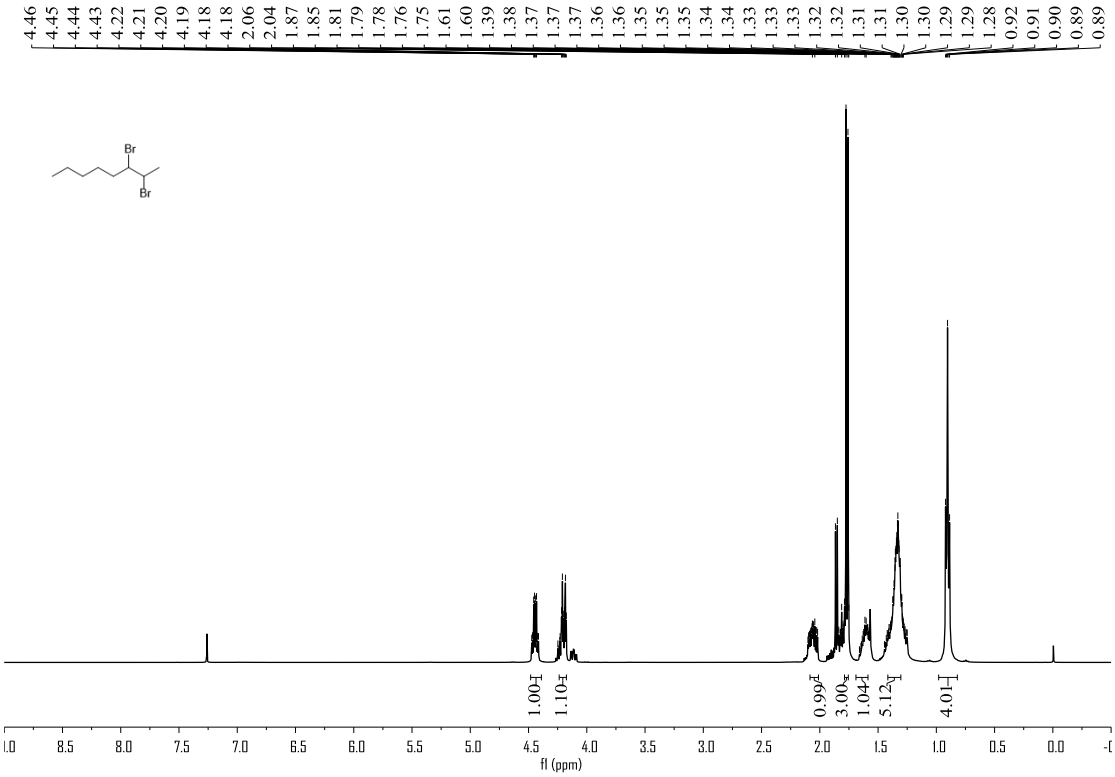

Figure S137. ^{13}C NMR (100 MHz, $CDCl_3$) spectrum of compound **6r**, related to **Figure 4**

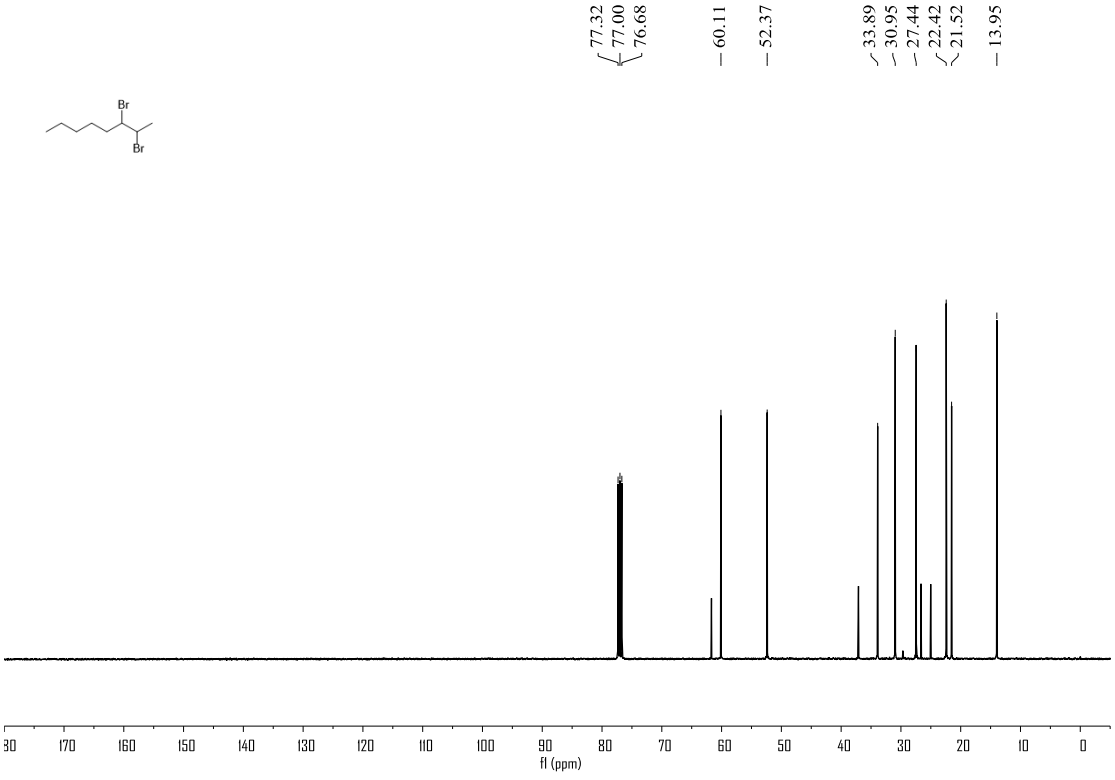

Figure S138. ^{1}H NMR (400 MHz, $CDCl_3$) spectrum of compound **6s**, related to **Figure 4**

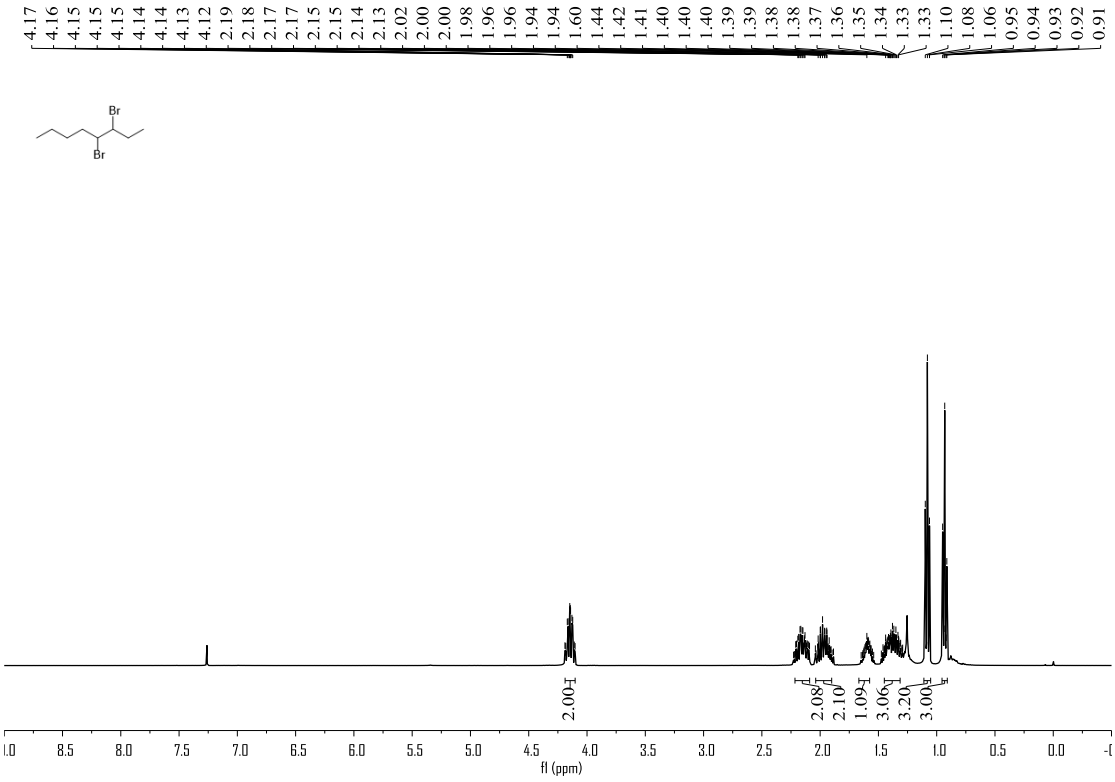

Figure S139. ^{13}C NMR (100 MHz, $CDCl_3$) spectrum of compound **6s**, related to **Figure 4**

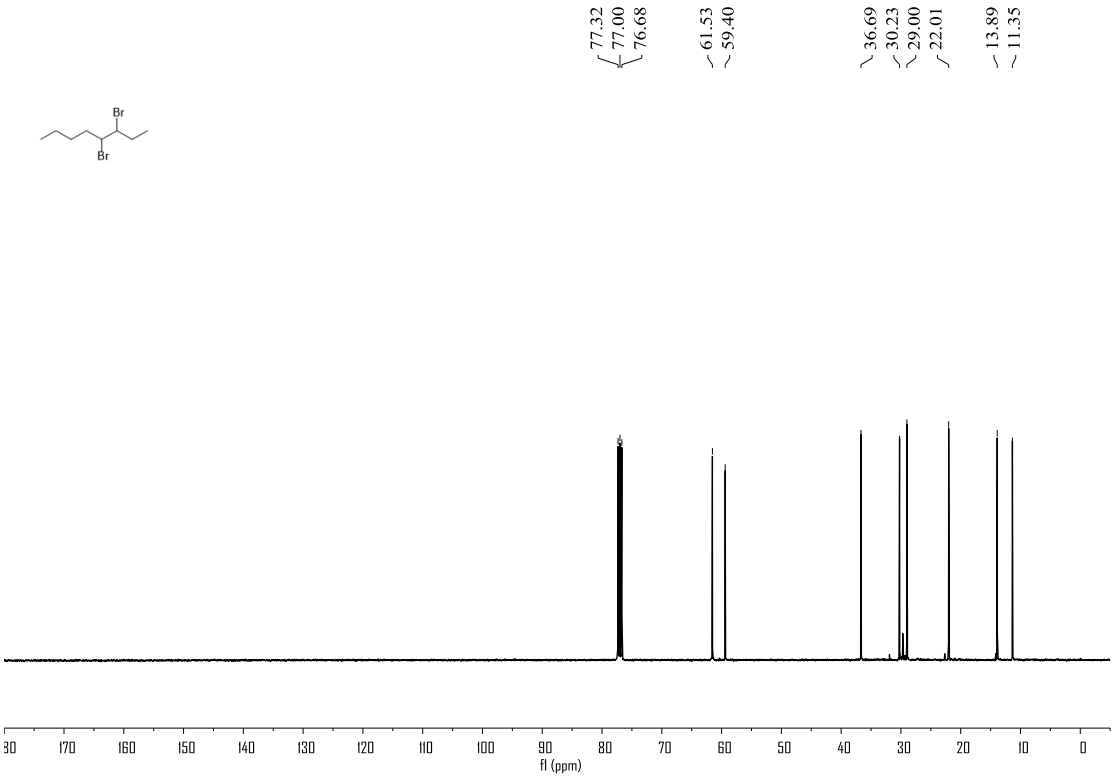

Figure S140. ^{1}H NMR (400 MHz, $CDCl_3$) spectrum of compound **6t**, related to **Figure 4**

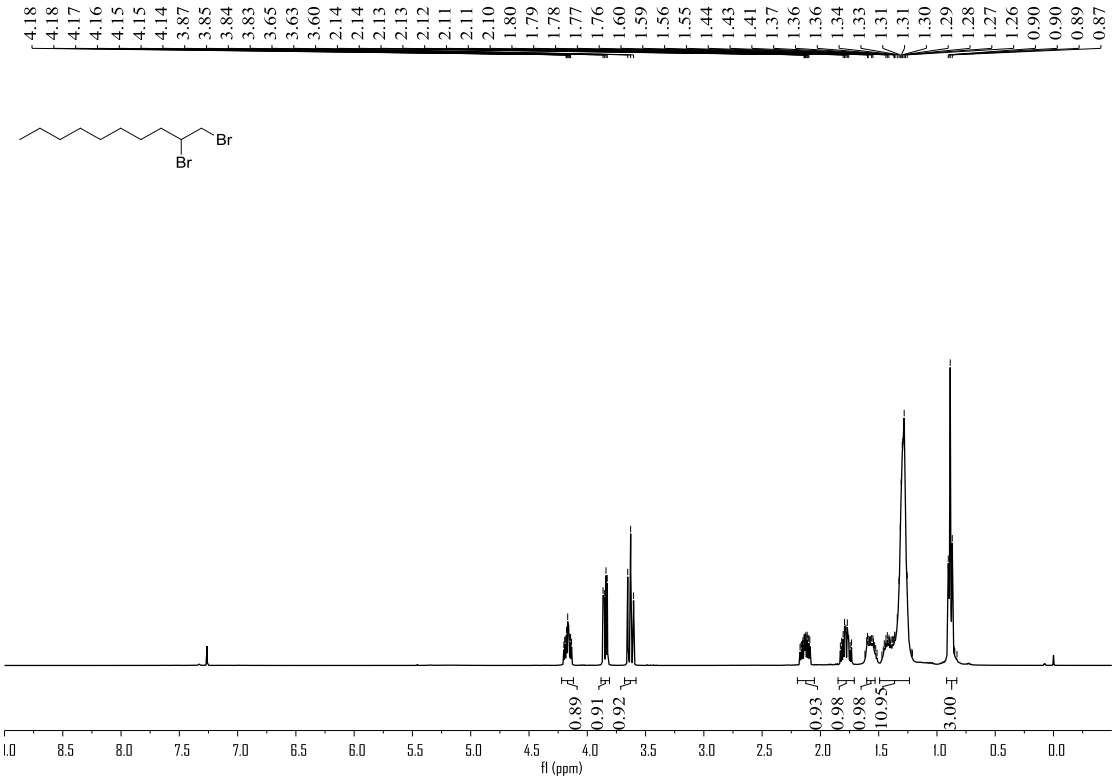

Figure S141. ^{13}C NMR (100 MHz, $CDCl_3$) spectrum of compound **6t**, related to **Figure 4**

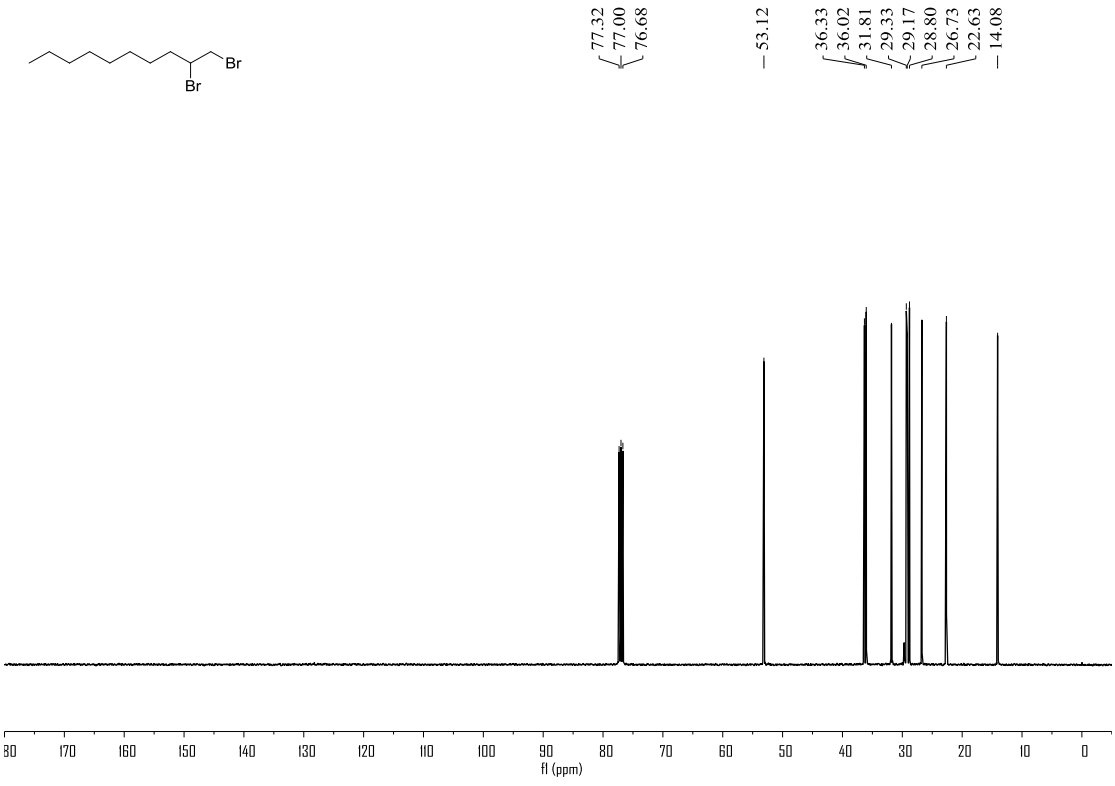

Figure S142. ^{1}H NMR (400 MHz, $CDCl_3$) spectrum of compound **6u**, related to **Figure 4**

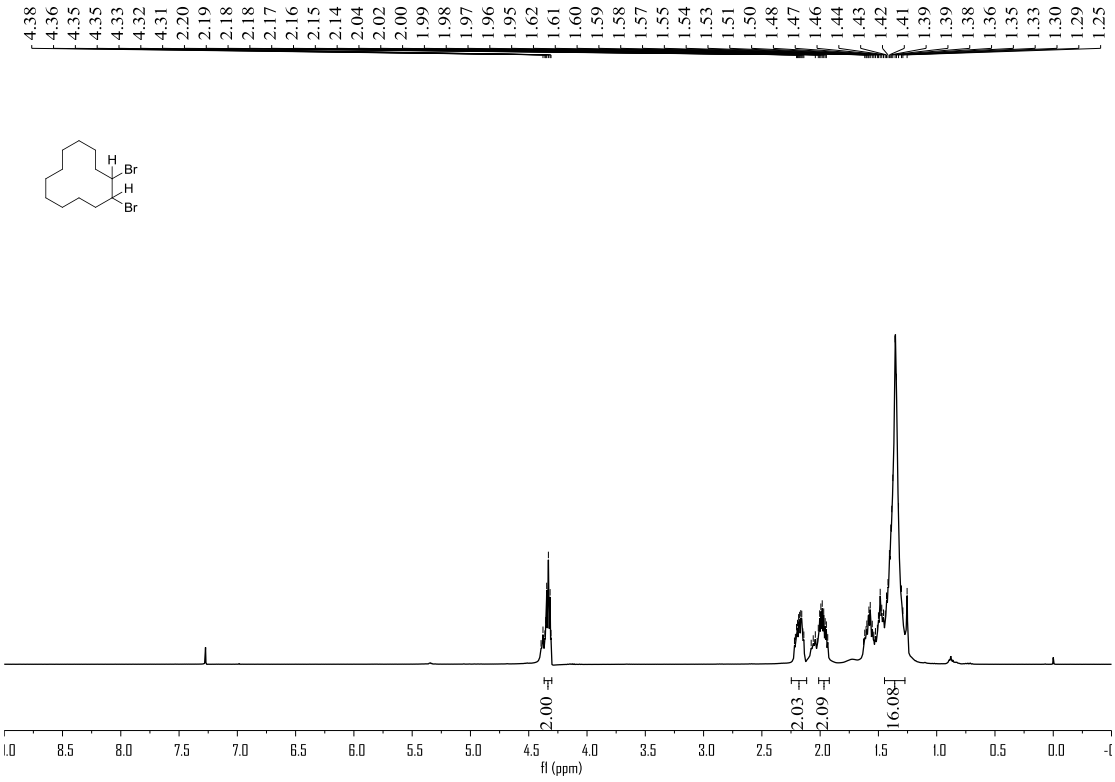

Figure S143. ^{13}C NMR (100 MHz, $CDCl_3$) spectrum of compound 6u, related to **Figure 4**

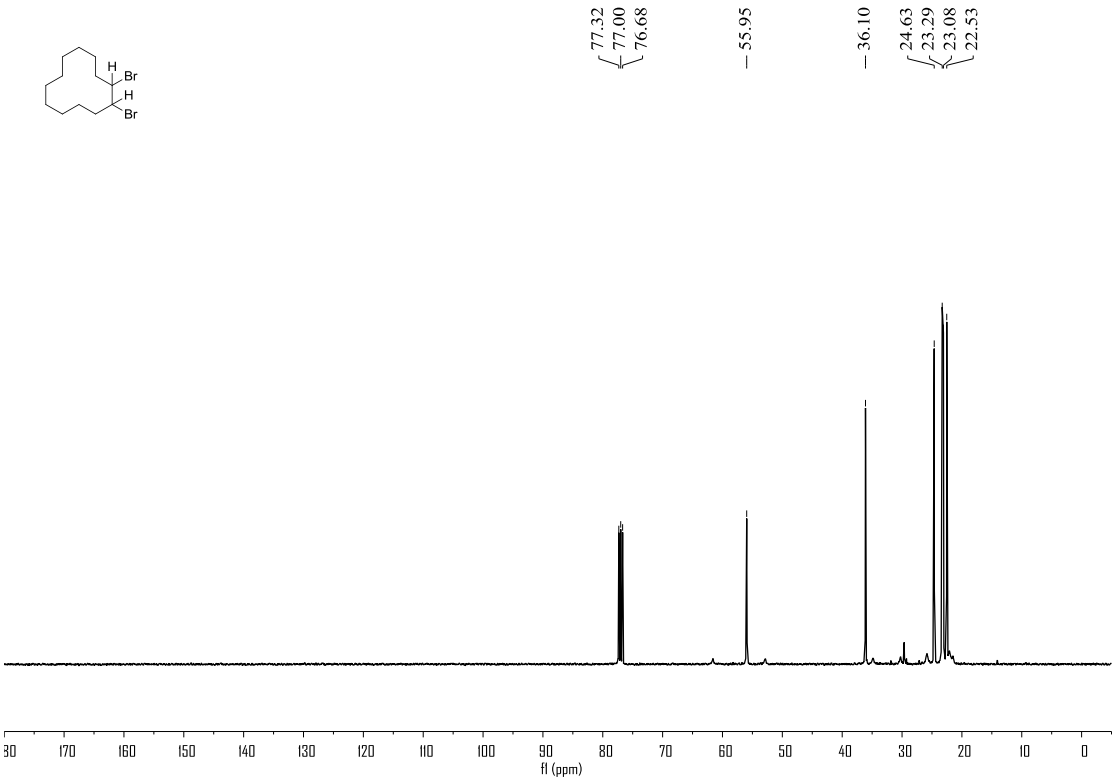

Figure S144. ^{1}H NMR (400 MHz, $CDCl_3$) spectrum of compound **6v**, related to **Figure 4**

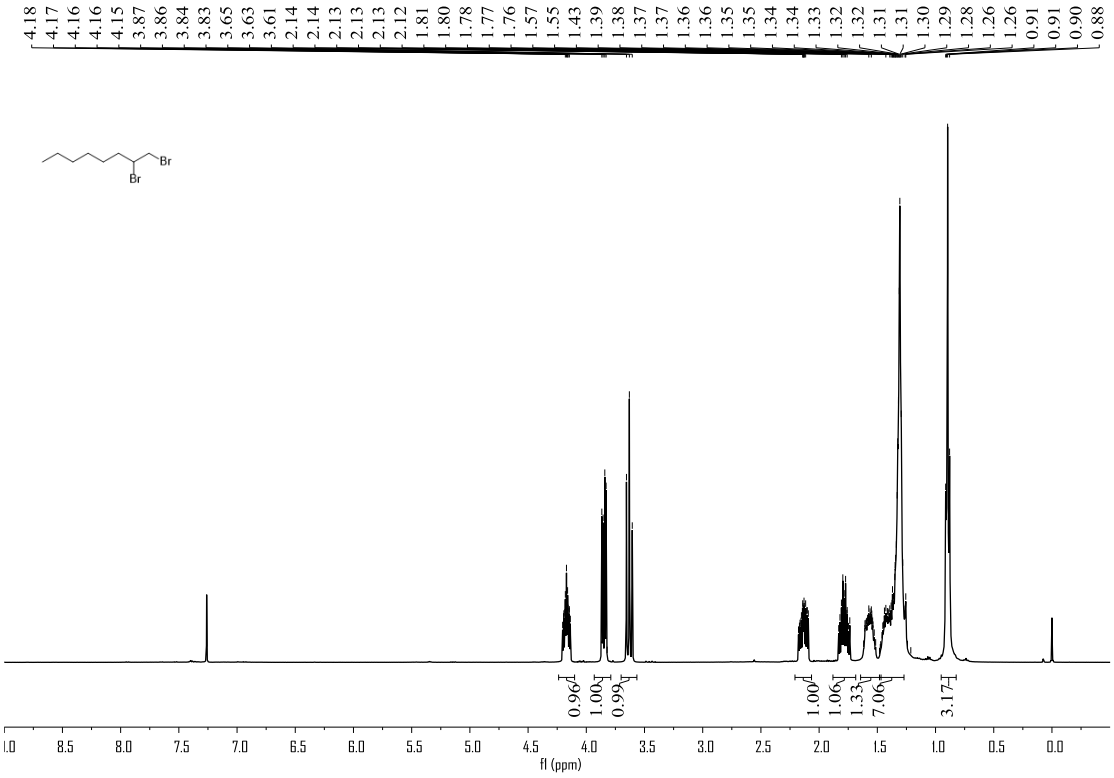

Figure S145. ^{13}C NMR (100 MHz, $CDCl_3$) spectrum of compound **6v**, related to **Figure 4**

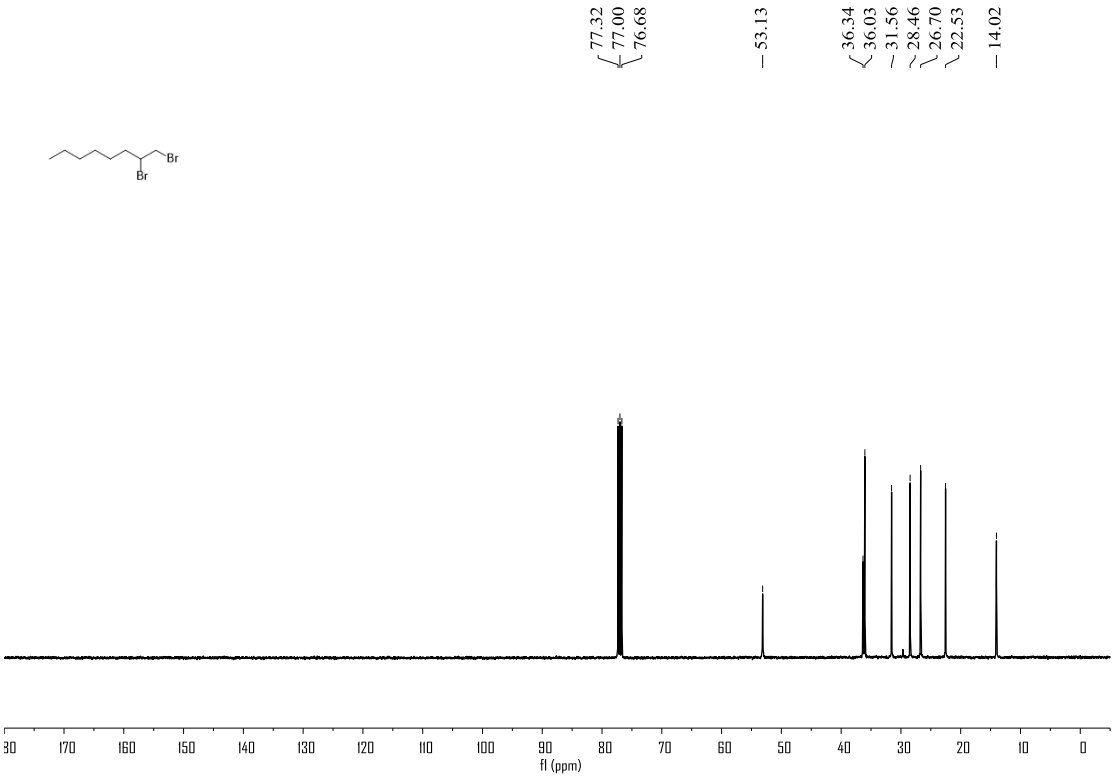

Figure S146. ^{1}H NMR (400 MHz, $CDCl_3$) spectrum of compound **6w**, related to **Figure 4**

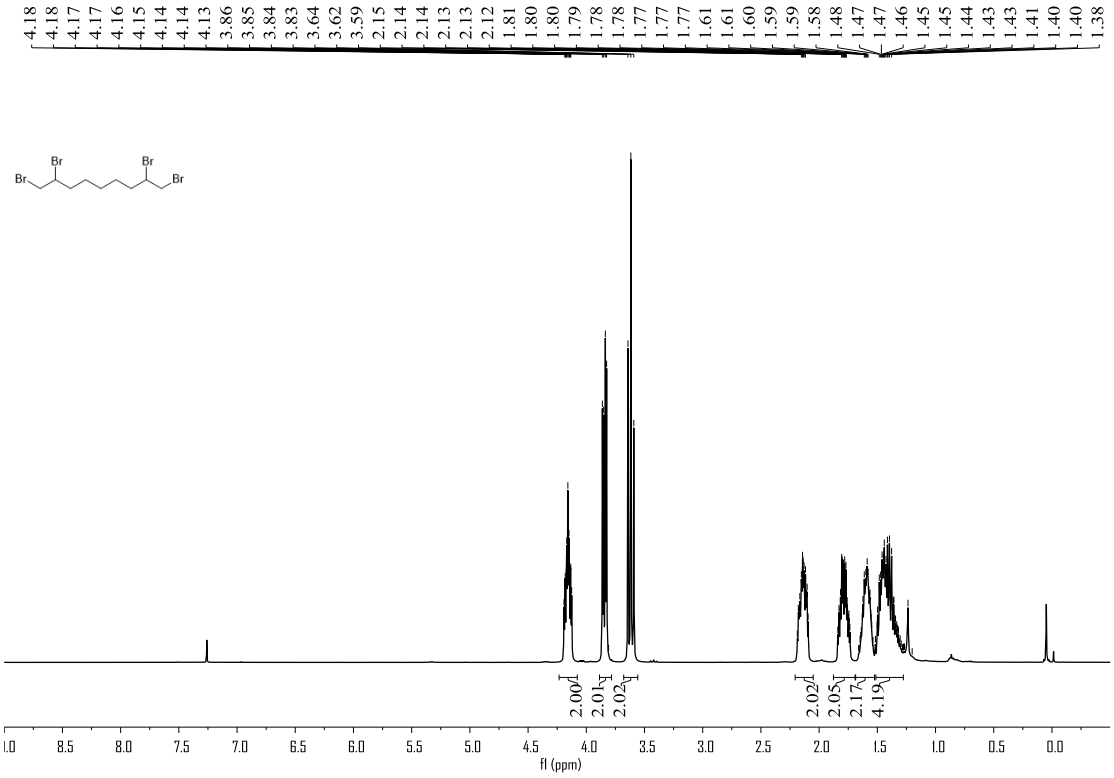

Figure S147. ^{13}C NMR (100 MHz, $CDCl_3$) spectrum of compound **6w**, related to **Figure 4**

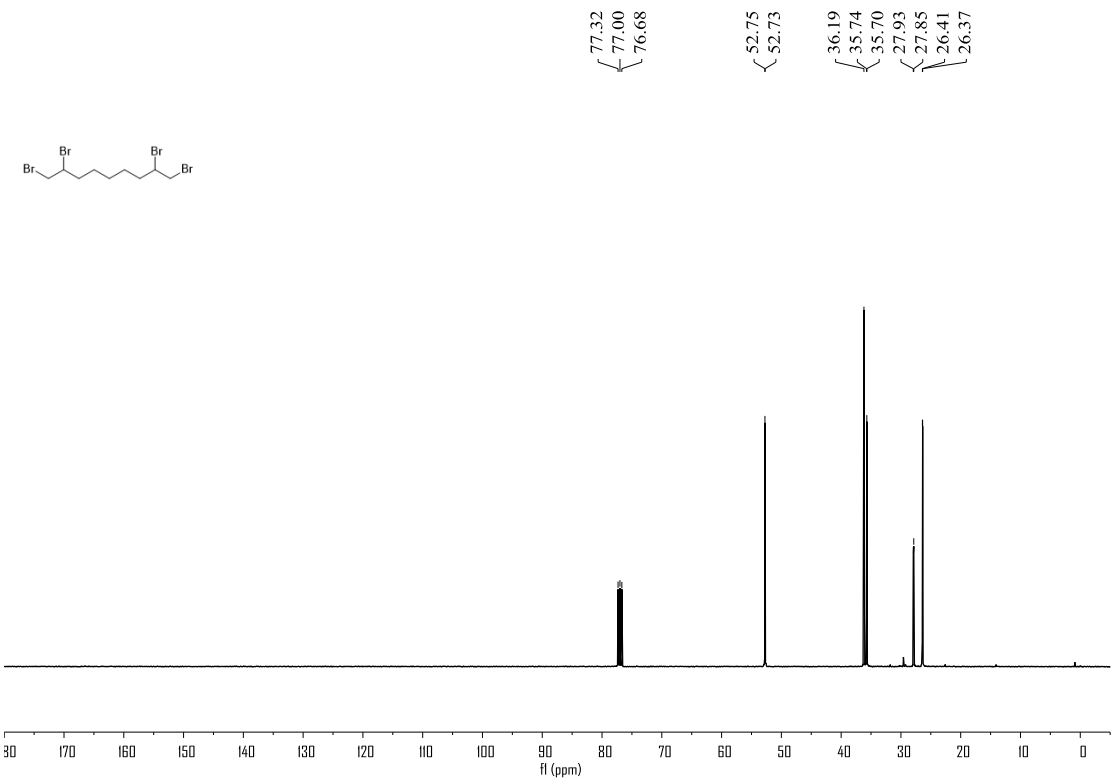

Figure S148. ^{1}H NMR (400 MHz, $CDCl_3$) spectrum of compound **6x**, related to **Figure 4**

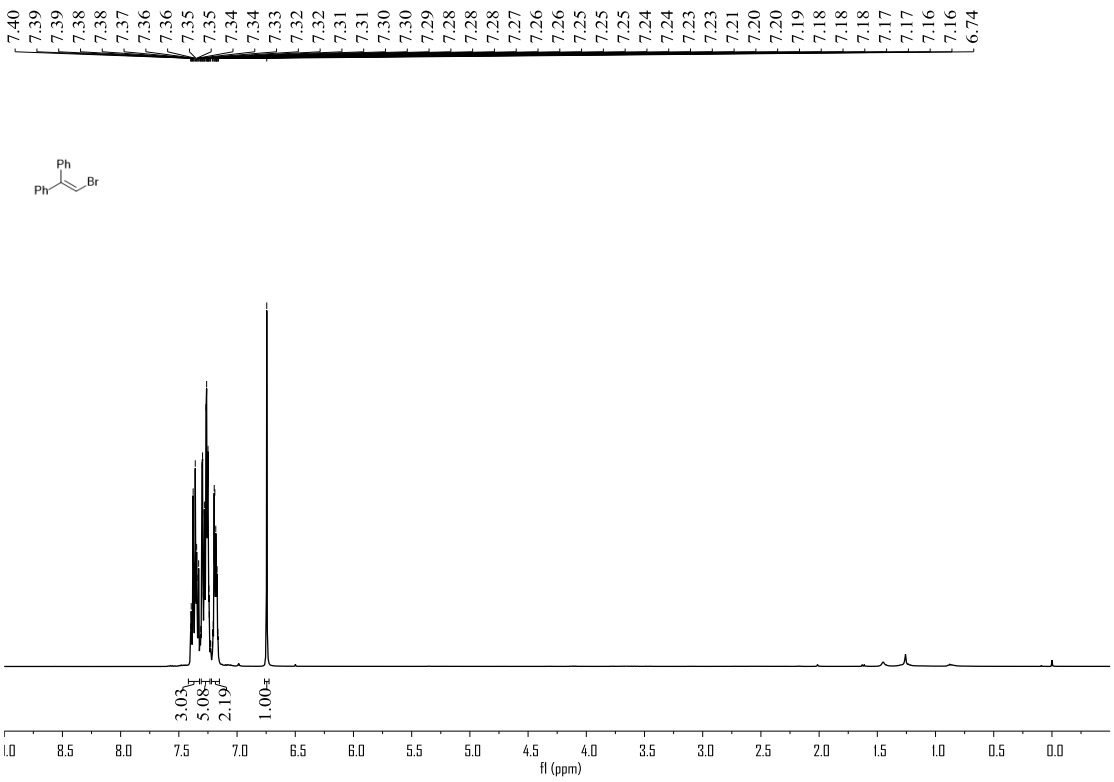

Figure S149. ^{13}C NMR (100 MHz, $CDCl_3$) spectrum of compound **6x**, related to **Figure 4**

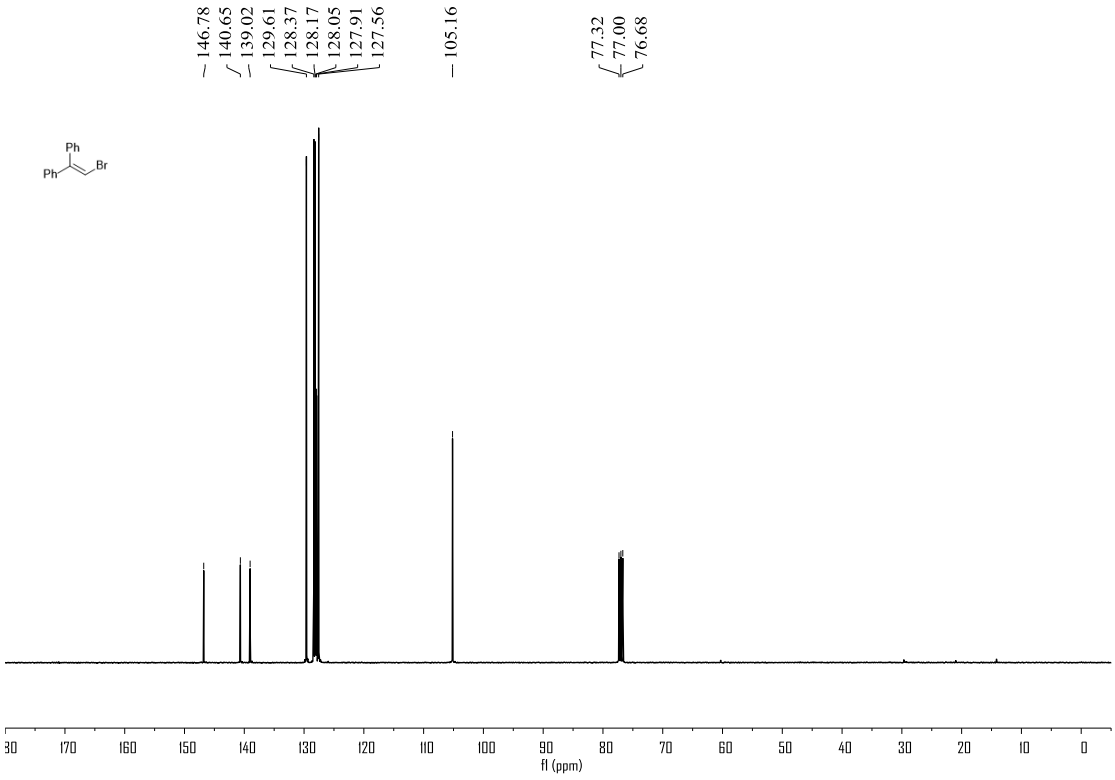

Figure S150. ^{1}H NMR (400 MHz, $CDCl_3$) spectrum of compound **8a**, related to **Figure 5**

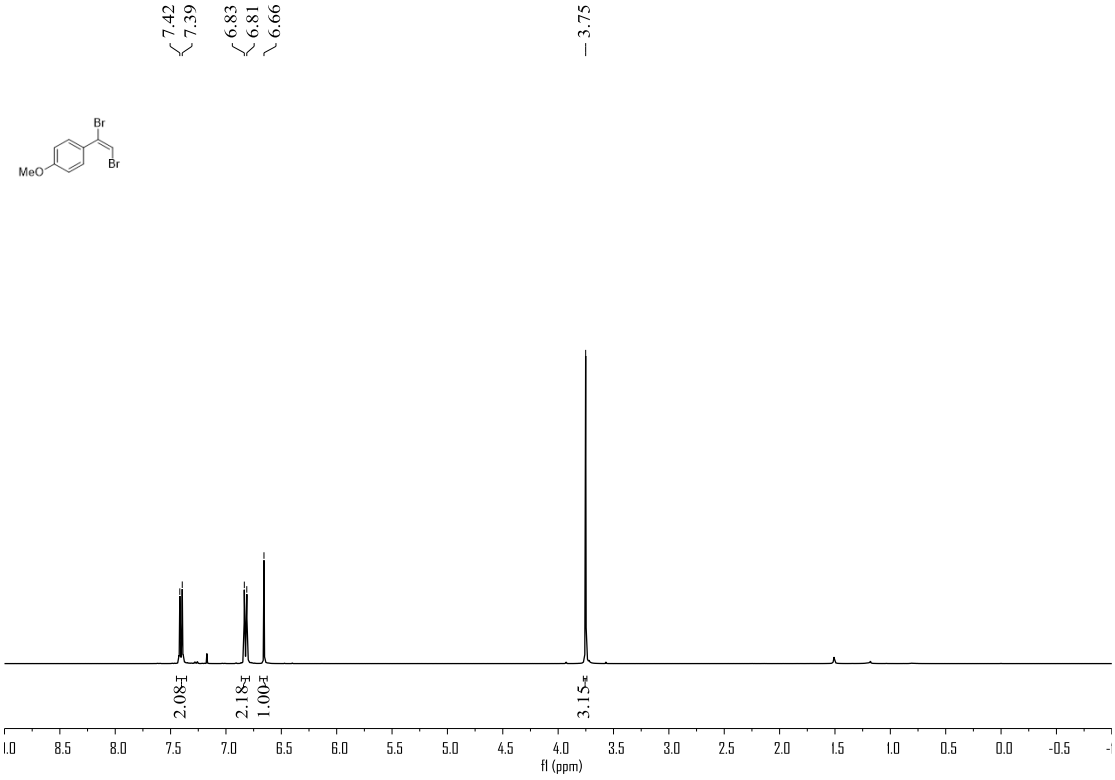

Figure S151. ^{13}C NMR (100 MHz, $CDCl_3$) spectrum of compound **8a**, related to **Figure 5**

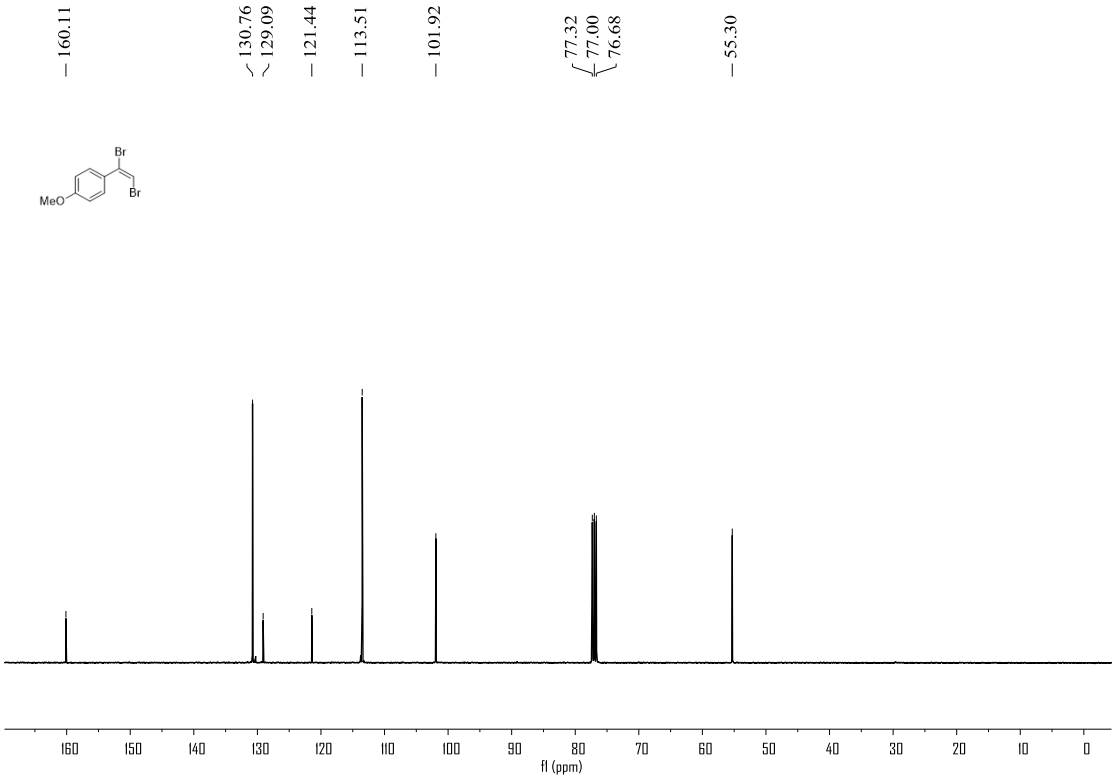

Figure S152. ^{1}H NMR (400 MHz, $CDCl_3$) spectrum of compound **8b**, related to **Figure 5**

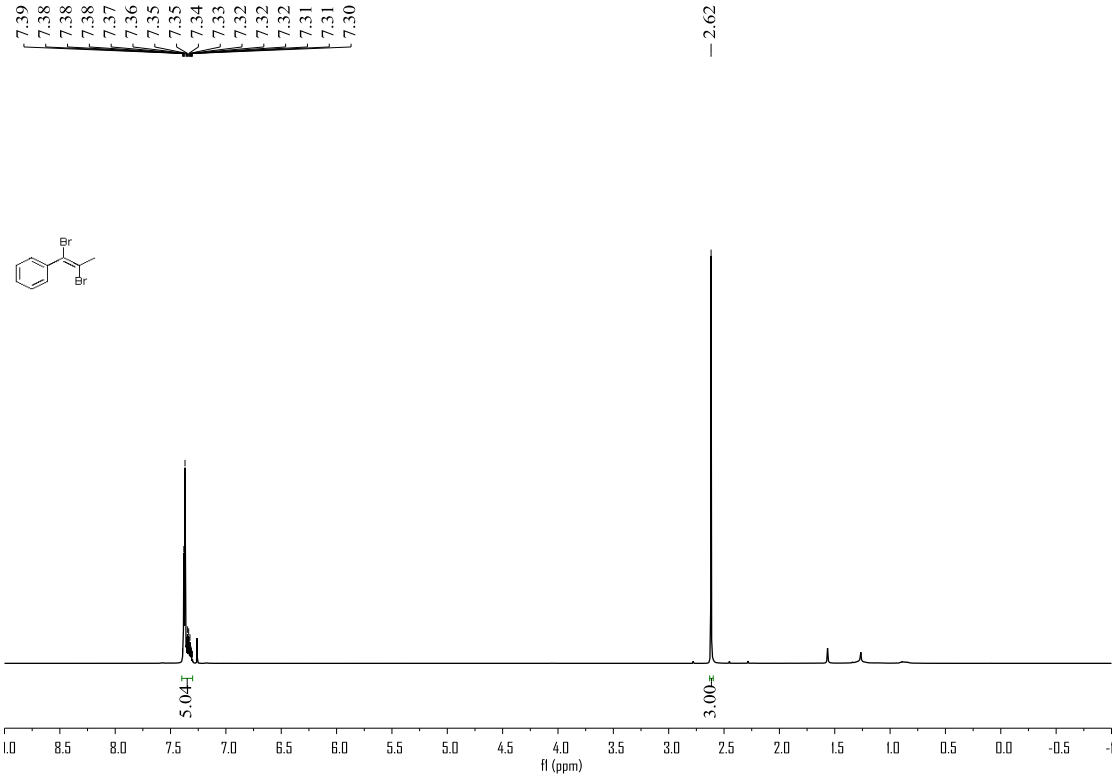

Figure S153. ^{13}C NMR (100 MHz, $CDCl_3$) spectrum of compound **8b**, related to **Figure 5**

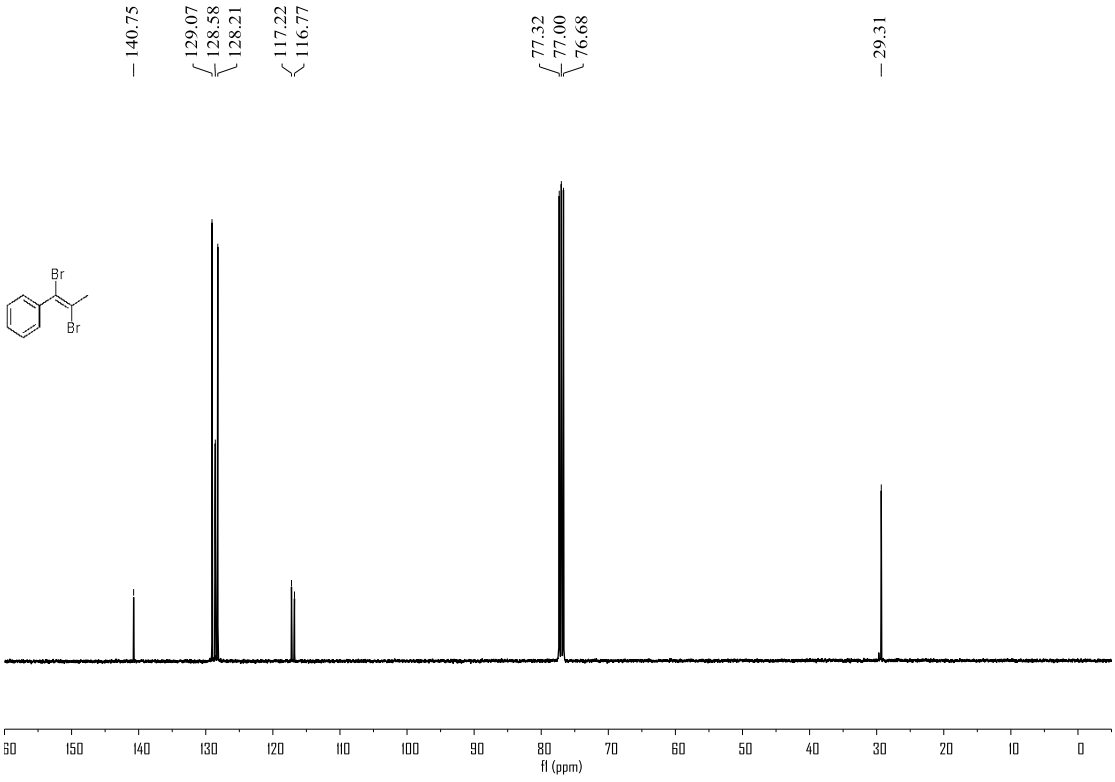

Figure S154. ^{1}H NMR (400 MHz, $CDCl_3$) spectrum of compound **10**, related to **Figure 7**

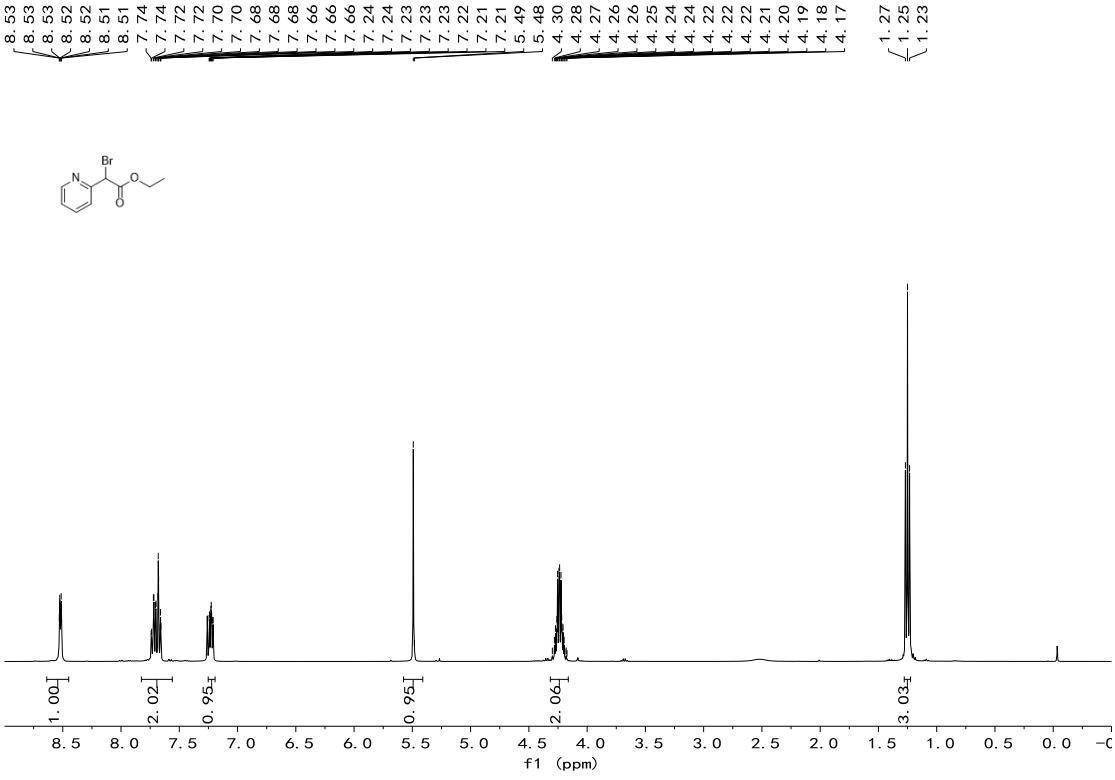

Figure S155. ^{13}C NMR (100 MHz, $CDCl_3$) spectrum of compound **10**, related to **Figure 7**

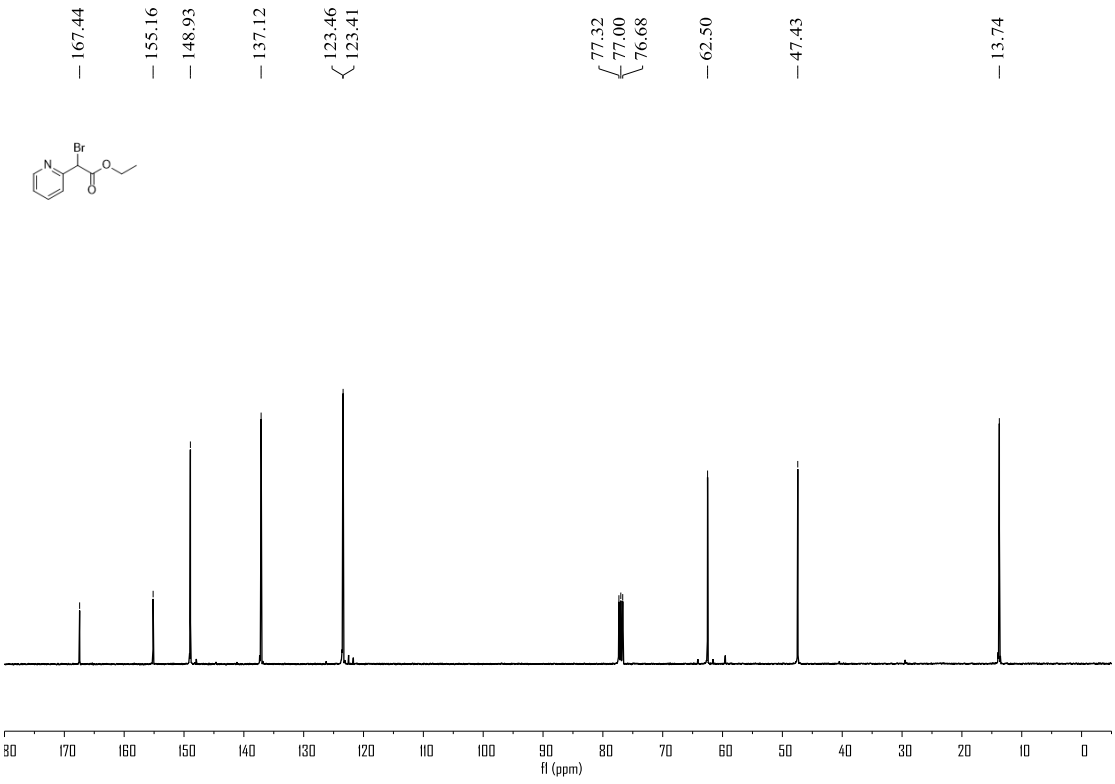

Figure S156. ^{13}C NMR (400 MHz, $CDCl_3$) spectrum of compound **11**, related to **Figure 7**

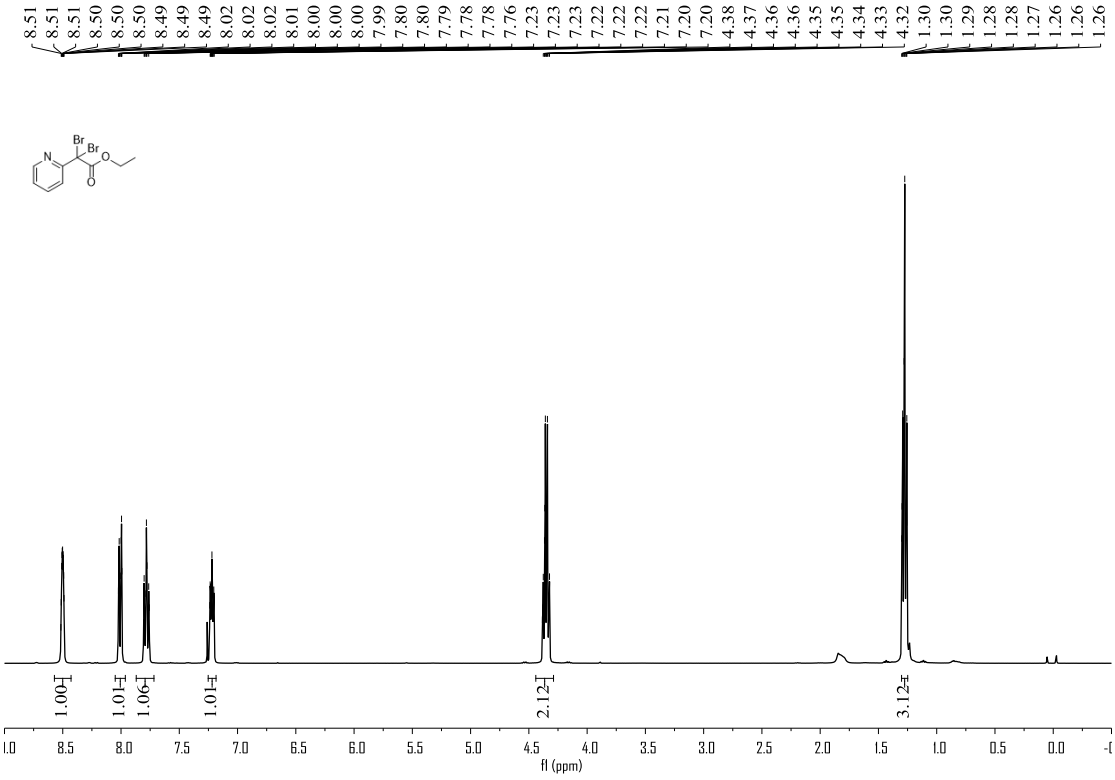

Figure S157. ^{13}C NMR (100 MHz, $CDCl_3$) spectrum of compound **11**, related to **Figure 7**

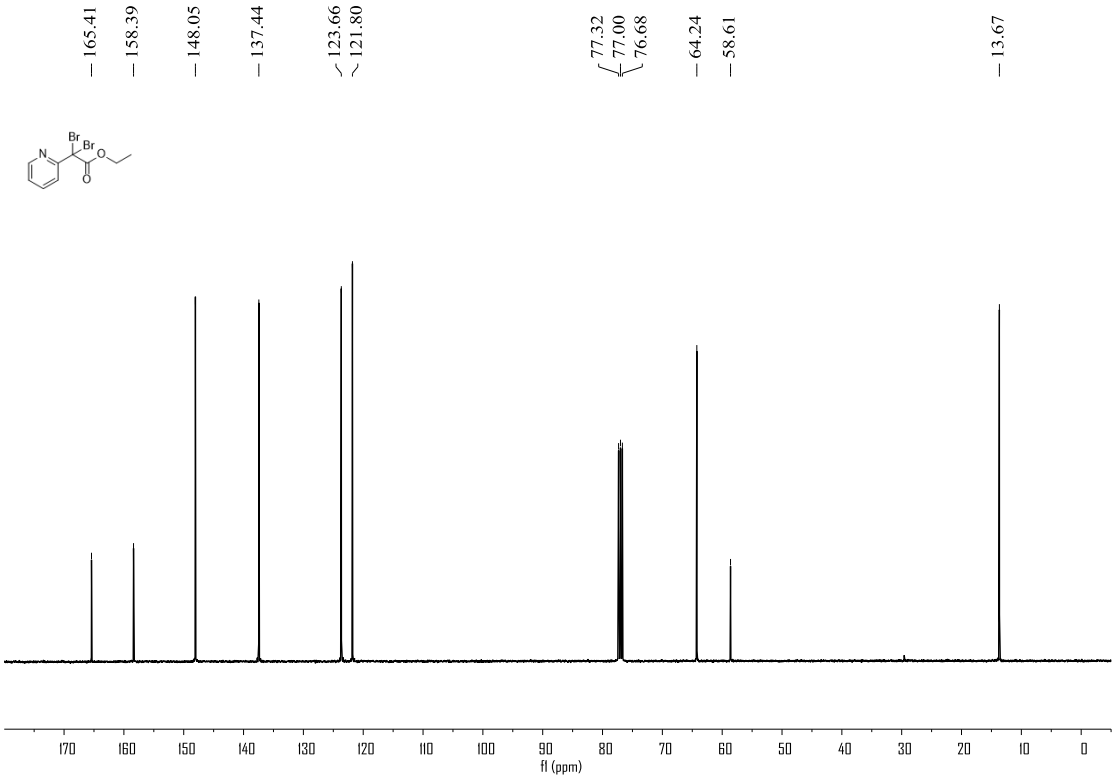

Figure S158. ^{1}H NMR (400 MHz, $CDCl_3$) spectrum of compound **13**, related to **Figure 7**

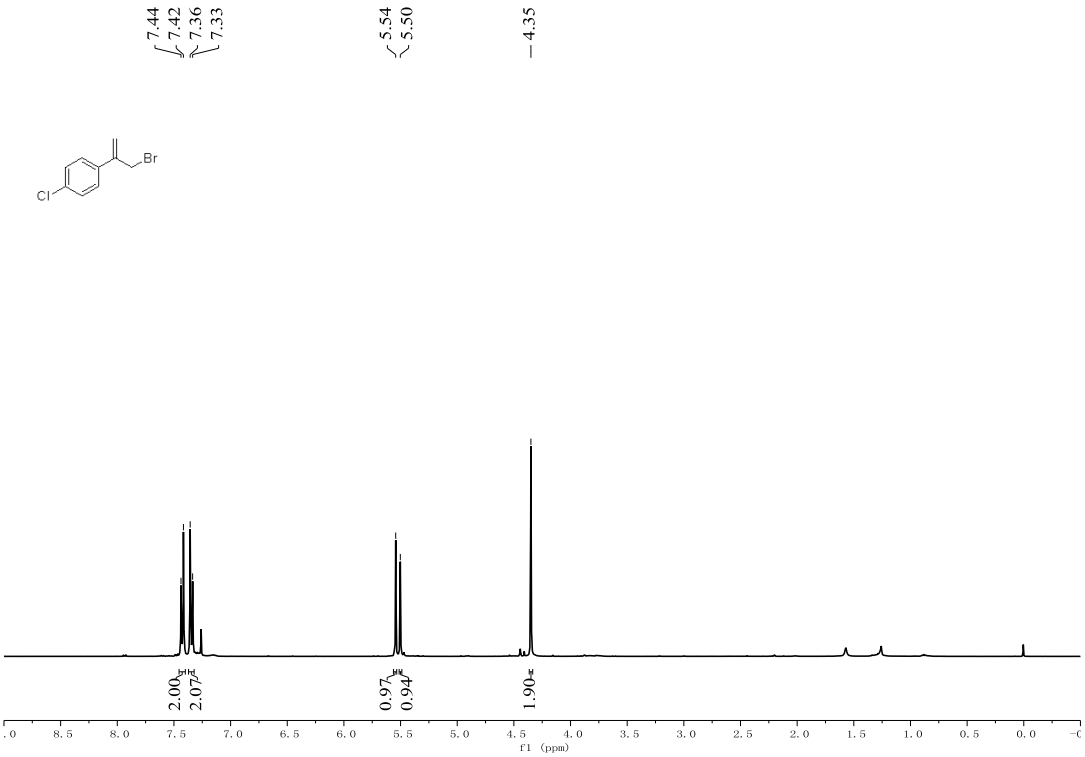

Figure S159. ^{13}C NMR (100 MHz, $CDCl_3$) spectrum of compound **13**, related to **Figure 7**

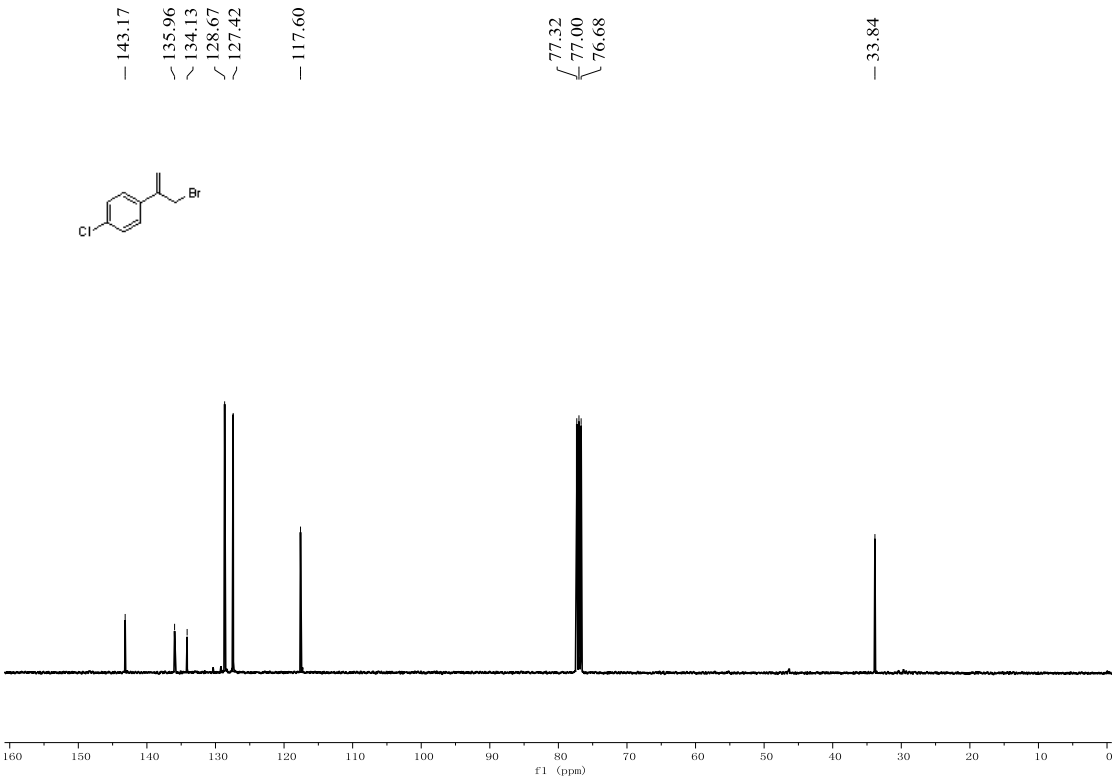

Transparent Methods

The instrument for electrolysis is dual display potentiostat (DJS-292B) (made in China). The anodic electrode was graphite rod (ϕ 6 mm) and cathodic electrode was platinum plate (15 mm × 15 mm × 0.3 mm). Thin layer chromatography (TLC) employed glass 0.25 mm silica gel plates. Flash chromatography columns were packed with 200-300 mesh silica gel in petroleum (boiling point, 60 to 90 ^{o}C). NMR spectra were recorded on a Bruker spectrometer at 400 MHz (^{1}H NMR), 100 MHz (^{13}C NMR), 376 MHz (^{19}F NMR), respectively. All chemical shifts are reported relative to tetramethylsilane and solvent peaks. ^{1}H, ^{13}C and ^{19}F NMR data spectra were reported in delta (δ) units, parts per million (ppm) downfield from the internal standard. Coupling constants are reported in Hertz (Hz).

General procedure for electrochemical oxidative C–H chlorination: In an undivided three-necked bottle (25 mL) equipped with a stir bar, **1** (0.3 mmol), **2a** (0.6 mmol, 35.1 mg), were combined and added. The bottle was equipped with graphite rod (ϕ 6 mm, about 18 mm immersion depth in solution) as the anode and platinum plate (15 mm × 15 mm × 0.3 mm) as the cathode and then charged with nitrogen. Under the protection of N_2, H_2O (0.5 mL) and DMF (10.5 mL) were injected respectively into the bottle via syringes. The reaction mixture was stirred and electrolyzed with a constant current of 12 mA at 80 ^{o}C for 3.5 h. When the reaction was finished, the solution was extracted with EtOAc (3×10mL) and H_2O (3×30mL). The combined organic layer was dried with Na_2SO_4, filtered. The solvent was removed with a rotary evaporator. The pure product was obtained by flash column chromatography on silica gel using petroleum ether and ethyl acetate as the eluent.

General procedure for electrochemical oxidative C–H bromination: In an undivided three-necked bottle (25 mL) equipped with a stir bar, **1** (0.3 mmol), **2b** (1.2 mmol, 123.5 mg.), were combined and added. The bottle was equipped with graphite rod (ϕ 6 mm, about 18 mm immersion depth in solution) as the anode and platinum plate (15 mm × 15 mm × 0.3 mm) as the cathode and then charged with nitrogen. Under the protection of N_2, H_2O (0.5 mL) and DMF (10.5 mL) were injected respectively into the bottle via syringes. The reaction mixture was stirred and electrolyzed with a constant current of 12 mA at 80 ^{o}C for 3.5 h. When the reaction was finished,

the solution was extracted with EtOAc (3×10mL) and H_2O (3×30mL). The combined organic layer was dried with Na_2SO_4, filtered. The solvent was removed with a rotary evaporator. The pure product was obtained by flash column chromatography on silica gel using petroleum ether and ethyl acetate as the eluent.

General procedure for electrochemical oxidative dibromination of alkenes: In an undivided three-necked bottle (25 mL) equipped with a stir bar, $^{n}Bu_4NBF_4$ (0.1 mmol, 33 mg) was added. The bottle was equipped with graphite rod (ϕ 6 mm, about 18 mm immersion depth in solution) as the anode and platinum plate (15 mm × 15 mm × 0.3 mm) as the cathode and then charged with nitrogen. Under the protection of N_2, **5** (0.5 mmol), **2c** (1.0 mmol, 113 uL, 48%), H_2O (0.2 mL) and CH_3CN (10.8 mL) were injected respectively into the bottle via syringes. The reaction mixture was stirred and electrolyzed with a constant current of 12 mA at room temperature for 3 h. The pure product was obtained by flash column chromatography on silica gel using petroleum ether as the eluent.

Procedure for gram scale synthesis of electrochemical oxidative C–H bromination (15 mmol scale): In an undivided three-necked bottle equipped with a stir bar, **1a** (15 mmol), **2b** (4 equiv.) were combined and added. The bottle was equipped with graphite rod (ϕ 6 mm) as the anode and platinum plate (15 mm × 15 mm × 0.3 mm) as the cathode. Under the air, H_2O (5 mL) and DMF (105 mL) were injected respectively into the bottle via syringes. The reaction mixture was stirred and electrolyzed with a constant current of 60 mA at 80 ^{o}C for 35 h. When the reaction was finished, the solution was extracted with EtOAc (3×50 mL) and H_2O (3×150 mL). The combined organic layer was dried with Na_2SO_4, filtered. The solvent was removed with a rotary evaporator. The pure product was obtained by flash column chromatography on silica gel using petroleum ether and ethyl acetate as the eluent.

Procedure for gram scale synthesis of electrochemical oxidative C–H bromination (50 mmol scale): In an undivided three-necked bottle equipped with a stir bar, **1a** (50 mmol), **2b** (4 equiv.) were combined and added. The bottle was equipped with graphite rod (ϕ 6 mm) as the anode and platinum plate (15 mm × 15 mm × 0.3 mm) as the cathode. Under the air, H_2O (5 mL) and DMF (105 mL) were injected respectively into the bottle via syringes. The reaction mixture was stirred

and electrolyzed with a constant current of 120 mA at 80 ^{o}C for 58.4 h. When the reaction was finished, the solution was extracted with EtOAc (3×100 mL) and H_2O (3×300 mL). The combined organic layer was dried with Na_2SO_4, filtered. The solvent was removed with a rotary evaporator. The pure product was obtained by flash column chromatography on silica gel using petroleum ether and ethyl acetate as the eluent.

Procedure for gram scale synthesis of electrochemical oxidative dibromination of alkenes: In an undivided three-necked bottle equipped with a stir bar. The bottle was equipped with graphite rod (ϕ 6 mm) as the anode and platinum plate (15 mm × 15 mm × 0.3 mm) as the cathode and then charged with nitrogen. Under the N_2, **5t** (200 mmol), **2c** (400 mmol, 48%), H_2O (4 mL) and CH_3CN (210 mL) were injected respectively into the bottle via syringes. The reaction mixture was stirred and electrolyzed with a constant current of 120 mA at room temperature for 120 h. The pure product was obtained by flash column chromatography on silica gel using petroleum ether as the eluent.

Procedure for cyclic voltammetry (CV)

Cyclic voltammetry was performed in a three-electrode cell connected to a schlenk line under nitrogen at room temperature. The working electrode was a steady glassy carbon disk electrode, the counter electrode was a platinum wire. The reference was an Ag/AgCl electrode submerged in saturated aqueous KCl solution. 11 mL mix-solvent (DMF/H_2O = 10.5/0.5) containing 0.01 M $^{n}Bu_4NBF_4$ were poured into the electrochemical cell in all experiments. The scan rate is 0.1 V/s, ranging from 0 V to 1.8 V.

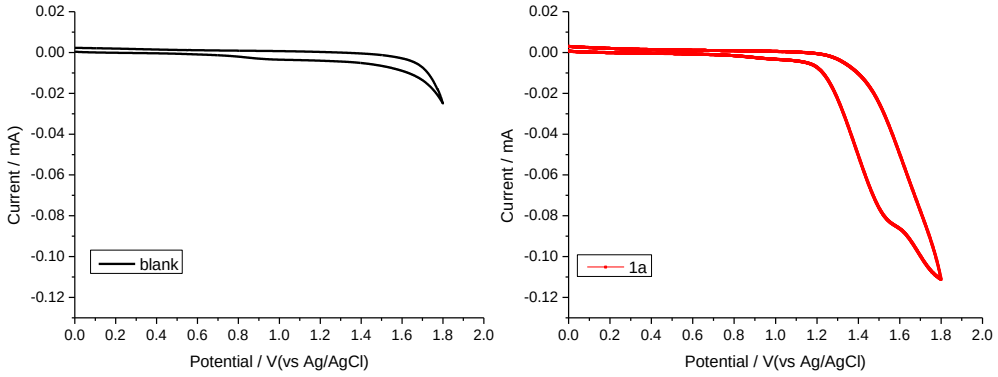

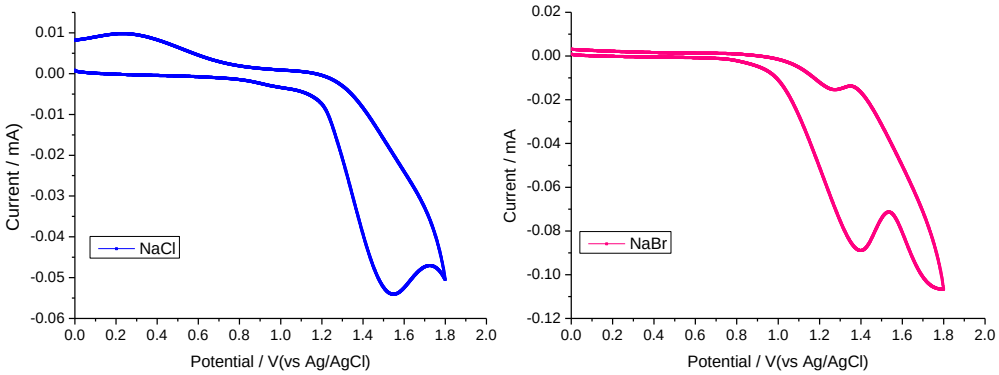

Fig. S160. Cyclic voltammograms.

Characterization of all compounds

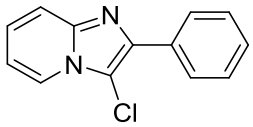

3-Chloro-2-phenylimidazo[1,2-a]pyridine (3a) (Xiao et al., 2015).

White solid was obtained in 81% isolated yield. ^{1}H NMR (400 MHz, $CDCl_3$) δ 8.13 (d, *J* = 8.1 Hz, 2H), 7.98 – 7.96 (m, 1H), 7.58 (d, *J* = 9.1 Hz, 1H), 7.46 (t, *J* = 7.7 Hz, 2H), 7.37 – 7.35 (m, 1H), 7.16 – 7.12 (m, 1H), 6.79 (t, *J* = 6.8 Hz, 1H); ^{13}C NMR (100 MHz, $CDCl_3$) δ 143.60, 139.66, 132.42, 128.49, 128.20, 127.41, 124.81, 122.61, 117.56, 112.85, 105.62.

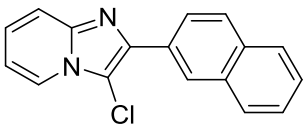

3-Chloro-2-(naphthalen-2-yl)imidazo[1,2-a]pyridine (3b).

White solid was obtained in 76% isolated yield. ^{1}H NMR (400 MHz, DMSO-d_6) δ 8.63 (s, 1H), 8.36 (d, *J* = 6.8 Hz, 1H), 8.27 – 8.25 (m, 1H), 8.02 (d, *J* = 8.5 Hz, 2H), 7.95 – 7.92 (m, 1H), 7.70 (d, *J* = 9.1 Hz, 1H), 7.57 – 7.52 (m, 2H), 7.41 – 7.37 (m, 1H), 7.10 (t, *J* = 6.6 Hz, 1H); ^{13}C NMR (100 MHz, $CDCl_3$) δ 143.72, 139.62, 133.36, 133.06, 129.85, 128.44, 128.08, 127.61, 126.69, 126.27, 126.17, 125.02, 124.92, 122.61, 117.53, 112.91, 105.94. HRMS (ESI): m/z calcd for $C_{17}H_{12}ClN_2$ $[M+H]^+$: 279.00684, found: 279.0688.

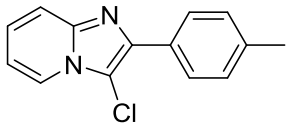

3-Chloro-2-(p-tolyl)imidazo[1,2-a]pyridine (3c) (Xiao et al., 2015).

White solid was obtained in 73% isolated yield. ^{1}H NMR (400 MHz, $CDCl_3$) δ 8.04 – 8.02 (m, 3H), 7.60 (d, *J* = 9.1 Hz, 1H), 7.28 – 7.266 (m, 2H), 7.19 – 7.15 (m, 1H), 6.86 – 6.82 (m, 1H), 2.39 (s, 3H); ^{13}C NMR (100 MHz, $CDCl_3$) δ 143.50, 139.77, 138.00, 129.57, 129.14, 127.25, 124.55, 122.45, 117.37, 112.63, 105.17, 21.22.

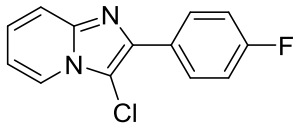

3-Chloro-2-(4-fluorophenyl)imidazo[1,2-a]pyridine (3d).

White solid was obtained in 70% isolated yield. ^{1}H NMR (400 MHz, $CDCl_3$) δ 8.14 – 8.06 (m, 3H), 7.61 (d, *J* = 9.1 Hz, 1H), 7.26 (m, 1H), 7.19 – 7.13 (m, 2H), 6.93–6.90 (m, 1H); ^{13}C NMR (100 MHz, $CDCl_3$) δ 163.91, 161.44, 143.59, 138.83, 129.21 (d, *J* = 8.2 Hz), 128.58 (d, *J* = 3.2 Hz), 124.98, 122.64, 117.51, 115.49 (d, *J* = 21.6 Hz), 112.96, 105.33; ^{19}F NMR (376 MHz, $CDCl_3$) δ –113.20. HRMS (ESI): m/z calcd for $C_{13}H_9ClFN_2$ $[M+H]^+$: 247.0433, found: 247.0436.

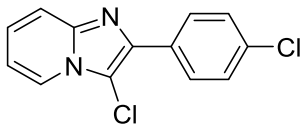

3-Chloro-2-(4-chlorophenyl)imidazo[1,2-a]pyridine (3e) (Xiao et al., 2015).

White solid was obtained in 75% isolated yield. ^{1}H NMR (400 MHz, $CDCl_3$) δ 8.06 – 8.01 (m, 3H), 7.59 (d, *J* = 9.1 Hz, 1H), 7.41 (d, *J* = 8.5 Hz, 2H), 7.23 – 7.19 (m, 1H), 6.88 (t, *J* = 6.8 Hz, 1H); ^{13}C NMR (100 MHz, $CDCl_3$) δ 143.50, 138.40, 133.93, 130.88, 128.58, 128.46, 124.96, 122.52, 117.46, 112.91, 105.59.

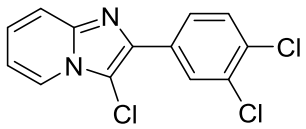

3-Chloro-2-(3,4-dichlorophenyl)imidazo[1,2-a]pyridine (3f).

White solid was obtained in 73% isolated yield. ^{1}H NMR (400 MHz, DMSO-d_6) δ 8.36 (d, J = 6.8 Hz, 1H), 8.21 (d, J = 1.8 Hz, 1H), 8.05 – 8.02 (m, 1H), 7.74 (d, J = 8.5 Hz, 1H), 7.66 (d, J = 9.1 Hz, 1H), 7.43 – 7.39 (m, 1H), 7.12 (t, J = 6.8 Hz, 1H); ^{13}C NMR (100 MHz, $CDCl_3$) δ 143.65, 137.25, 132.72, 132.50, 132.06, 130.39, 128.97, 126.31, 125.35, 122.66, 117.65, 113.22, 106.09. HRMS (ESI): m/z calcd for $C_{13}H_8Cl_3N_2$ $[M+H]^+$: 296.9748, found: 296.9740.

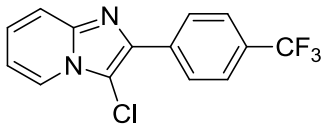

3-Chloro-2-(4-(trifluoromethyl)phenyl)imidazo[1,2-a]pyridine (3g).

White solid was obtained in 73% isolated yield. ^{1}H NMR (400 MHz, DMSO-d_6) δ 8.34 (d, J = 6.9 Hz, 1H), 8.24 (d, J = 8.1 Hz, 1H), 7.80 (d, J = 8.3 Hz, 1H), 7.66 (d, J = 9.1 Hz, 1H), 7.40 – 7.36 (m, 1H), 7.11 – 7.07 (m, 1H); ^{13}C NMR (100 MHz, $CDCl_3$) δ 143.77, 138.10, 135.97, 129.83 (q, J = 32.4 Hz) , 127.45, 125.36 (q, J = 4.0 Hz), 125.37, 124.15 (q, J = 270.0 Hz), 122.69, 117.75, 113.21, 106.49; ^{19}F NMR (376 MHz, $CDCl_3$) δ –62.53. HRMS (ESI): m/z calcd for $C_{14}H_9ClF_3N_2$ $[M+H]^+$: 297.0401, found: 297.0405.

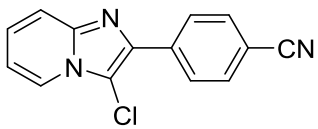

4-(3-Chloroimidazo[1,2-a]pyridin-2-yl)benzonitrile (3h).

White solid was obtained in 62% isolated yield. ^{1}H NMR (400 MHz, $CDCl_3$) δ 8.28 – 8.26 (m, 2H), 8.13 – 8.11 (m, 1H), 7.75 – 7.73 (m, 2H), 7.64 (d, J = 9.1 Hz, 1H), 7.33 – 7.28 (m, 1H), 6.01 – 6.97 (m, 1H); ^{13}C NMR (100 MHz, $CDCl_3$) δ 143.80, 137.41 (d, J = 2 Hz), 136.89, 132.18, 127.53, 125.62, 122.73, 118.81, 117.79, 113.44, 111.27, 106.93. HRMS (ESI): m/z calcd for $C_{14}H_9ClN_3$ $[M+H]^+$: 254.0480, found: 254.0485.

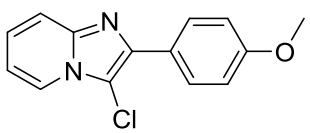

3-Chloro-2-(4-methoxyphenyl)imidazo[1,2-a]pyridine (3i) (Xiao et al., 2015).

White solid was obtained in 30% isolated yield. ^{1}H NMR (400 MHz, $CDCl_3$) δ 8.09 – 8.07 (m, 3H), 7.62 (d, *J* = 9.1 Hz, 1H), 7.24 – 7.20 (m, 1H), 7.02 (d, *J* = 8.7 Hz, 2H), 6.90 (t, *J* = 6.8 Hz, 1H), 3.86 (s, 3H); ^{13}C NMR (100 MHz, $CDCl_3$) δ 159.62, 143.54, 139.62, 128.74, 125.03, 124.65, 122.52, 117.33, 113.93, 112.70, 104.76, 55.25.

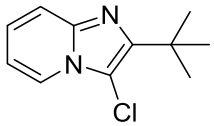

2-(Tert-butyl)-3-chloroimidazo[1,2-a]pyridine (3j) (Li et al., 2018).

Light yellow liquid was obtained in 68% isolated yield. ^{1}H NMR (400 MHz, $CDCl_3$) δ 8.03 (d, *J* = 6.9 Hz, 1H), 7.59 (d, *J* = 9.1 Hz, 1H), 7.19 – 7.15 (m, 1H), 6.86 (t, *J* = 6.8 Hz, 1H), 1.51 (s, 9H); ^{13}C NMR (100 MHz, $CDCl_3$) δ 149.42, 142.16, 123.69, 122.00, 117.22, 112.35, 104.33, 32.87, 29.49.

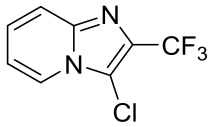

3-Chloro-2-(trifluoromethyl)imidazo[1,2-a]pyridine (3k).

White solid was obtained in 73% isolated yield. ^{1}H NMR (400 MHz, DMSO-d_6) δ 8.47 – 7.45 (m, 1H), 7.77 – 7.74 (m, 1H), 7.56 – 7.51 (m, 1H), 7.26 – 7.23(m, 1H); ^{13}C NMR (100 MHz, $CDCl_3$) δ 143.40, 130.8 (q, *J* = 38.5 Hz), 126.57, 123.13, 121.09 (q, *J* = 267.0 Hz), 118.89, 114.51, 108.92; ^{19}F NMR (376 MHz, $CDCl_3$) δ –61.77. HRMS (ESI): m/z calcd for $C_8H_5ClF_3N_2$ $[M+H]^+$: 221.0088, found: 221.0091.

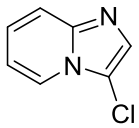

3-Chloroimidazo[1,2-a]pyridine (3l) (Li et al., 2018).

Light yellow oil was obtained in 37% isolated yield. ^{1}H NMR (400 MHz, $CDCl_3$) δ 8.05 (d, *J* = 6.9 Hz, 1H), 7.61 – 7.56 (m, 2H), 7.22 – 7.18 (m, 1H), 6.91 (t, *J* = 6.8 Hz, 1H); ^{13}C NMR (100 MHz, $CDCl_3$) δ 144.29, 130.00, 124.06, 122.37, 117.88, 112.76, 109.40.

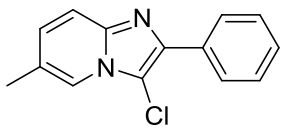

3-Chloro-6-methyl-2-phenylimidazo[1,2-a]pyridine (3m) (Xiao et al., 2015).

Light yellow liquid was obtained in 87% isolated yield. ^{1}H NMR (400 MHz, $CDCl_3$) δ 8.14 – 8.11 (m, 2H), 7.83 (s, 1H), 7.52 – 7.45 (m, 3H), 7.38 – 7.33 (m, 1H), 7.06 – 7.33 (m, 1H), 2.33 (s, 3H); ^{13}C NMR (100 MHz, $CDCl_3$) δ 142.66, 139.37, 132.63, 128.40, 127.96, 127.91, 127.24, 122.62, 120.21, 116.81, 105.11, 18.25.

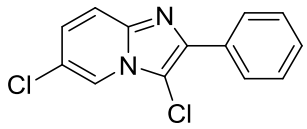

3,6-Dichloro-2-phenylimidazo[1,2-a]pyridine (3n) (Xiao et al., 2015).

White solid was obtained in 76% isolated yield. ^{1}H NMR (400 MHz, DMSO-d_6) δ 8.49 – 8.48 (m, 1H), 8.70 – 8.05 (m, 2H), 7.67 (d, *J* = 9.6 Hz, 1H), 7.52 – 7.48 (m, 2H), 7.42 – 7.36 (m, 2H); ^{13}C NMR (100 MHz, $CDCl_3$) δ 141.93, 140.71, 131.96, 128.53, 128.47, 127.36, 126.26, 121.41, 120.55, 117.93, 106.08.

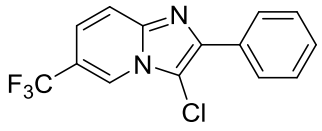

3-Chloro-2-phenyl-6-(trifluoromethyl)imidazo[1,2-a]pyridine (3o).

White solid was obtained in 78% isolated yield. ^{1}H NMR (400 MHz, DMSO-d_6) δ 8.75 (s, 1H), 8.10 –8.07 (m, 2H), 7.85 (d, *J* = 9.5 Hz, 1H), 7.61 – 7.58 (m, 1H), 7.53 – 7.50 (m, 2H), 7.45 – 7.40 (m, 1H); ^{13}C NMR (100 MHz, $CDCl_3$) δ 143.32, 141.61, 131.67, 128.79, 128.63, 127.48, 123.35 (q, *J* = 270.0 Hz), 121.8 (q, *J* = 5.7 Hz), 120.72 (q, *J* = 2.6 Hz), 118.32, 117.4 (q, *J* = 34.4

Hz), 107.21; ^{19}F NMR (376 MHz, $CDCl_3$) δ –62.14. HRMS (ESI): m/z calcd for $C_{14}H_9ClF_3N_2$ $[M+H]^+$: 297.0400, found: 297.0361.

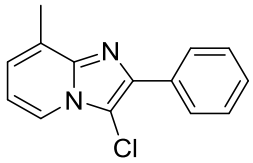

3-Chloro-5-methyl-2-phenylimidazo[1,2-a]pyridine (3p).

Light yellow oil was obtained in 83% isolated yield. ^{1}H NMR (400 MHz, $CDCl_3$) δ 8.04 – 8.02 (m, 2H), 7.79 (d, *J* = 6.8 Hz, 1H), 7.36 (t, *J* = 7.6 Hz, 2H), 7.25 (t, *J* = 7.4 Hz, 1H), 6.86 (d, *J* = 6.9 Hz, 1H), 6.65 (t, *J* = 6.9 Hz, 1H), 2.53 (s, 3H); ^{13}C NMR (100 MHz, $CDCl_3$) δ 143.99, 139.25, 132.75, 128.44, 128.00, 127.64, 127.58, 123.52, 120.45, 112.84, 105.86, 16.47. HRMS (ESI): m/z calcd for $C_{14}H_{12}ClN_2$ $[M+H]^+$: 243.0684, found: 243.0690.

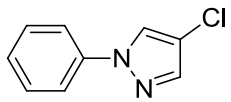

4-Chloro-1-phenyl-1H-pyrazole (3q) (Wang et al., 2016).

White solid was obtained in 90% isolated yield.^{1}H NMR (400 MHz, $CDCl_3$) δ 7.81 (s, 1H), 7.55 (s, 1H), 7.55 – 7.51 (m, 2H), 7.39 – 7.32 (m, 2H), 7.25 – 7.19 (m, 1H); ^{13}C NMR (100 MHz, $CDCl_3$) δ 139.70, 139.46, 129.55, 127.01, 124.84, 118.96, 112.39.

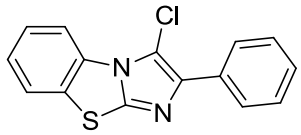

3-Chloro-2-phenylbenzo[d]imidazo[2,1-b]thiazole (3r).

Yellow solid was obtained in 68% isolated yield.^{1}H NMR (400 MHz, $CDCl_3$) δ 8.01 (d, *J* = 8.2 Hz, 1H), 7.90 (d, *J* = 7.0 Hz, 2H), 7.49 (d, *J* = 8.0 Hz, 1H), 7.33 (t, *J* = 7.7 Hz, 2H), 7.26 – 7.13 (m, 3H); ^{13}C NMR (100 MHz, $CDCl_3$) δ 145.90, 140.77, 132.24, 132.18, 129.78, 128.37, 127.65, 126.47, 125.90, 124.99, 123.95, 113.23, 108.27. HRMS (ESI): m/z calcd for $C_{15}H_{10}ClN_2S[M+H]^+$: 285.0248, found:285.0258.

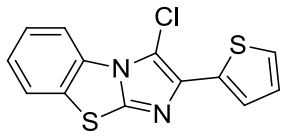

3-Chloro-2-(thiophen-2-yl)benzo[d]imidazo[2,1-b]thiazole (3s).

Yellow solid was obtained in 62% isolated yield. ^{1}H NMR (400 MHz, $CDCl_3$) δ 8.19 (d, *J* = 8.5 Hz, 1H), 7.62 (d, *J* = 3.7 Hz, 1H), 7.53 (d, *J* = 8.0 Hz, 1H), 7.31 – 7,27 (m, 1H), 7.25 – 7.18 (m, 2H), 7.02 – 7.00 (m, 1H).;^{13}C NMR (100 MHz, $CDCl_3$) δ 147.93, 139.79, 135.43, 132.54, 129.88, 127.45, 125.81, 125.13, 125.08, 124.29, 124.03, 113.26, 90.78. HRMS (ESI): m/z calcd for $C_{13}H_8ClN_2S_2$ $[M+H]^+$: 290.9812, found: 290.9816.

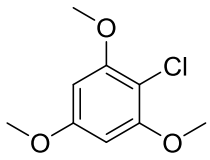

2-Bromo-1,3,5-trimethoxybenzene (3t) (Tang et al., 2018).

White solid was obtained in 77% isolated yield. ^{1}H NMR (400 MHz, $CDCl_3$) δ 6.18 (s, 2H), 3.88 (s, 6H), 3.81 (s, 3H); ^{13}C NMR (100 MHz, $CDCl_3$) δ 159.37, 156.49, 102.61, 91.55, 56.24, 55.48.

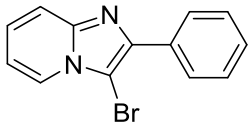

3-Bromo-2-phenylimidazo[1,2-a]pyridine (4a) (Zhou et al., 2016).

White solid was obtained in 87% isolated yield. ^{1}H NMR (400 MHz, DMSO-d_6) δ 8.35 (d, *J* = 6.9 Hz, 1H), 8.10 – 8.08 (m, 2H), 7.66 (d, *J* = 9.1 Hz, 1H), 7.51 – 7.47 (m, 2H), 7.42 – 7.35 (m, 2H), 7.09 – 7.05 (m, 1H); ^{13}C NMR (100 MHz, DMSO-d_6) δ 144.87, 141.39, 132.81, 128.58, 128.27, 127.36, 125.87, 124.58, 117.09, 113.64, 91.65.

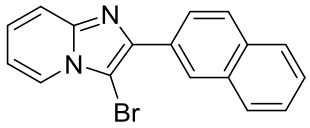

3-Bromo-2-(naphthalen-2-yl)imidazo[1,2-a]pyridine (4b) (Zhou et al., 2016).

White solid was obtained in 66% isolated yield. ^{1}H NMR (400 MHz, DMSO-d_6) δ 8.64 (s, 1H), 8.40 (d, *J* = 6.8 Hz, 1H), 8.27 – 7.25 (m, 1H), 8.03 – 8.00 (m, 2H), 7.95 – 7.93 (m, 1H), 7.70 (d, *J* = 9.0 Hz, 1H), 7.57 – 7.52 (m, 2H), 7.42 – 7.38 (m, 1H), 7.10 (t, *J* = 6.8 Hz, 1H); ^{13}C NMR (100 MHz, $CDCl_3$) δ 145.37, 142.37, 133.22, 133.00, 130.17, 128.37, 127.93, 127.55, 127.01, 126.21, 126.10, 125.37, 125.06, 123.78, 117.41, 112.94, 91.91.

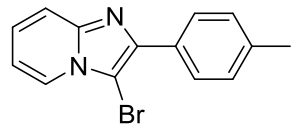

.

3-Bromo-2-(p-tolyl)imidazo[1,2-a]pyridine (4c) (Zhou et al., 2016).

White solid was obtained in 91% isolated yield. ^{1}H NMR (400 MHz, $CDCl_3$) δ 8.01 (d, *J* = 6.9 Hz, 1H), 7.92 (d, *J* = 8.2 Hz, 2H), 7.51 (d, *J* = 9.1 Hz, 1H), 7.19 – 7.15 (m, 2H), 7.13 – 7.09 (m, 1H), 6.79 – 6.75 (m, 1H), 2.29 (s, 3H); ^{13}C NMR (100 MHz, $CDCl_3$) δ 145.32, 142.67, 138.23, 129.85, 129.19, 127.76, 125.05, 123.90, 117.46, 112.99, 91.41, 21.33.

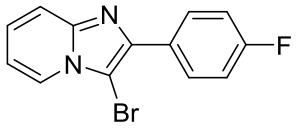

3-Bromo-2-(4-fluorophenyl)imidazo[1,2-a]pyridine (4d) (Zhou et al., 2016).

White solid was obtained in 76% isolated yield. ^{1}H NMR (400 MHz, $CDCl_3$) δ 8.14 – 8.09 (m, 3H), 7.61 (d, *J* = 9.1 Hz, 1H), 7.26 – 7.22 (m, 1H), 7.19 – 7.13 (m, 2H), 6.92 – 6.89 (m, 1H); ^{13}C NMR (100 MHz, $CDCl_3$) δ162.68 (d, *J* = 248.0 H), 145.31, 141.69, 129.55 (d, *J* = 8.2 Hz), 128.95 (d, *J* = 3.2 Hz), 125.12, 123.85, 117.45, 115.36 (d, *J* = 21.5 Hz), 113.01, 91.32; ^{19}F NMR (376 MHz, $CDCl_3$) δ –13.19.

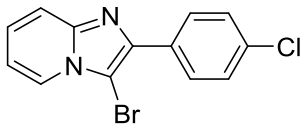

3-Bromo-2-(4-chlorophenyl)imidazo[1,2-a]pyridine (4e) (Zhou et al., 2016).

White solid was obtained in 59% isolated yield. ^{1}H NMR (400 MHz, $CDCl_3$) δ 8.12 (d, *J* = 6.9 Hz, 1H), 8.09 – 8.05 (m, 2H), 7.61 (d, *J* = 9.1 Hz, 1H), 7.45 – 7.41 (m, 2H), 7.26 – 7.22 (m, 1H), 6.93

– 6.89 (m, 1H); ^{13}C NMR (100 MHz, $CDCl_3$) δ 145.32, 141.34, 134.15, 131.22, 128.98, 128.61, 125.37, 123.91, 117.51, 113.20, 91.74.

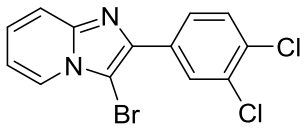

3-Bromo-2-(3,4-dichlorophenyl)imidazo[1,2-a]pyridine (4f) (Zhou et al., 2016).

White solid was obtained in 74% isolated yield. ^{1}H NMR (400 MHz, DMSO-d_6) δ 8.36 (d, J = 6.9 Hz, 1H), 8.25 (d, J = 2.0 Hz, 1H), 8.08 – 8.06 (m, 1H), 7.73 (d, J = 8.4 Hz, 1H), 7.65 (d, J = 9.1 Hz, 1H), 7.43 – 7.39 (m, 1H), 7.13 – 7.10 (m, 1H); ^{13}C NMR (100 MHz, $CDCl_3$) δ 145.40, 140.10, 132.80, 132.70, 132.25, 130.39, 129.44, 126.78, 125.71, 124.01, 117.65, 113.47, 92.14.

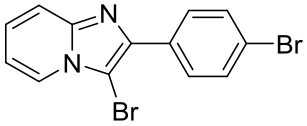

3-Bromo-2-(4-bromophenyl)imidaz[1,2-a]pyridine (4g) (Salgado-Zamora et al., 2008).

White solid was obtained in 58% isolated yield. ^{1}H NMR (400 MHz, DMSO-d_6) δ 8.33 (d, J = 6.9 Hz, 1H), 8.04 – 8.02 (m, 2H), 7.68 – 7.63 (m, 3H), 7.40 – 7.36 (m, 1H), 7.08 (t, J = 6.8 Hz, 1H); ^{13}C NMR (100 MHz, DMSO-d_6) δ 144.78, 140.15, 131.89, 131.34, 129.00, 125.86, 124.39, 121.40, 116.96, 113.57, 91.59.

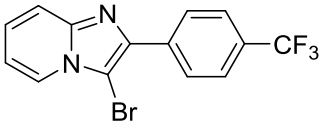

.

3-Bromo-2-(4-(trifluoromethyl)phenyl)imidazo[1,2-a]pyridine (4h) (Zhou et al., 2016).

White solid was obtained in 67% isolated yield. ^{1}H NMR (400 MHz, DMSO-d_6) δ 8.36 – 8.34 (m, 1H), 8.27 (d, J = 8.1 Hz, 2H), 7.82 (d, J = 8.2 Hz, 2H), 7.68 – 7.65 (m, 1H), 7.41 – 7.37 (m, 1H), 7.11 – 7.07 (m, 1H); ^{13}C NMR (100 MHz, DMSO-d_6) δ 145.03, 139.70, 136.79, 128.33 (q, J = 32 Hz) , 127.73, 126.36, 125.48 (q, J = 3.7 Hz), 124.76, 124.35 (q, J = 271 Hz), 117.29, 113.99, 92.85; ^{19}F NMR (376 MHz, $CDCl_3$) δ –62.54.

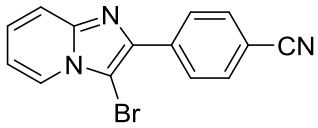

4-(3-Bromoimidazo[1,2-a]pyridin-2-yl)benzonitrile (4i).

White solid was obtained in 56% isolated yield. ^{1}H NMR (400 MHz, DMSO-d_6) δ 8.44 (d, J = 5.6 Hz, 1H), 8.30 (d, J = 7.1 Hz, 2H), 7.98 (d, J = 7.2 Hz, 2H), 7.71 (d, J = 8.8 Hz, 1H), 7.45 (t, J = 7.5 Hz, 1H), 7.15 (s, 1H); ^{13}C NMR (100 MHz, DMSO-d_6) δ 144.98, 139.33, 137.15, 132.28, 127.55, 126.28, 124.56, 118.49, 117.15, 113.88, 110.42, 92.90. HRMS (ESI): m/z calcd for $C_{14}H_9BrN_3$ $[M+H]^+$: 297.9974, found: 297.9967.

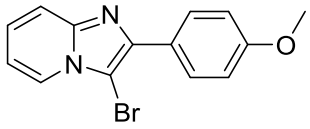

3-Bromo-2-(4-methoxyphenyl)imidazo[1,2-a]pyridine (4j) (Zhou et al., 2016).

White solid was obtained in 74% isolated yield. ^{1}H NMR (400 MHz, DMSO-d_6) δ 8.35 – 8.33 (m, 1H), 8.05 – 8.01 (m, 2H), 7.65 – 7.62 (m, 1H), 7.38 – 7.34 (m, 1H), 7.08 – 7.04 (m, 3H), 3.81 (s, 3H); ^{13}C NMR (100 MHz, DMSO-d_6) δ 159.37, 144.76, 141.38, 128.70, 125.71, 125.19, 124.48, 116.85, 114.06, 113.48, 90.68, 55.25 (d, J = 7.3 Hz).

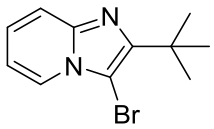

3-Bromo-2-(tert-butyl)imidazo[1,2-a]pyridine (4k) (Li et al., 2018).

Light yellow oil was obtained in 83% isolated yield. ^{1}H NMR (400 MHz, $CDCl_3$) δ 8.12 (d, J = 6.9 Hz, 1H), 7.60 (d, J = 9.0 Hz, 1H), 7.21 – 7.17 (m, 1H), 6.89 – 7.86 (m, 1H), 1.53 (s, 9H); ^{13}C NMR (100 MHz, $CDCl_3$) δ 151.84, 143.75, 124.08, 123.22, 117.19, 112.59, 90.06, 33.06, 29.67.

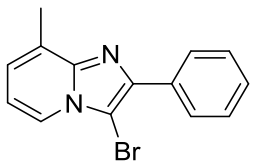

3-Bromo-8-methyl-2-phenylimidazo[1,2-a]pyridine (4l) (Zhou et al., 2016).

Light yellow oil was obtained in 93% isolated yield. ^{1}H NMR (400 MHz, $CDCl_3$) δ 8.04 – 8.01 (m, 2H), 7.87 (d, *J* = 6.8 Hz, 1H), 7.37 (t, *J* = 7.6 Hz, 2H), 7.27 (t, *J* = 7.4 Hz, 1H), 6.89 – 6.87 (m, 1H), 6.66 (t, *J* = 6.9 Hz, 1H), 2.54 (s, 3H); ^{13}C NMR (100 MHz, $CDCl_3$) δ 145.58, 142.00, 133.01, 128.32, 128.01, 127.92, 127.46, 123.70, 121.65, 112.86, 91.88, 16.47.

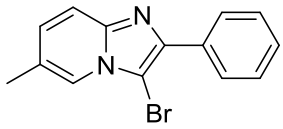

3-Bromo-6-methyl-2-phenylimidazo[1,2-a]pyridine (4m) (Zhou et al., 2016).

Light yellow oil was obtained in 83% isolated yield. ^{1}H NMR (400 MHz, DMSO-d_6) δ 8.16 (s, 1H), 8.09 – 8.07 (m, 2H), 7.56 (d, *J* = 9.2 Hz, 1H), 7.49 (t, *J* = 7.6 Hz, 2H), 7.39 (t, *J* = 7.4 Hz, 1H), 7.24 – 7.21 (m, 1H), 2.35 (s, 3H); ^{13}C NMR (100 MHz, $CDCl_3$) δ 144.31, 142.11, 132.85, 128.32, 128.19, 128.04, 127.65, 122.79, 121.50, 116.73, 91.14, 18.24.

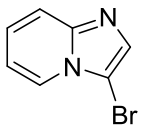

3-Bromoimidazo[1,2-a]pyridine (4n) (Pelleter et al., 2009).

Light yellow oil was obtained in 61% isolated yield. ^{1}H NMR (400 MHz, $CDCl_3$) δ 8.07–8.05 (m, 1H), 7.60 (d, *J* = 9.1 Hz, 1H), 7.56 (s, 1H), 7.21 – 7.17 (m, 1H), 6.90–6.86 (m, 1H); ^{13}C NMR (100 MHz, $CDCl_3$) δ 145.55, 133.36, 124.19, 123.42, 117.68, 112.82, 94.46.

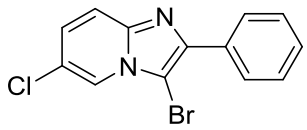

3-Bromo-6-chloro-2-phenylimidazo[1,2-a]pyridine (4o).

White solid was obtained in 90% isolated yield. ^{1}H NMR (400 MHz, DMSO-d_6) δ 8.48 (d, *J* = 1.1 Hz, 1H), 8.07 (d, *J* = 7.6 Hz, 2H), 7.69 (d, *J* = 9.5 Hz, 1H), 7.50 (t, *J* = 7.5 Hz, 2H), 7.43 – 7.39 (m, 2H); ^{13}C NMR (100 MHz, $CDCl_3$) δ 143.65, 143.48, 132.24, 128.51, 128.46, 127.73, 126.50, 121.84, 121.49, 117.86, 92.11. HRMS (ESI): m/z calcd for $C_{13}H_9BrClN_2$ $[M+H]^+$: 306.9632, found: 306.9621.

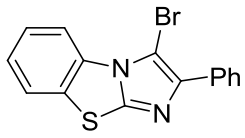

3-Bromo-2-phenylbenzo[d]imidazo[2,1-b]thiazole (4p).

White solid was obtained in 44% isolated yield.^{1}H NMR (400 MHz, $CDCl_3$) δ 8.24 (d, *J* = 8.2 Hz, 1H), 7.92 (d, *J* = 7.0 Hz, 2H), 7.53 (d, *J* = 7.9 Hz, 1H), 7.35 (t, *J* = 7.6 Hz, 2H), 7.29 – 7.17 (m, 3H); ^{13}C NMR (100 MHz, $CDCl_3$) δ 147.89, 143.89, 132.82, 132.53, 129.98, 128.33, 127.83, 127.07, 125.73, 125.09, 124.03, 113.51, 91.81.HRMS (ESI): m/z calcd for $C_{15}H_{10}BrN_2S$ $[M+H]^+$: 328.9743, found: 328.9757.

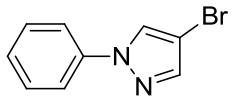

4-Bromo-1-phenyl-1H-pyrazole (4q) (Song et al., 2015).

White solid was obtained in 80% isolated yield. ^{1}H NMR (400 MHz, $CDCl_3$) δ 7.93 (s, 1H), 7.68 (s, 1H), 7.66 – 7.61 (m, 2H), 7.49 – 7.42 (m, 2H), 7.35 – 7.28 (m, 1H); ^{13}C NMR (100 MHz, $CDCl_3$) δ 141.43, 139.52, 129.48, 126.98, 126.95, 118.93, 95.56.

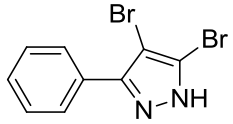

4,5-Dibromo-3-phenyl-1H-pyrazole (4r) (Trofimenko et al., 2007).

White solid was obtained in 68% isolated yield. ^{1}H NMR (400 MHz, $CDCl_3$) δ 10.84 (s, 1H), 7.75 – 7.64 (m, 2H), 7.54 – 7.37 (m, 3H); ^{13}C NMR (100 MHz, $CDCl_3$) δ 142.78, 129.65, 129.36, 128.94, 127.40, 127.25, 95.22.

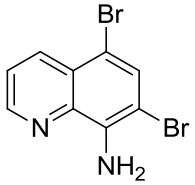

5,7-Dibromoquinolin-8-amine (4s) (da Silva et al., 2007).

Yellow solid was obtained in 80% isolated yield. ^{1}H NMR (400 MHz, $CDCl_3$) δ 8.73 – 8.72 (m, 1H), 8.36 – 8.33 (m, 1H), 7.76 (s, 1H), 7.48-7.45 (m, 1H), 5.35 (s, 2H); ^{13}C NMR (100 MHz, $CDCl_3$) δ 148.22, 141.93, 138.09, 135.66, 133.10, 126.61, 122.37, 106.75, 103.17.

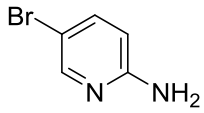

5-Bromopyridin-2-amine (4t) (Li et al., 2013).

White solid was obtained in 60% isolated yield. ^{1}H NMR (400 MHz, DMSO-d_6) δ 7.98 – 7.90 (m, 1H), 7.50 – 7.47 (m, 1H), 6.47 – 6.37 (m, 1H), 6.14 (s, 2H); ^{13}C NMR (100 MHz, $CDCl_3$) δ 156.96, 148.43, 140.15, 110.09, 108.16.

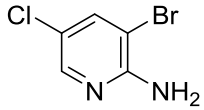

3-Bromo-5-chloropyridin-2-amine (4u).

Yellow solid was obtained in 49% isolated yield. ^{1}H NMR (400 MHz, $CDCl_3$) δ 7.95 (d, J = 2.2 Hz, 1H), 7.63 (d, J = 2.2 Hz, 1H), 5.19 (s, 2H); ^{13}C NMR (100 MHz, $CDCl_3$) δ 154.16, 145.06, 139.42, 119.94, 103.95. HRMS (ESI): m/z calcd for $C_5H_5BrClN_2$ $[M+H]^+$: 206.9319, found: 206.9330.

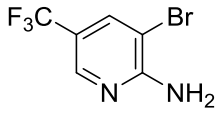

3-Bromo-5-(trifluoromethyl)pyridin-2-amine (4v).

White solid was obtained in 60% isolated yield. ^{1}H NMR (400 MHz, DMSO-d_6) δ 8.25 (d, J = 1.1 Hz, 1H), 8.00 (d, J = 2.0 Hz, 1H), 7.04 (s, 2H); ^{13}C NMR (100 MHz, $CDCl_3$) δ 157.77, 144.58 (q, J = 4.0 Hz)), 144.56, 123.29 (q, J = 271.1 Hz), 117.71 (q, J = 33.6 Hz), 103.44; ^{19}F NMR (376 MHz, $CDCl_3$) δ –61.18. HRMS (ESI): m/z calcd for $C_6H_5BrF_3N_2$ $[M+H]^+$: 240.9583, found: 240.9584.

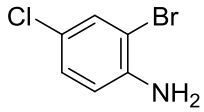

2-Bromo-4-chloroaniline (4w) (Li et al., 2013).

White solid was obtained in 59% isolated yield. ^{1}H NMR (400 MHz, $CDCl_3$) δ 7.36 (d, *J* = 2.3 Hz, 1H), 7.04 – 7.01 (m, 1H), 6.61 (d, *J* = 8.6 Hz, 1H), 4.01 (s, 2H); ^{13}C NMR (100 MHz, $CDCl_3$) δ 142.73, 131.62, 128.18, 122.75, 116.09, 108.98.

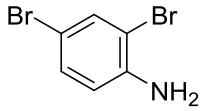

2,4-Dibromoaniline (4x) (Li et al., 2013).

White solid was obtained in 57% isolated yield. ^{1}H NMR (400 MHz, $CDCl_3$) δ 7.49 (d, *J* = 2.1 Hz, 1H), 7.16 – 7.13 (m, 1H), 6.57 (d, *J* = 8.5 Hz, 1H), 3.99 (s, 2H); ^{13}C NMR (100 MHz, $CDCl_3$) δ 143.11, 134.22, 130.98, 116.56, 109.40, 109.36.

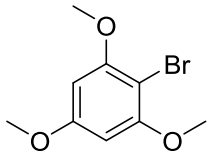

2-Bromo-1,3,5-trimethoxybenzene (4y) (Tang et al., 2018).

White solid was obtained in 85% isolated yield. ^{1}H NMR (400 MHz, $CDCl_3$) δ 6.14 (s, 2H), 3.85 (s, 6H), 3.79 (s, 3H); ^{13}C NMR (100 MHz, $CDCl_3$) δ 160.30, 157.24, 91.70, 91.44, 56.12, 55.31.

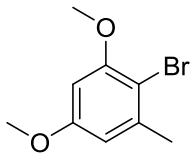

2-Bromo-1,5-dimethoxy-3-methylbenzene (4z) (Davis et al., 2000).

White solid was obtained in 83% isolated yield. ^{1}H NMR (400 MHz, $CDCl_3$) δ 6.41 (d, *J* = 2.7 Hz, 1H), 6.33 (d, *J* = 2.7 Hz, 1H), 3.84 (s, 3H), 3.77 (s, 3H), 2.38 (s, 3H); ^{13}C NMR (100 MHz, $CDCl_3$) δ 159.24, 156.56, 139.68, 107.19, 105.03, 97.16, 56.14, 55.33, 23.43.

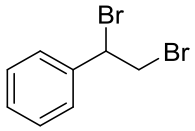

(1,2-Dibromoethyl)benzene (6a) (Martins et al., 2018).

White solid was obtained in 73% isolated yield.^{1}H NMR (400 MHz, $CDCl_3$) δ 7.42 – 7.30 (m, 5H), 5.15 – 5.11 (m, 1H), 4.08 – 3.98 (m, 2H); ^{13}C NMR (100 MHz, $CDCl_3$) δ 138.53, 129.10, 128.78, 127.59, 50.86, 35.00.

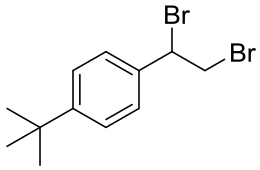

1-(Tert-butyl)-4-(1,2-dibromoethyl)benzene (6b) (Martins et al., 2018).

Colorless oil was obtained in 50% isolated yield. ^{1}H NMR (400 MHz, $CDCl_3$) δ 7.43 – 7.37 (m, 2H), 7.36 – 7.32 (m, 2H), 5.19 – 5.15 (m, 1H), 4.13 – 3.99 (m, 2H), 1.33 (s, 9H); ^{13}C NMR (100 MHz, $CDCl_3$) δ 152.26, 135.51, 127.26, 125.78, 51.23, 35.14, 34.69, 31.22.

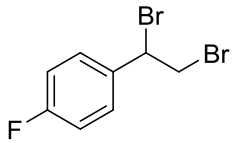

1-(1,2-Dibromoethyl)-4-fluorobenzene (6c) (Wilson et al., 2018).

White solid was obtained in 74% isolated yield. ^{1}H NMR (400 MHz, $CDCl_3$) δ 7.48 – 7.31 (m, 2H), 7.15 – 7.02 (m, 2H), 5.16 – 5.12 (m, 1H), 4.10 – 4.05 (m, 1H), 4.01 – 3.95 (m, 1H); ^{13}C NMR (100 MHz, $CDCl_3$) δ162.77 (d, *J* = 249.1 Hz), 134.52 (d, *J* = 4Hz), 129.48 (d, *J* = 9 Hz), 115.85 (d, *J* = 22 Hz) 49.79, 34.97; ^{19}F NMR (376 MHz, $CDCl_3$) δ -111.64.

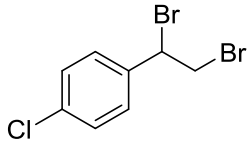

1-Chloro-4-(1,2-dibromoethyl)benzene (6d) (Martins et al., 2018).

Yellow oil was obtained in 77% isolated yield. ^{1}H NMR (400 MHz, $CDCl_3$) δ 7.38 – 7.33 (m, 4H), 5.13 – 5.09 (m, 1H), 4.09 – 4.05 (m, 1H), 4.00 – 3.94 (m, 1H); ^{13}C NMR (100 MHz, $CDCl_3$) δ 137.10, 134.89, 129.03, 128.98, 49.53, 34.65.

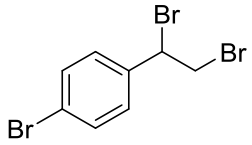

1-Bromo-4-(1,2-dibromoethyl)benzene (6e) (Karki et al., 2015).

Yellow oil was obtained in 80% isolated yield. ^{1}H NMR (400 MHz, $CDCl_3$) δ 7.57 – 7.48 (m, 2H), 7.35 – 7.23 (m, 2H), 5.12 – 5.08 (m, 1H), 4.08 – 4.04 (m, 1H), 3.97 (t, *J* = 10.6 Hz, 1H); ^{13}C NMR (100 MHz, $CDCl_3$) δ 137.60, 132.00, 129.25, 123.10, 49.54, 34.57.

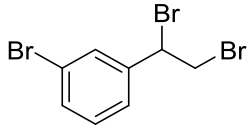

1-Bromo-3-(1,2-dibromoethyl)benzene (6f).

Yellow oil was obtained in 58% isolated yield. ^{1}H NMR (400 MHz, $CDCl_3$) δ 7.55 (t, *J* = 1.9 Hz, 1H), 7.48 – 7.46 (m, 1H), 7.34 – 7.31 (m, 1H), 7.25 – 7.22 (m, 1H), 5.07 – 5.03 (m, 1H), 4.06 – 4.02 (m, 1H), 3.95 (t, *J* = 10.6 Hz, 1H); ^{13}C NMR (100 MHz, $CDCl_3$) δ 140.71, 132.18, 130.72, 130.28, 126.29, 122.65, 49.21, 34.55. HRMS (EI): m/z calcd for $C_8H_7Br_3$ $[M]^+$: 339.8098, found: 339.8105.

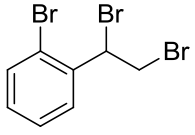

1-Bromo-2-(1,2-dibromoethyl)benzene (6g).

Yellow oil was obtained in 57% isolated yield. ^{1}H NMR (400 MHz, $CDCl_3$) δ 7.61 – 7.59 (m, 1H), 7.56 – 7.53 (m, 1H), 7.41 – 7.37 (m, 1H), 7.22 – 7.18 (m, 1H), 5.74 – 5.70 (m, 1H), 4.10 – 4.07 (m, 2H); ^{13}C NMR (100 MHz, $CDCl_3$) δ 137.53, 133.24, 130.29, 128.28, 128.13, 124.32, 48.32, 33.70. HRMS (EI): m/z calcd for $C_8H_7Br_3$ $[M]^+$: 339.8098, found: 339.8094.

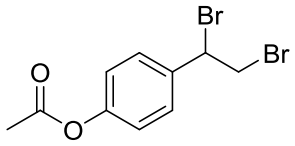

4-(1,2-Dibromoethyl)phenyl acetate (6h) (Rej et al., 2017).

White solid was obtained in 70% isolated yield. ^{1}H NMR (400 MHz, $CDCl_3$) δ 7.47 – 7.37 (m, 2H), 7.18 – 7.08 (m, 2H), 5.16 – 5.12 (m, 1H), 4.08 – 4.04 (m, 1H), 3.98 (t, *J* = 10.5 Hz, 1H), 2.29 (s, 3H); ^{13}C NMR (100 MHz, $CDCl_3$) δ 168.97, 150.89, 135.99, 128.76, 121.87, 50.03, 34.95, 21.07.

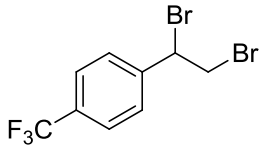

1-(1,2-Dibromoethyl)-4-(trifluoromethyl)benzene (6i).

Yellow oil was obtained in 40% isolated yield. ^{1}H NMR (400 MHz, $CDCl_3$) δ 7.64 (d, *J* = 8.2 Hz, 2H), 7.51 (d, *J* = 8.1 Hz, 2H), 5.16 – 5.12 (m, 1H), 4.09 – 4.05 (m, 1H), 3.98 (t, *J* = 10.7 Hz, 1H); ^{13}C NMR (100 MHz, $CDCl_3$) δ 142.45, 131.11 (q, *J* = 32.7 Hz), 128.13, 125.83 (q, *J* = 3.8 Hz), 123.73 (q, *J* = 270.6 Hz), 48.88, 34.28; ^{19}F NMR (376 MHz, $CDCl_3$) δ –62.71. HRMS (EI): m/z calcd for $C_9H_7Br_2F_3$ $[M]^+$: 329.8867, found: 329.8869.

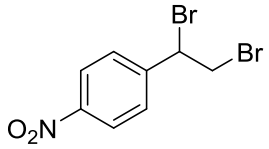

1-(1,2-Dibromoethyl)-4-nitrobenzene (6j).

Colorless oil was obtained in 41% isolated yield. ^{1}H NMR (400 MHz, $CDCl_3$) δ 8.35 – 8.13 (m, 2H), 7.78 – 7.47 (m, 2H), 5.19 – 5.15 (m, 1H), 4.11 – 4.07 (m, 1H), 3.98 (t, *J* = 10.8 Hz, 1H); ^{13}C NMR (100 MHz, $CDCl_3$) δ 148.01, 145.45, 128.76, 124.04, 47.77, 33.86. HRMS (ESI): m/z calcd for $C_8H_7Br_2NNaO_2$ $[M+Na]^+$: 329.8736, found: 329.8732.

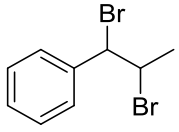

(1,2-Dibromopropyl)benzene (6k) (Kulangiappar et al., 2016).

White solid was obtained in 86% isolated yield. ^{1}H NMR (400 MHz, $CDCl_3$) δ 7.41 – 7.27 (m, 5H), 5.03 (d, J = 10.2 Hz, 1H), 4.63 – 4.55 (m, 1H), 2.03 (d, J = 6.5 Hz, 3H); ^{13}C NMR (100MHz, CDCl3) δ 140.46, 128.70, 128.55, 127.65, 59.11, 51.10, 25.75.

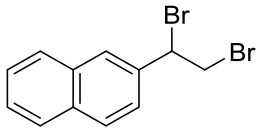

2-(1,2-Dibromoethyl)naphthalene (6l) (Song et al., 2015).

White solid was obtained in 43% isolated yield. ^{1}H NMR (400 MHz, $CDCl_3$) δ 7.98 – 7.81 (m, 4H), 7.55 – 7.51 (m, 3H), 5.37 – 5.33 (m, 1H), 4.19 – 4.14 (m, 2H); ^{13}C NMR (100 MHz, $CDCl_3$) δ 135.68, 133.48, 132.88, 129.05, 128.16, 127.74, 127.39, 126.87, 126.65, 124.34, 51.34, 34.78.

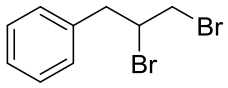

(2,3-Dibromopropyl)benzene (6m) (Karki et al., 2015).

Yellow oil was obtained in 86% isolated yield. ^{1}H NMR (400 MHz, $CDCl_3$) δ 7.40 – 7.27 (m, 5H), 4.41 – 7.35 (m, 1H), 3.86 – 3.82 (m, 1H), 3.67 – 3.62 (m, 1H), 3.55 – 3.50 (m, 1H), 3.18 – 3.12 (m, 1H); ^{13}C NMR (100 MHz, $CDCl_3$) δ 136.81, 129.46, 128.46, 127.16, 52.38, 41.97, 36.02.

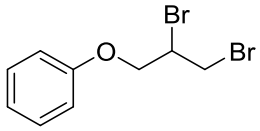

(2,3-Dibromopropoxy)benzene (6n) (Song et al., 2015).

Light yellow oil was obtained in 38% isolated yield. ^{1}H NMR (400 MHz, $CDCl_3$) δ 7.43 – 7.28 (m, 2H), 7.07 – 7.00 (m, 1H), 7.00 – 6.93 (m, 2H), 4.48 – 4.42 (m, 1H), 4.40 – 4.35 (m, 2H), 4.02 – 3.87 (m, 2H); ^{13}C NMR (100 MHz, $CDCl_3$) δ 157.90, 129.55, 121.62, 114.82, 69.03, 47.72, 32.74.

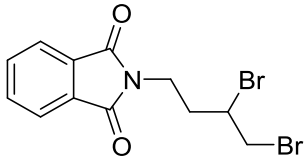

2-(3,4-Dibromobutyl)isoindoline-1,3-dione (6o).

Colorless oil was obtained in 70% isolated yield. ^{1}H NMR (400 MHz, DMSO-d_6) δ 7.84 – 7.79 (m, 4H), 4.94 – 4.43 (m, 1H), 4.00 – 3.96 (m, 1H), 3.92 – 3.88 (m, 1H), 3.80 – 3.71 (m, 2H), 2.42 – 4.34 (m, 1H), 2.20 – 2.01 (m, 1H). ^{13}C NMR (100 MHz, DMSO-d_6) δ 167.83, 134.33, 131.67, 123.00, 51.56, 38.45, 35.61, 34.99. HRMS (ESI): m/z calcd for $C_{12}H_{11}Br_2NNaO_2$ $[M+Na]^+$: 381.9049, found: 381.9048.

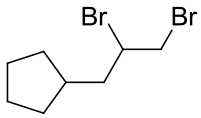

(2,3-Dibromopropyl)cyclopentane (6p).

Colorless oil was obtained in 77% isolated yield. ^{1}H NMR (400 MHz, $CDCl_3$) δ 4.18 – 4.11 (m, 1H), 3.92 – 3.80 (m, 1H), 3.64 – 3.59 (m, 1H), 2.20 – 1.96 (m, 2H), 1.95 – 1.73 (m, 3H), 1.73 – 1.46 (m, 4H), 1.31 – 1.12 (m, 1H), 1.10 – 1.01 (m, 1H); ^{13}C NMR (100 MHz, $CDCl_3$) δ 52.70, 42.68, 38.00, 37.10, 32.80, 31.44, 25.03, 24.97. HRMS (EI): m/z calcd for $C_8H_{14}Br_2$ $[M]^+$: 267.9462, found: 267.9452.

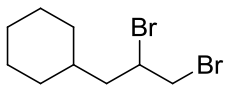

(2,3-Dibromopropyl)cyclohexane (6q).

Colorless oil was obtained in 85% isolated yield. ^{1}H NMR (400 MHz, $CDCl_3$) δ 4.31 – 4.13 (m, 1H), 3.8 – 3.84 (m, 1H), 3.70 – 3.49 (m, 1H), 2.01 – 1.94 (m, 1H), 1.85 – 1.49 (m, 7H), 1.31 – 1.15 (m, 3H), 1.09 – 0.95 (m, 1H), 0.93 – 0.77 (m, 1H); ^{13}C NMR (100 MHz, $CDCl_3$) δ 50.99, 43.95, 37.21, 35.52, 33.77, 31.48, 26.40, 26.12, 25.83. HRMS (EI): m/z calcd for $C_9H_{16}Br_2$ $[M]^+$: 281.9619, found: 281.9622.

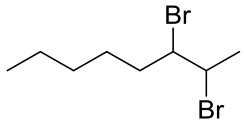

2,3-Dibromooctane (6r) (Badetti et al., 2016).

Colorless oil was obtained in 80% isolated yield. ^{1}H NMR (400 MHz, CDCl3) δ 4.47 – 4.41 (m, 1H), 4.25 – 4.18 (m, 1H), 2.08 – 2.01 (m, 1H), 1.77 (d, *J* = 6.7 Hz, 3H), 1.66 – 1.58 (m, 1H), 1.43 – 1.28 (m, 5H), 0.98 – 0.82 (m, 4H); ^{13}C NMR (100 MHz, $CDCl_3$) δ 60.11, 52.37, 33.89, 30.95, 27.44, 22.42, 21.52, 13.95.

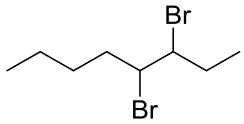

3,4-Dibromooctane (6s) (Conte et al., 1994).

Colorless oil was obtained in 71% isolated yield. ^{1}H NMR (400 MHz, $CDCl_3$) δ 4.19 – 4.10 (m, 2H), 2.22 – 2.09 (m, 2H), 2.04 – 1.90 (m, 2H), 1.65 – 1.54 (m, 1H), 1.49 – 1.26 (m, 3H), 1.08 (t, *J* = 7.2 Hz, 3H), 0.93 (t, *J* = 7.2 Hz, 3H); ^{13}C NMR (100 MHz, $CDCl_3$) δ 61.53, 59.40, 36.69, 30.23, 29.00, 22.01, 13.89, 11.35.

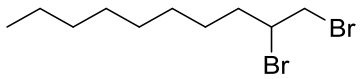

1,2-Dibromodecane (6t) (Song et al., 2015).

Colorless oil was obtained in 89% isolated yield. ^{1}H NMR (400 MHz, $CDCl_3$) δ 4.22 – 4.12 (m, 1H), 3.87 – 3.83 (m, 1H), 3.63 (t, *J* = 10.0 Hz, 1H), 2.20 – 2.05 (m, 1H), 1.83 – 1.73 (m, 1H), 1.60 – 1.53 (m, 1H), 1.49 – 1.24 (m, 11H), 0.92 – 0.83 (m, 3H); ^{13}C NMR (100 MHz, $CDCl_3$) δ 53.12, 36.33, 36.02, 31.81, 29.33, 29.17, 28.80, 26.73, 22.63, 14.08.

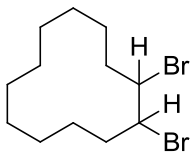

1,2-Dibromocyclododecane (6u).

Light yellow oil was obtained in 73% isolated yield. ^{1}H NMR (400 MHz, $CDCl_3$) δ 4.37 – 4.30 (m, 2H), 2.22 – 2.14 (m, 2H), 2.08 – 1.93 (m, 2H), 1.45 – 1.27 (m, 16H); ^{13}C NMR (100 MHz, $CDCl_3$) δ 55.95, 36.10, 24.63, 23.29, 23.08, 22.53. HRMS (EI): m/z calcd for $C_{12}H_{22}Br_2$ $[M]^+$: 324.0088, found: 324.0093.

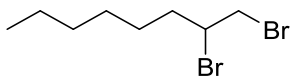

1,2-Dibromooctane (6v) (Martins et al., 2018).

Colorless oil was obtained in 83% isolated yield; ^{1}H NMR (400 MHz, $CDCl_3$) δ 4.24 – 4.10 (m, 1H), 3.87 – 3.82 (m, 1H), 3.63 (t, *J* = 10.0 Hz, 1H), 2.18 – 2.09 (m, 1H), 1.88 – 1.69 (m, 1H), 1.64 – 1.47 (m, 1H), 1.48 – 1.27 (m, 7H), 0.95 – 0.82 (m, 3H); ^{13}C NMR (100 MHz, $CDCl_3$) δ 53.13, 36.34, 36.03, 31.56, 28.46, 26.70, 22.53, 14.02.

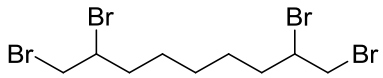

1,2,8,9-Tetrabromononane (6w).

Colorless oil was obtained in 89% isolated yield. ^{1}H NMR (400 MHz, $CDCl_3$) δ 4.23 – 4.08 (m, 2H), 3.86 – 3.81 (m, 2H), 3.62 (t, *J* = 10.0 Hz, 2H), 2.21 – 2.05 (m, 2H), 1.88 – 1.69 (m, 2H), 1.69 – 1.52 (m, 2H), 1.51 – 1.28 (m, 4H); ^{13}C NMR (100 MHz, $CDCl_3$) δ 52.75, 52.73, 36.19, 35.74, 35.70, 27.93, 27.85, 26.41, 26.37. HRMS (ESI): m/z calcd for $C_9H_{16}Br_3$ $[M\text{-}Br]^+$: 360.8802, found: 360.8803.

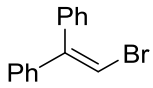

(2-Bromoethene-1,1-diyl)dibenzene (6x) (Bi et al., 2017).

Light yellow oil was obtained in 95% isolated yield. ^{1}H NMR (400 MHz, $CDCl_3$) δ 7.41 – 7.32 (m, 3H), 7.31 – 7.23 (m, 5H), 7.22 – 7.16 (m, 2H), 6.74 (s, 1H); ^{13}C NMR (100 MHz, $CDCl_3$) δ 146.78, 140.65, 139.02, 129.61, 128.37, 128.17, 128.05, 127.91, 127.56, 105.16.

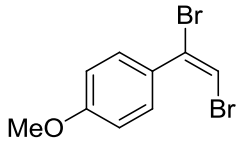

(E)-1-(1,2-dibromovinyl)-4-methoxybenzene (8a) (Song and Li et al., 2015).

Colorless oil was obtained in 65% isolated yield. ^{1}H NMR (400 MHz, $CDCl_3$) δ 7.41 (d, *J* = 8.9 Hz, 2H), 6.82 (d, *J* = 8.9 Hz, 2H), 6.66 (s, 1H), 3.75 (s, 3H); ^{13}C NMR (100 MHz, $CDCl_3$) δ 160.11, 130.76, 129.09, 121.44, 113.51, 101.92, 55.30.

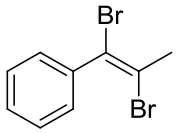

(E)-(1,2-dibromoprop-1-en-1-yl)benzene (8b). (Kikushima et al., 2010).

Colorless oil was obtained in 33% isolated yield. ^{1}H NMR (400 MHz, $CDCl_3$) δ 7.40 – 7.30 (m, 5H), 2.62 (s, 3H); ^{13}C NMR (100 MHz, $CDCl_3$) δ 140.75, 129.07, 128.58, 128.21, 117.22, 116.77, 29.31.

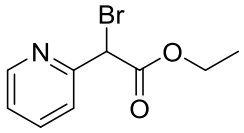

Ethyl 2-bromo-2-(pyridin-2-yl)acetate (10).

Light yellow oil was obtained in 54% isolated yield. ^{1}H NMR (400 MHz, $CDCl_3$) δ 8.64 – 8.45 (m, 1H), 7.82 – 7.56 (m, 2H), 7.24 – 7.21 (m, 1H), 5.49 (s, 1H), 4.30 – 4.17 (m, 2H), 1.25 (t, *J* = 7.1 Hz, 3H); ^{13}C NMR (100 MHz, $CDCl_3$) δ 167.44, 155.16, 148.93, 137.12, 123.46, 123.41, 62.50, 47.43, 13.74. HRMS (ESI): m/z calcd for $C_9H_{10}BrNNaO_2$ $[M+Na]^+$: 265.9787, found: 265.9788.

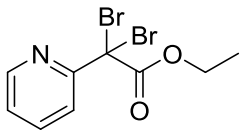

Ethyl 2,2-dibromo-2-(pyridin-2-yl)acetate (11).

Light yellow oil was obtained in 40% isolated yield. ^{1}H NMR (400 MHz, $CDCl_3$) δ 8.57 – 8.43 (m, 1H), 8.02 – 7.99 (m, 1H), 7.81 – 7.76 (m, 1H), 7.24 –7.20 (m, 1H), 4.44 – 4.29 (m, 2H), 1.30 – 1.25 (m, 3H); ^{13}C NMR (100 MHz, $CDCl_3$) δ 165.41, 158.39, 148.05, 137.44, 123.66, 121.80,

64.24, 58.61, 13.67. HRMS (ESI): m/z calcd for $C_9H_9Br_2NNaO_2$ $[M+Na]^+$: 343.8892, found: 343.8889.

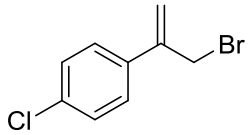

1-(3-Bromoprop-1-en-2-yl)-4-chlorobenzene (13) (Gonzalez-de-Castro et al., 2015).

Colorless oil was obtained in 32% isolated yield.^{1}H NMR (400 MHz, $CDCl_3$) δ 7.43 (d, *J* = 8.6 Hz, 2H), 7.35 (d, *J* = 8.7 Hz, 2H), 5.54 (s, 1H), 5.50 (s, 1H), 4.35 (s, 2H); ^{13}C NMR (100 MHz, $CDCl_3$) δ 143.17, 135.96, 134.13, 128.67, 127.42, 117.60, 33.84.

Supplemental References

Xiao, X., Xie, Y., Bai, S., Deng, Y., Jiang, H., and Zeng, W. (2015). Transition-Metal-Free Tandem Chlorocyclization of Amines with Carboxylic Acids: Access to Chloroimidazo[1,2-a]pyridines. Org. Lett. *17*, 3998-4001.

Li, J., Tang, J., Wu, Y., He, Q., and Yu, Y. (2018). Transition-metal-free regioselective C–H halogenation of imidazo[1,2-a]pyridines: sodium chlorite/bromite as the halogen source. RSC Adv. *8*, 5058-5062.

Tang, R.-J., Milcent, T., and Crousse, B. (2018). Regioselective Halogenation of Arenes and Heterocycles in Hexafluoroisopropanol. J. Org. Chem. *83*, 930-938.

Zhou, X., Yan, H., Ma, C., He, Y., Li, Y., Cao, J., Yan, R., and Huang, G. (2016). Copper-Mediated Aerobic Oxidative Synthesis of 3-Bromoimidazo[1,2-a]pyridines with Pyridines and Enamides. J. Org. Chem. *81*, 25-31.

Salgado-Zamora, H., Velazquez, M., Mej á, D., Campos-Aldrete, M. E., Jimenez, R., Cervantes, H. (2008). Influence of the 2-aryl group on the ipso electrophilic substitution process of 2-arylimidazo[1,2-*A*] pyridines. Heterocycl. Commun. *14*, 27-32.

Pelleter, J., and Facile, F.R. (2009). Fast and Safe Process Development of Nitration and Bromination Reactions Using Continuous Flow Reactors. Org. Process Res. Dev. *13*, 698-705.

Li, X.-L., Wu, W., Fan, X.-H., and Yang, L.-M. (2013). A facile, regioselective and controllable bromination of aromatic amines using a $CuBr_2$/Oxone system. RSC Adv. *3*, 12091-12095.

Davis, F.A., Mohanty, P.K., Burns, D.M., and Andemichael, Y.W. (2000). Sulfinimine-Mediated Asymmetric Synthesis of 1,3-Disubstituted Tetrahydroisoquinolines: A Stereoselective Synthesis of cis- and trans-6,8-Dimethoxy-1,3-dimethyl-1,2,3,4-tetrahydroisoquinoline. Org. Lett. *2*, 3901-3903.

Martins, N.S., and Alberto, E.E. (2018). Dibromination of alkenes with LiBr and H_2O_2 under mild conditions. New J. Chem.*42*, 161-167.

Wilson, K.L., Murray, J., Jamieson, C., and Watson, A.J.B. (2018). Cyrene as a Bio-Based Solvent for the Suzuki-Miyaura Cross-Coupling. Synlett *29*, 650-654.

Karki, M., and Magolan, J. (2015). Bromination of Olefins with HBr and DMSO. J. Org. Chem. *80*, 3701-3707.

Rej, S., Pramanik, S., Tsurugi, H., and Mashima, K. (2017). Dehalogenation of vicinal dihalo compounds by 1,1`-bis(trimethylsilyl)-1H,1` H-4,4`-bipyridinylidene for giving alkenes and alkynes in a salt-free manner. Chem. Commun. *53*, 13157-13160.

Kulangiappar, K., Ramaprakash, M., Vasudevan, D., and Raju, T. (2016). Electrochemical bromination of cyclic and acyclic enes using biphasic electrolysis. Synth. Commun. *46*, 145-153.

Song, S., Li, X., Sun, X., Yuana, Y., and Jiao, N. (2015). Efficient bromination of olefins, alkynes, and ketones with dimethyl sulfoxide and hydrobromic acid. Green Chem. *17*, 3285-3289.

Badetti, E., Romano, F., Marchiò, L., Taşkesenlioğlu, S., Daştan, A., Zonta, C., and Licini, G. (2016). Effective Bromo and Chloro Peroxidation Catalysed by Tungsten (VI) Amino Triphenolate Complexes. Dalton Trans. *45*, 14603-14608.

Conte, V., Furia, F.D., and Moro, S. (1994). Mimicking the Vanadium Bromoperoxidases Reactions: Mild and Selective Bromination of Arenes and Alkenes in a Two-Phase System. Tetrahedron Lett. *35*, 7429-1432.

Bi, M.-X., Qian, P., Wang, Y.-K., Zha, Z.-G., and Wang, Z.-Y. (2017). Decarboxylative bromination of α,β-unsaturated carboxylic acids via an anodic oxidation. Chin. Chem. Lett. *28*, 1159-1162.

Wang, M., Zhang, Y., Wang, T., Wang, C., Xue, D., and Xiao, J. (2016). Story of an Age-Old Reagent: An Electrophilic Chlorination of Arenes and Heterocycles by 1-Chloro-1,2-benziodoxol-3-one. Org. Lett. *18*, 1976-1979.

Song, S., Sun, X., Li, X., Yuan, Y., and Jiao, N. (2015). Efficient and Practical Oxidative Bromination and Iodination of Arenes and Heteroarenes with DMSO and Hydrogen Halide: A Mild Protocol for Late-Stage Functionalization. Org. Lett. *17*, 2886-2889.

Trofimenko, S., Yap, G. P. A., Jove, F. A., Claramunt, R. M. Garca, M. A., Dolores Santa Maria, M. Alkorta, I., and Elguero, J. (2007). Structure and tautomerism of 4-bromo substituted 1H-pyrazoles. Tetrahedron *63*, 8104-8111.

da Silva, L. E., Joussef, A. C., Pacheco, L. K., and da Silva, D. G., Steindel, M., Rebelo, R. A., and Schmidt, B. (2007). Synthesis and in vitro evaluation of leishmanicidal and trypanocidal activities of N-quinolin-8-yl-arylsulfonamides. Bioorg Med Chem *15*, 7553-7560.

Song, S., Li, X., Sun, X., Yuan, Y., and Jiao, N. (2015). Efficient bromination of olefins, alkynes, and ketones with dimethyl sulfoxide and hydrobromic acid. Green Chem. *17*, 3285-3289.

Kikushima, K., Moriuchi, T., and Hirao, T. (2010). Oxidative bromination reaction using vanadium catalyst and aluminum halide under molecular oxygen.Tetrahedron Lett. *51*, 340-342.

Gonzalez-de-Castro, A., and Xiao, J. (2015). Green and Efficient: Iron-Catalyzed Selective Oxidation of Olefins to Carbonyls with O_2. J. Am. Chem. Soc. *137*, 8206-8218.